FINAL REPORT

Environmentally Sustainable Liquid Gas Generator Formulations Program

SERDP Project WP-2400

MAY 2019

Eleonora Dimas
Dr. Gary Holland
Robert Masse
Scott Dawley
Nicholas Brown
Dr. Robert Holmes
Dr. Donald Tzeng
Aerojet Rocketdyne

Dr. Jaime Neidert
Dr. Greg Drake
AMRDEC

Dr. Adam Brand
AFRL

Dr. William Eck
USA-PHC

Dr. Dominic Di Toro
University of Delaware

Distribution Statement A
This document has been cleared for public release

SERDP
DOD ▪ EPA ▪ DOE

Page Intentionally Left Blank

This report was prepared under contract to the Department of Defense Strategic Environmental Research and Development Program (SERDP). The publication of this report does not indicate endorsement by the Department of Defense, nor should the contents be construed as reflecting the official policy or position of the Department of Defense. Reference herein to any specific commercial product, process, or service by trade name, trademark, manufacturer, or otherwise, does not necessarily constitute or imply its endorsement, recommendation, or favoring by the Department of Defense.

Page Intentionally Left Blank

REPORT DOCUMENTATION PAGE

Form Approved
OMB No. 0704-0188

The public reporting burden for this collection of information is estimated to average 1 hour per response, including the time for reviewing instructions, searching existing data sources, gathering and maintaining the data needed, and completing and reviewing the collection of information. Send comments regarding this burden estimate or any other aspect of this collection of information, including suggestions for reducing the burden, to Department of Defense, Washington Headquarters Services, Directorate for Information Operations and Reports (0704-0188), 1215 Jefferson Davis Highway, Suite 1204, Arlington, VA 22202-4302. Respondents should be aware that notwithstanding any other provision of law, no person shall be subject to any penalty for failing to comply with a collection of information if it does not display a currently valid OMB control number.
PLEASE DO NOT RETURN YOUR FORM TO THE ABOVE ADDRESS.

1. REPORT DATE *(DD-MM-YYYY)*	2. REPORT TYPE	3. DATES COVERED *(From - To)*
05/10/2019	SERDP Final Report	2/15/2015 - 2/15/2019

4. TITLE AND SUBTITLE
Environmentally Sustainable Liquid Gas Generator Formulations

5a. CONTRACT NUMBER
5-C-0002

5b. GRANT NUMBER

5c. PROGRAM ELEMENT NUMBER

6. AUTHOR(S)
Eleonora Dimas

5d. PROJECT NUMBER
WP-2400

5e. TASK NUMBER

5f. WORK UNIT NUMBER

7. PERFORMING ORGANIZATION NAME(S) AND ADDRESS(ES)
Aerojet Rocketdyne
11411 139th Pl NE.
Redmond, WA 98052

8. PERFORMING ORGANIZATION REPORT NUMBER
TRPL-317202

9. SPONSORING/MONITORING AGENCY NAME(S) AND ADDRESS(ES)
Strategic Environmental Research and Development Program
4800 Mark Center Drive, Suite 17D03
Alexandria, VA 22350-3605

10. SPONSOR/MONITOR'S ACRONYM(S)
SERDP

11. SPONSOR/MONITOR'S REPORT NUMBER(S)
WP-2400

12. DISTRIBUTION/AVAILABILITY STATEMENT
DISTRIBUTION STATEMENT A. Approved for public release: distribution unlimited.

13. SUPPLEMENTARY NOTES

14. ABSTRACT
Anhydrous hydrazine represents the state of the art for liquid monopropellants. It has proven performance, manageable handling characteristics and a mature supply chain. It is, however, toxic and flammable so there are limitations to its use – especially shipboard. In addition, its output as a rocket propellant is modest in comparison to liquid bipropellants and metallized solid propellants.

AF-M315E is a recently-developed liquid monopropellant which is demonstrating some success at replacing hydrazine. It is much less toxic, non-flammable and has higher output as a rocket propellant. However, it may not represent the optimal blend of performance and safety properties. AF-M315E achieves its high output at the expense of high combustion temperature and slow ignition response. In addition, since it is classified as an explosive material, there are restrictions on its storage and handling.

15. SUBJECT TERMS
Environmentally Sustainable, Liquid Gas, Generator Formulations

16. SECURITY CLASSIFICATION OF:			17. LIMITATION OF ABSTRACT	18. NUMBER OF PAGES	19a. NAME OF RESPONSIBLE PERSON
a. REPORT	b. ABSTRACT	c. THIS PAGE			Eleonora Dimas
UNCLASS	UNCLASS	UNCLASS	UNCLASS	234	19b. TELEPHONE NUMBER *(Include area code)* 540-854-2199

Page Intentionally Left Blank

Table of Contents

1.0 Objective……7
2.0 Technical and Program Objective……..……8
3.0 Results and Discussion……..17
3.1 Definition of Requirements……18
3.2 Task 1 Subscale Laboratory Characterization and Evaluation……..…21
3.2.1 Candidate Materials and Eliminated Families……..21
3.2.2 Theoretical Performance Calculations…….28
3.2.3 ESOH Screening: QSAR/QSAR Software Model Case Study……33
3.3 Task 2 Scale-up and Subscale Screening……...36
3.3.1 Initial Laboratory Results……..36
3.3.2 Aerojet Rocketdyne Synthesis Efforts…….39
3.3.3 AMRDEC Synthesis Evaluations…….41
3.3.4 AR Initial Propellant Evaluations…….43
3.3.5 AFRL Propellant Evaluations and Development……..46
3.4 US, Army Public Health Center Toxicology Evaluation Summary…….48
3.5 Task 3 Safety Characterization and Hazard Classification……51
3.5.1 Formulation Downselection……..51
3.5.2 Safety Hazards Summary……..52
3.6 Task 4 Scale-up and Workhorse Testing Performance Validation ……..56
4.0 Summary……83
4.1 Propellant Rankings……..…85
5.0 References……..86
6.0 Appendices ……89

List of Tables

3.1-1 Threshold and Optimum Performance Metrics for WP-2400 Propellant……..18

3.2-1 Summary of EILs Evaluate in Task 1……21

3.2-2 Regression independent variable predictors……28

3.2-3 Solver Methods Results by Ionic Liquids…….31

3.2-4 Summary of Experimental Ionic Liquids (IL) Data……...32

3.2-5 List of Energetic Ionic Liquids and Reference Compounds to be studied……....34

3.2-6 List of Chemical Parameters to be Estimated for the Energetic Ionic Liquids (EIL) Compounds……..34

3.2-7 Stop/Go schemed table to compounds parameters relative to hydrazine……35

3.3-1 Summary of Task 2 Material Candidates……36

3.3-2 EILs Propellant Blends Performance……44

3.3-3 Summary of EIL Propellant Formulations……46

3.4-1 Characterization Criteria used in the Development of Safety and Occupational Health Severity…….49

3.4-2 Stoplight chart of examined compounds……49

3.4-3 Selected SERDP compounds for Bioaccumulation, Toxicity and Exotoxicity….…..50

3.5-1 Formulation Components……51

3.6-1 Propellant Candidate Summary…….52

3.6-2 Summary of Diluted 315F and M824S……53

3.6-3 Sensitivity Results of 1-methyl-4-amino-triazolium Nitrate…….55

3.7-1 List of Candidate Propellant Tested with Characteristic Metrics……..57

3.7-2 Nominal Operating Conditions…….59

3.7-3 Planned Hot Fire Test Matrix……..59

3.7-4 Test 1 As-Run Test Matrix……..61

3.7-5 Test 2 As-Run Test Matrix……..65

3.7-6 Test 3 As-Run Test Matrix……..71

3.7-7 Test 4 As Run Test Matrix……76

List of Figures

2.0-1 Technical Approach…….9

3.0-1 SERDP Report Overview……..……17

3.0-1 SERDP Program Overview……17

3.2-1 Final Minitab Regression Equation for Flame Temperature…….29

3.2-2 Final Minitab Regression Residuals for Isp……...……30

3.2-3 Excel snip of the color coded trends for visualization……..…….32

3.3-1 Overview of promising EILs from Task 2…….42

3.3-2 DSCs of AMRDEC EILs and AN Mixtures……..……45

3.6-1 DSC for Carbohydrazide nitrate based propellant.....55

3.6-2 Comparison of titanium curves for carboyhydrazide nitrate based propellants……57

3.7-1 Laboratory Mod (Heavyweight) Test Thruster……..…58

3.7-2 Stability assessment Seq 2 (0.5/5 sec on/off) pulses of Diluted M315E..…….62

3.7-3 Selected extended stability assessment sequence pulse overlap of Diluted M315E…….63

3.7-4 Diluted M315E Five-second burn exceeded at progressively reduced catalyst bed preheat temperature……..……..…64

3.7-5 Stability assessment Seq 2 (0.5/5 sec on/off) pulses of M315F……..….66

3.7-6 Selected extended stability assessment sequence pulse overlays of M315F……67

3.7-7 M315F Five-second burns executed at progressively reduced catalyst bed preheat temperature……....68

3.7-8 Video images from five-second burn initiated from 288ºC (550º) preheat temperature of M824S……..70

3.7-9 Stability assessment Seq 2 (0.5/5 sec on/off) pulses of M824S……..72

3.7-10 Selected extended stability assessment sequence pulse overlay of M824S…….72

3.7-11 Five-second burns executed at progressively reduced catalyst bed preheat temperature of Carbohydrazinium Nitrate…….…….74

3.7-12 Rise in temperature measured by Tplenum vs catalyst bed preheat temperature……74

3.7-13 Stability assessment Seq 2 (0.5/5 sec on/off) pulses of Carbohydrazinium Nitrate……77

3.7-14 Selected extended stability assessment sequence pulse overlay of Carbohydrazinium Nitrate……77

3.7-15 Carbohydrazinium Nitrate Five-second burns executed progressively reduced catalyst bed preheat temperature……78

3.7-16 Chamber pressure 50% response time vs preheat temperature for all propellants….....79

3.7-17 Chamber pressure 10% response time vs preheat temperature for all propellant ……80

3.7-18 Comparison of estimated moving average Isp propellants tested……..81

List of Acronyms

AF-M315E ..... USAF blend of HAN, HEHN, AN, H2O

AFRL ..... US Air Force Research Laboratory

AMRDEC ..... US Army Missile R+D and Engineering Command

AN ..... Ammonium Nitrate, NH4NO3

AR ..... Aerojet Rocketdyne

Bmim ..... butyl, methyl-imidazole

C-103 ..... alloy

cP ..... centipoise, viscosity units

DOT ..... US Department of Transportation

EIL ..... Energetic Ionic Liquid

Emim ..... Ethyl-, methyl-imidazole

ESOH ..... Environmental Safety and Occupational Health

GHS ..... Globally Harmonized System

HAN ..... HydroxylAmmonium Nitrate

HEATN ..... Hydroxy-Ethyl-Amino-Triazolium Nitrate

HEHN ..... HydroxyEthyl Hydrazinium Nitrate

HN ..... Hydrazinium Nitrate

IPA ..... Isopropyl Alcohol

LFERs ..... Linear free energy relationships

LMP-103S ..... blend of A-DN, NH3, AN, H2O

MATN ..... Methyl-Amino-Triazolium Nitrate

MW ..... Molecular Weight

pp-LFER ..... Abraham poly-parameter linear free energy

QSAR ..... Quantitative Structure Activity Relationship

QSPR ..... Quantitative Structure Property Relationship

Tc ..... Theoretical Combustion Temperature, K

TZM ..... high temperature alloy

USA-PHC ..... Army Public Health Center

1. Objective and Summary

Anhydrous hydrazine represents the state of the art for liquid monopropellants. It has proven performance, manageable handling characteristics and a mature supply chain. It is, however, toxic and flammable so there are limitations to its use – especially shipboard. In addition, its output as a rocket propellant is modest in comparison to liquid bipropellants and metallized solid propellants.

AF-M315E is a recently-developed liquid monopropellant which is demonstrating some success at replacing hydrazine. It is much less toxic, non-flammable and has higher output as a rocket propellant. However, it may not represent the optimal blend of performance and safety properties. AF-M315E achieves its high output at the expense of high combustion temperature and slow ignition response. In addition, since it is classified as an explosive material, there are restrictions on its storage and handling.

The WP-2400 Environmentally Sustainable Liquid Gas Generator Formulations Program seeks to retain some of the performance and handling improvements demonstrated by AF-M315E while recouping some of the operability and versatility associated with hydrazine. In particular, the program is striving to reduce the combustion temperature and ignition response characteristics of the non-toxic monopropellants so that it can approach the expectations established from hydrazine-based systems.

During the course of this 4 year effort, material candidates based on ionic liquids were evaluated as possible hydrazine replacements. The program evaluated cations from the triazole, tetrazole, pyrimidium, hydrazide and imidazole family, and the perchlorate, dinitramides and nitrate anions. Initial evaluations examined the performance, sensitivity, catalytic response, thermal stability and toxicity of each candidate. Overall the triazoles and hydrazides exhibited acceptable properties. Both candidate families exhibited good ignition, heat of formulation and reactivity. The imidizoles were the first to be eliminated from further evaluations due to poor performance while the tetrazoles were eliminated due to thermal stability concerns and the pyrimidiums due to poor catalytic ignition. Nitrates were determined as the only acceptable cation. Perchlorates were eliminated due to environmental concerns while dinitramides exhibited unacceptable low exotherm temperatures.

The program then focused on propellant development and downselection of the following formulations summarized in Table 1.1-1. Each formulation utilized water as the coolant to achieve the required flame temperature of <1450K. All formulations down selected exhibited acceptable sensitivity and thermal stability. The 1-methyl-4-amino-1,2,4-triazolium nitrate candidate was selected because of its good performance and potential for improved toxicity. Scale-up of this formulation was cancelled due to environmentally unfriendly impurities (silver) present in the 1-methyl-4-amino-1,2,4-triazolium nitrate. Additional work is required to improve the synthesis of this material prior to continuing work. The carbohydrazinium nitrate formulation was

downselected because of its high performance and the commercial availability/low cost of carbohydrazide. A diluted M315 formulation was selected due to its high maturity level and ability to meet the program flame temperature requirement. M315F was selected due to its low toxicity since it replaces HAN as its oxidizer with ammonium nitrate. The final candidate selected was M824S which has improved thermal stability.

Table 1.1-1 Propellant Summary

Candidate	Ingredients	Oxidizer	Benefits
1-methyl-4-amino-1,2,4-triazolium nitrate	Synthesized at AR Sacramento	HAN	Good performance and toxicity
Carbohydrazinium Nitrate	Synthesized from Carbohydrazide at AR Redmond	No Oxidizer	Good performance and commercially available
Diluted M315E	HEHN	HAN	Reduced flame temperature compared to M315E
M315F	HEHN	AN	Low toxicity
M824S	HEATN	HAN	Increased thermal stability

Hot fire testing was conducted on the carbohydrazinium nitrate, diluted M315E, M315F and M824S. All propellants demonstrated case-specific minimum preheat temperatures from which stable operation of a heavyweight lab model thruster could be successfully initiated. AF-M315F and Carbohydrazinium nitrate-based propellants respectively exhibited typical benign washouts at 288 ºC (550 ºF) and 260 ºC (500 ºF). Testing conducted on M824S showed concerns with incomplete combustion. Diluted M315E, Carbohydrazinium nitrate and M315F showed that with proper preheating, formulations could be utilized as environmentally friendly hydrazine replacements. Even though hot fire testing showed promise for the formulation candidates, additional work is required to further optimize and mature the formulation candidates.

2. Technical and Program Approach

The technical approach for the program is to investigate ionic liquids (IL) for use as hydrazine replacements while retaining the desirable features of the hydrazine system (low flame temperature, catalyst bed ignition, commercial materials). Ionic liquid monopropellants achieve technical performance through increased density and improved packing. In addition, low volatility aids in operator handling and minimum exposure. Detailed requirements are given in section 3.1. Progress in Tasks 1 and 2 are detailed in this final report.

The program approach is outlined in the following graphic, Figure 2.0-1. It starts with Task 1 modeling efforts (thermodynamic performance, ESOH / toxicological) on individual components and compositions; candidates that pass this preliminary screening are only then admitted to the laboratory, in small amounts, for sensitivity and stability screening, Task 1. Acceptable stability and sensitivity / handling characteristics allow quantities to scale up to levels suitable for small scale mix studies and performance assessments, Task 2. Successful mixes and scale-up efforts on materials and compositions exhibiting suitable performance in crude laboratory testing would then be subjected to larger scale sensitivity testing Task 3, required to transport materials from their point of origin to the site of testing, Task 4, in a heavyweight "workhorse" thruster. Those scaled-up materials from Task 3 are also subjected to more rigorous in vitro and in vivo ESOH testing ,Task 5.

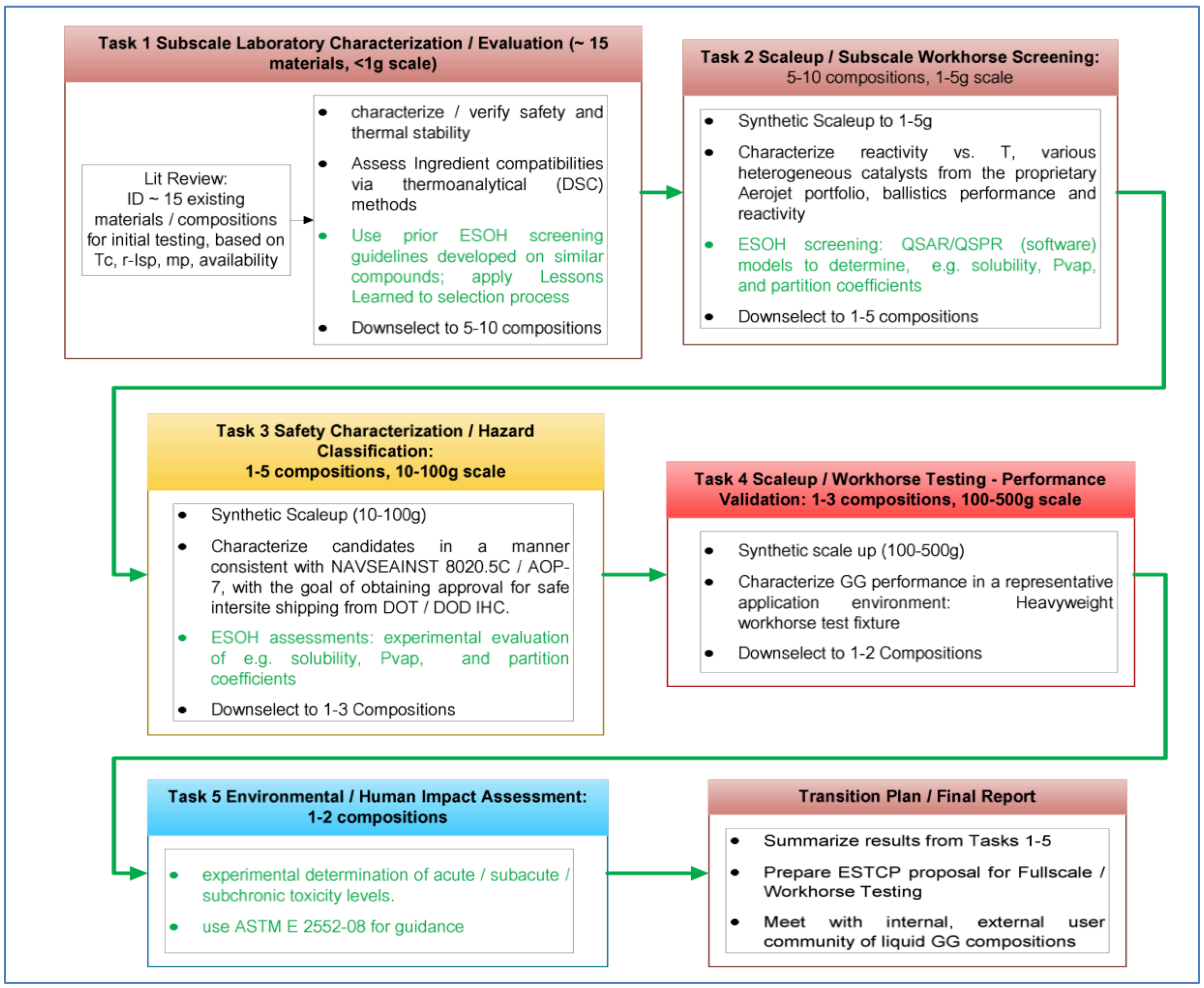

Figure 2.0-1 Technical Approach

2.1 Task 1 Subscale Laboratory Characterization and Evaluation:

In Task 1, a literature review focused on the identification of 15-20 chemical constituents which will form the backbone of candidate materials for further characterization, development and down selection through the course of this program. This selection of the candidate materials was based on a paper trade study of known materials and novel compositions, and reviewed by the Aerojet Rocketdyne-AFRL-AMRDEC team with the sponsor. Theoretical thermochemical calculations were run to ensure that combustion temperatures are within criteria identified. Assessment of the composition and exhaust products to evaluate environmental and human impacts allowed determination of SERDP objectives.

An initial laboratory effort for characterization/verification, safety, and thermal stability using minimal quantities of material allowed screening of ingredients to eliminate materials not compliant with requirements. Ingredient compatibilities were studied via thermoanalytical methods prior to incorporating any new material into propellants. Initial candidates were also screened for environmental and human safety using guidelines developed in the course of prior research efforts of ionic liquids, avoiding known detrimental chemical markers such as longer aliphatic side chains and aromatic functionalities.

Differential scanning calorimetry (DSC) and thermal gravimetric analyses (TGA) was used for measurement of thermal stability and melt /glass points. Material hazards sensitivity was assessed using drop hammer closed brass cup testing, electrostatic discharge (ESD), and friction sensitivity. Safe handling of material required the components / compositions to be at an improved sensitivity level over reference materials (RDX, HMX (or propyl nitrate).

2.2 Task 2 Scale-up/Subscale Screening

Based on the screening efforts of Task 1, approximately 5-10 compositions were evaluated for ballistics performance and reactivity assessed vs. various heterogeneous catalysts from the proprietary Aerojet portfolio. ESOH screening proceeded to predictive computational tools (QSAR/QSPR) to determine, e.g. solubility, vapor pressure and partition coefficients. Suitable candidates were scaled up in quantity, further characterized for safety, thermal stability and materials compatibility, and subjected to Ballistics Performance Evaluation by, e.g. Pino and strand burner testing. Upon verification of safety, thermal stability, performance and toxicology, a downselected subset of materials are scaled to levels required for experimental verification of safe handling / shipping and environmental compliance in Task 3.

Target compounds were synthesized at all locations at the 1-5g level. Once the compounds were made, they were subjected to hazard testing (impact, friction, ESD). They were also characterized for thermal stability (DSC, TGA) and structurally confirmed by proton and C-13 NMR, and FT-IR. New formulations during the course of this effort were subjected to a similar series of hazards and thermal stability testing.

Quantitative structure activity relationships (QSARs) was employed by the University of Delaware to help guide selection of candidate propellant formulations. The QSAR approach is well known for estimating physical properties that impact bioaccumulation and narcosis: water solubility, Henry's law constant, vapor pressure, adsorption coefficient (Koc) on soil, and octanol-water partition coefficient (Kow). Use of QSAR modeling for salts- the type of compounds of interest in this effort- is less well established than for neutral molecules. Therefore, the modeling assessment was performed using methodology and tools developed by Dr. Dominic Di Toro of the University of Delaware under SERDP Project ER-1734. Dr. Di Toro's project team previously tested the predictive ability of QC methods (COSMO-SAC and SM5) as well as other commonly used estimation methods applied to munitions chemicals, and the QC methods were clearly superior. In their SERDP project, these researchers combined estimation methods to produce optimal estimates using a technique successfully applied to estimating atomization enthalpy using the estimates from multiple functionals in QC density functional theory. Dr. Di Toro's models are being applied to predict bioconcentration factors (BCFs) in the absence of metabolism.

Screening criteria at the one to five gram scale included differential scanning calorimetry (DSC) and thermal gravimetric analyses (TGA) (for characterization of thermal stability and freezing/glass points); viscosities were measured using a piston style viscometer (approximately 2 grams of sample required); and mechanical sensitivity was tested using a drop hammer closed brass cup, sliding friction using unglazed ceramic tiles; and electrostatic discharge testing. Several important criteria are used in screening the ionic liquid candidates and eutectic mixtures and include: 1) a positive catalyst response in open drop tests with neat monopropellant ingredients and/or ionic liquid mixtures as monopropellants; 2) reasonable liquidous range for final usage in desired monopropellant application(s), i.e. will have a melting/glass point <-50ºC; and 3) will have working liquid viscosity < 1,000 cP at ambient laboratory conditions (20ºC).

Given that all current monopropulsion systems involve catalytic reactors, the most straightforward next generation sustainable, non-hydrazine system would also involve decomposition of the liquid on a heterogeneous catalyst bed. The majority of current monopropellant engines, as well as current liquid GGs such as the F-16 EPU, are based upon decomposition / ignition of the liquid with the Shell-405 catalyst. This is an alumina-supported iridium catalyst. Aerojet now manufactures the similar S405 catalyst since Shell-405 is no longer in production. Aerojet has developed a broad portfolio of heterogeneous catalysts, similar to S-405 but with different active metals – e.g. precious metals such as Pd, Rh, Pt and more cost-effective Fe-Co-Ni systems. Performance of the candidate propellant compositions is being evaluated against different catalysts in an attempt to optimize performance.

Preliminary reactivity screening was conducted with simple spot-plate testing. Pino testing was used to further the evaluation of propellant decomposition catalysts; the process is also be adapted for non-catalytic reactors. Pino testing provides two valuable pieces of information:

exhaust gas temperature rise rate (the time in milliseconds that it takes the exit gas temperature to rise a specified amount over the initial starting temperature) and overall temperature achieved.

A higher exit gas temperature indicates better catalytic / reaction performance, i.e., more complete decomposition of the propellant, and greater thrust. Similarly, the shorter the exit gas temperature rise rate, the better the performance. A short rise rate indicates faster ignition of the propellant. Conventional Pino testing typically involves placing a catalyst sample into a holder, suddenly immersing it into a pool of propellant, and measuring the temperature-versus-time response of a thermocouple in the sample holder. The most common procedure employs a heated catalyst sample and ambient-temperature propellant.

Catalytic reactivity will be complemented by liquid strand combustion characterization. This will provide a general characterization of combustion behavior as a function of pressure - an essential parameter in the development of new liquid propellants. Just as important in propellant development is an understanding of the linear velocity of propellant combustion for establishing safe operating conditions for the system. If the propellant combustion velocity significantly exceeds the propellant feed rate, burn back of the propellant through the feed line can occur. In this event a catastrophic failure may ensue. Thus, operational safety dictates a good knowledge of the propellant combustion and its variation with pressure.

2.3 Task 3 Safety Characterization/Hazard Classifications:

While screening tests of energetic materials can be accomplished on small scales using materials transported in approved containers, more extensive testing will require larger quantities of material, as well as extensive characterization of material hazards and safe handling. To this end, we are characterizing a down selected subset of 1-5 candidates in a manner consistent with NAVSEAINST 8020.5C / AOP-7, with the goal of obtaining approval for intersite shipping from DOT / DOD IHC. Furthermore, in order to characterize safe handling domains for energetic liquids intended for transfer from a holding tank to a combustion reactor, Adiabatic Compression Sensitivity for this down selected subset will be undertaken. Human / environmental assessments will graduate to experimental evaluation of those physical properties previously determined predictively. Upon demonstration of safe handling / shipping and environmental compliance, 1-3 down selected formulations will be identified for further scale-up to quantities suitable for workhorse performance testing in Task 4.

Those candidates that pass the Task 2 criteria of catalyst bed reactivity, thermal stability, reasonable viscosity measurements, low melting point, and satisfactory safety test values, can then be scaled to the 100 gram quantities in the same laboratories at AMRDEC upon mutual agreement by the entire team effort. After the scale-up, physical and chemical properties of the desired candidates will be checked and verified to ensure that critical behaviors important to the success of the target solution are maintained. These laboratories already have an established protocol (approved SOP) for handling up to 100 gram quantities of Class 1.1 materials in synthetic

procedures. The environmental fate and transport of new materials is an important factor that relies on multiple, complex phenomena within the environment. Such phenomena are not easily quantifiable. Vapor pressure is often a key parameter for transmission of the subject material via atmosphere to other environmental compartments. However, in the case of salts, particularly ILs, the vapor pressures of these materials are principally negligible. In contrast, the transmission of these ionic materials can be significant through water or in the soil. Thus it is critical that knowledge of the aqueous solubility and of the partition coefficients between environmental compartments of a substance is determined as soon as practicable.

During Task 3, up to three propellant candidates will be selected for experimental verification of water solubility, Koc, Kow, sorption and dissolution rate. An early experimental assessment of these basic physical properties will help assure the program's direction toward identifying propellant candidates with reduced environmental impacts.

Likewise the test area for carrying out interim hazard classification card gap testing is within the same restricted test area inside of Redstone Arsenal, and will require no special efforts to transport from the laboratories to the test area to carry out testing. Upon approval of the cognizant shipping authorities, compounds with satisfactory purity will be sent via exempt pipe containers to Redmond facility and/or Government Labs for testing at small motor levels.

An important safety issues arises when a liquid propellant is transferred or pumped from the storage tank through feed lines to the combustion chamber. If the lines contain entrained air bubbles, vapor bubbles, or even bubbles generated from propellant decomposition, the rapid closure or opening of online valves may cause a sudden compression of the liquid and, as a result, an explosion may occur. Furthermore, pumping propellants at considerably high flow rates, as it is required in many applications, can cause cavitation and may introduce vapor bubbles into the liquid.

In the proposed effort, an AFRL apparatus will be used for assessment of the sensitivity of the propellant toward mechanical shocks (Adiabatic Compression Tester). The propellant sample is placed into a 316 stainless steel U-tube, and the sample is then exposed to an abrupt mechanical shock produced by the rapid introduction of nitrogen gas into the tube at a pressure between 3.45 and 20.7 MPa (500 to 3000 psi). A pressurization rate of 827 MPa/sec (120,000 psi/sec) is measured for the apparatus operated at 20.7 MPa driving pressure. The propellant is equilibrated to 25ºC and the nitrogen pressure set at 3.45 MPa for a driving pressure ratio of 35/1. A positive reaction of the propellant to adiabatic compression results in a deformed and possibly fragmented steel tube. Tests are performed and compared to hydrazine.

2.4 Task 4 Scaleup/Workhourse Testing-Performance Validation:

With approval to safely transport larger quantities of material, propellant candidates determined to have suitable ESOH, performance, and ignition characteristics will be scaled up to support hot-fire validation testing.. This testing will entail test under operational flow rates ranging from low to high, at conditions from hot / cold, and for both short and extended discharges. Such testing will rigorously probe the ignition repeatability of the gas generant on the selected catalyst over the range of operational conditions, as well as provide a means to measure its performance lifetime. The 1-2 formulations demonstrating the most promising performance will be identified and down selected for further environmental / human impact assessment of acute / sub-acute / sub chronic toxicity levels

As far as scaling towards a 500 gram capacity AMRDEC will use multiple runs at a 100 gram scale to generate quantities for IHC testing internally. The first 500 grams of each of the two materials produced will be dedicated for DOT shipping classification tests. Final products will be shipped to Redmond under DOT classification.

All workhorse testing will be performed in subscale test hardware to minimize cost and thereby maximize the scope of evaluated propellants; however target test parameters (e.g. chamber pressure, catalyst bedloading) will be established as necessary for scale-up to several-hundred lbf thrust. All facilities needed to complete the planned scope of the test effort currently exist in an operational state, thereby representing substantial savings to this SERDP program. Aerojet's versatile micro-feed system enables efficient operational screen tests of up to thirty seconds with minimal propellant waste associated with system internal hold-up volume, thereby allowing test of small batch propellants prior to investing in fabrication process scale-up necessary to operate typical test systems. Propellants yielding favorable results can then be produced in larger quantities for more extensive long-duration testing in Aerojet's larger hot-fire facility. As these systems were designed specifically for the testing of unproven propellants, both incorporate a number of safety features designed to eliminate the risk of damage by upstream propagation of ignition.

An existing subscale heavyweight test gas generator will be employed in all tests. This fully disassembled workhorse apparatus, pivotal in the development of Aerojet's HAN-based propellant technologies including the recent IR&D efforts focused on low-flame temperature blends, incorporates a highly interchangeable architecture such that catalysts, catalyst bed geometry, injection scheme, chamber pressure, and thrust density may be readily tailored as required for a given candidate propellants, as well as iterated for purposes of performance optimization. Aerojet's existing catalysts encompass a range of active metals of interest likely to be effective with a wide variety of propellants. A key advantage of the test apparatus' flexibility is that each propellant performance may first be vetted at lower thrust density before graduating to the higher performance requirements typically necessary for DACS-type applications. All internal components of the reactor are constructed of chemically inert materials, such that a wide range of propellants may be tested while leaving the system fully reusable. Instrumentation includes a

pressure transducer monitoring chamber pressure and roughness penetrating thermocouples to measure reaction and effluent gas temperatures.

The test effort will employ special test methodologies developed over Aerojet's twenty years' experience developing advanced monopropellants now well proven to facilitate the quantitative assessment of the ignition characteristics of even high pressure-burnrate-exponent propellants in unstable injection schemes without damage to test hardware. Thus, the robust planned test program will not be susceptible to schedule impacts in the event a down-selected propellant yields behavior inconsistent with predictions based on preliminary screening.

2.5 Task 5 Environmental/Human Impact Assessments:

The proposed effort will extend the physical properties study with an experimental determination of acute / sub-acute / subchronic toxicity levels using for guidance ASTM E 2552-08 for the top 1-2 candidates as determined in Task 4.

During Task 4, up to two propellants will be down selected for Tier 1 acute, sub-acute, and subchronic toxicity testing. The testing protocols will generally follow those performed during prior efforts by this program team during the development of monopropellant AF-M315E. Thus, initial toxicity testing of the propellants will consist of the following acute studies: dermal irritation, dermal sensitization, oral toxicity, and the bacterial reverse mutation test. An acute toxicity study will be administered by the oral route to rats. The purpose of the study will be to assess the short-term toxicity of candidate propellant when administered by a single oral dose to rats. Based on the OECD 425 Acute Oral Toxicity Statistical Program with the default sigma of 0.5, the dose level increased or decreased as each level is tested. The following variables and end points are expected to be evaluated in this study: clinical signs, body weights and gross necropsy. The acute oral LD50 of the propellant will be estimated and compared to the oral LD50 of hydrazine (60 mg/kg in the rat).

An acute skin irritation study of propellant candidate is anticipated through administration by the dermal route to rabbits. The purpose of this study is to assess the irritant and/or corrosive effects of propellant when administered by a single dermal dose to rabbits. Exposure to the propellant is judged by evaluation of degree/extent of erythema at the test sites by the 1-hour scoring interval. Assessment of resolution of the dermal irritation will be performed post-dose. Under the conditions of the test, the propellant action as an irritant to the skin of the rabbit can be based on the EPA-FIFRA Dermal Irritation Descriptive Classification. For comparison purposes, hydrazine is considered as a strong irritant (and is known as a corrosive).

A sensitization study will be undertaken for propellant candidate administered by the dermal route using the modified buehler design. The dermal sensitization potential of propellant is evaluated in Hartley derived albino guinea pigs. An α-hexylcinnamaldehyde (HCA) positive

control group consisting of 10 HCA test and 10 HCA control guinea pigs are included in this study to assure test fidelity. Based on the results of this study, the propellant candidate's propensity as a contact sensitizer in guinea pigs is determined. Hydrazine by comparison is a known strong allergen or potent sensitizing agent. An Ames evaluation of propellant candidate for mutagenic activity is anticipated using Salmonella-Escherichia coli microsome plate incorporation assay. Control values will be employed for consistency.

The propellant candidate will be judged for mutagenic propensity under the test conditions used in this study. Results of all Phase III tests will then be compiled. Thus, an experimental measure of the improvement in endpoint impacts between the new monopropellant and the current state-of-the-art monopropellant will be established.

The results of Task 5 will be reported in a separate report once testing is complete. All samples for testing have been shipped to the Army Public Health Center.

2.6 Task 6 Final Report:

Results obtained in Tasks 1-5 of this program effort will be summarized in a Final Report and submitted to the customer.

3. Final Results and Discussion:

3.0 Program Review Structure

The WP-2400 program has taken place during the last four years and has amounted to a significant amount of data and knowledge that will be presented in this section. The information will be introduced and discussed as shown in Figure 3.0-1 which is provided throughout the text a roadmap.

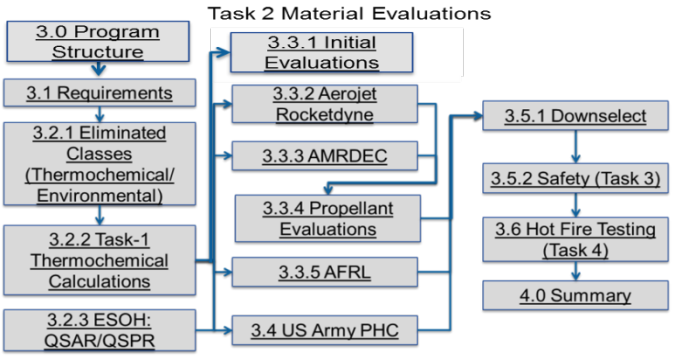

Figure 3.0-1 SERPD Report Overview

In addition Figure 3.0-2 is presented in order to provide an overall summary of the candidate families evaluated and propellants downselected during this effort.

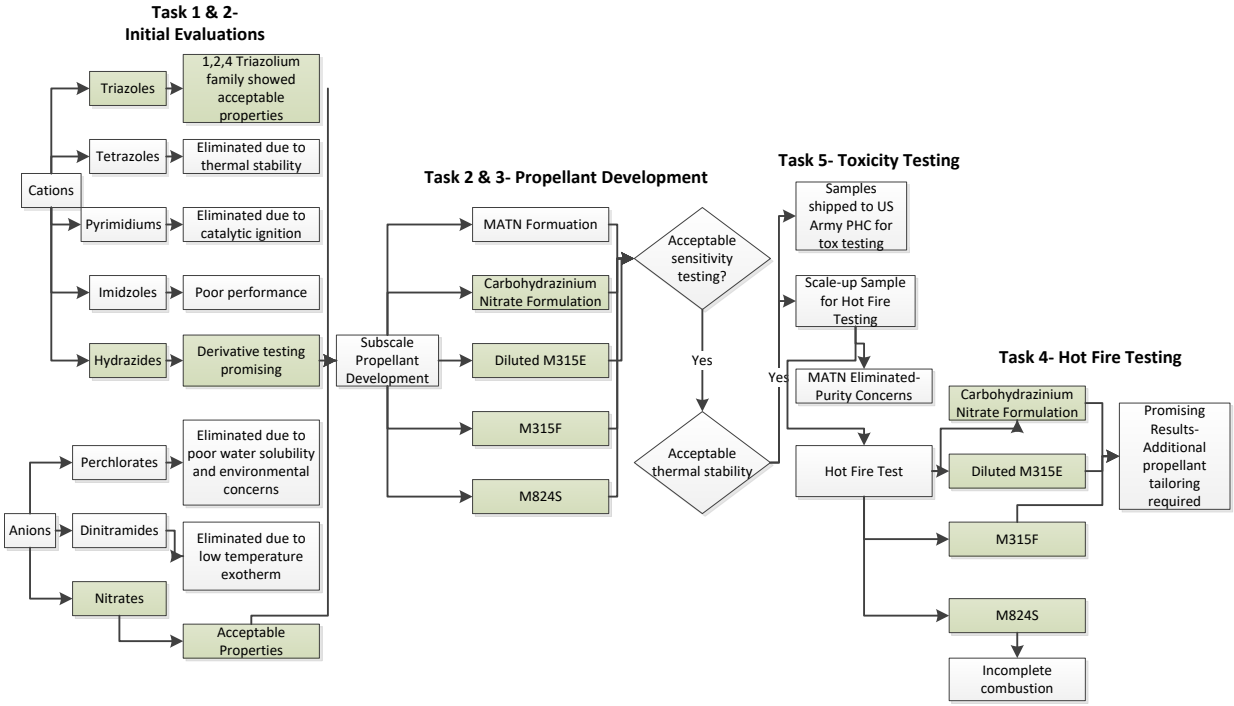

Figure 3.0-2 SERDP Program Overview

3.1 Definition of Requirements

The initial proposal provided a table of performance metrics for this propellant development effort. Two existing propellants were used as reference standards: anhydrous hydrazine and AF-M315E.

The following Table 3.1-1 and discussion represent our minimum (threshold) and optimum performance metrics for our propellant candidates.

Table 3.1-1 Threshold and Optimum Performance Metrics for WP-2400 Propellant

Metric	Threshold	Optimum
Storage Temperature (min, ºC)	0	-54
ρIsp (% vs Hydrazine)	+20	>30
Storage Stability	<1.0	<0.1
Low Toxicity		
Mutagenicity (Ames Test)	2/5	0/5
Acute Toxicity (Mammalian Surrogate, LD 50, mg/L)	≥50	>2000
Micro-Tox(Aquatic, LD50, mg/L)	≥1.0	>100
Combustion Temperature T_c (K)	<1900	<1450
Liquid Viscosity (cP, 20ºC)	<1000	-1
Decomposition Onset (DSC, ºC)	150 min	>150
Synthesis Steps	≤4	<2
Flash Point (Closed Cup, ºC)	>51	Non-Flammable
Hazards Classification	≥US DOT 1.3	US DOT 9
Ignition Response Delay	=AF-M315E	=Hydrazine

Storage Temperature (min, °C): Liquid propellant systems that freeze (2 °C, hydrazine) or become extremely viscous (-20 °C, AF-M315E) require additional engineering controls to maintain system temperature which limits mission applications and increases costs Tactical munitions often have a very low operation limit of -65F (-54 °C). The optimum propellant would be usable down to - 54°C but we will not exclude materials that have higher melt/freeze points; up to 0°C.

ρ*Isp (% vs Hydrazine): Density Isp is a measure of thrust efficiency. It describes the amount of thrust available per unit of propellant volume. Higher performing, denser propellants can be packaged more efficiently. Using hydrazine as the reference (ρ*Isp = 245 s/cc), propellants with ρ*Isp > 30% higher (~320s/cc) will be identified but materials with +20-30% ρ*Isp will not be excluded. The high-performing advanced monopropellant AF-M315E has ρ*Isp >+50% over hydrazine. Identification will occur through theoretical calculations parametrically assessing performance versus composition at varying water levels, oxidizer/fuel ratios, and other important parameters.

Storage Stability (% mass loss, 24 hours, 75 °C): Storage stability is an important parameter for both propellant safety and environmental cost considerations. Unstable propellant is dangerous and requires costly disposal and replacement. We can roughly equate a <1.0% mass loss with a 10 year storage stability expectation. Propellants achieving this threshold stability will be included in

our study with goals of obtaining materials with much higher thermal stability; <0.1 % mass lost over the test duration. AF-M315E has reported 0.43%/day mass loss.

Low Toxicity: Significant detail has been added to this requirement versus the material presented in our original proposal.

Mutagenicity - The Ames test examines test materials vs. 5 strains of microorganisms.

Materials which do not result in mutation of the microorganisms are preferred, since EPA considers any positive test in the 5 standard strains, with or without microsomal activation, to be a positive test for mutagenicity. Testing of AF-M315E showed 2 positives for mutation. This is our threshold performance for a new propellant. Optimally we would find 0/5.

Acute Toxicity (Mammalian Surrogate, Neutral Red) - LD50 (oral, rat) is 60 mg/kg for hydrazine. The criterion for Category 3 acute toxicity under the Globally Harmonized System (GHS) is 50-300 mg/kg, which closely follows the accepted acute oral toxicity value for hydrazine. The "limit test" for acute oral toxicity is 2000 mg/kg, indicating no toxicity, so this would be the optimum goal. Testing on AF-M315E put its acute toxicity at 350 mg/kg.

Aquatic Toxicity (Micro-Tox) - The lower limit for acute aquatic toxicity in both the GHS and the Army Public Health Center (APHC) classification criteria is 1.0 mg/L, indicating this is an appropriate threshold. The upper limit for Category III acute aquatic toxicity under both the GHS and the APHC classification scheme is 100 mg/L, making it the optimum level.

Combustion Temperature, Tc (K): The propellant combustion temperature (Tc) drives not only performance, but also a range of thruster design considerations. High Tc is good for performance, but severely restricts engineering options. Most notably, high Tc destroys the catalyst used for ignition of the propellant. Hydrazine has a relatively low Tc; ~1250K. The highly active ɣ-alumina-based catalyst used for hydrazine systems is stable up to about 1450K before it is badly degraded. Other less-active catalyst systems are stable up to 1900K. AF-M315E, with a Tc of >2100K, employs low-activity ceramic catalysts. Optimally we would have a propellant with a Tc <1450K, but we will work with and develop propellants with Tc up to 1900K.

Tc also drives considerations on the materials used to construct the thrusters or gas generator devices. Based on our experience with hydrazine propellant systems, we expect that nickel/cobalt-based super alloys (e.g. Inconel, Hastelloy, Haynes) could be used for thrusters or gas generators where the Tc was ≤1450K. Hotter burning propellant formulations, up to 1900K, would possibly employ molybdenum or niobium-based alloys such as TZM or C-103 with oxidation inhibiting coatings such as 512A/E. Thrusters using AF-M315E with Tc>2100K currently employ rhenium-based alloys with an oxidation-resistant iridium liner.

Liquid Viscosity: Propellant viscosity drives engineering requirements for propellant storage and distribution in the propulsion system and thruster. Hydrazine has water-like viscosity (1 cP) and represents our optimum performance. AF-M315E is significantly more viscous (25 cP). The

threshold for propellant viscosity will be 1000 cP which may be reached for some of the ionic-liquid or gel-based propellant systems.

Decomposition Onset: This parameter predicts both propellant hazards and also propellant ignition. A low decomposition onset is undesirable since it implies the propellant will readily decompose or auto-ignite if accidentally exposed to fire during storage or handling. Conversely a very high decomposition onset indicates possible difficulties with propellant ignition. AF-M315E has a DSC decomposition onset above 150º C; its other safety and storage properties are acceptable. We will adopt this as our threshold requirement and optimally have a more stable propellant.

Synthesis Steps: Preparation of the propellant and its ingredients represents both a fiscal and environmental cost. Optimally we will be able to prepare our propellant ingredients with a minimal (<2) number of process steps from readily available raw materials. It is expected that some ingredients/formulations will use materials which are currently not readily available and may require more (up to 4) steps to synthesize.

Flash Point: Flash point is used in assigning the flammability/combustibility designations for storage and handling. Hydrazine has a flash point of 51º C and carries a "Flammable" (Class 6) DOT labelling requirement. While we would accept a propellant with similar flammability (threshold), we would optimally have a non-flammable formulation.

Hazard Classification: Hazard class 1.3 is the most severe hazard class that we will consider as a product of this effort (threshold). AF-M315E is assigned hazard class 1.3 or 1.4 depending on packaging. Optimally our propellant would achieve a class 9 designation. Other propellants - notably gas generating formulations used for air bags - have been assigned to class 9. Class 9 generally carries fewer restrictions on handling and storage versus Class 1.

Ignition Response Delay: This parameter is highly dependent on device and test parameters and there is no standard test method. As a minimum we will provide propellants which have ignition response equivalent to AF-M315E. Optimally, the response will be much faster and approach that of hydrazine.

Summary: Based on the threshold and optimum requirements, candidate systems will be ranked relative to these criteria and selected

3.2 Task 1 Subscale Laboratory Characterization and Evaluation:

3.2.1 Candidate Materials/Eliminated Compounds

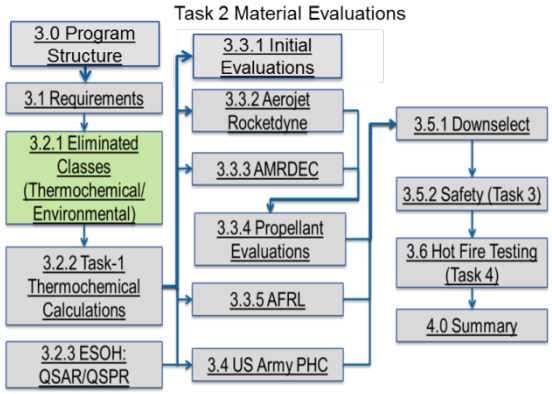

During the course of 4 years, over 70 possible material candidates have been evaluated as possible hydrazine replacements at AMRDEC, AFRL and AR. All materials evaluated have been summarized in Table 3.2-1. Given the numerous chemical structures and overlapping identities structures were provided with a nomenclature (code) and documented with both this code, reference number and the compound name for clarity. Families of materials evaluated included cations of triazoles, tetrazoles, pyrimidiums, imidzoles, and hydrazides, and anions of perchlorates, dinitramides and nitrates. Multiple families of compounds were eliminated during initial literature evaluations prior to thermochemical and synthesis evaluations. Families eliminated included perchlorates (due to water solubility and environmental impacts) and dinitramides (due to low temperature exotherm). Perchlorates and dinitramides are not included in Table 3.2-1 due to early elimination. For all materials considered in Task 1 please refer to appendix A.

Table 3.2-1 Summary of EILs Evaluated in Task 1

Ref #	Compound Code	Chemical Name	Molecular Formula	Molecular Structure	ΔH_f [kcal/mole]	Density [g/cm^3]
1	M123TN1	1-methyl-3H-1,2,3-triazolium nitrate	$C_3H_6N_4O_3$	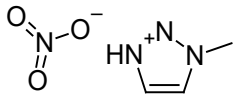	-5	1.44
2	HM124TN2	1 methyl-3 hydroxylmethy l 4-H-1,2,4 triazolium nitrate	$C_4H_7N_4O_4$	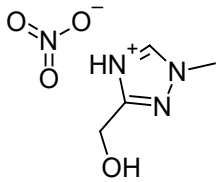	-90	1.53
3	124TN3	1-methyl-4-H-1,2,4 triazolium nitrate	$C_3H_6N_4O_3$	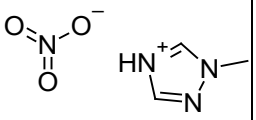	-27	1.44
4	HE124TN4	1-hydroxyethyl-4-H-1,2,4 triazolium nitrate	$C_4H_8N_4O_4$	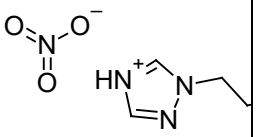	-86	1.45
5	HEK123TN5	1-H-5 hydrazinium-1,2,4 triazolium nitrate	$C_3H_7N_7O_4$	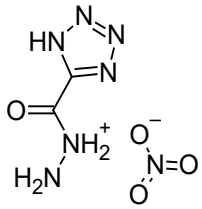	-80	1.70
6	A124TN6	1-H-3-amino-4-H-1,2,4 triazolium nitrate	$C_2H_5N_5O_3$	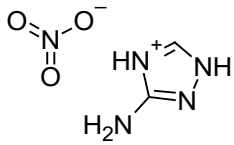	-41	1.60
7	DA124TN7	1-H-3,5-diamino-4-H-1,2,4 triazolium nitrate	$C_2H_6N_6O_3$	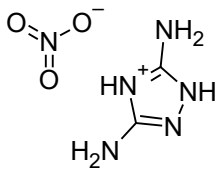	-56	1.64

8	A1234TN8	1H,4H,5-amino-1,2,3,4 tetrazolium nitrate	$C_1H_4N_6O_3$		-7	1.74
9	DA124TN9	1H-3,4-diamino-1,2,4-triazolium	$C_2H_6N_6O_3$		-11	1.60
10	A124TN10	1H-4-amino-1,2,4 triazolium nitrate	$C_2H_4N_5O_3$		0	1.65
11	MA1234TN11	1-methyl-4H-5amino1,2,3,4 tetrazolium nitrate	$C_2H_6N_6O_3$		-12	1.64
12	DA123TN12	1,3-diamino-1,2,3 triazolium nitrate	$C_2H_6N_6O_3$		+55	1.71
13	DA124TN13	1,4-diamino-1,2,4-triazolium nitrate	$C_2H_6N_6O_3$		+25	1.71
14	DA13IN14	1,3-diamino-1,3-imidizolium nitrate	$C_3H_7N_5O_3$		0	1.63
15	DHAPN15	1, 2-dihydroxy-3-aminopropane nitrate	$C_3H_{10}N_2O_5$		-180	1.43

16	MAPDW16	3-methylammonium-1, 2-propanediol nitrate	$C_4H_{12}N_2O_5$		-185	1.24
17	DMAPDW17	3-Dimethylammonium-1, 2-propanediol nitrate	$C_5H_{14}N_2O_5$		-190	1.15
18	DEAPDN18	3-Diethylammonium-1, 2-propanediol nitrate	$C_7H_{18}N_2O_5$		-200	1.12
19	MGAN19	*N*-methyl-D-glucammonim nitrate	$C_7H_{17}N_2O_8$		-350	1.52
20	MPPDN20	3-Morpholinium-1, 2-propanediol nitrate	$C_7H_{17}N_3O_6$		-270	1.36
21	AMPPN21	1-Amino-4-methylpiperazinium nitrate	$C_5H_{13}N_4O_3$		-50	1.31
22	MPPN22	1-methyl-piperazinium nitrate	$C_5H_{14}N_3O_3$		-75	1.25

23	DM124TN23	1,4-Dimethyl-1,2,4-triazolium Nitrate	$C_4H_8N_4O_3$		-30	1.36
24	AM1234TN24	5-amino-1-methyltetrazolium Nitrate	$C_2H_6N_6O_3$		-10	1.56
25	CIN124T25	1,2,4-Triazole-1-carboximidamidimium Nitrate	$C_3H_6N_6O_3$		-65	1.65
26	HEA124TN26	1-(2-hydroxyethyl)-4-amino-1,2,4-triazolium nitrate	$C_4H_9N_5O_4$		-75	1.47
27	HEAHM124TN27	1-(2-hydroxyethyl)-4-amino-3, 5-hydroxymethyl 1,2,4-triazolium nitrate	$C_6H_{13}N_5O_6$		-185	1.57
28	AHM124TN28	4-amino-3, 5-hydroxymethyl 1,2,4-triazolium nitrate	$C_4H_9N_5O_5$		-110	1.69
29	HM124TN29	1,4-di-H-3, 5-hydroxymethyl 1,2,4,triazolium nitrate	$C_4H_8N_4O_5$		-140	1.70

30	MA123TN30	1-amino-3-methyl 1,2,3-triazolium nitrate	$C_3H_7N_5O_3$		35	1.57
31	HEA123TN31	1-amino-3-(2-hydroxyethyl) 1,2,3-triazolium nitrate	$C_4H_9N_5O_4$		-30	1.53
32	N/A	carbohydrazide	$C_1H_6N_4O_1$			1.34
33	CDN	carbohydrazinium nitrate	$C_1H_7N_5O_4$		NL	
34	HEHN	2-hydroxyethylhydrazinium nitrate	$C_2H_9N_3O_4$		-98	1.43
35	HEH	2-hydroxyethylhydrazine	$C_2H_8N_2O_1$		NL	1.12
37	MA124TN33	1-methyl-4-amino-1,2,4-triazolium nitrate	$C_3H_6N_3O_4$		13.8	1.60
38	DA124TN32	3,4-diamino-1,2,4-triazolium nitrate	$C_3H_7N_6O_3$		-11	1.60
39	A123TN34	1-amino-1,2,3-triazolium nitrate	$C_2H_4N_5O_3$		NL	NL

40	MA123TN	3-methyl-1-amino-1,2,3-triazolium nitrate	$C_2H_5N_5O_3$		35	1.57
41	TAPYRN	1-H-2,4,6-triamino pyrimidium nitrate	$C_2H_5N_6O_3$		NL	NL
42	EMIMN	Ethyl methyl imidazolium nitrate	$C_3H_5N_5O_3$		NL	NL
43	BHIMN	Bis hydroxyl imidazolium nitrate	$C_3H_5N_5O_3$		NL	NL
44	1HE4ATN	1-hydroxyethyl-4-amino-1,2,4-triazolium nitrate	$C_4H_9N_5O_4$		NL	NL
45	AM124TN	4-amino-1,2,4-triazolium nitrate	$C_2H_5N_5O_3$		-20	1.60
46	HAM124TN	1-H-3-amino-1,2,4-triazolium nitrate	$C_3H_6N_4O_3$		-27	1.44
48	HD124TN	1-H-3,5-diamino-1,2,4-triazolium nitrate	$C_2H_6N_6O_3$		-56	1.64

49	3A124TN	3-amino-1,2,4-triazolium nitrate	$C_2H_5N_5O_3$	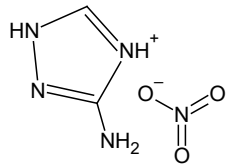	-41	1.60
50	4M5ATN	4-methyl-5-amino-1,2,3,4-tetrazolium nitrate	$C_2H_6N_6O_3$	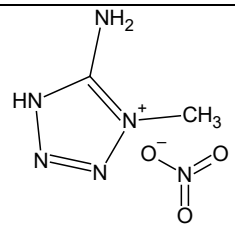	NL	NL
51	13BHIN	1,3-bis-hydroxylimidazolium nitrate	$C_3H_5N_3O_5$	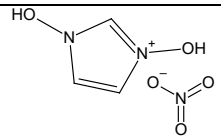	NL	NL

3.2.2 Theoretical Performance Calculations

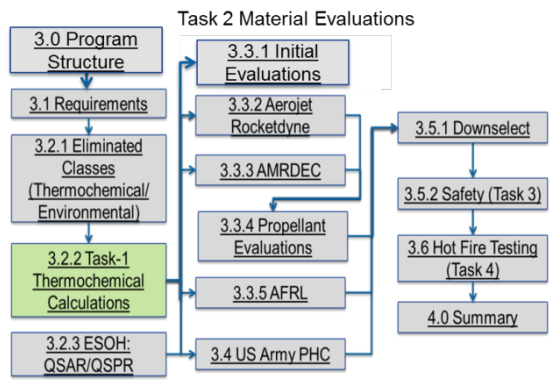

Initial thermochemical analyses on the ionic liquids were performed to assess and identify trends in performance. For this, all ionic liquids were initially run in a parametric fashion. The molecular formula, heat of formation and density were the inputs for the thermochemical program. The wt% of water, HAN and the ionic liquid were parametrically varied according to the input deck shown in Appendix B. Then, the I_{sp} and Flame Temperature were determined at each condition, for each ionic liquid. These data were imported into an excel spreadsheet in order to assess initial trends and ionic liquid viability. From here, the data was regressed in order to quantify the effects of molar atomic composition and heat of formation of each ionic liquid on the resultant I_{sp} and flame temperature.

At each condition, the moles of carbon, hydrogen, nitrogen and oxygen were determined based on the molar composition of the propellant. Additionally the heat of formation of the ionic liquid was calculated at each condition by multiplying the number of moles of the ionic liquid by its standard heat of formation. These variables were the primary set of data that were used for the regression analysis. Table 3.2-2 shows all the parameters that were used in the regression and the rationale behind their inclusion. These 5 sets of data were incorporated in the regression analysis to assess their effects on the I_{sp} and flame temperature of the resultant propellant. The initial fit of the regression was only fair, and the identified outliers from the regression were looked at, culled if necessary, and the regression was rerun.

Table 3.2-2 Regression independent variable predictors

Variable	**Rationale for Inclusion**
Moles of Hydrogen	Molar thermodynamics
Moles of Oxygen	Molar thermodynamics
Moles of Nitrogen	Molar thermodynamics
Moles of Carbon	Molar thermodynamics
Standard Enthalpy of formation	Molar thermodynamics
Moles of Oxygen to Moles of Carbon	Air to fuel ratio
Moles of HAN to Moles of Ionic Liquid	Used to resolve differences in molecular weight
Moles of Water	Used in thermochemical program
Moles of HAN	Used in thermochemical program
Moles of Ionic Liquid	Used in thermochemical program

The residual plots for the flame temperature regression are shown in Figure 3.2-1 and the regression equation is equation 1. the "Normal Probability Plot" shows a group of non-normality at the lower left side of the graph, but good agreement everywhere else. The "Versus Fits" plot displays a section of concentrated occurrences flanked by outliers on both sides of the concentration. The "Histogram" shows that the residuals are roughly normally distributed, while the very condensed "Versus Order" plot shows the sinusoidal behavior of the values of the residuals. If expanded and examined, the "Versus Order" plot would show that the period of the sinusoid corresponds to the end of a run (Appendix B, Table 1) for an ionic liquid.

The regression equation for flame temperature shows that the individual molar values of Carbon, Hydrogen, Nitrogen and Oxygen were not good at determining the flame temperature. The identified variables were: moles of water, moles of HAN, Moles of HAN/Moles of Ionic Liquid, oxygen to carbon ratio, and the heat of formation.

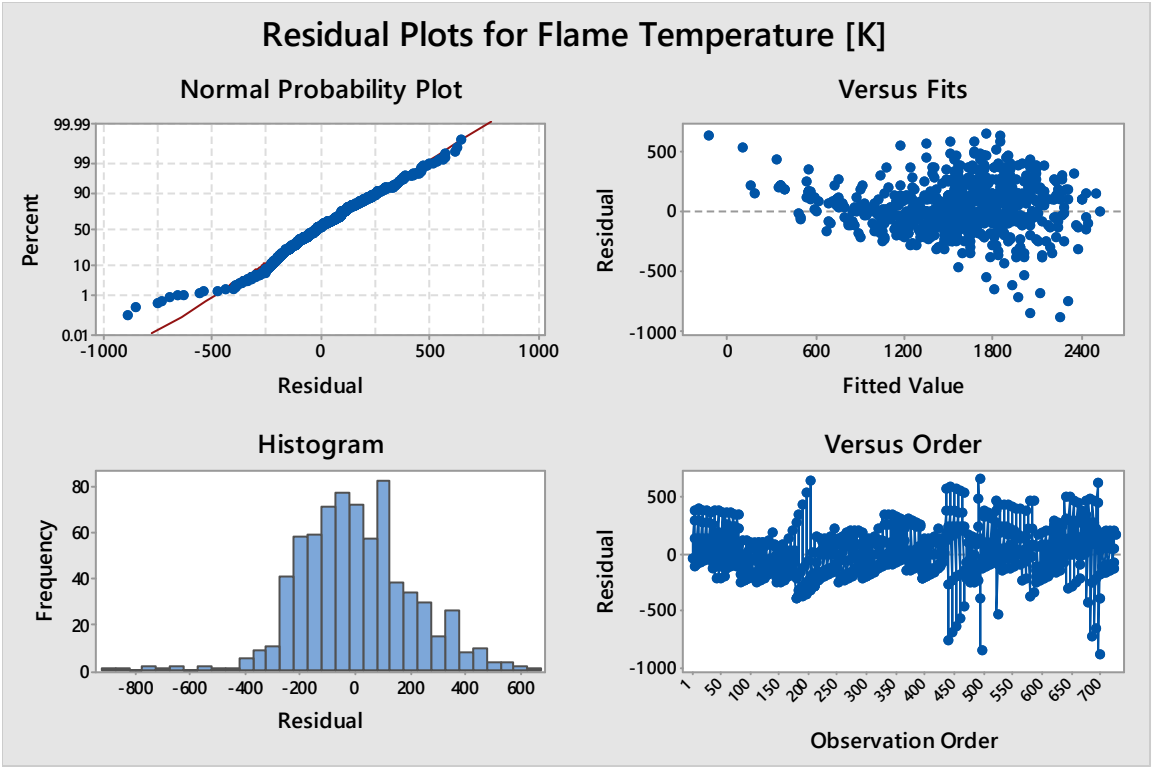

Figure 3.2-1 Final Minitab Regression Equation for Flame Temperature

Tc, K = 3694.2 - 833.6 mol water - 1620 mol han - 9.57 Mol Han/Mol IL - 5.498 O/C Ratio + 9.234 Hf [kcal]

Equation 1: *Minitab Regression Equation for Flame Temperature*

The residual plots for the Isp regression are shown in Figure 3.2-2 and the regression equation is equation 2. The "Normal Probability Plot" shows a group of non-normality at the lower left side and upper right side of the graph, but good agreement everywhere else. The "Versus Fits" plot displays a section of concentrated occurrences flanked by outliers on both sides of the concentration similar to the versus fits plot for flame temperature. The "Histogram" shows that the residuals are normally distributed, while the very condensed "Versus Order" plot shows the sinusoidal behavior of the values of the residuals. If expanded and examined, the "Versus Order" plot would show that the period of the sinusoid corresponds to the end of a run (Appendix A) for an ionic liquid.

The regression equation for Isp shows that the individual molar values of Carbon, Hydrogen, Nitrogen and Oxygen were good at determining the flame temperature. The identified variables were: moles of water, moles of HAN, Moles of HAN/Moles of Ionic Liquid, oxygen to carbon ratio, the heat of formation, and individual molar values.

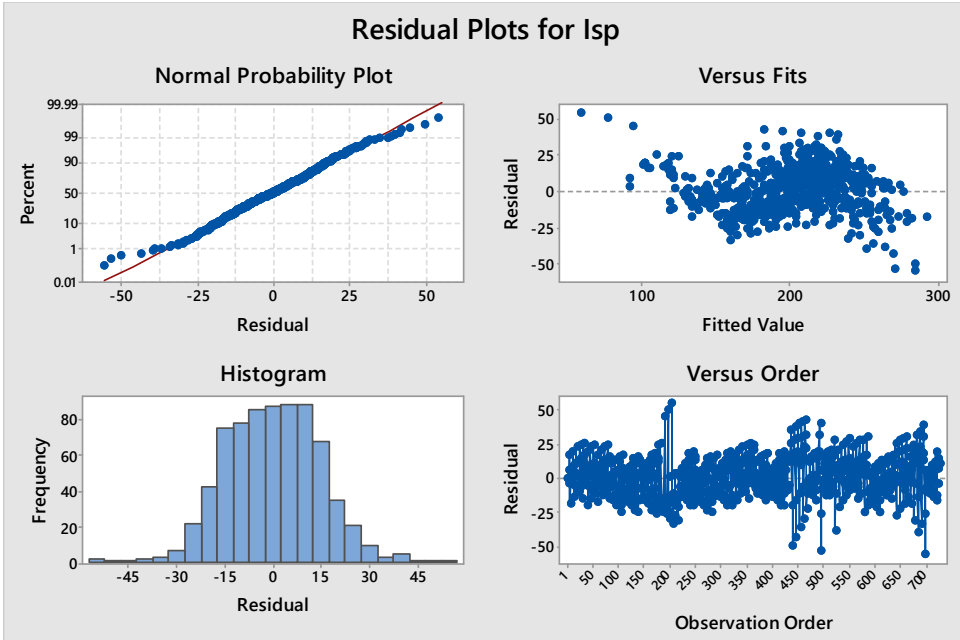

Figure 3.2-2 Final Minitab Regression Residuals for Isp

Isp = 5.63 mol water + 221.71 mol han + 45.11 mol C + 14.05 mol H + 26.18 mol N
+ 86.89 mol O
+ 1.384 Hf [kcal] - 0.8803 Mol Han/Mol IL - 0.4817 O/C Ratio

Equation 2: *Minitab Regression Equation for Isp*

Global Evaluation of Compounds

Solver Method:

After the regressions were run, and the fit was determined to be sufficient, the Identified variables and each ionic liquid were put through a solver method to maximize Isp while keeping the flame temperature at or below 1450 K. The regression equations were used to determine the Isp and flame temperature of each ionic liquid propellant The solver method would make use of the Excel add-in Solver package for data analysis. The selected solving method was GRG Nonlinear, and the total sum of all Isp for all ionic liquids was set to be maximized. The wt % composition of water, HAN and ionic liquid were set to change in order to solve the equations. In almost all instances, the equation was solved to a flame temperature of 1450 K. From here a visual inspection of the results was used to determine which kind of molecule (moles of each species) produced the most optimal results.

Table 3.2-3 Solver Methods Results by Ionic Liquid

Ionic Liquid	Isp $\left[\frac{lb_f\, s}{in^3}\right]$	Ivol $\left[\frac{lb_f\, s}{lb_m}\right]$
HM124TN2	194.77	10.69
124TN3	194.04	10.61
HEK1234TN5	193.05	10.76
A124TN6	192.13	10.61
DA124TN7	193.35	10.70
A1234TN8	188.20	10.54
DA124TN9	192.27	10.62
A124TN10	190.46	10.59
MA1234TN11	192.29	10.67
DA13IN14	194.02	10.77
AHM124TN28	194.21	10.82
AM1234TN24	192.25	10.58
AMppN21	201.15	10.83
CIN124T25	194.73	10.79
DEAPDN18	208.23	10.80
DHA PN15	197.44	10.68
DMAPDN17	203.23	10.63
HEA123TN31	194.61	10.71
HEA124N26	195.76	10.68
HEA124N27	198.00	10.87
HEHN	188.92	10.13
HM124TN29	194.34	10.84
MAPDN16	200.48	10.61
MA123TN30	193.29	10.69
MGAN19	203.56	11.02
Mp PDN20	208.72	10.97
MPp N22	204.42	10.93
DA124TN13	191.60	10.70
Carbohydrazide	204.12	10.75
MA124TN33	200.18	10.93
AM124TN	191.96	10.61
HAM124TN	194.94	10.65
HD124TN	188.35	10.44
3A124TN	190.70	10.54
	Mean	10.70
	Median	10.69
	Standard Deviation	0.16

A picture of a portion of one of the excel spreadsheets used in the analyses is shown in Figure 3.2-3. The purpose of this figure is to help identify the effects of the ionic liquid molecular formula, molecular weight and heat of formation on the Isp from the solver method. In most cases, excluding outliers and carbohydrazide, the following was determined to be the ideal archetype for an ionic liquid candidate (listed items are per mole of ionic liquid):

- 4 or more carbon atoms
- 9 or more hydrogen atoms

- 4 or fewer nitrogen atoms
- 4 or more oxygen atoms
- High molecular weight
- Highly negative heat of formation

	Moles of Species						
Ionic Liquid	C	H	N	O	MW	Hf [kcal]	Isp
M123TN1	3	6	4	3	146	-5	193.52
HM124TN2	4	7	4	4	175	-90	194.77
124TN3	3	6	4	3	146	-27	194.04
HEK1234TN5	3	7	7	4	205	-80	193.05
A124TN6	2	5	5	3	147	-41	192.13
DA124TN7	2	6	6	3	162	-56	193.35
A1234TN8	1	4	6	3	148	-7	188.20
DA124TN9	2	6	6	3	162	-11	192.27
A124TN10	2	4	5	3	146	0	190.46
MA1234TN11	2	6	6	3	162	-12	192.29
DA13IN14	3	7	5	3	161	0	194.02
AHM124TN28	4	9	5	5	207	-110	194.21
AM1234TN24	2	6	6	3	162	-10	192.25
AMppN21	3	13	4	3	153	-50	201.15
CIN124T25	3	6	6	3	174	-65	194.73
DEAPDN18	7	18	2	5	210	-200	208.23
DHA PN15	3	10	2	5	154	-180	197.44
DMAPDN17	5	14	2	5	182	-190	203.23
HEA123TN31	4	9	5	4	191	-30	194.61
HEA124N26	4	9	5	4	191	-75	195.76
HEA124N27	6	13	5	6	251	-185	198.00
HEHN	9	2	3	4	216	-10.8	193.32
HM124TN29	4	8	4	5	192	-140	194.34
MAPDN16	4	12	2	5	168	-185	200.48
MA123TN30	3	7	5	3	161	35	193.29
MGAN19	7	17	2	8	257	-350	203.56
Mp PDN20	7	17	3	6	239	-270	208.72
MPp N22	5	14	3	3	164	-75	204.42
DA124TN13	2	6	6	3	162	25	191.60
Carbohydrazide	1	6	4	1	90	-22	204.12
M124TN34	3	7	5	0	161	-175	200.18
AM124TN	2	5	5	3	147	-20	191.96
HAM124TN	3	6	4	3	146	-27	194.94
HD124TN	2	6	6	3	162	-56	188.35
3A124TN	2	5	5	3	147	-41	190.70

Figure 3.2-4 Excel snip of the color coded data trends used for visualization. In all instances, red indicates a larger magnitude value, while green indicates a smaller magnitude value

The above analysis allowed for the downselect of candidates that met both performance and flame temperature goals for program effort. Promising candidates included but not limited to 1-methyl-4-amino-1,2,4-triazolium nitrate (MA124TN34 ref 36), Carbohydrazinium nitrate (CDN, ref 33), 1,2-dihydroxy-3-aminopropane nitrate(DHAPN15, ref 15), 3-methylammonium-1,2-propanediol nitrate (MAPDW16, ref 16) and 1-amino-4-methyl piperazinium nitrate (AMPPN21, ref 21).

3.2.3 ESOH screening: QSAR/ QSPR Software Models Case Study

In addition to the thermochemical calculations described above, environmental evaluations were conducted at the University of Delaware in order to begin understanding the environmental benefits of EILs. Under the direction of Professor Dom Di Toro, the University of Delaware team used Abraham poly-parameter linear free energy (pp-LFER) models to predict thermodynamic properties related to the fate and transport of a selection of energetic ionic liquids (EILs). These predictions were based on existing Abraham solute descriptors (E, S, A, B, V) for the neutralized form of the EIL cations with applied empirical corrections for both the cation charge effect as well as the effect of the counter anion (NO_3-). These corrections were based on a training set of octanol-water partition coefficients for structurally similar ionic liquid (IL) compounds. However, empirical corrections could not be made for the remaining thermodynamic properties, since similar training sets were not available. Consequently, relative predictions for the remaining thermodynamic properties were obtained, with absolute prediction values requiring further calibration with additional training sets.

Estimating Physical Chemical Parameters of Energetic Ionic Liquid (EIL) Ion-Pairs Experimental Data – Imidazolium & pyridinium-based ILs

While experimental data for energetic ionic liquids is sparse, data for similarly-structured ionic liquids (i.e., imidazolium- and pyridinium-based ionic liquids) are not. Significant experimental data for aqueous solubility, octanol-water partition coefficients, hydrophobicity, activated carbon-water, soil-water partition coefficients, and toxicity exist for these classes of ILs. A summary of significant sources of experimental data is shown in the table below.

Table 3.2.4. Summary of Experimental Ionic Liquid (IL) Data.

Parameter	Ionic Liquids[a,b]	N	Notes	Reference
K_{ow}	Im, Py	67		Lee, Lin (2013)
K_{ow}	Im, Py	46		Cho et. al (2011)
S_w	Im, Py	37		Cho et. al (2011)
K_{GAC}, K_{oc}	Im	16, 3		Jungnickel et. al (2011)
EC_{50}	Im, Py	50	ACheI, vibrio fischeri, E coli, lemna minor, daphnia magna	Pham, Cho (2009)

[a]Imidazolium-based (Im), [b]Pyridinium-based (Py)

Energetic Ionic Liquids (EILs)

For this study 10 EILs and 3 neutral reference energetic compounds were selected. The table below summarizes the various EILs and their structural composition.

Table 3.2.5. List of Energetic Ionic Liquids and Reference Compounds to be Studied.

No	Energetic Ionic Liquids
1	Ammonium Nitrate
2	Hydrazinium Nitrate (HN)

3	HydroxyEthylHydrazinium Nitrate
4	4-Amino-1,2,4-Triazolium Nitrate
5	***4-Amino-1-Methyl-1,2,4-Triazolium Nitrate[1]***
6	Guanidinium Nitrate
7	MonoAmino-Guanidinium Nitrate
8	1-Hydroxyethan-1,2,4-Triazolium Nitrate
9	1-amino-1,2,3-triazolium Nitrate
	Reference Compounds
1	***Hydrazine[2]***
2	5-Amino-Tetrazole
3	3-Nitro-1,2,4-Triaminotriazol-5-One

[1]Aerojet Rocketdyne selected EIL compound, [2]Primary reference compound

Physical Chemical Parameters

The following thermodynamic properties were generated in order to estimate the extent of toxicity, fate and transport of candidate EIL compounds (Table 3.2.6):

Table 3.2.6. List of Physical Chemical Parameters to be Estimated for the Energetic Ionic Liquid (EIL) Compounds.

Parameter	Description	Significance
S_w	Water solubility	This parameter is used to calculate the soil saturation limit for single hazardous substances
K_{aw}	Henry's law constant	This parameter is used to calculate the volatility of a compound
p/po|l	Vapor pressure (liquid)	This parameter examines the pure liquid phase and will impact inhalation and eye irritation
K_{oc}	Affinity to organic carbon (sorption)	This parameter is useful in predicting the mobility of organic soil contaminants
K_{ow}	Lipid solubility (octanol/water coefficient)	This parameter is a relative indicator of the tendency of an organic compound to adsorb to soil and living organisms

The relative trends for each EIL and reference compound are shown in Table 3.2.7. The red/green highlight indicates whether the compound had a better parameter value than hydrazine (green) or worse (red). The magnitude values are also shown to provide resolution between compounds with the same highlight color.

Table 3.2.7. Stop/Go schemed table for compound parameters relative to hydrazine

	Parameter				
Energetic Ionic Liquids	$\log S_w$	$\log K_{aw}$	$p/p_o\|_l$	$\log K_{oc}$	$\log K_{ow}$
Ammonium Nitrate	2.25	3.2	0.5	1.05	-6.2
Hydrazinium Nitrate (HN)	2.6	7	-3	0.85	-7
HydroxyEthylHydrazinium Nitrate	2.05	9.2	-5.9	0.8	-7.1
4-Amino-1,2,4-Triazolium Nitrate	2	7.9	-4.5	1.5	-6.5
4-Amino-1-Methyl-1,2,4-Triazolium Nitrate [1]	0.75	6	-4	1.95	-5.2
Guanidinium Nitrate	1.7	7.2	-4.3	1.25	-6.35
MonoAmino-Guanidinium Nitrate	1.75	10.9	-7.6	0.75	-7.8
1-Hydroxyethan-1,2,4-Triazolium Nitrate	0.25	7	-5.5	2.2	-5
1-amino-1,2,3-triazolium Nitrate	1.9	7.3	-4.2	1.5	-6.4
Reference Compounds					
Hydrazine [2]	2.6	7	-3	0.85	-2.1
5-Amino-Tetrazole	1.8	11.8	-7.2	1.05	-2.05
3-Nitro-1,2,4-Triaminotriazol-5-One	1.78	9.8	-6.3	1.4	-1.9

Summary/Lessons Learned

While absolute predictions of the remaining thermodynamic properties cannot be made without additional calibration, the pp-LFER models have been demonstrated to correctly rank the training set ILs as well as the energetic compounds of interest. These estimates of the thermodynamic parameters for the candidate EIL compounds can be used to down select ideal compounds for further testing as well as formulation development as outlined in the scope of work for the project.

It is clear that the nitrate-containing EILs follow similar trends for the thermodynamic properties discussed above ($\log K_{ow}$, $\log K_{aw}$, $\log K_{oc}$). This suggests that for the properties of the tight ion pair, selection of an EIL with a low vapor pressure (relative to hydrazine), will not preclude the selection of an EIL compound with low lipophilicity ($\log K_{ow}$), low affinity for sorption onto organic carbon / soil ($\log K_{oc}$), or low fugacity when dissolved in an aqueous phase ($\log K_{aw}$). Further, the low vapor pressures and Henry's law constants computed by EPI suite for the nitrate-containing EILs is consistent with low vapor pressures observed for other IL salts and ionic species in general. Finally, the ability of the Abraham pp-LFER to accurately rank the imidazolium and pyridinium-based ILs in the training set strongly suggests the applicability of the method for the structurally similar energetic compounds and their counter-ions. However, further work is necessary to more accurately determine the appropriate anion fragment values for 5-aminotetrazolate (5AT) and NTO in octanol –water as well as N anion fragment values for the remaining physical chemical parameters, in order to accurately determine the magnitudes of the EILs, relative to the reference compounds for the remaining thermodynamic properties.

3.3 Task 2 Scale-up/Subscale Screening:

3.3.1 Initial Laboratory Results

Syntheses of promising candidates were conducted at AMRDEC and Aerojet Rocketdyne under the direction of Dr. Gregory Drake. Compounds synthesized at Aerojet Rocketdyne were limited and only included synthesis routes being with commercially available precursors and simple synthesis, while synthesis requiring higher skill sets were conducted at AMRDEC. All materials evaluated are summarized below in Table 3.3-1. Each material is color coded green, red and yellow which represents if the material was deemed acceptable to go forward in Task 3or eliminated from further consideration. Desired results included thermal stability of <2% weight loss after 48 hours at 75ºC, less than 3 synthesis steps, melting point of <40ºC, decomposition temperature of >150ºC and performance ≥ hydrazine. A specific metric for water solubility was not determined. Acceptable solubility was determined by preparing 50:50 solutions at ambient temperature and then samples were cooled to determine if candidate stayed in solution.

Table 3.3-1 Summary of Task 2 Material Candidates.

Ref #	Compound Code	Chemical Name	Location	Material Status
1	M123TN1	1-methyl-3H-1,2,3-triazolium nitrate	AMRDEC	Poor Thermal Stability
2	HM124TN2	1 methyl-3 hydroxylmethyl 4-H-1,2,4 triazolium nitrate	AMRDEC	Poor thermal stability
3	124TN3	1-methyl-4-H-1,2,4 triazolium nitrate	AMRDEC	Poor thermal stability
5	HEK123TN5	1-H-5 hydrazinium-1,2,4 triazolium nitrate	AMRDEC	High Melting Point
6	A124TN6	1-H-3-amino-4-H-1,2,4 triazolium nitrate	AMRDEC	Poor Solubility in water
9	DA124TN9	1H-3,4-diamino-1,2,4-triazolium	AMRDEC	Eliminated due to discoloration and aging concerns
11	MA1234TN11	1-methyl-4H-5amino1,2,3,4 tetrazolium nitrate	AMRDEC	Poor Solubility in water
12	DA123TN12	1,3-diamino-1,2,3 triazolium nitrate	AMRDEC	Poor Thermal Stability
13	DA124TN13	1,4-diamino-1,2,4-triazolium nitrate	AMRDEC	Good Thermal Stability
14	DA13IN14	1,3-diamino-1,3-imidizolium nitrate	AMRDEC	Poor Performance
15	DHAPN15	1, 2-dihydroxy-3-aminopropane nitrate	AMRDEC	Concern with reactivity
16	MAPDW16	3-methylammonium-1, 2-propanediol nitrate	AMRDEC	Catalytic Ignition Concerns with S405
17	DMAPDW17	3-Dimethylammonium-1, 2-propanediol nitrate	AMRDEC	Catalytic Ignition Concerns with S405
18	DEAPDN18	3-Diethylammonium-1, 2-propanediol nitrate	AMRDEC	Catalytic Ignition Concerns with S405

19	MGAN19	*N*-methyl-D-glucammonim nitrate	AMRDEC	Catalytic Ignition Concerns with S405
20	MPPDN20	3-Morpholinium-1, 2-propanediol nitrate	AMRDEC	Catalytic Ignition Concerns with S405
21	AMPPN21	1-Amino-4-methylpiperazinium nitrate	AMRDEC	Catalytic Ignition Concerns with S405
22	MPPN22	1-methyl-piperazinium nitrate	AMRDEC	Catalytic Ignition Concerns with S405
23	DM124TN23	1,4-Dimethyl-1,2,4-triazolium Nitrate	AMRDEC	Low reactivity with S405 but good thermal stability
24	AM1234TN24	5-amino-1-methyltetrazolium Nitrate	AMRDEC	Synthesis Issues
25	CIN124T25	1,2,4-Triazole-1-carboximidamidimium Nitrate	AMRDEC	Poor Performance
30	MA123TN30	1-amino-3-methyl 1,2,3-triazolium nitrate	AMRDEC	Synthesis Issues
31	HEA123TN31	1-amino-3-(2-hydroxyethyl) 1,2,3-triazolium nitrate	AMRDEC	Synthesis Issues
33	CDN	Carbohydrazinium nitrate	Aerojet Rocketdyne	Downselected-Acceptable hazards and thermal stability
34	HEHN	2-hydroxyethylhydrazinium nitrate	AFRL	Downselected-Acceptable Thermal Stability and Historical Experience
37	MA124TN33	1-methyl-4-amino-1,2,4-triazolium nitrate	Aerojet Rocketdyne	Downselected-Acceptable hazards and thermal stability

38	DA124TN32	3,4-diamino-1,2,4-triazolium nitrate	AMRDEC	High MP, purification issues and poor thermal stability
39	A123TN34	1-amino-1,2,3-triazolium nitrate	Aerojet Rocketdyne	Poor Thermal Stability
40	MA123TN	3-methyl-1-amino-1,2,3-triazolium nitrate	Aerojet Rocketdyne	Synthesis issue and poor thermal stability
41	TAPYRN	1-H-2,4,6-triamino pyrimidium nitrate	AMRDEC	High Melting Point (255C)
42	EMIMN	Ethyl methyl imidazolium nitrate	AMRDEC	Poor Performance and low solubility in AN
43	BHIMN	Bis hydroxyl imidazolium nitrate	AMRDEC	Poor Performance
44	1HE4ATN	1-hydroxyethyl-4-amino-1,2,4-triazolium nitrate	AMRDEC	Good thermal stability
45	AM124TN	4-amino-1,2,4-triazolium nitrate	Aerojet Rocketdyne	Good MP but poor weight loss
46	HAM124TN	1-H-3-amino-1,2,4-triazolium nitrate	AMRDEC	High Melting Point
48	HD124TN	1-H-3,5-diamino-1,2,4-triazolium nitrate	AMRDEC	Mod High Melting Point and Low solubility in water
49	3A124TN	3-amino-1,2,4-triazolium nitrate	AMRDEC	High Melting Point and not liquid with water at room temperature
50	4M5ATN	4-methyl-5-amino-1,2,3,4-tetrazolium nitrate	AMRDEC	Low solubility in water

51	13BHN	1,3-bis-hydroxylimidazolium nitrate	ARFL	Poor hazards

3.3.2 Aerojet Rocketdyne Synthesis Efforts

Small quantities (1-10 grams) of candidate materials that were produced in Redmond for sensitivity evaluations included 1,4-dimethyl-1,2,4-triazolium iodide, 4-amino-1,2,4-triazolium nitrate (AM124TN, Ref 45), 1-methyl-4-amino-1,2,4 triazolium nitrate (MA124TN33, Ref 37) , 1-amino-1,2,3-triazolium nitrate (A123TN34, Ref 39) and 3-methyl-1-amino-1,2,3-triazolium nitrate (MA123TN, Ref 40).

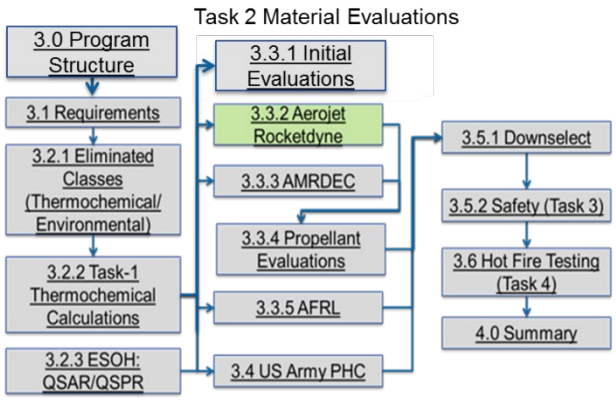

1,4-dimethyl-1,2,4-triazolium iodide was obtained from commercial sources (Aldrich) and converted to the nitrate by ion exchange per H Xue et al. (Shreeve) (Chem. Mater., 2005, 17, 191-198.)

4-amino-1,2,4-triazolium nitrate (A124TN, Ref 45) was prepared from commercially obtained 4-amino-1,2,4 triazole per Drake (G. W. Drake, et. al, Propellants Explos. Pyrotech. 2003, 28, 174 - 180). 4-amino-1,2,4-triazole was dissolved in methanol; concentrated HNO_3 was slowly added to a 1:1 stoichiometric ratio. Precipitate was isolated by filtration and recrystallized twice with methanol and diethyl ether. The white salt obtained melted at 60-63 ºC, and the onset of decomposition onset occurred at ~200 ºC, both consistent with Drake's report (60 ºC and 190 ºC respectively).

1-methyl-4-amino-1,2,4 triazolium nitrate (MA124TN33, Ref 37) was prepared using commercially obtained 4-amino-1,2,4 triazole which was converted to 1-methyl-4-amino-1,2,4 triazolium nitrate (MA124TN33, Ref 37) using the procedure described by G Drake et al., AFRL-PR-ED-TP-2003-033. Commercial 4-amino-1,2,4-triazole was dissolved in isopropyl alcohol; methyl iodide was added in excess and the reaction was allowed to proceed under darkness for days. The white precipitate was collected (1-methyl-4-amino-1,2,4-triazolium iodide) by filtration and characterized by a melting point of 99 ºC (Drake reports mp=98 ºC, Shreeve reports 101 ºC). The iodide salt was washed with IPA and diethyl ether, then dissolved into methanol and an AgNO3 water solution dropwise. An additional 4 hours of stirring was allowed. The AgI precipitate was removed by filtration. The filtrate was then concentrated under rotavapor. The concentrated filtrate was stored in a methanol and diethyl ether mixture and refrigerated, then the yellow oily liquid product was collected. The filtrated was further stripped

of solvent under high vacuum overnight. The melting point was unable to be determined clearly, but it was confirmed that the melting point was below -45 ºC (Drake reports -55-56 ºC, Shreeve -60 ºC).

The two IL nitrate salts 1-amino-1,2,3-triazolium nitrate (A123TN34, Ref 39) and 3-methyl-1-amino-1,2,3-triazolium nitrate (MA123TN, Ref 40) based upon 1,2,3-triazole ring, 1-amino-1,2,3-triazolium nitrate (A123TN34, Ref 39) and 3-methyl-1-amino-1,2,3-triazolium nitrate (MA123TN, Ref 40) were synthesized according to published methods (G. Drake, et al., J. Heterocyclic Chem., 42, 19 (2005) and J. Chem. Cryst., Vol. 37, No. 1, (2007).), and characterized by FT-IR and DSC studies. Glyoxal bishydrazone was prepared according to a modified method published by Dr. Greg Drake. Subsequently, the hydrazone was oxidized with manganese dioxide in acetonitrile to produce 1-amino-1,2,3-triazole (A123TN, Ref 39).

Half of the 1-amino-1,2,3-triazole was then dissolved in acetonitrile and allowed to react with nitric acid. The obtained nitrate salt was a pale pink solid powder. It was not clear the cause for pink discoloration. The discoloration is suspected to be caused by the residue of manganese from previous step or due to the instability of the 1-amino-1,2,3-triazole ring. DSC indicated a melting point of 93°C (literature mp ~ 99 °C) and an onset thermal decomposition temperature of 108°C. It was noted that the relatively low decomposition temperature presents a thermal stability challenge for its propellant formulation.

The other half of 1-amino-1,2,3-triazole was reacted with methyl iodide in acetonitrile to affect methylation. The resulting iodide compound then reacted with $AgNO_3$ in water for 2hr. The filtration of AgI and the subsequent solvent removal produced a white solid. A melting point of 86-88° C (literature: mp ~ 86-88 °C) and an onset decomposition temperature of 185°C were reported for this chemical. DSC indicated that 1-amino-3-methyl-1,2,3-triazolium nitrate is thermally more stable than 1-amino-1,2,3-triazolium nitrate.

3.3.3 AMRDEC Synthesis Evaluations

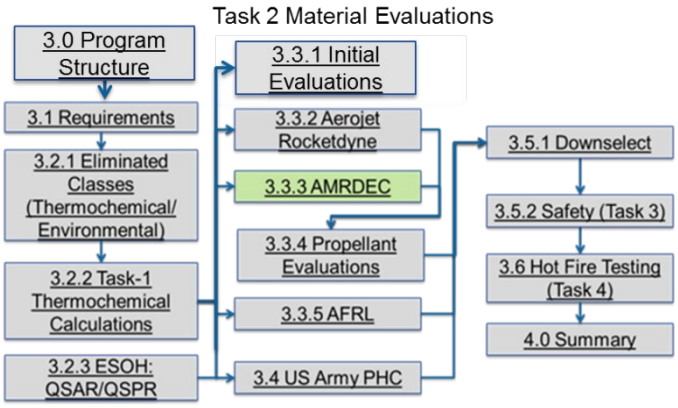

In addition to the above materials, AMRDEC evaluated a number of candidate salts. The salts evaluated included 1, 2-dihydroxy-3-aminopropane (DHAPN15, Ref 15), 3-methylammonium-1, 2-propanediol (MAPDW16, Ref 16), 3-Dimethylammonium-1, 2-propanediol (DMAPDW1, Ref14), 3-Diethylammonium-1, 2-propanediol (DEAPDN18, Ref 18) , 3-Morpholinium-1,2-propanediol (MPPDN20, Ref 20), 1-Amino-4-

methylpiperazine (AMPPN21), and 1-methyl-piperazine (MPPN22). However, the general lack of N-N bonding in these candidates rendered the likelihood of catalytic ignition problematic (as employed in hydrazine systems); these candidates were not further explored.

Target candidates were further refined to include the following design features:

- Active N-NH_2 functionalities
    - Offers best historical evidence for good ignition (an implied similarity to Hydrazine)
    - Good heat of formation
    - Best chance of activity even with high water dilution
- Active Heterocyclic centers
    - 1,2,4- triazoles
    - 1,2,3- triazoles
    - 1,2,3,4-tetrazoles
- Higher nitrogen content
    - Translates to less oxygen (oxidizer) demand
- Higher density
- Initial candidates will remain with nitrate anion (NO_3-)
    - Should limit solubility issues of metathesis in-situ
    - Enhances water solubility

Preliminary candidates that met above requirements are summarized in the figure below.

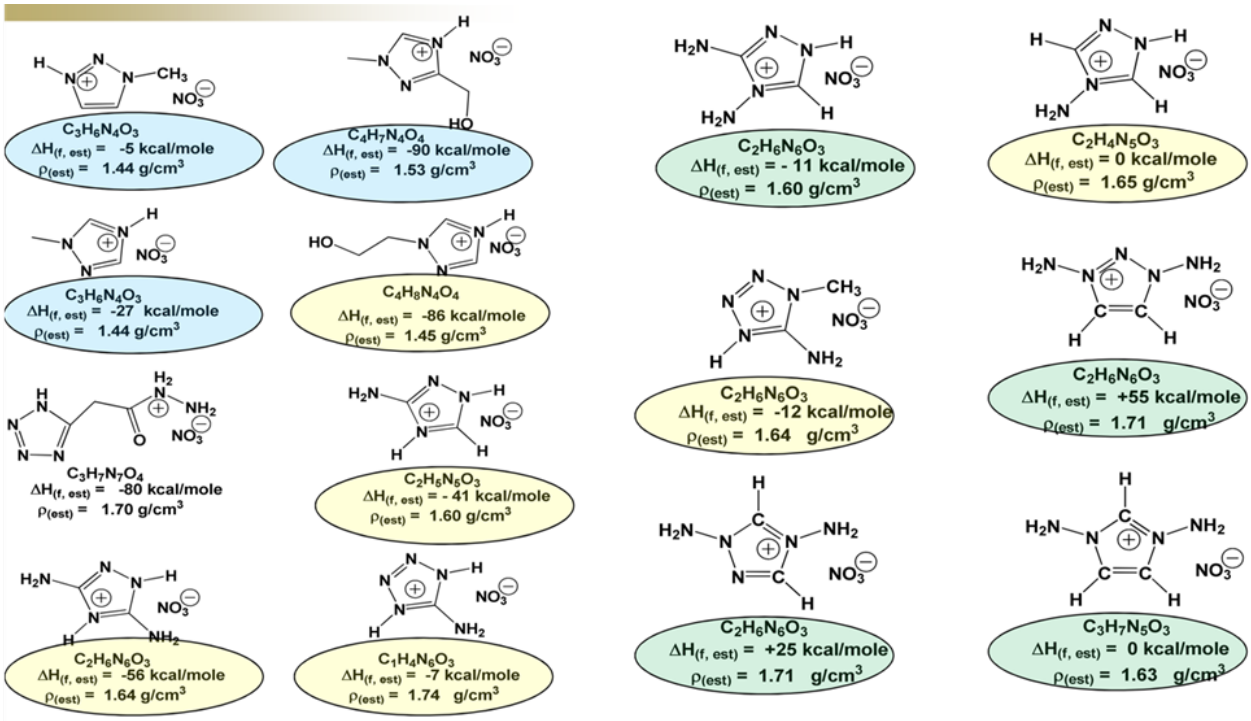

Figure 3.3-1 Overview of promising EILs from Task 2

Of the candidates identified, several materials were down-selected as potential additives for liquid monopropellants, based on reasonable oxygen balance, heat of formation, low impact/friction sensitivity, and thermal stability. Of these 1-H-3-amino-1,2,4-triazolium nitrate (A124TN6, ref 6), 1-H-4-methyl-5-amino-1,2,3,4-tetrazolium nitrate (MA1234TN11, ref 11), 1-H-3,5-diamino-1,2,4-triazolium nitrate (DA124TN7, ref 7), 1,4-dimethyl-1,2,4-triazolium nitrate (DM124TN23, ref 23), and 1-H-2,4,6-triamino-pyrimidinium nitrate (TAPTRN, ref 41), were scaled to multi-gram levels at AMRDEC and transported via DOT shipping container to the Aerojet Rocketdyne Redmond Facility and US Army - Public Health Center (USA-PHC) for further examination. Both A124TN6 and DA124TN23 passed the TGA stability test, losing less than 0.4% mass over 48 hours. The thermal stability of 1-methyl-3-hydroxymethyl-4-H-1,2,4-triazolium nitrate (HM124TN2, ref 2) was deemed unacceptable due to the large mass loss after 48 hours. This can be attributed to the volatility of the parent heterocycles all of which have low melting points and in some case lack basicity of the parent heterocycles.

The scale-up chemistry of 1-amino-3-R- substituted-1,2,3-triazolium salts was halted due to competing side reactions and troublesome silver metathesis reactions, creating impure materials which are essentially impossible to further purify without catastrophic yield losses.

Several N, N'-diamino-1,2,4 azolium materials, though of high interest, were dropped from further consideration in light of literature indications of high impact and/or high friction sensitivity of these highly endothermic salts. Attempts to synthesize some materials for formulation studies were thwarted by troublesome purification or inadequate thermal stability.

3.3.4 AR Initial Propellant Evaluations

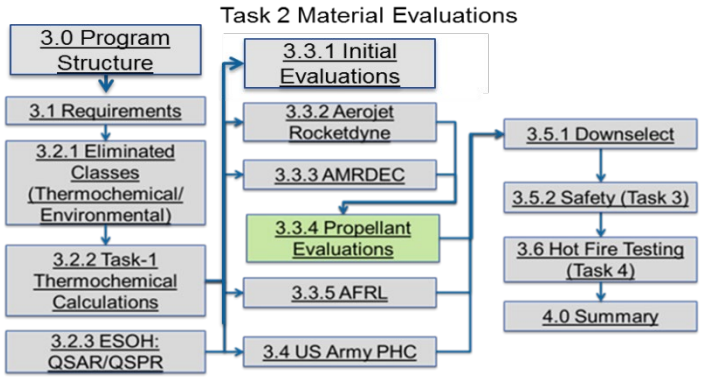

Material candidates synthesized and deemed acceptable (i.e. sensitivity, thermal stability, ect) by AMRDEC were shipped to AR Redmond for formulation development and screening. The materials shipped included 1-H-3-amino-1,2,4-triazolium nitrate, 1-H-3,5-diamino-1,2,4-triazolium nitrate, 1,4-dimethyl-1,2,4-triazolium nitrate, 1-methyl-5-amino-4H-1,2,3-tetrazolium nitrate and 2,4,6-triamino-1H-pyrimindium nitrate. In addition, materials synthesized by AR were also evaluated. Formulation development looked at evaluating HAN and AN as oxidizers while using water as the coolant.

Formulations based on 1-R-4-R'-1,2,4-Triazolium Nitrate (R=NH_2, CH_3; R'=H, CH_3) were produced at the 5 gram level and submitted for small scale laboratory testing. Compositions considered the triazolium salt plus oxidizer (ammonium nitrate or hydroxylammonium nitrate) and

coolant (water). Combustion models (CEA/ArChem) were run to optimize stoichiometry and flame temperature (See thermochemical section). Compositions based on the computed fuel-oxidizer-coolant ratios were subsequently prepared in the laboratory. Room temperature liquids having combustion temperatures within the target range (Tc<1500 K) were prepared for each of these salt systems, and at least 2 compositions were identified with melting points below -23°C with impact hazard testing meeting the goal of E50>20 kg-cm (low sensitivity). The two blends in green are predicted to be capable of meeting program requirements. Preliminary thermal stability testing (weight loss, 48 hours / 75ºC) was encouraging for the 1,2,4 Triazolium nitrates but 1,2,3 Triazolium work was discontinued due to thermal stability concerns.

Table 3.3-2 EILs Propellant Blends Performance

Blends Chemicals	Blend Composition	Density (g/cc)	Tc (K)	Isp (s)	Comments on Exhaust Gas
1-amino-4-methyl-1,2,4 triazolium nitrate:AN:H2O	100%	1.55	1783	268/258	CH4 0.0012: Carbon soot at exit: Water 0.002
	57:43	1.555	2273	247/235	Water: 0.2878
	57:43:20= 44:33:23	1.376	1532	232/222	H2O 0.429
	60:20:20	1.356	1473	236/226	CH4 0.00003; Water 0.29
1-amino-1,2,3 triazolium nitrate:AN:H2O	100%	1.63	2458	280/268	Carbon soot at the exit; Water 0.12; Trace of NH3
	66.7:33.3	1.644	2238	259/249	Water 0.313
	64:36:43= 45:25:30	1.387	1523	224/215	Water: 0.53; Trace NH3
Diluted M315E	77.3:22.7	1.322	1487	223/214	Water: 0.67; Trace NH3

Initial evaluation of AMRDEC candidates used small scale 50:50 mixtures of the AMRDEC energetics with AN oxidizer and probed for formation of low-melting eutectic formation using DSC. The presence of a new endothermic DSC peak at temperatures below the melting point (or structural phase transition in the case of AN) was taken as supportive of eutectic formation. In each mixture containing AN, a disappearance of energetic material melting point was observed. This was interpreted as evidence of some degree of miscibility with AN. New

endotherms at ~125, 20, 110 and 90ºC are suggestive of eutectic formation in the mixtures of AN with 3-amino-1,2,4-triazolium Nitrate (3A124TN, ref 49), 2,4,6-Triamino-Pyrimidium Nitrate (TAPYRN, ref 41), 3,5-diamino-1,2,4-triazolium Nitrate and 1,4-dimethyl-1,2,4-triazolium Nitrate (DM124TN23, ref 23). However, this test did not reveal clear indication of mixture melting points. Additional DSC obtained from the AMRDEC candidates can be found in Appendix D.

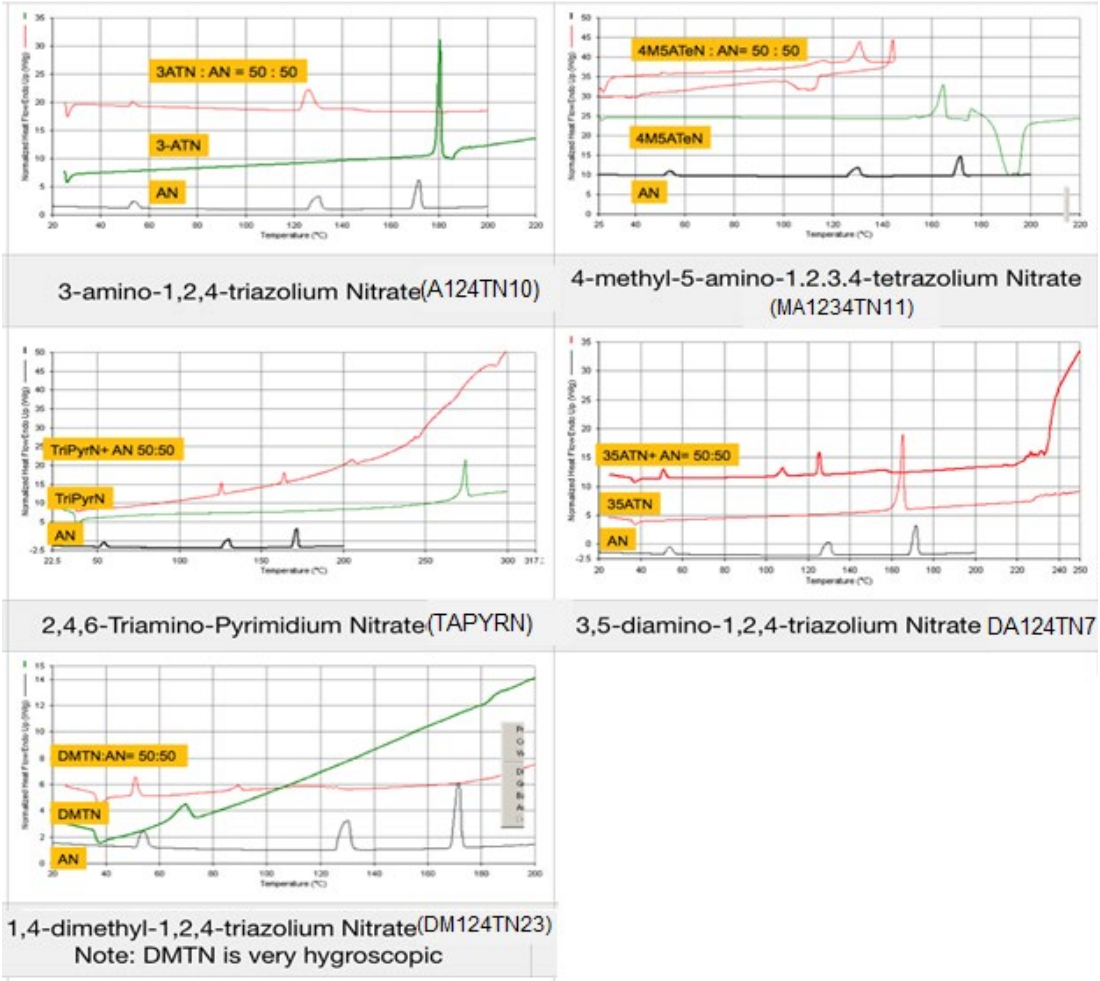

Figure 3.3-2 DSCs of AMRDEC EILs and AN Mixtures

Small quantities (~0.3g) of the mixtures were prepared, allowing for deviation in baseline formulation in order to prepare a homogeneous aqueous propellant (i.e. Ratios were allowed to deviate from baseline to yield complete miscibility solubility). While the ingredients all have significant solubility in water, only the DM124TN23 (1,4-dimethyl-1,2,4-triazolium nitrate) had high enough solubility in water and water/AN solutions to afford a credible propellant blend. DM124TN23, AN and water (DM124TN23: AN : Water = 33.7 : 42.4 : 23.9) formed a RT liquid with predicted combustion temperature (Tc= 1242K, Isp=214/205s) close to the desired value(1500K). All small scale samples produced for initial solubility evaluations are summarized in table 3.3-3 below.

Table 3.3-3. Summary of EIL Propellant Formulations

Fuel Abbreviation	Fuel	Formulation	Fuel to Oxidizer Blend	Fuel to Oxidizer Blend Density g/cc	Flame Temperature, Tc (K)	Isp, sec	Gas Composition at Chamber
A124TN10			A124TN10: AN (r=) 66.7: 33.3	1.644	2238	264/254	H2O 0.313
			A124TN10:AN:Water 64:36:43 (45:25:30)	1.387	1523	224/215	H2O 0.53
A124TN	3-amino-1,2,4-triazolium nitrate	C2H5N5O3	A124TN: AN (r=1.53) 71.4:28.6	1.634	2006	249/239	H2O 0.2840
			A124TN:AN:Water 71:29:20 (59.2:24.2:16.7) R=1.364	1.478	1494	222/212	CO 0.086, CO2 0.087, H2O 0.37353, N2 0.28
MA1234TN11	4-methyl-5-amino-1,2,3,4-tetrazolium nitrate	C2H6N6O3	MA1234TN11:AN (r=1.7)76.9:23.1	1.659	2117	253/246	H2O 0.2446
			MA1234TN11:AN:Water (r=1.44) 76.5:18.5:20.0 (61.5:18.5:20)	1.466	1482	226/216	H2O 0.379
A124TN10			A124TN10: (AN(r=1.7) 76.9:23.1	1.627	2128	254/247	CO 0.16 CO2 0.04 H2O 0.24
			A124TN10:AN:H2O (r=1.44)76.5:18.5:20.0 (61.5:18.5:20)	1.446	1490	226/217	CO 0.085, CO2 0.071 and H2O 0.339
DA124TN32	3,5-diamino-1,2,4-trizolium nitrate	C2H6N6O3	DA124TN32: AN (r=1.59) 71.4:28.6	1.656	1756	237/227	CO 0.133 CO2 0.06 H2O 0.27
			DA124TN32: AN :H2O (r=1.46) 71.4:28.6:12 63.8:25.5:10.7	1.5473	1454	221/211	CO 0.12, CO2 0.07, H2 0.22, H2O 0.35m N2 0.24
MA1234TN			MA1234TN: AN 57:43	1.555	2273	247/235	H2O 0.29
			MA1234TN: AN:H2O 57:43:20 44:33:23	1.376	1532	232/222	CO 0.08, CO2 0.085, H2 0.168, H2O 0.45, N2 0.212
DM124TN23	1,4-dimethyl-1,2,4-triazolium nitrate	C4H8N4O3	DM124TN23: AN 40:60:0 (1.5)	1.3208	1990	257/247	CO 0.14, CO2 0.07, H2O 0.355 and H2 0.171
			DM124TN23:AN:H2O 40:60:20 33:50:17 (r=1.36	1.424	1502	229/219	

3.3.5 AFRL Propellant Evaluations and Development

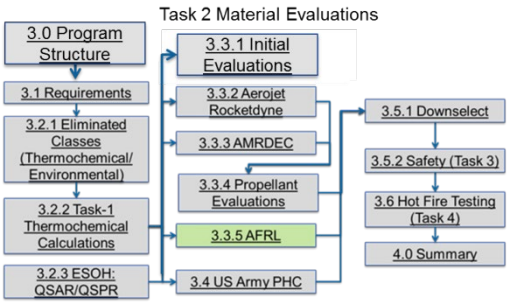

In parallel to AR and AMRDEC material and propellant evaluations, AFRL Edwards conducted evaluations that focused on HAN propellant development. In addition AFRL also focused on M315E modification and improvements that could meet SERPD WP-2400 requirements.

HAN Propellant Development

At the Air Force Research Lab, HAN based IL formulations were evaluated. Several low combustion temperature HAN-based monopropellant formulations were characterized and down selected for future thruster firing demonstrations; this work is described in greater detail in Appendix E. Most of these formulations are promising variants of formulations that have been worked on in the past at AFRL and possess at least a small concentration of HAN due to the limited number of viable oxidizers available, and the wide liquidous range they afford. Although in certain cases quite successful, the incorporation of HAN imparts some undesirable properties to the propellant to include limited compatibility with other ingredients and system materials, sensitivity to impurities leading to poor thermal stability, and poor ignitability. The latter trait becomes even more pronounced when a diluent such as water is added to drive down the combustion temperature. Nevertheless, these challenges can be overcome as shown with the success of M315E.

HAN Reduction Studies

AFRL/AMRDEC explored the use of molecules which are oxygen balanced or near balanced and catalytically reactive to minimize the need for HAN. Although in certain cases quite successful, the incorporation of HAN imparts some undesirable properties to the propellant. However, use of HAN expands the range of fuel-rich IL candidate materials and therefore allows added possibilities for replacement compositions.

One such family of candidate materials are the 3-oxy-5-nitrotetrazolate (ONT) salts first synthesized by SRI international (Schmidt). ONT salts were looked at by AFRL in 2006 as potential melt cast explosives for Insensitive Munitions and they demonstrated decent thermal stability and small-scale hazards. These materials were never evaluated in monopropellant formulations. The theoretical Isp (vacuum) of these materials are very high due to the positive heat of formation. If they should be found to be suitably reactive on a catalyst, one of the challenges will be to find eutectic mixtures and diluents capable of yielding a low melting formulation. Theoretical calculations with AONT and water show that up to 30% water may be added to achieve the maximum desired 1900ºC combustion temperature while maintaining an equivalent Isp to hydrazine. Other balanced compounds of which small lab samples exist at AFRL for catalytic reactivity screening are also listed below. All of the compounds are capable of making the theoretical Isp and combustion temperature goals if formulated appropriately with

small amounts of oxidizers (e.g. AN) and a diluent like water. The exhaust products indicate primarily N2, CO2 and H2O are present with no solid particulate and little to no methane.

1-hydroxy-3-oxoimidazole was synthesized in good yields from formic acid and hydroxyl amine in regards to published procedures. It is a white solid with a strong melt and violent decomposition at 165-170ºC at 10ºC/minute by scanning differential calorimetry in sealed aluminum pans. 1-hydroxy-3-oxoimidazole is poorly soluble in water and under very basic conditions reverts back to its starting materials, i.e. one cannot make the anion to alkylate for other derivatives. Subsequent efforts in creating the simple nitrate salt using 90% nitric acid in methanol at ice water temperatures in acetonitrile, were successful in creating highly crystalline material by careful recrystallization using solvent/anti solvent methods, generating 1,3-bis-hydroxylimidazolium nitrate that was recovered in high yields. However, this material was extremely sensitive to simple impact tests and differential scanning calorimetry found a surprisingly thermally unstable material, which exploded ~80ºC with much violence (slight damage to DSC was incurred). Hence forth this material was immediately destroyed and no further efforts are planned with it. This behavior of N-Oxide based heterocycles is not uncommon due to the weak endothermic N-O bond. Likewise it mirrors the behavior of simple 1-amino-1,2,3-triazolium nitrate which was also found to be extremely unstable. Based on these unsuitable characteristics, this line of research was discontinued.

3.4. U.S. Army Public Health Center Toxicology Evaluation Summary

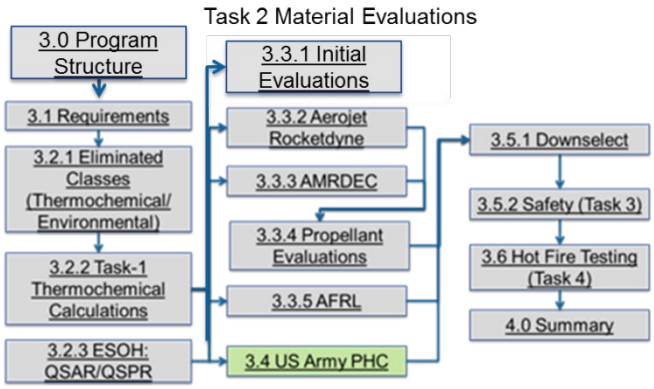

The toxicology assessment for the environmentally sustainable liquid gas generator formulations was conducted by Dr. S. William Eck and his team. Persistence, bioaccumulation, human health toxicity, and ecotoxicity were assigned to general categories of risk (i.e., low, moderate, or high) using criteria modified from Howe et al. (2006). Table 3.4-1 describes the criteria used in the categorization, though the relative proportions of each substance were also factored into the final assessment. In addition, classification in the Globally Harmonized System (GHS; OSHA 2012) is also included for many of these compounds (See Appendix F).

If no experimental data can be located in the literature, toxicity values for the various parameters were predicted using Quantitative Structure Activity Relationship (QSAR) software where possible. Modeling packages include US EPA's EPI Suite™ 4.0 (USEPA, 2008a), ECOSAR™ (USEPA, 2007) and TOPKAT (BIOVIA Inc.). (EPI Suite™ and ECOSAR™ are trademarks of the USEPA.)

Table 3.4-1. Categorization Criteria used in the Development of Environmental Safety and Occupational Health Severity (modified from Howe et al. 2006)

	Low	**Moderate**	**High**
PERSISTENCE	Readily biodegrades (<28 days)	Degradation ½ life: water <40 days , soil <120 days	Degradation ½ life: water >40 days soil > 120 days
TRANSPORT	Water sol. < 10 mg/L log K_{OC} > 2.0	Water sol. 10-1000 mg/L log K_{OC} 2.0-1.0	Water sol. > 1000 mg/L log Koc <1.0
BIOACCUMULATION	log K_{OW} <3.0	log K_{OW} 3.0-4.5	log K_{OW} >4.5
TOXICITY	No evidence of carcinogenicity/ mutagenicity; Subchronic LOAEL > 200 mg/kg-d	Mixed evidence for carcinogenicity/mutagenicity (B2, 2); Subchronic LOAEL 5-200 mg/kg-d	Positive corroborative evidence for carcinogenicity /mutagenicity; LOAEL < 5 mg/kg-d
ECOTOXICITY	Acute LC_{50}/LD_{50} >1 mg/L or 1500 mg/kg; Subchronic EC_{50} >100 µg/L or LOAEL >100 mg/kg-d	Acute LC_{50}/LD_{50} 1-0.1 mg/L or 1500-150 mg/kg; Subchronic EC_{50} 100-10 µg/L or LOAEL – 10-100 mg/kg-d	Acute LC_{50}/LD_{50}<100 µg/L or <150 mg/kg; Subchronic LOAEL <10 mg/kg-d

Notes:
mg/L - milligrams per liter
LOAEL - lowest-observed adverse effect level
LC_{50} – concentration expected to result in 50 percent lethality to a population of test animals.
mg/kg-d - milligrams per kilogram per day
µg/L - micrograms per liter

The full report and tables are available in appendix F. A summary of the results is presented in table 3.4-2.

Table3.4-2: Stoplight chart of the examined compounds

Name	Persistence	Transport	Bioaccumulation	Toxicity	Ecotoxicity
Hydroxyl ammonium Nitrate					
Hydroxy ethyl hydrazinium nitrate					
Ammonium nitrate					
Bipyridyl					

1-Methyl-4-amino-1,2,4,triazolium nitrate					
Carbohydrazide		**ND**	**ND**	**ND**	
Hydrazine					

ND = No data or insufficient data

Hydrazine was the most hazardous compound, while ammonium nitrate was shown to be the least hazardous. There was insufficient/little data on carbohydrazide. Most of the EIL's showed bad transport values which was expected since they are salts and readily dissociate in water.

Table 3.4-3: Selected SERDP compounds Examined for Bioaccumulation, Toxicity and Ecotoxicity, Eck

Name	Persistence	Transport	Bioaccumulation	Toxicity	Ecotoxicity
1-Methyl-1,2,4-triazolium nitrate	**ND**	**ND**			
3,5-Diamino-1,2,4-triazolium nitrate	**ND**	**ND**			
1-Methyl-3-methoxy-1,2,4-triazolium nitrate	**ND**	**ND**			
N-1-Ethoxy-1,2,4-triazolium nitrate	**ND**	**ND**			
3-Amino-1,2,4-triazolium nitrate	**ND**	**ND**			
5-Aminotetrazolium nitrate	**ND**	**ND**			
3,4-Diamino-1,2,4-triazolium nitrate	**ND**	**ND**			
1-Methyl-5-aminotetrazolium nitrate	**ND**	**ND**			
1,4-Diamino-1,2,4-triazolium nitrate	**ND**	**ND**			
1-H-4-Amino-1,2,4-triazolium nitrate	**ND**	**ND**			
1,3-Diamino-1,2,3-triazolium nitrate	**ND**	**ND**			
1,3-Diamino-1H-imidazol-3-ium nitrate	**ND**	**ND**			

ND = No data or insufficient data

Persistence and Transport were not examined for these EIL's, but the transport should be assumed to be red for most of the EIL's given their ionic salt nature and their inherent high dissociation constants. Persistence should be yellow for most of the EIL's as well. A more in depth Excel spreadsheet of these data is available in the appendix.

Table 3.4-4 Formulation Components

Chemical Substance	Percent composition*	CAS Number
M315E Han-base (AFRL 315E)		
Hydroxyl ammonium nitrate (HAN)		13465-08-2
HEHN	34	109-84-2
S-HAN5**	34	N/A Mixture
AN	5	6484-52-2
Bipyridyl	1	366-18-7
M315F Mod (No HAN) (AFRL 315F)		
HEHN	34	109-84-2
AN	17	6484-52-2
Bipyridyl	0.3	366-18-7
Hydroxylethyl triazolium (AFRL 824S)		
HEATN	24	N/A
S-HAN5**	51	N/A Mixture
AN	5	6484-52-2
Bipyridyl	1	366-18-7
1-Methyl-4-amino-1,2,4-triazolium nitrate [AMTN] (AFRL 1107P)		
AMTN	20	N/A
HEHN	5	109-84-2
S-HAN5**	47	N/A Mixture
Carbohydrazide [CBZ]		
Carbohydrazide		497-18-7

*Percent compositions brought to 100% by addition of water.
**Stabilized HAN containing 1 wt% 2-bipyridyl and 5 wt% AN

3.6 Task 3 Safety Characterization/Hazard Classifications:

3.6.1 Formulation Downselection

During Task 3 the following 5 candidates were selected for scale-up and safety/hazards characterization, summarized in table 3.6-1. All formulations were required to exceed the performance of hydrazine, along with having improved toxicity. In addition, all ingredients used in each candidates must be commercially available or simple synthesis (<3 Steps).

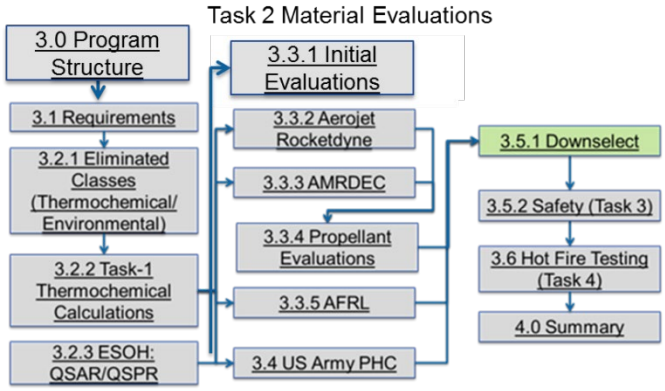

Table 3.6-1 Propellant Candidate Summary

Candidate	Ingredient	Oxidizer	Isp	Tc (K)	Synthesis	Hazards/ Thermal Stability	Toxicity (Data to date)	Cost	Hot Fire Test	Overall Benefits
1-methyl-4-amino-1,2,4-triazolium nitrate	Synthesis at AR	HAN	203	1452	Issue with purity of scaled- up synthesized material	Acceptable properties		High Cost	NT	Good performance & toxicity
Carbohydrazinium nitrate	Synthesis at AR	No Oxidizer	226	1322	Easy synthesis from commercially available materials	Acceptable properties	TBD	Low Cost	Good Stability	Good performance & commercially available
Diluted M315E	HEHN	HAN	221	1453	Scaled-up and cost effective relative to hydrazine	Acceptable properties	Improved over N2H4	Low Cost	Good Stability	Modified heritage & characterized formulation

M315F	HEHN	AN	239	1457	Comparable to M315E using low-cost AN	Acceptable properties	Improved over N2H4	Low cost	Good Stability	Increased stability & low toxicity
M824S	HEATN	HAN	243	1900	Improved cost to Hydrazine	Acceptable properties	TPB	Medium cost	Combustion concerns	Increased thermal stability

3.6.2 Safety and Hazards Summary

Diluted M315E, M315F and M824S Results

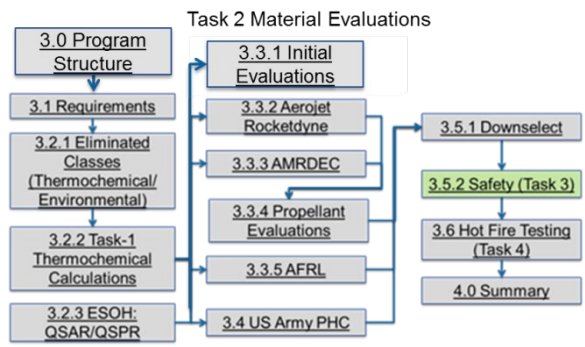

The safety and hazards data for Diluted M315E, M315F and M824S were provided by Adam Brand from AFRL. The propellant performance characteristics, hazards, and physical properties are presented in Table 3.6-2. A clear distinction can be made between ionic liquid monopropellants and hydrazine in regards to an immense increase in combustion temperature, yet similar performance. Hydrazine has a high performance relative to its low combustion temperature due to the low molecular weight gases (N_2, H_2, NH_3) it outputs during catalytic decomposition in a thruster. On the contrary and in the case of the carbon-containing ionic liquids, an oxidizer must be used to balance the formulation for complete combustion. Since this produces higher molecular weight gases, the Isp detriment must be offset by a higher combustion temperature. Although the theoretical Isp of 315E-D and 1028B do not surpass hydrazine, the ρ-Isp still outperforms hydrazine by 20 to 30%. The real performance gain for the ionic liquids originates in their superior density (~1.4 vs 1.0 g/mL). More importantly, however, the ionic nature of the formulations imparts many favorable traits in regards to propellant hazards such as lower: vapor toxicity, flammability, and handling concerns.

The formulations were largely insensitive to friction and ESD, with the exception of 315F. The four formulations containing HAN had friction and ESD values at the upper end of the test equipment. This is expected, as the ionic nature of the constituents makes them highly electrically conductive. The impact sensitivities of the propellants were in line with typical ionic

liquid monopropellants, noting that the maximum value is 200 N. The 315F formulation containing AN had a higher sensitivity to impact and friction. Although this friction sensitivity is higher than other ionic liquid monopropellants, it should still be comparatively safe in day-to-day use. In conjunction with the Zero-Card NOL Card Gap results, all of these formulations would be considered a Class 1.3 explosive.

Table 3.6-2 Summary of Diluted M315E, 315F and M824S.

Candidate	**315E-D**	**315F**	**M824S**
Density (g/mL)	1.318	1.393	1.402
Impact(kg·cm, 5 neg)	128	100	133
Friction (N, 5 neg)	>353	88	>353
ESD, (J)	>1	>9.4	>9.4
TGA (% wt loss/day, 75ºC)	0.43	0.20	0.43
NOL Card Gap (0 cards)	Neg	Neg	Neg
Adiabatic Compression (25ºC)	10/10 Neg at 200:1	5/5 Neg at 135:1	5/5 Neg at 200:1

Another attractive property of the formulations is their thermal stability. All of the blends had less than 1 percent weight decomposition per day at 75 °C. Notably, the formulations lacking HAN as the primary oxidizer (315F and 1028B) had a weight loss only half that of the other formulations. This provides further impetus for identifying more formulations that omit HAN as the oxidizer. To gauge the thermal stability of the triazole formulations, a simulated slow cook off in a TGA (3ºC/hour ramp to 60 °C, 3 hour soak) was performed on undiluted 315E, 1107P, and 824S. The onset temperatures of the three blends were found to be 137, 113, and 141 °C, respectively. It was evident that MA124TN was decidedly less thermally stable than HEA124TN26 in a similar propellant system. In-house studies have found that this is likely due to the stabilizing effect of the hydroxyethyl group (on HEA124TN26) to HAN.

<u>Carbohydrazinium Nitrate Results</u>

Since the fourth propellant had not been previously assessed for handling safety, sensitivity testing was performed at AR Redmond as described below to verify it safe to handle prior to delivery for hot-fire test.

Impact Testing

Impact testing was determined using a 2-kg drop weight on a Technoproducts drop-weight tester, the test propellant yielded 50% positive results at an impact level of 118 kg-cm. The

carbohydrazide nitrate-based propellant showed no evidence of induced reaction when subjected to an electrostatic discharge imparted by hand-held Tesla coil. Sensitivity testing is summarized in table 3.6-2.

Table 3.6-2 Summary of Carbohydrzide Nitrate Candidate

Candidate **Density (g/mL)** **Impact(kg·cm, 5 neg)**	**M315E** 1.318 128	**Carbohydrazide** 1.460 118
Friction (N, 5 neg)	>353 (N, 5 neg)	NT
ESD, (J)	>1	>1
TGA (% wt loss/day, 75ºC) **NOL Card Gap (0 cards)**	0.43 Neg at 0	0.43 NT
Adiabatic Compression (25ºC)	10:10 Neg at 200:1	NT

Differential scanning calorimetry was performed on 4.5-4.6 mg samples of the carbohydrazide nitrate-based propellant over a temperature range of 0-350ºC at 20ºC/min using a Perkin Elmer DSC 7 Differential Scanning Calorimeter. Unperforated capsules were employed for all cases tested. As evident in the example trace presented in Figure 3.6-1, no exothermic behavior (negative in the plot) was observed below 200 ºC. The small endotherm between 150 and 180 ºC was demonstrated to be repeatable, but irreversible – as interrogated by a follow-up case where the endotherm manifested upon the first but not second heating of a sample initially heated to 200 ºC, cooled to 30 ºC and then reheated to 350ºC.

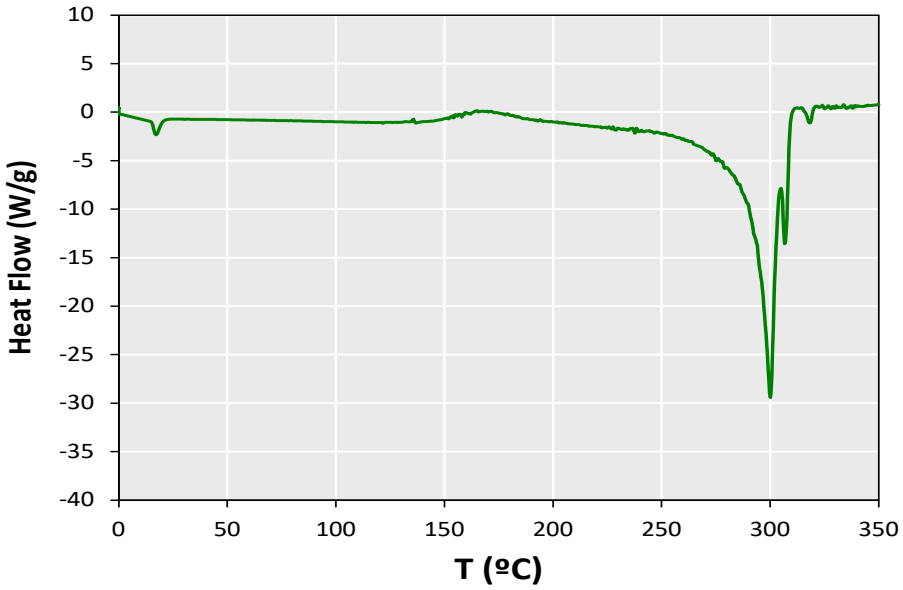

Figure 3.6-1 Differential scanning calorimetry heat flow for carbohydrazide nitrate-based propellant

1-methyl-4-amino-1,2,4-triazolium Nitrate Candidate

Initial results from Task 2 showed great potential for the 1-methyl-4-amino-1,2,4-triazolium nitrate EIL candidate. Testing showed acceptable sensitivity, thermal stability and sufficient solubility in water. In addition the candidate used commercially available starting materials and simple synthesis reactions. It is because of these reasons that 1-methyl-4-amino-1,2,4-triazolium nitrate was selected as the programs 5th candidate. The candidate was then scaled-up to 100 grams to support Task-3 and Task-4 efforts.

The 1-methyl-4-amino-1,2,4-triazolium nitrate was scaled-up at Aerojet Rocketdyne Sacramento. Once scale-up was complete, sensitivity testing was repeated to compare to previous results. Sensitivity was deemed acceptable and is summarized in Table 3.6-3.

Table 3.6-3. Sensitivity Results of 1-methyl-4-amino-1,2,4-triazolium nitrate

Test	Threshold	1-methyl-4-amino-1,2,4-triazolium nitrate
ESD (Joules)	>1.0	>1.0
Exotherm Onset DTA (ºF)	>150	464
Bureau of Mines Impact , E_{50} (kg·com)	>100	>100

Propellant development continued and a 5 gram verification batch was started. It was noted that once the 1-methyl-4-amino-1,2,4-triazolium nitrate was mixed with S-HAN-5 a white precipitate formed and became silver overnight. ICP was performed on the 1-methyl-4-amino-1,2,4-triazolium nitrate and verified a silver contamination. FTIR was also conducted but did not indicate any other organic contaminates. Purification efforts to remove the silver contaminate included filtering through silica gel and a liquid-liquid extraction with diethyl ether. Both methods proved ineffective in removing silver and propellant scale-up of this formulation was discontinued.

3.7 Task 4 Scale-up/Workhorse Testing-Performance Validation:

Testing Scope

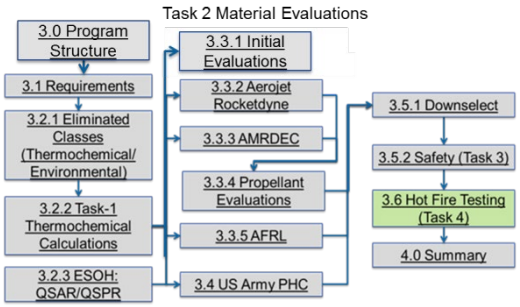

This section describes heavyweight test hardware, requirements, and procedures for hot-fire testing conducted on the Strategic Environmental Research and Development Program (SERDP). Environmentally Sustainable Liquid Gas Generator Formulations program to assess the

performance of a series of candidate reduced-flame-temperature green propellants, summarized in Table 3.7-1 as follows:

Table 3.7-1 List of Candidate Propellants Tested with Characteristic Metrics

Propellant	Constituents (by weight)	Predicted Flame Temp (ºC)	Density (g/cc)	Isp (sec)	Source
1. Diluted AF-M315E	SHAN5: 34% HEHN: 34% Water: 32%	1113	1.318	212	AFRL
2. AF-M315F	AN: 17% HEHN: 73% Water: 10%	1120	1.393	219	AFRL
3. AF-M824S	SHAN5: 51% HEATN: 24% Water: 25%	1627	1.402	243	AFRL
4. CHN-based Propellant	CHN: 74.5% EAN: 10.5% Water: 15%	1322	1.460	226	AR

AN = Ammonium Nitrate
HAN = Hydroxylammonium nitrate
HEHN = Hydroxyethylhydrazinium nitrate
SHAN5 = Stabilized HAN containing 1 wt% 2-bipyridyl and 5 wt% AN.
HEATN = 1-hydroxyethyl-4-amino-1,2,4-triazolium nitrate.

CHN = Carbohydrazide mononitrate
EAN = Ethylammonium nitrate

Objectives of the test program were to:

- Verify basic operability of a standardized laboratory heavyweight thruster on each propellant.
- Determine minimum preheat temperature for catalytic ignition.
- Perform a stability assessment over a mission-representative range of duty cycles.

Thruster Overview

Testing was conducted using the Rocketdyne P/N 42719-301 heavyweight thruster configured as depicted in Figure 3.7-1. Catalyst bed heating was accomplished via a 570W swage-tube heater (not shown in the figures) wrapped around the thrust chamber body. The thruster was packed with LCH-241 catalyst. Because the short total operational duration associated with the limited available quantities of the experimental propellants can be expected to deplete a negligible fraction of the catalyst bed's demonstrated life capability, all testing was performed using a single thruster pack.

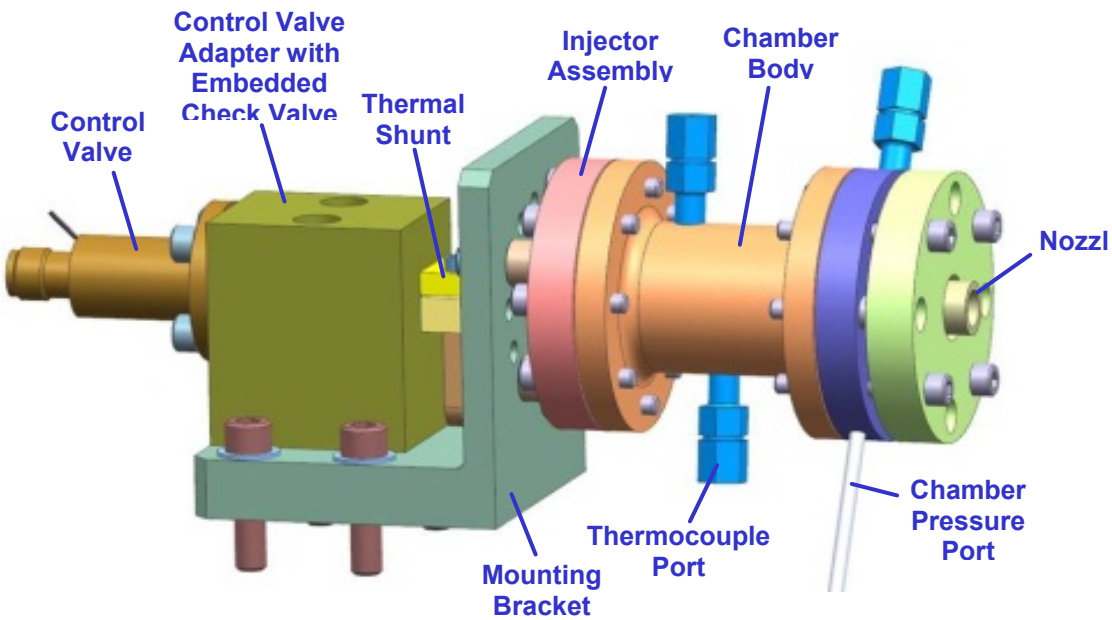

Figure 3.7-1 Laboratory Mode (Heavyweight) Test Thruster

Hot-Fire Conditions

Nominal target operational conditions for all testing are listed in Table 3.7-2. Inlet pressures are the total pressure prior to the start of the run.

Table 3.7-2 Nominal Operating Conditions

Parameter	Value
Piston Tank Gas Pressure	245 psig*
Steady-State Thruster Chamber Pressure	200 psia
Steady-State Thrust	1 N
Steady-State Propellant Flow Rate	0.5 g/sec

*Adjusted as required to achieve nominal chamber pressure based on data from Initial firing.

Hot-Fire Matrix

Thruster testing proceeded with the execution of the matrix presented in Table 3.7-3. As-run deviations (repeats of runs or modifications to the execution order enacted where deemed prudent by the cognizant project engineer) are noted with the reported results for each test.

Table 3.7-3 Planned Hot-Fire Test Matrix

Seq.	Duty Cycle On (sec)	Duty Cycle Off (sec)	# of Pulses	Time to Next Sequence	Purpose	Preheat Temp (ºF)
1	0.12	5	10	As required to cool to preheat temperature for next run	Preliminary Stability Assessment.	900
2	0.5	5	10			
3	15	0	1			
4	1	0	1	10 sec	Hot start.	As left by previous sequence
5	5	0	1	As required to cool to preheat temperature for next run.	Minimum Catbed Preheat Assessment. Additional sequences may be added at PE's discretion. Once found, go to 14.	800
6	5	0	1			700
7	5	0	1			600
8	5	0	1			550
9	5	0	1			500
10	5	0	1			450
11	5	0	1			400
12	5	0	1			350
13	5	0	1			300
14	0.5	5	10	Allow to cool to <1100 ºF	Extended stability assessment.	>800
15	0.5	2	10			
16	0.5	1	10			
17	0.5	0.5	10			
18	0.5	0.25	10			
19	0.5	0.1	10			
20	0.5	0.05	10			
21	0.5	0.02	10			
22	0.02	5	10			
23	0.05	5	10			
24	0.25	5	10			
25	0.5	5	10			
26	60	0	1	As required to cool to preheat temperature for next run.	Long Burn for SS performance assessment. Repeat as necessary to consume remaining propellant.	900

Notes:

- Propellant will be at ambient temperature.
- Firings will be at sea level.

- Preheat temperature refers to Tbed1.
- Target preheat temperature (Tbed1) set by heating above listed start temperature before turning off heaters and allowing test to automatically start once temperature fell to specified value.
- In the event any test sequence aborts, Cognizant PE will review data to determine if testing will be resumed or discontinued.

Test Results

Test 1: Diluted AF-M315E Propellant

Propellant composition (by weight): 34% SHAN5/34% HEHN/32% Water

Test Operations Summary:

- Initial tank pressure was set to 275 psig, corresponding to a thruster non-operating feed pressure of 2963 kPa (415 psig).
- Initial stability assessment Sequences 1-4 completed normally. During operation thruster feed pressure was observed to drop to approximately 2860 kPa (400 psig), but also shifted up and down by a similar amount due to drift in the pressure regulator (resolved for subsequent tests by adding a ballast tank to the outlet).
- Minimum catalyst bed preheat sequences were initiated per plan at 427 ºC (800 ºF) and successful starts were demonstrated down to 260 ºC (500 ºF) (Seq. 9). Chamber pressure rise time became progressively slower as preheat temperature was reduced, with a change in the inflection of the rise profile and significantly extended tail-off noted for the 500 ºC case. The thruster rapidly washed out when restart was attempted from 232 ºC (450 ºF) catalyst bed preheat temperature on the subsequent sequence.
- Propellant tank pressure was lowered to 1860 kPa (255 psig) (corresponding to a thruster feed pressure of 2791 kPa (390 psig)) to reduce propellant consumption/adjust thrust closer to the target 1-N.
- The thruster was reheated and Sequences 14-21 completed normally as planned. Feed pressure dropped indicating the propellant tank had run to empty approximately five pulses into Sequence 21.
- The tank was reloaded with propellant and Sequence 26 executed ahead of schedule to purge any bubbles potentially inadvertently introduced into the feedlines.
- Testing then proceeded with a repeat of Sequence 22 followed by Sequences 23-25.

- Testing concluded with a repeat of Sequence 26 to consume remaining expellable propellant, completing an additional 28.8 seconds of normal steady-state operation before falling feed and chamber pressure triggered an automatic shut-down as the tank ran empty.

A summary of all completed test sequences is compiled in Table 3.7-4.

Table 3.7-4 Test 1 As-Run Test Matrix

File	Seq.	Tank Pressure (psig)	Pfeed (psig)	Duty Cycle On (sec)	Duty Cycle Off (sec)	# of Pulses	Time to Next Sequence	Purpose	Preheat Temperature (ºF)	Comments/Observations
1								Preheat		
3	1	275	415	0.12	5	10	As required to cool to preheat temper-ature for	Preliminary Stability Assessment.	900	
4	2	275	415	0.5	5	10				
5	3	275	415	15	0	1				
5	4	275	415	1	0	1	10 sec	Hot start.	As left by previous sequence	
6	5	275	415	5	0	1	As required to cool to preheat temperature for next run.	Minimum Catalyst Bed Preheat Temperature Assessment.	800	
7	6	275	415	5	0	1			700	
8	7	275	415	5	0	1			600	
9	8	275	415	5	0	1			550	
10	9	275	415	5	0	1			500	
11	10	275	415	0.4	0	1			450	Visible smoke exiting thruster nozzle. Shut down on low Pc.
12	14	255	390	0.5	5	10	Allow to cool to <1100 ºF	Extended stability assessment.	>800	
13	15	255	390	0.5	2	10				
14	16	255	390	0.5	1	10				
15	17	255	390	0.5	0.5	10				
16	18	255	390	0.5	0.25	10				
17	19	255	390	0.5	0.1	10				
18	20	255	390	0.5	0.05	10				
19	21	255	390	0.5	0.02	10				
20	22	255	390	0.02	5	5				Ran out of propellant.
22								Preheat		
23	26	255	390	60	0	1	As required to cool to preheat temperature for next run.	Long Burn for SS performance assessment. Repeat as necessary to consume remaining propellant.	>800	Inserted to purge any bubbles that may have been introduced during tank refilling.
24	22	255	390	0.02	5	10	Allow to cool to <1100 ºF	Extended stability assessment.	>800	
25	23	255	390	0.05	5	10				
26	24	255	390	0.25	5	10				
27	25	255	390	0.5	5	10				
28	26	255	390	60	0	1	As required to cool to preheat temperature for next run.	Long Burn for SS performance assessment. Repeat as necessary to consume remaining propellant.	>800	Ran out of propellant.

Stability Testing: Diluted AF-M315E Propellant

Beginning-of-test stability and pulse-mode-performance characteristics were generally similar to prior tests operated on diluted AF-M315E propellant, the most notable distinction from operation on undiluted propellant being a lower relative increase in response time for each successive pulse owed the diminished rate of catalyst bed heating by the less energetic propellant variant. Chamber pressure traces for the ten pulses of Sequence 2 are shown superimposed in

Figure 3.7-2 for illustration, where pulse order is denoted by a progressive color shift from blue to red. Selected pulse-mode sequences from the extended stability test segment encompassing a broadened duty cycle range are similarly presented in Figure 3.7-3. No indication of chamber pressure spiking or sining was observed at any time during the test.

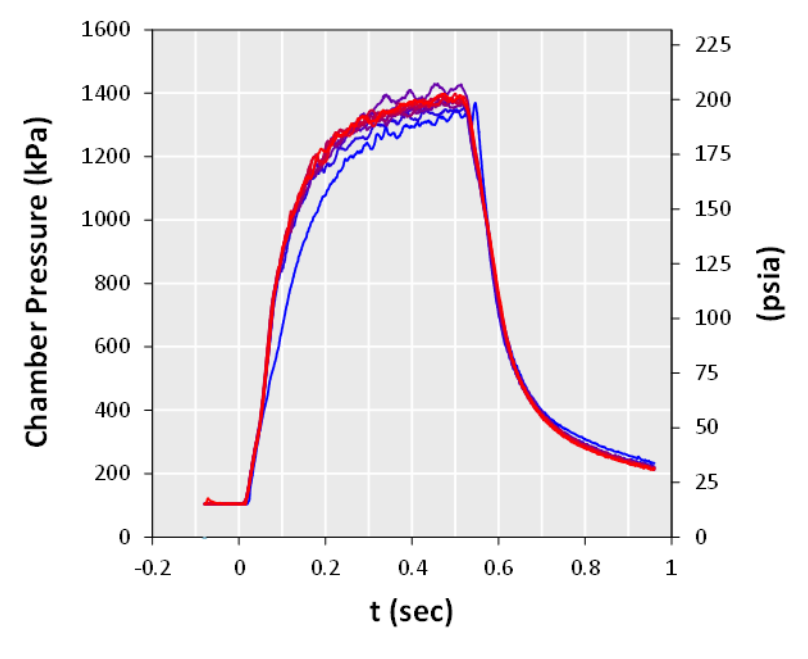

Figure 3.7-2 Stability assessment Seq. 2 (0.5/5 sec on/off) pulse overlay of Diluted M315E

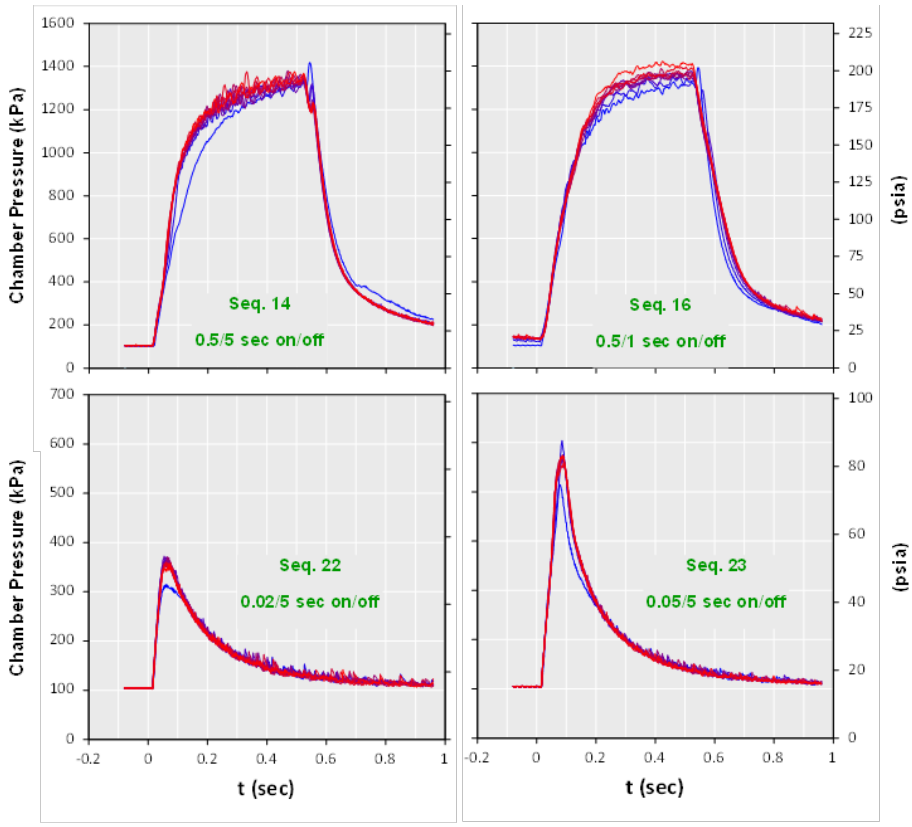

Figure 3.7-3 Selected extended stability assessment sequence pulse overlays of Diluted M315E

Minimum Preheat Temperature: Diluted AF-M315E Propellant

Chamber pressure traces for the series of five-second burns initiated from progressively lower catalyst bed preheat temperatures are superimposed for comparison in Figure 3.7-4**Error! Reference source not found.**. Consistent with prior tests, thruster response time is seen to fall initially incrementally and then more precipitously with each decrement, ultimately resulting in a marginally successful start at 288 ºC (500 ºF) followed by rapid washout at 232 ºC (450 ºF). Tail-off times demonstrate a corresponding trend, indicating the five seconds of commanded operation to be insufficient for the larger initial propellant puddle formed within the catalyst bed during colder starts to fully resolve. Temperature measured at the edge of the plenum region downstream of the bed plate was observed to rise approximately 23 ºF over the five-second operating interval for the case started from 427 ºC, compared to 33 ºF for the 288 ºC case, with the subsequent 260 ºC start case showing an increase of only 29 ºC, likely principally as the result of the reduction in effective operational duration affected by the slow start.

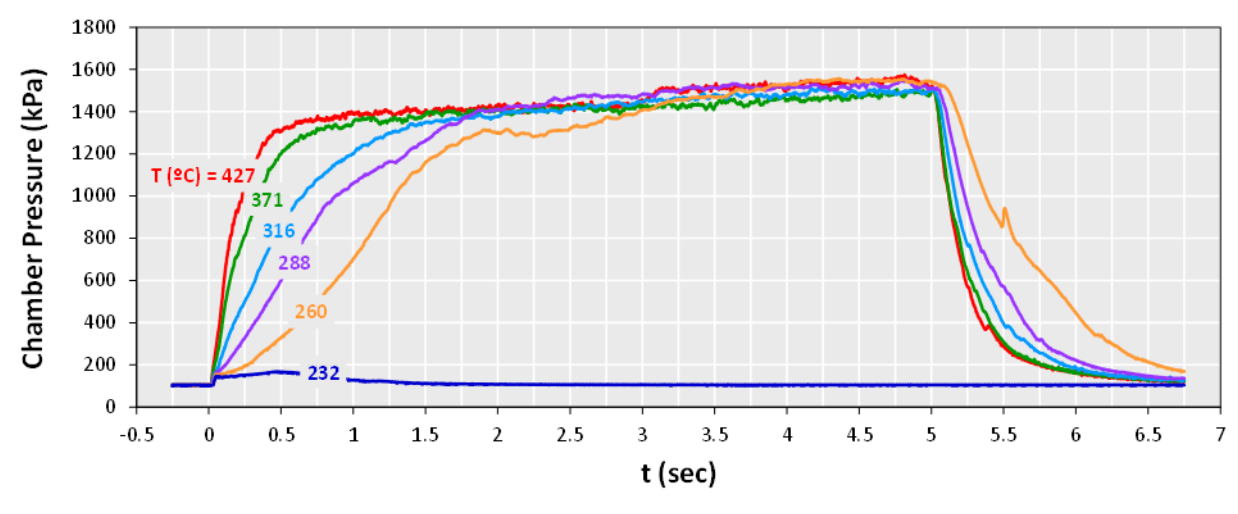

Figure 3.7-4 Diluted M315E Five-second burns executed at progressively reduced catalyst bed preheat temperature, T

Test 2: AF-M315F Propellant

Propellant composition (by weight): 17% AN/73% HEHN/10% Water

Test Operations Summary:

1.0 Based on the rate of propellant consumption observed in the prior test, initial tank pressure was set to 1791 kPa (245 psig), corresponding to a thruster non-operating feed pressure of 2626 kPa (366 psig).

2.0 Initial stability assessment Sequences 1-4 completed normally. During operation thruster feed pressure was observed to drop to 2563 kPa (357 psig).

3.0 Propellant tank pressure was increased to 1894 kPa (260 psig), corresponding to thruster non-operating/operating feed pressures of 2790/2720 kPa (390/380 psig) to adjust thrust closer to the nominal target 1-N without overly increasing the anticipated consumption rate of the limited available quantity of the experimental propellant.

4.0 Minimum catalyst bed preheat sequences were initiated per plan at 427 ºC (800 ºF) and successful starts were demonstrated down to 316 ºC (600 ºF) (Seq 7). Chamber pressure rise time initially demonstrated similar reduction with reduced preheat temperature to that observed for the Test 1 diluted AF-M315E control. However, the thruster rapidly washed out when

restart was attempted from 228 ºC (550 ºF), 50 ºC (100 ºF) higher than that required to achieve the same result in the control case.

5.0 The thruster was allowed to cool and reheated in association with a break for lunch.

6.0 Propellant tank pressure was increased to 1929 kPa (265 psig), corresponding to a non-operating thruster feed pressure of approximately 2812 kPa (393 psig).

7.0 Sequences 14-20, 22, and 23 were completed normally as planned, with Sequences 21, 24, and 25 omitted to preserve adequate propellant for a final steady-state burn (Sequence 26) of sufficient duration for the catalyst bed to approach thermal equilibrium.

8.0 Testing concluded with Sequence 26, which consumed all remaining expellable propellant over 27 seconds of normal steady-state operation.

A summary of all completed test sequences is compiled in Table 3.7-5Table.

Table 3.7-5 Test 2 As-Run Test Matrix

File	Seq.	Tank Pressure (psig)	Pfeed (psig)	Duty Cycle On (sec)	Duty Cycle Off (sec)	# of Pulses	Time to Next Sequence	Purpose	Preheat Temperature (ºF)	Comments/Observations
1								Preheat		
4	1	245	357	0.12	5	10	As required to cool to preheat temper-ature for	Preliminary Stability Assessment.	900	
5	2	245	357	0.5	5	10				
6	3	245	357	15	0	1				
6	4	245	357	1	0	1	10 sec	Hot start.	As left by previous sequence	
7	5	260	380	5	0	1	As required to cool to preheat temperature for next run.	Minimum Catalyst Bed Preheat Temperature Assessment.	800	
8	6	260	380	5	0	1			700	
9	7	260	380	5	0	1			600	
10	8	260	380	0.4	0	1			550	Visible smoke exiting thruster nozzle. Shut down on low Pc.
11								Preheat (after breaking for lunch)		
12	14	265	383	0.5	5	10	Allow to cool to <1100 ºF	Extended stability assessment.	>800	
13	15	260	383	0.5	2	10				
14	16	260	383	0.5	1	10				
15	17	260	383	0.5	0.5	10				
16	18	260	383	0.5	0.25	10				
17	19	260	383	0.5	0.1	10				
18	20	260	383	0.5	0.05	10				
19	22	260	383	0.02	5	10				
20	23	260	383	0.05	5	10				
21	26	260	383	27	0	1	As required to cool to preheat temperature for next run.	Long Burn for SS performance assessment. Repeat as necessary to consume remaining propellant.	>800	Ran out of propellant.

Stability Testing: AF-M315F Propellant

Beginning-of-test stability and pulse-mode-performance characteristics were generally similar the diluted AF-M315E control (Test 1), save for a small degree of increased chamber

pressure roughness. Chamber pressure traces for the ten pulses of Sequence 2 are shown superimposed in Figure 3.7-5 with pulse order denoted by color progression from blue to red. The same selection of pulse-mode sequences from the extended duty-cycle stability test segment as for the preceding test are likewise presented in Figure 3.7-6. No indication of chamber pressure spiking or sining was observed at any time during the test.

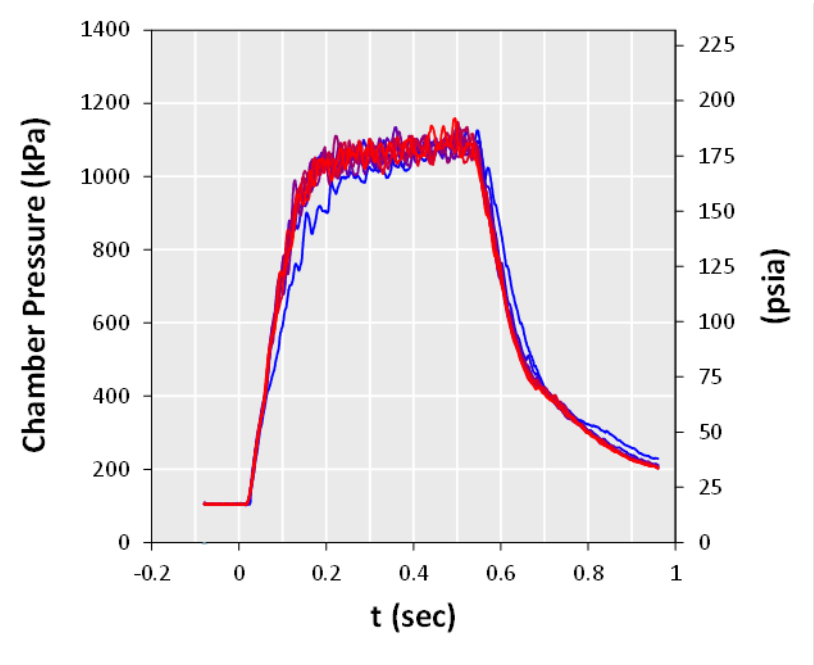

Figure 3.7-5 Stability assessment Seq. 2 (0.5/5 sec on/off) pulses of M315F

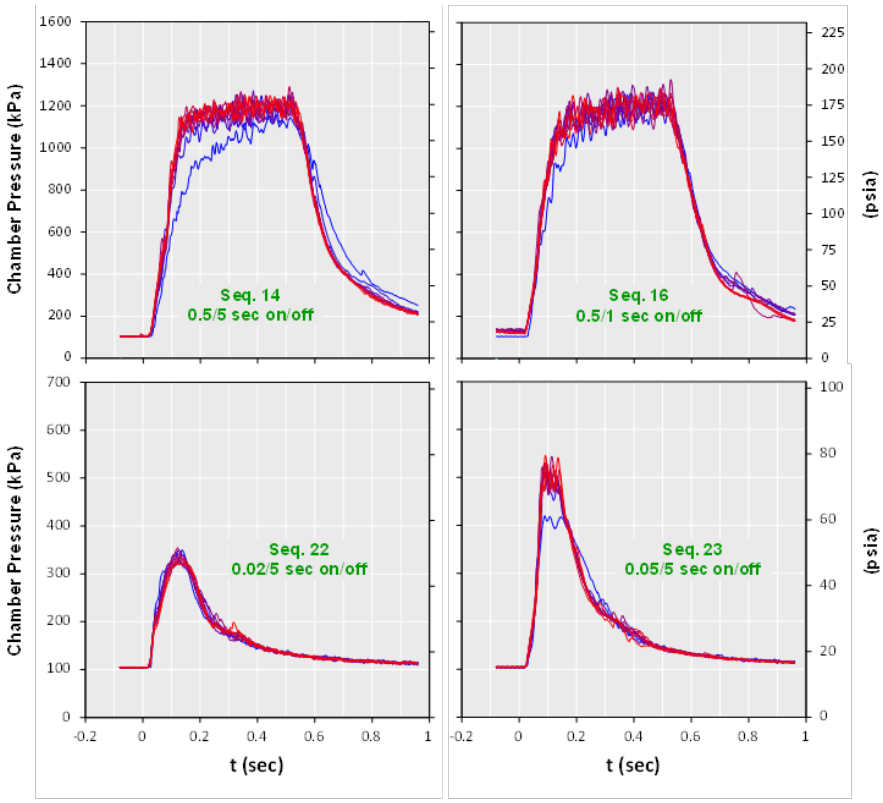

Figure 3.7-6 Selected extended stability assessment sequence pulse overlays of M315F

Minimum Preheat Temperature: AF-M315F Propellant

Chamber pressure traces for the series of five-second burns initiated from progressively lower catalyst bed preheat temperatures are superimposed for comparison in Figure 3.7-7. The initial slope of the chamber pressure rise for each start is seen to fall more quickly than for the preceding control case, although overall response times remain similar, with failure to start due to washout setting in at approximately 50 ºC (100 ºF) higher preheat temperature. Also notable is that chamber pressure does not demonstrate the slow upward drift of the five-second burn duration as was observed in the Test 1 control case. Feed manifold pressure does not show a similar trend, leaving differences in combustion characteristics as probably cause for the discrepancy. Notably, temperature measured by the plenum thermocouple (Tplenum) rises by 3 ºC (5 ºF) over the burn duration versus 8 ºC (15 ºF) for the control case, suggesting a lower relative flame temperature despite the approximately equal values predicted by chemical equilibrium calculations. While the downstream-most thermocouple at the edge of the catalyst bed (Tbed2) correspondingly showed a 1 ºC (2 ºF) rise vs. 6 ºC (10 ºF) for Test 1, the upstream thermocouple located at the catalyst bed wall (Tbed1) remained essentially constant throughout the burn for both tests.

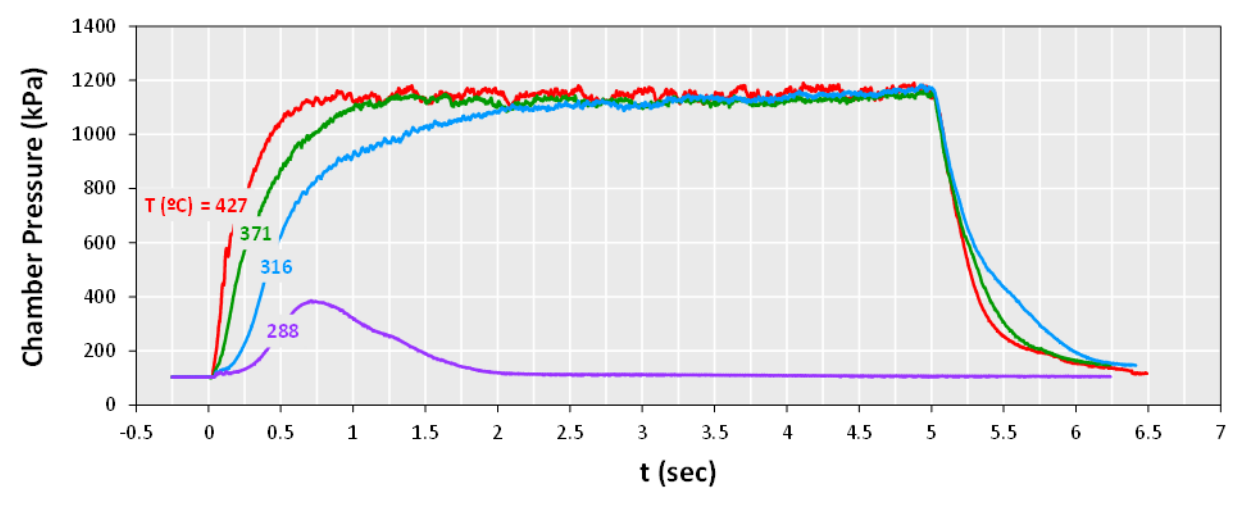

Figure 3.7-7 M315F Five-second burns executed at progressively reduced catalyst bed preheat temperature

Test 3: AF-M824S Propellant

Propellant composition (by weight): 15% SHAN5/24% HEATN/25% Water

Test Operations Summary:

- Based on the rate of propellant consumption observed in the prior test, initial tank pressure was set to 1791 kPa (245 psig), corresponding to a thruster non-operating feed pressure of 2653 kPa (370 psig).
- Initial stability assessment Sequences 1-4 completed normally, save that the very first pulse of the test exhibited an erratic chamber pressure profile. During operation thruster feed pressure was observed to drop to 2591 kPa (361 psig).
- Minimum catalyst bed preheat sequences were initiated per plan at 427 ºC (800 ºF) and successful starts were demonstrated down to 288 ºC (550 ºF) (Seq 8). Occasional wisps of smoke were observed in the plume during the burn started from 371 ºC (700 ºF), progressing to substantial evidence of incomplete combustion for the subsequent two sequences, particularly following shutdown where thick smoke was observed to billow from the nozzle (See Figure 3.7-8). Pressure traces for these burns appeared normal. The

thruster immediately shut down as the result of an ignition chamber pressure spike when restart from 500 ºC preheat temperature was attempted.

- Sequences 14, 16, 22, 23, and 20 were completed (in the order listed) normally as planned, with remaining planned sequences omitted to preserve adequate propellant for a final steady-state burn (Sequence 26) of sufficient duration for the catalyst bed to approach thermal equilibrium.
- Testing concluded with Sequence 26, which consumed all remaining expellable propellant over 18 seconds of normal steady-state operation.

1. Initially preheated above the target 288 ºC (550 ºF) start temperature, the catalyst bed heaters are deactivated and the firing sequence set to automatically initiate once Tbed1
falls to the target value.

2. A large puff of smoke is observed to exit the thruster nozzle upon initial start-up.

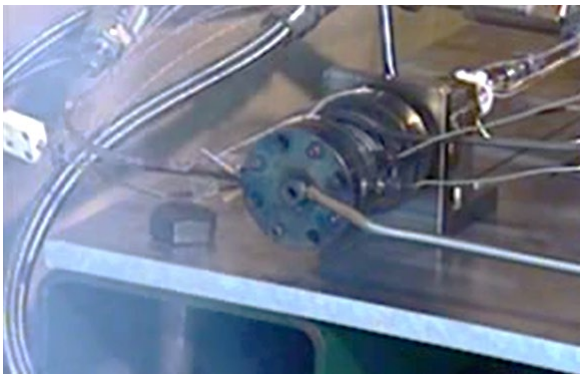

3. Chamber pressure rises and levels off. Throughout the burn, diffuse smoke visible in the plume steadily accumulates in the test cell.

4. A dense smoke is observed exiting the nozzle immediately upon shutdown and persisting for approximately ten seconds. Thereafter smoke continues to billow from the nozzle at low velocity, diminishing to negligible despite intermittent resurgences over an approximately 20 second interval.

Figure 3.7-8 Video images from five-second burn initiated from 288 ºC (550 ºF) preheat temperature

A summary of all completed test sequences is compiled in Table 3.7-6.

Table 3.7-6 Test 3 As-Run Test Matrix

File	Seq.	Tank Pressure (psig)	Pfeed (psig)	Duty Cycle On (sec)	Duty Cycle Off (sec)	# of Pulses	Time to Next Sequence	Purpose	Preheat Temperature (ºF)	Comments/Observations
1								Preheat		
2	1	245	370	0.12	5	10	As required to cool to preheat temper-ature for next run.	Preliminary Stability Assessment.	900	Erratic first pulse. Normal thereafter.
3	2	245	370	0.5	5	10				
4	3	245	370	15	0	1				
4	4	245	370	1	0	1	10 sec	Hot start.	As left by previous sequence	
5	5	245	370	5	0	1	As required to cool to preheat temperature for next run.	Minimum Catalyst Bed Preheat Temperature Assessment.	800	
6	6	245	370	5	0	1			700	Wisps of smoke seen in plume.
7	7	245	370	5	0	1			600	Significant smoke exiting nozzle, particularly after shutdown.
8	8	245	370	5	0	1			550	Significant smoke exiting nozzle, particularly after shutdown.
9	9	245	370	1.1	0	1			500	Shut down resulting from ignition chamber pressure spike.
10	14	245	370	0.5	5	10	Allow to cool to <1100 ºF	Extended stability assessment.	>800	
11	16	245	370	0.5	1	10				
12	22	245	370	0.02	5	10				
13	23	245	370	0.05	5	10				
14	20	245	370	0.5	0.05	10				
15	26	245	370	17.7	0	1	As required to cool to preheat temperature for next run.	Long Burn for SS performance assessment. Repeat as necessary to consume remaining propellant.	>800	Ran out of propellant.

Stability Testing: AF-M824S Propellant

Beginning-of-test stability and pulse-mode-performance characteristics were generally similar to the diluted AF-M315E control (Test 1). Chamber pressure traces for the ten pulses of Sequence 2 are shown superimposed in Figure 3.7-9 with pulse order denoted by color progression from blue to red. The same selection of pulse-mode sequences from the extended duty-cycle stability test segment as for the preceding test, shown in Figure 3.7-10, likewise exhibit similar roughness, with the sharper peak observed for pulse sequence 23 (0.05/5 sec on/off) comprising the most discernible difference. No indication of chamber pressure instability was observed for all sequences started from >288 ºC (550 ºF) (chamber pressure spiking was observed for the lowest-temperature starts discussed in the next section).

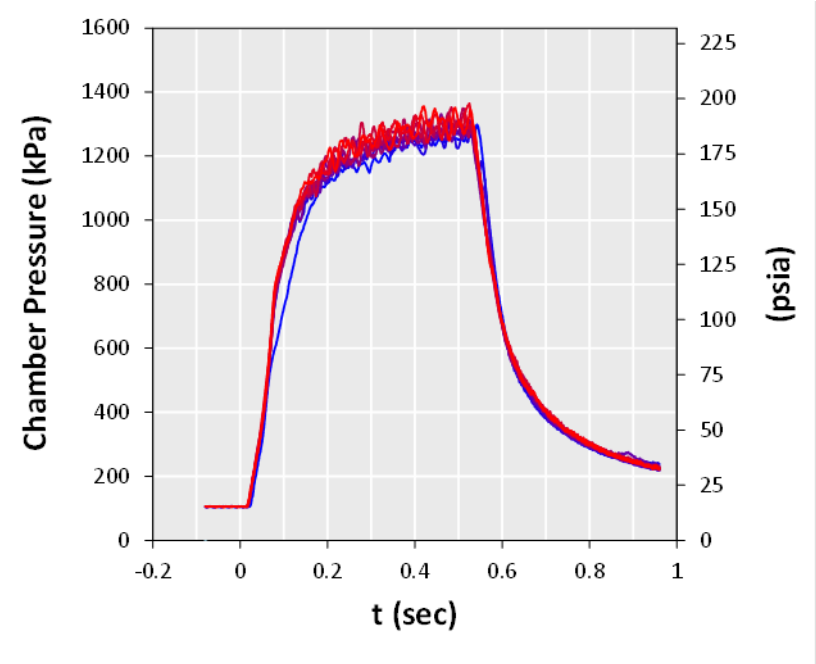

Figure 3.7-9 Stability assessment Seq. 2 (0.5/5 sec on/off) pulses of M824S

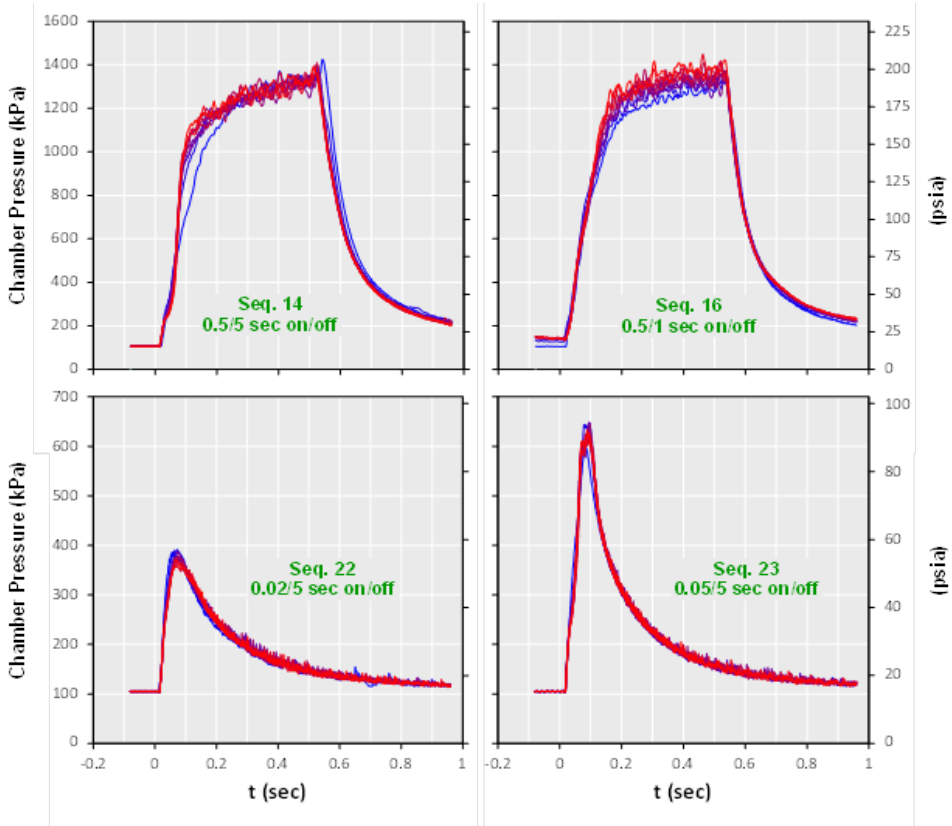

Figure 3.7-10 Selected extended stability assessment sequence pulse overlays of M824S

Minimum Preheat Temperature: AF-M824S Propellant

Chamber pressure traces for the series of five-second burns initiated from progressively lower catalyst bed preheat temperatures are superimposed for comparison in Figure 3.7-11. Response time is observed to fall less with each preheat temperature decrement. An initially small ignition overshoot appears at 316 ºC (600 ºF), increasing incrementally for the subsequent 288 ºC (550 ºF) start but precipitously thereafter, resulting in a 3150 kPa (442 psig) chamber pressure spike and automated test shutdown when restart was attempted from 260 ºC 500 ºF. Also distinct is that chamber pressure is not observed to asymptote toward a common start-temperature-independent steady pressure within the duration of the burns as in the prior test cases. That is demonstrated instead an evident correlation where lower temperature ignition transients resolve (at least initially) into reduced-chamber-pressure modes of operation suggests the normally highly transient state of increased catalyst bed flooding (with unreacted propellant) expected to develop during startup may exhibit greater persistence for the AF-824S propellant, presumably as a result of poorer upstream heat transfer and/or heat generation by the incomplete combustion indicated in the videographic data. This hypothesis is corroborated by the data plotted in Figure 3.7-12, where the increase in temperature measured at the edge of the plenum downstream of the catalyst bed (Tplenum) over each run demonstrates an opposite trend from that observed in Test 1 and the positive variance with the difference between initial catalyst bed and propellant flame temperatures as would be expected for complete combustion. Notably, the temperature at the plenum wall rose less than half as much as for the diluted AF-M315E control case, despite the significantly higher theoretical flame temperature of the AF-M824S propellant.

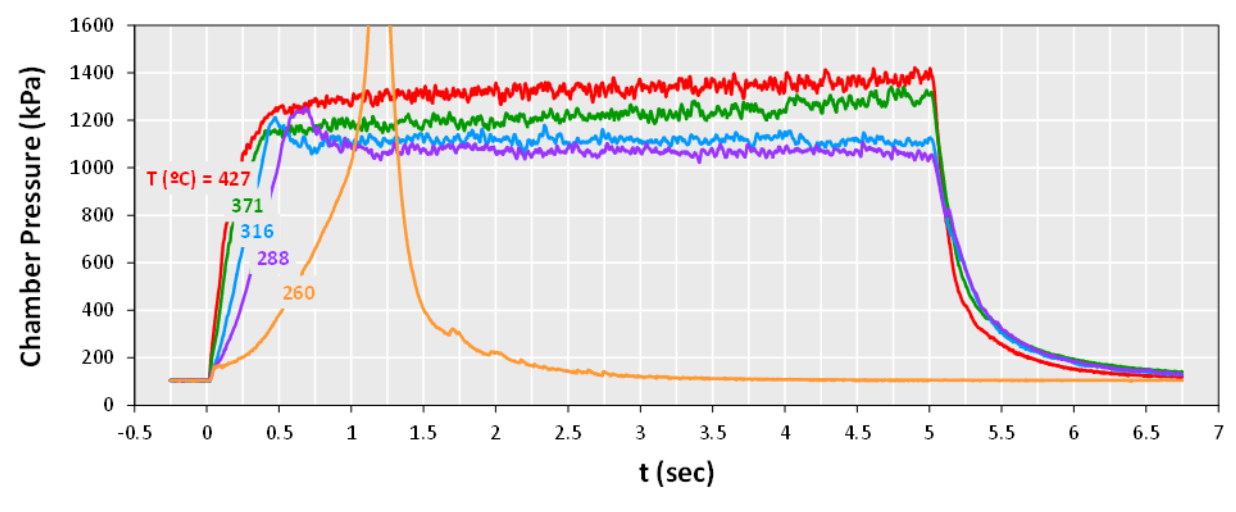

Figure 3.7-11 : M824S Five-second burns executed at progressively reduced catalyst bed preheat temperature

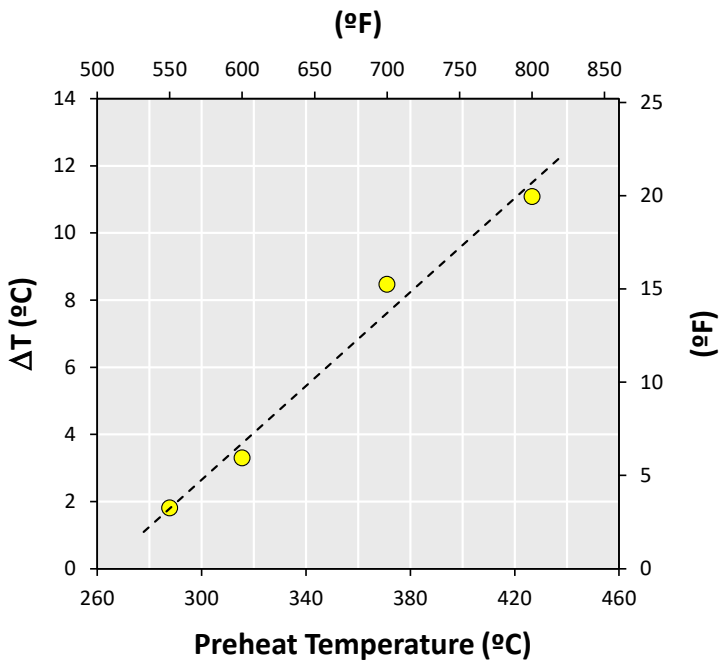

Figure 3.7-12 Rise in temperature measured by Tplenum vs. catalyst bed preheat temperature (Tbed1)

Test 4: Carbohydrazide Nitrate-Based Propellant

Propellant composition (by weight): 74.5% Carbohydrazide nitrate/10.5% EAN/15% Water

Hot-Fire Test Operations Summary:

1 Tank pressure was set to 1791 kPa (245 psig), corresponding to a thruster non-operating feed pressure of 2653 kPa (370 psig).

2 Initial stability assessment Sequences 1-4 completed normally, save that the very first pulse of the test exhibited an erratic chamber pressure profile. During operation thruster feed pressure was observed to drop to 2598 kPa (362 psig).

3 Minimum catalyst bed preheat sequences were initiated per plan at 427 ºC (800 ºF), but halted after the first sequence in order to increase feed pressure to 2030 kPa (280 psig) to increase steady-state chamber pressure (and thrust) for better comparability to the prior tests. Thereafter, the thruster was reheated, and Sequence 5 repeated, followed by the planned series of progressively lower temperature starts. Chamber pressure rise time demonstrated similar reduction with reduced preheat temperature as observed for the Test 1 diluted AF-M315E control. The thruster rapidly washed out when restart was attempted from 260 ºC (500 ºF), 29 ºC (50 ºF) higher than that required to achieve the same result in the control case.

4 Sequences 14, 16, 22, 15, 23, 24 and 17 were executed and completed (in the order listed) normally, with remaining planned sequences omitted to preserve propellant for the final steady-state burn (Sequence 26).

5 Testing concluded with Sequence 26, which consumed all remaining expellable propellant in just under 10 seconds of normal steady-state operation.

A summary of all completed test sequences is compiled in Table 3.7-7.

Table 3.7-7: Test 4 As-Run Test Matrix

Seq.	Tank Pressure (psig)	Pfeed (psig)	Duty Cycle On (sec)	Duty Cycle Off (sec)	# of Pulses	Time to Next Sequence	Purpose	Preheat Temperature (ºF)	Comments/Observations
							Preheat		
1	245	370	0.12	5	10	As required to cool to preheat temper-ature for next run.	Preliminary Stability Assessment.	900	
2	245	370	0.5	5	10				
3	245	370	15	0	1				
4	245	370	1	0	1	10 sec	Hot start.	As left by previous sequence	
5	245	370	5	0	1			800	
							Preheat		
5	280	420	5	0	1	As required to cool to preheat temperature for next run.	Minimum Catalyst Bed Preheat Temperature Assessment.	800	
6	280	420	5	0	1			700	
7	280	420	5	0	1			600	
8	280	420	5	0	1			550	
9	280	420	5	0	1			500	Visible smoke exiting thruster nozzle. Shut down on low Pc.
14	280	420	0.5	5	10	Allow to cool to <1100 ºF	Extended stability assessment.	>800	
16	280	420	0.5	1	10				
22	280	420	0.02	5	5				
15	280	420	0.5	2	10				
23	280	420	0.05	5	10				
24	280	420	0.25	5	10				
17	280	420	0.5	0.5	10				
26	280	420	60	0	1	As required to cool to preheat temperature for next run.	Long Burn for SS performance assessment. Repeat as necessary to consume remaining propellant.	>800	Ran out of propellant.

Stability Testing: Carbohydrazide Nitrate-Based Propellant

Beginning-of-test stability and pulse-mode-performance characteristics were generally similar to the diluted AF-M315E control case except as exhibiting a substantially greater, but acceptable, degree of chamber pressure roughness. Chamber pressure traces for the ten pulses of Sequence 2 are shown superimposed Figure 3.7-13 with pulse order denoted by color progression from blue to red. Pulse-mode sequences from the extended duty-cycle stability test segment, shown in Figure 3.7-14, likewise exhibit similarly increased roughness compared to the prior tests, save where comprising pulses of insufficient duration for chamber pressure to approach steady-state levels (Sequence 22). No indication of appreciable chamber pressure instability (spiking or large-scale signing) was observed throughout the test.

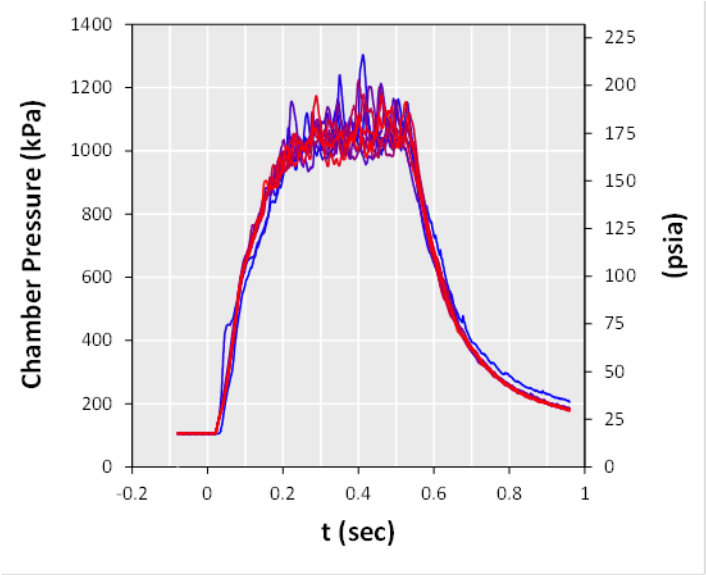

Figure 3.7-13: Stability assessment Seq. 2 (0.5/5 sec on/off) pulses of Carbohydrazide Nitrate Candidate

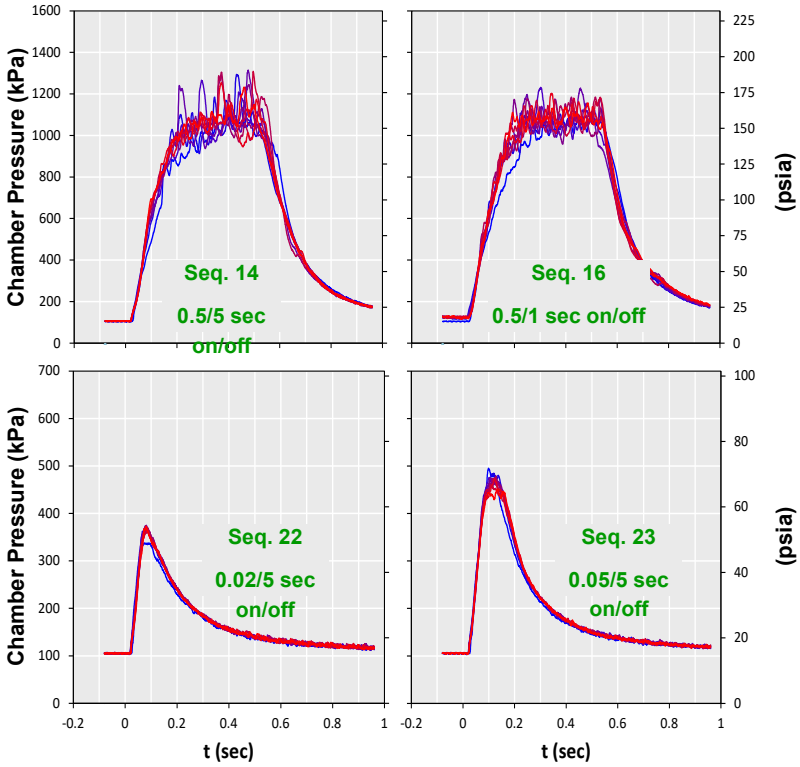

Figure 3.7-14 Selected extended stability assessment sequence pulse overlays of Carbohydrazide Nitrate Candidate

Minimum Preheat Temperature: Carbohydrazide Nitrate-Based Propellant

Chamber pressure traces for the series of five-second burns initiated from progressively lower catalyst bed preheat temperatures, superimposed for comparison in Figure 3.7-15, demonstrate similar overhaul behavior as was seen in the diluted AF-M315E control-case test, with a consistently more abrupt roll-over from the slope of the pressure rise to steady-state being the most notable difference. While thruster response time exhibited nearly identical fall-off with each preheat decrement as the control case, washout occurred at 28 ºC (50 ºF) higher start temperature. Interpolation based on the severity of the observed washouts suggests the actual difference in minimum start temperature to be closer to 17 ºC (30 ºF). Interestingly, tail-off times demonstrated significantly less corresponding variation than in the case of the control propellant, suggesting reduced liquid bed penetration at the moment of thruster shut-down.

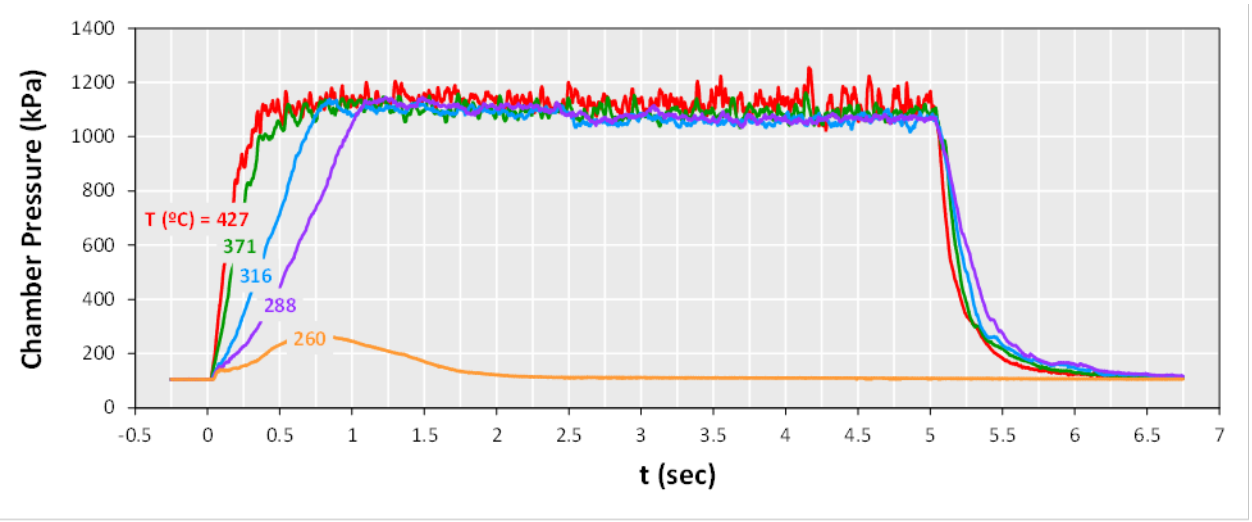

Figure 3.7-15 Carbohydrazide Nitrate Candidate Five-second burns executed at progressively reduced catalyst bed preheat temperature

Data Analysis

Response Time Comparison

Whereas conventional hydrazine thrusters may be started from catalyst bed preheat temperatures as low as -40 ºC/ºF, state-of-the-art AF-315E thrusters require a minimum preheat temperature of 316 ºC (600 ºF) to reliably start, a performance feature principally determined by the propellant's activity with the best-known catalyst for it, that being iridium metal. Owed its direct impact on thruster required preheat power, minimum start temperature is, therefore, readily

identified as a key propellant performance metric. To facilitate such a comparison, response time to 50% steady-state chamber pressure (taken as the average chamber pressure over the last one second of each run) is plotted vs. preheat temperature in Figure 3.7-16 for each of the propellants investigated in the present test series, yielding the following observations:

1. The diluted AF-M315E, AF-315F, and CBH-based propellants demonstrated nearly identical response times, irrespective of the fact that the latter two propellant washed out at respectively 50 ºC (100 ºF) and 28 ºC (50 ºF) higher preheat temperature.
2. The AF-M824S propellant exhibited substantially faster response times over the entire range tested than the lower temperature propellants, despite the signs of incomplete combustion evident in the videographic data.
3. At elevated start temperatures response time appeared to asymptote to a similar limit 50% response time of ~0.14 sec for all propellants tested.

Response characteristics show better differentiation in the plot to 10% chamber pressure presented in Figure 3.7-17. The response time data rank according to a general, but not absolute correlation with flame temperature.

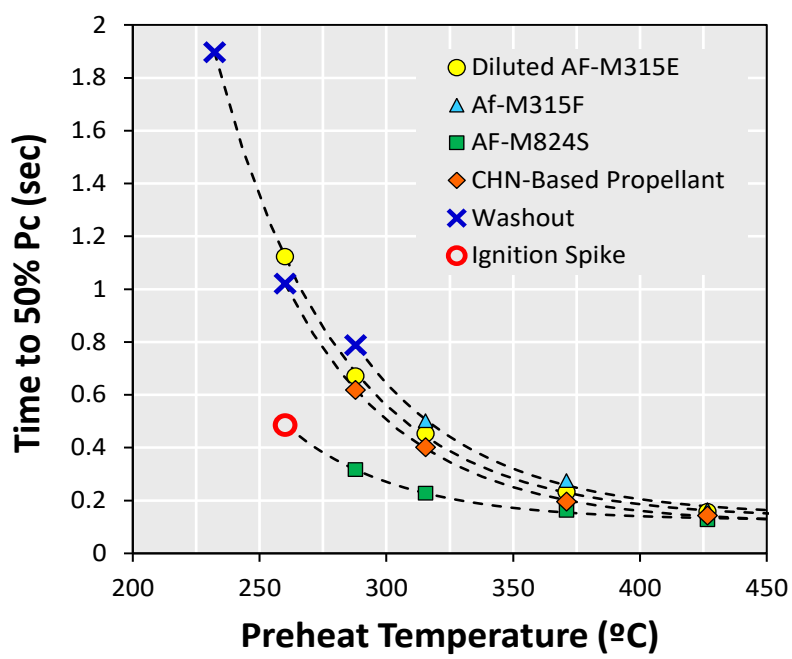

Figure 3.7-16 Chamber pressure 50% response time vs. preheat temperature for all propellants tested

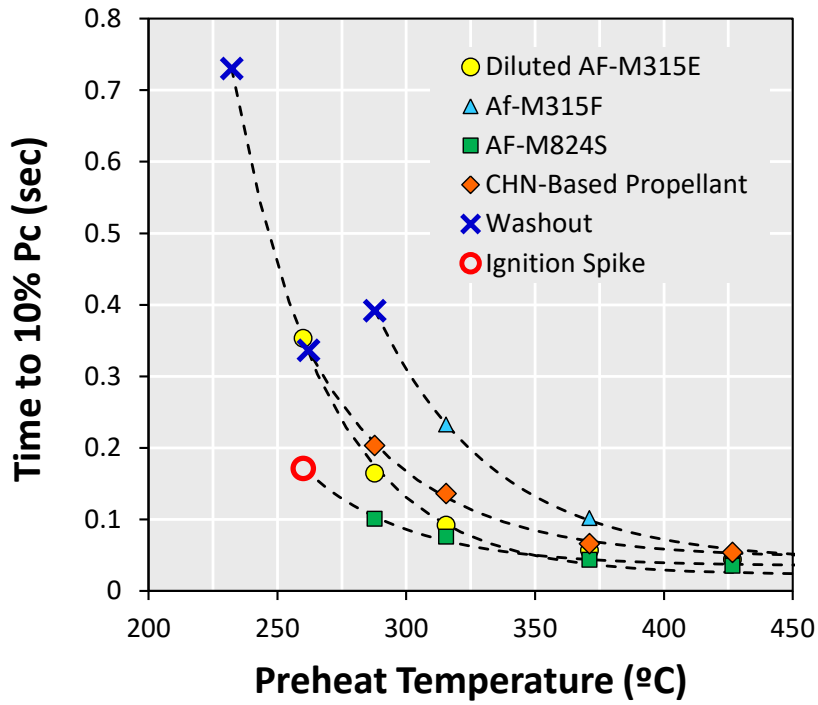

Figure 3.7-17 Chamber pressure 10% response time vs. preheat temperature for all propellants tested

Specific Impulse

While the test setup incorporated no means of direct thrust measurement, delivered thrust for each test performed on the present effort can be estimated from chamber pressure by leveraging reference thrust data taken during testing of the functionally equivalent (in terms of catalyst bed and throat diameter) GR-1 thruster conducted on the Green Propellant Infusion Mission (GPIM) and approximating thrust coefficient as unchanged. Taken in conjunction with measured propellant tank piston displacement (via the integral linear variable differential transformer), computed curves of approximate delivered Isp over the course of the extended burns concluding each test are presented in Figure 3.7-18. The present data have been scaled to estimate predicted performance in an corresponding flight-like thruster by setting similarly-calculated Isp for data taken previously for the same lab model thruster operating on full-strength AF-M315E propellant as corresponding to values derived from flow-rate and thrust stand measurements taken during GPIM flight-weight thruster testing (226 sec at 1 N thrust). The resulting traces, depicting the evolution of estimated delivered Isp as the heavyweight lab model thruster steadily warms, generally trend toward the theoretical values of delivered vacuum Isp (see Table) for each propellant, with the exception of the carbohydrazide-based propellant case, where the final burn is

of insufficient duration to facilitate a reasonable assessment. It should be noted that observable difference in the relative rise rates of the various traces are not directly meaningful in the same respect, however, being strongly influenced by relative differences in operating thrust. (Owed the limited propellant quantities available and variability in viscosity of the various propellants tested, it proved impractical to achieve close matching of the operating point across all tests.)

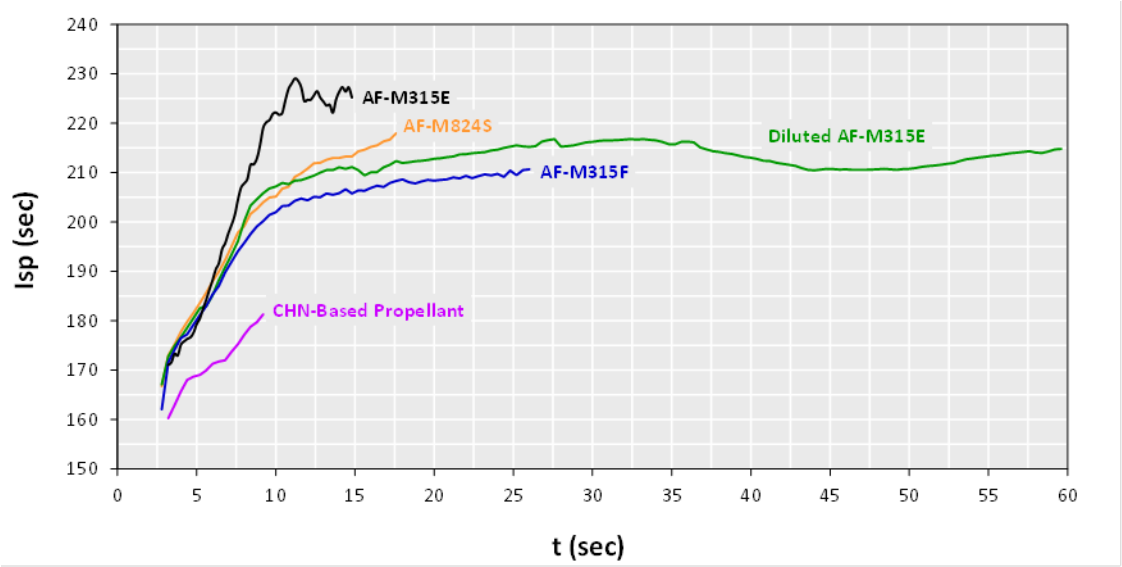

Figure 3.7-18 Comparison of estimated moving average Isp for propellants tested

Conclusions

Three new green monopropellant blends and one diluted AF-M315E control-case propellant were hot-fire tested on the Strategic Environmental Research and Development Program. All propellants demonstrated case-specific minimum preheat temperatures from which stable operation of a heavyweight lab model thruster could be successfully initiated. Whereas the AF-M315F and carbohydrazide nitrate-based propellants respectively exhibited typical benign washouts at 288 ºC (550 ºF) and 260 ºC (500 ºF), the AF-M825S propellant was seen to rise to reduced post-ignition-transient steady-state chamber pressure as starts from progressively lower preheat temperature were similarly attempted, ultimately giving way to substantially delayed ignition followed by a chamber pressure spike when operation was initiated from 260 ºC (500 ºF). While in all cases requiring moderately higher preheat temperatures than the 260 ºC (500 ºF) of diluted AF-M315E control case, the tested experimental propellants provide an expanded range of formulations delivering similar Isp versus flame temperature while offering other potential benefits such as reduced viscosity and enhanced storage stability.

Recommendations for Future Work

Findings of the four propellant hot-fire tests and subsequent data analysis conducted on the SERDP program reveal a number of opportunities where follow-on investigation would potentially significantly further the state-of-the-art, as follows:

1. A better understanding of what factors affect the observed 100 ºC discrepancy in the minimum required start temperature between the AF M315F experimental propellant versus AF M315E would provide invaluable insight, particularly in light of the fact that this difference is not accompanied by an appreciable corresponding difference in chamber pressure response time at equivalent start temperatures. Whereas the two propellants vary significantly in both equivalence ratio and the substitution of AN versus HAN as the oxidizer, the performance of a test with an intermediate propellant variant, either employing AN at equivalence ratio closer to AF-315E or at similar equivalence ratio to AF M315F using HAN instead of AN, would facilitate the isolation of these variables.

2. The mechanism leading to the propensity for chamber pressure spikes and ignition observed for the HEATN-based AF M824S propellant should be further explored. This is particularly of interest owed the significantly lower rise in chamber pressure response time with reduced start temperature demonstrated by the propellant. Pragmatically, the potential to produce a hybrid blend coupling the accelerated response times with more favorable stability characteristics by combining HEATN with other constituents, such as those comprising the other propellants tested, merits investigation.

3. Demonstrating competitively low minimum start and similar response characteristics to the other propellants investigated, the completed test series establishes carbohydrazide nitrate-based propellants as a potentially promising alternative to AN or HAN. However, based on thermal stability test results obtained on the present effort, a necessary first step toward practical implementation will be to establish an better understanding of stability-related formulation constraints and/or determine a method to improve the fundamental storage stability of the carbohydrazide nitrate.

4.0 Summary

Candidate formulations were identified that met program requirements for performance, flame temperature, and showed significantly improved toxicity over hydrazine. During the course of the WP-2400 effort, the partnership between AFRL, AMRDEC, University of Delaware, Army Public Health Center and AR has allowed for the evaluation of over 70 EILs and the synthesis of over 20 candidates. This successful effort was only possible by the collaboration combining propulsion, predictive modeling and toxicity testing. The program assessed triazoles, tetrazoles, pyrimidiums, dinitramides, and imidazoles cations and nitrate anions as possible less toxic hydrazine replacements. The results from Task 1and 2 allowed the team to focus on candidates that possessed characteristics that maximized safety/stability, reactivity and system compatibility. The ideal features were determined to be an active N-NH2 functionality which provides good ignition, heat of formation and reactivity along with active heterocyclic centers (i.e. 1,2,4-triazoles), higher nitrogen content and higher density. Undesirable features which prevented candidates from being selected were thermal stability, catalytic activity, performance, safety hazards and difficulty in synthesis.

Overall the program was able to select less toxic candidate formulations as hydrazine replacements for Hot Fire testing. All candidates exhibited acceptable sensitivity (i.e. ESD, impact, thermal stability) and were successfully scaled-up for Hot Fire testing. With the appropriately heated catalyst bed, the hot fire testing showed rapid ignition and stable combustion. Each candidate selected for testing had unique characteristics: Both HAN oxidized and non-HAN oxidized formulations were evaluated with a variety of cations including HEHN, HEATN and CDN. The cation MATN was too difficult to purify and the impurities represented a toxicity challenge.

The formulations identified were not fully optimized; performance measurements in flight weight hardware need to be made to provide accurate performance assessment. Since the candidate formulations possess low flame temperature they should be compatible in existing hardware and therefore can be readily assessed. This technology will require heated catalyst beds; tuning of the catalyst bed technology will further improve design performance.

Final toxicological testing is being conducted and will further guide final formulation selection. This testing will be conducted by the Army Public Health Center and will cover toxicity, mutagenicity and other environmental characteristics.

The SERDP WP-2400 effort brought together unique organizations and technical expertise to tackle the complex technical challenge of providing a monopropellant formulation with the attributes of hydrazine while eliminating its characteristic toxicity. This successful effort provides the foundation for the elimination of hydrazine as a monopropellant fuel.

4.1 Formulation Rankings

Candidate	Ingredient	Oxidizer	Isp	Tc (K)	Synthesis	Hazards/ Thermal Stability	Toxicity (Data to date)	Cost	Hot Fire Testing	Maturity Level	Ranking (1 Best-5 Worst)	Overall Benefits
1-methyl-4-amino-1,2,4-triazolium nitrate	Synthesis at AR	HAN	203	1452	Issue with purity of scaled- up synthesized material	Acceptable properties	Expected	High Cost	NT	Low	5 -Synthesis issue with purity causes concern with material cost and reproducibility	Good performance & toxicity
Carbohydrazinium nitrate	Synthesis at AR	No Oxidizer	226	1322	Easy synthesis from commercially available materials	Acceptable properties	TBD	Low Cost	Good Stability	Low	2 Low maturity level but high performance and commercially available	Good performance & commercially available
Diluted M315E	HEHN	HAN	221	1453	Scaled-up and cost effective relative to hydrazine	Acceptable properties	Improved over N2H4	Low Cost	Good Stability	High	2 -High Maturity	Modified heritage & characterized formulation
M315F	HEHN	AN	239	1457	Comparable to M315E using low-cost AN	Acceptable properties	Improved over N2H4	Low cost	Good Stability	Medium	2 Improved toxicity and good performance	Increased stability & low toxicity
M824S	HEATN	HAN	243	1900	Improved cost to Hydrazine	Acceptable properties	TBD	Medium cost	Combustion concerns	Medium	4 Incomplete combustion is a concern	Increased stability & low toxicity

5 References

Brand, A., Hawkins, T. W., Drake, G., Ismail, I. M., Warmoth, G., & Hudgens, L. (2006). Energetic Ionic Liquids as TNT Replacements.

Chatel, G., Pereira, J., Debbeti, V., Green, H. W., 2014. (2014). Mixing ionic liquids–"simple mixtures" or 'double salts'? *Green Chemistry*, *16*, 2051–2083.

Christofferson, S., Wucherer, E., & Zube, D. (2001). Tools for monopropellant catalyst development (p. 463). Presented at the 37th Joint Propulsion Conference, Salt Lake City, UT: American Institute of Aeronautics and Astronautics. http://doi.org/10.2514/6.2001-3941

Clark, P. E., Clow, A., Easterbrook, E. K., Haendler, H. M., & Iddles, H. A. (1949). Ternary Systems with Ammonium Nitrate and Guanidine Nitrate. *The Journal of Physical Chemistry*, *53*(7), 1009–1015. http://doi.org/10.1021/j150472a003

Drake, G., Hawkings, T., Hall, L., Boatz, J., & Vij, A. (n.d.). Experimental and Theoretical Study of l,5-diamlno-l,2,3,4-Tetrazolium Perchlorate. *Researchgate.Net*

Drake, G., Hawkins, T., Brand, A., Hall, L., Mckay, M., Vij, A., & Ismail, I. (2003). Energetic, Low-Melting Salts of Simple Heterocycles. *Propellants, Explosives, Pyrotechnics*, *28*(4), 174–180. http://doi.org/10.1002/prep.200300002

Drake, G., Hawkins, T., Brand, A., Hall, L., Mckay, M., Vij, A., & Ismail, I. (2003). Energetic, Low-Melting Salts of Simple Heterocycles. *Propellants, Explosives, Pyrotechnics*, *28*(4), 174–180. http://doi.org/10.1002/prep.200300002

Drake, G., Hawkins, T., Brand, A., Hall, L., Mckay, M., Vij, A., & Ismail, I. (2003). Energetic, Low-Melting Salts of Simple Heterocycles. *Propellants, Explosives, Pyrotechnics*, *28*(4), 174–180. http://doi.org/10.1002/prep.200300002

Drake, G., Hawkins, T., Tollison, K., Brand, A., & Mckay, M. (2003). Low Melting Salts. Presented at the JANNAF PDCS Meeting.

Drake, G., Kaplan, G., Hall, L., Hawkins, T., & Larue, J. (2006). A new family of energetic ionic liquids 1-amino-3-alkyl-1,2,3-triazolium nitrates. *Journal of Chemical Crystallography*, *37*(1), 15–23. http://doi.org/10.1007/s10870-005-9021-0

Driscoll, E., & Spores, R. (2015). Establishing a Complete Product Line Life Cycle for Green Propellants (pp. 1–16). Presented at the Green Monopropellant Alternatives to Hydrazine JANNAF/NIRPS Joint Technical Interchange Meeting.

G. W. Drake, et. al, Propellants Explos. Pyrotech. 2003, 28, 174 - 180) (xref)

Galbraith, L. D., Holland, G. F., Poole, D. R., & Mitchell, R. M. (1995, June 13). Apparatus for suppressing a fire. *US Patent Office*. US Patent Office.

H Xue et al. (Shreeve) Chem. Mater., 2005, 17, 191-198. (xref)

Hawkins, T. (2011). R&D of Energetic Ionic Liquids (pp. 1–25). Presented at the Partners in Environmental Technology.

Hawkins, T. W., Brand, A. J., Mckay, M., & Tinnirello, M. (2012). Research and Development of Energetic Ionic Liquids. Presented at the 243rd American Chemical Society ACS National Meeting.

Hawkins, T. W., Drake, G. W., & Brand, A. J. (2010). Energetic ionic liquids. *US Patent Office*. US Patent Office.

Kamal, F., Yann, B., Rachid, B., & Kappenstein, C. (2011). Application of ionic liquids to space propulsion. In *Applications of Ionic Liquids in Science and Technology* (pp. 447–466).

Sackheim, R. L., & Masse, R. K. (2014). Green propulsion advancement: challenging the maturity of monopropellant hydrazine. *Journal of Propulsion and Power*, *30*, 265–276.

Scheffee, R. S., & Wheatley, B. K. (1998, December 15). Eutectic mixtures of ammonium nitrate, guanidine nitrate and potassium perchlorate. *US Patent Office*.

Scheffee, R. S., & Wheatley, B. K. (1998, March 10). Eutectic mixtures of ammonium nitrate and amino guanidine nitrate. *US Patent Office*. US Patent Office.

Singh, R. P., Verma, R. D., Meshri, D. T., & Shreeve, J. M. (2006). Energetic Nitrogen-Rich Salts and Ionic Liquids. *Angewandte Chemie International Edition*, *45*(22), 3584–3601. http://doi.org/10.1002/anie.200504236

Smiglak, M., Metlen, A., & Rogers, R. D. (2007). The second evolution of ionic liquids: from solvents and separations to advanced materials--energetic examples from the ionic liquid cookbook. *Accounts of Chemical Research*, *40*(11), 1182–1192. http://doi.org/10.1021/ar7001304

Tao, G.-H., Guo, Y., Joo, Y.-H., Twamley, B., & Shreeve, J. M. (2008). Energetic nitrogen-rich salts and ionic liquids: 5-aminotetrazole (AT) as a weak acid. *Journal of Materials Chemistry*, *18*(45), 5524–15. http://doi.org/10.1039/b811506k

Tao, G.-H., Guo, Y., Joo, Y.-H., Twamley, B., & Shreeve, J. M. (2008). Energetic nitrogen-rich salts and ionic liquids: 5-aminotetrazole (AT) as a weak acid. *Journal of Materials Chemistry*, *18*(45), 5524–15. http://doi.org/10.1039/b811506k

Welton, T. (1999). Room-Temperature Ionic Liquids. Solvents for Synthesis and Catalysis. *Chemical Reviews*, *99*(8), 2071–2084. http://doi.org/10.1021/cr980032t

Wilson, K. A., Wilson, M. A., Poole, D. R., Holland, G. F., Primex Technologies, Inc. (1999). Low temperature autoigniting propellant composition.

Wucherer, E. J., & Holland, G. F. (2001, April 17). Fire suppression composition and device. *US Patent Office*. US Patent Office.

Wucherer, E. J., Cook, T., Stiefel, M., Humphries, R., & Parker, J. (2003). Hydrazine catalyst production-sustaining S-405 technology. Presented at the 39th Joint AIAA/ASME/SAE/ASEE Joint Propulsion Conference, Huntsville, AL: American Institute of Aeronautics and Astronautics. http://doi.org/10.2514/6.2003-5079

Xue, H., Gao, H., Twamley, B., & Shreeve, J. M. (2007). Energetic Salts of 3-Nitro-1,2,4-triazole-5-one, 5-Nitroaminotetrazole, and Other Nitro-Substituted Azoles †. *Chemistry of Materials*, *19*(7), 1731–1739. http://doi.org/10.1021/cm062964g

Xue, H., Gao, Y., Twamley, B., & Shreeve, J. M. (2005). New Energetic Salts Based on Nitrogen-Containing Heterocycles. *Chemistry of Materials*, *17*(1), 191–198.

Zhang, Q., & Shreeve, J. M. (2014). Energetic Ionic Liquids as Explosives and Propellant Fuels: A New Journey of Ionic Liquid Chemistry. *Chemical Reviews*, *114*(20), 10527–10574. http://doi.org/10.1021/cr500364t

Zhang, Q., & Shreeve, J. M. (2014). Energetic Ionic Liquids as Explosives and Propellant Fuels: A New Journey of Ionic Liquid Chemistry. *Chemical Reviews*, *114*(20), 10527–10574. http://doi.org/10.1021/cr500364t

G. Drake, et al., "Energetic, low-melting salts of simple heterocycles," Propellants, Explosives, Pyrotechnics, vol. 28, no. 4, pp. 174-180, 2003.

P. Nancarrow and H. Mohammed, "Ionic Liquids in Space Technology–Current and Future Trends," ChemBioEng Reviews, 2017.

Q. Zhang and J. N. M. Shreeve, "Energetic ionic liquids as explosives and propellant fuels: a new journey of ionic liquid chemistry," Chemical reviews, vol. 114, no. 20, pp. 10527-10574, 2014.

C. H. McLean, et al., "Green propellant infusion mission program overview, status, and flight operations," in 51st AIAA/SAE/ASEE Joint Propulsion Conference, Orlando, 2015.

R. A. Spores, et al., "GPIM AF-M315E propulsion system," in 51st AIAA/SAE/ASEE Joint Propulsion Conference, Orlando, 2015.

I. M. Ismail and T. W. Hawkins, "Adiabatic Compression Sensitivity of Liquid Fuels and Monopropellants," DTIC, 1999.

P. Quach, G. Warmoth and A. Brand, "Adiabatic Compression Sensitivity of AF-M315E," in 51st AIAA/SAE/ASEE Joint Propulsion Conference, Orlando, 2015.

D. B. Scharfe, G. Gabrang, P. Adkison, et al., "Microreactor testing with AF-M315E," in JANNAF Propulsion Meeting, Phoenix, 2016.

P. Adkison, G. Gabrang, et al., "Drop In Testing of AFM315E and AFM315Q with Busek 0.5N Thruster," in JANNAF Propulsion Meeting, Phoenix, 2016.

F. Kamal, B. Yann, B. Rachid and K. Charles, "Application of ionic liquids to space propulsion," Applications of Ionic Liquids in Science and Technology, 2011.

T. W. Hawkins, A. J. Brand, M. B. McKay and M. Tinnirello, "Reduced toxicity, high performance monopropellant at the US Air Force Research Laboratory (No. AFRL-RZ-ED-TP-2010-219," DTIC, 2010.

A. J. Brand and G. W. Drake, "Energetic hydrazinium salts". U. S. Patent 6,218,577, 17 April 2001.

6 Appendices

Appendix A- Summary of Material Candidates and Properties

Compound Name	Molecular Formula CHNO	MW, g/mol	ΔH_0^f, kJ/mol (est)	$\Delta H_{(f, est)}$, kcal/mol	$\rho_{(est)}$, g/cc	mp, °C	DSC (exo) Onset, °C	Wt loss % (TGA, 48 h @ 75° C)	Impact, kg-cm	Friction, N	ESD Sensitivity* (J)	Availability: Commercial ("C") 1-3 Step ("13") Multistep ("M")
1,2,3-Triazoles												
1,2,3-Triazolium Nitrate			272.142	65.0	1.57	110	125	73.50	200			13
1,2,3-triazole perchlorate						73	200	0.05	5			13
1,2,3-triazole dinitramide					1.64	61	80		5			13
1-Amino-1,2,3-triazolium nitrate (tbd)			119.3	28.5	1.75	99	178	50.00				13
1-methyl-1,2,3-triazolium nitrate	C3H6N4O3	146	-20.934	-5.0	1.44	105	200	50.00				M
1-amino-3-methyl-1, 2, 3-triazolium nitrate	C3H7N5O3	161.1	146.538	35.0	1.57 (1.61)	87	185	0.01	200	>371		13
1-amino-3-ethyl-1,2,3-triazolium nitrate (1b)						30	165	unk				

1-amino-3-propyl-1,2,3-triazolium nitrate (1c)						33	165	unk				
1-amino-3-(2-propenyl)-1,2,3-triazolium nitrate (1d)						8	135	unk				
1-amino-3-butyl-1,2,3-triazolium nitrate (1e)						48	175	unk				
1-amino-3-(2-hydroxyethyl)-1,2,3-triazolium Nitrate	C4H9N5O4	191.14	-125.604	-30.0	1.53	-	unk	unk				M
1,3-Diamino-1,2,3-triazolium nitrate	C2H6N6O3		230.274	55.0	1.71	-	unk	unk				M
1,2,4-Triazoles												
1,2,4-triazole nitrate	[C2H4N3]NO3 = C2H4N4O3	132	-142.3512	-34.0	1.55	137	182	0.88	200			13
1,2,4-triazole perchlorate			-71.1756	-17.0		-	285	0.03	114			13
1,2,4-triazole dinitramide						75	120	1.62	98			13
1-Amino-1,2,4-triazolium Nitrate	C2H5N5O3		46	11.0	1.51	-62	217	unk				

[1-amino-124-Triazolium][3-nitro-124Tri-5-one] Shreeve #2	[C2H5N4][C2HN4O3]= C4H6N8O3		498.8	119.1	1.67	71	188	unk				M
1-amino-4-methyl-1,2,4-Triazolium Nitrate	C3H7N5O3	161	-174.68	-41.7	1.51	-62	217	unk				
1-methyl-5-amino-1,2,4-Triazolium Nitrate	C3H6N3O4		nr			-60	221	unk				
1,4-Diamino-1,2,4-triazolium nitrate	C2H6N6O3	162	104.67	25.0	1.71	-	212	unk	175	80		13
1-(2-hydroxyethyl-4-amino-1,2,4-triazolium Nitrate	C4H9N5O4	191	-314.01	-75.0	1.47	-	unk					13
N-1-Ethoxy-1,2,4-triazolium nitrate	C4H6N4O4		-360.0648	-86.0	1.45	-	unk					
1-Methyl-1,2,4-triazolium nitrate	C3H6N4O3	146	-113.0436	-27.0	1.44	125	220	50.00				13
1-Methyl-3-methoxy-1,2,4-triazolium nitrate (1-methyl-3-hydroxymethyl-4-H-1,2,4-triazolium nitrate)	C4H7N4O4	175	-376.812	-90.0	1.53	90	150	50.00				13

1-Methyl-4-Amino-1,2,4-Triazolium Nitrate (1M4ATN)	C3H7N5O3	161	93.36564	22.3	1.55	54	185					13
1,4-Dimethyl-1,2,4-triazolium nitrate (DMTN)	C4H8N4O3	160.11	**-125.604**	-30.0	1.32	1	212	unk	175	80		13
[4-amino, 1-Ethyl-1,2,4-triazolium][nitrate], [AETri]NO3						-5	160					

3-Amino-1,2,4-triazolium nitrate (3ATN)	C2H5N5O3	147	-171.6588	-41.0	1.6	179	188	0.40	175	80		13
3,4-Diamino-1,2,4-triazolium nitrate (34ATN)	C2H6N6O3		-46.0548	-11.0	1.6	-	unk					13
3,5-Diamino-1,2,4-triazolium nitrate (35ATN)	C2H6N6O3		-234.4608	-56.0	1.63	160	180	0.40	175	240		13

4-Amino-1,2,4-triazolium nitrate (4ATN)	C2H5N5O3	179	-83.736	-20.0	1.65	69	180	0.58	200			13
[4-amino-1,2,4-triazolium] perchlorate [ATri]ClO4			20.934	5.0	1.78	84	210	0.02	30			
[4-amino-1,2,4-triazolium] dinitramide, [ATri]DN						20	146	0.29	5			
4A-124Tri-5AT [4-amino-1,2,4-Triazolium][5AT]; Shreeve#6)	C2H5N4 CH2N5 =C3H7N9		565	134.9	1.62	114	unk					13
3-4-5-TriAmino-124-Triazolium Nitrate				-63.0	1.52	206	245	0.20	200			
[1-amino-124-Triazolium][3-nitro-124Tri-5-one] Shreeve #2	[C2H5N4][C2HN4O3]= C4H6N8O3		498.8	119.1	1.67	71	188					M

4A-1Et-124Tri-5AT 4-amino-1-ethyl-1,2,4-triazolium (5AT) Shreeve #8	C4H9N4 CH2N5 =C5H11N9		523.4	125.0	1.39	-38	unk					M
4A-1Me-124Tri-5AT 4-amino-1-methyl-1,2,4-triazolium (5AT) Shreeve #7	C3H7N4 CH2N5 =C4H9N9		546	130.4	1.46	-24	unk					M
Tetrazoles												
[1-amino-4,5-dimethyltetrazolium][nitrate]	C3H8N6O3		146		1.5	-59	170					
1-Methyl-5-aminotetrazolium nitrate (4-methyl-5-amino?) (4M5ATeN)	C2H6N6O3		-50.2416	-12.0	1.64	162	178	unk	175	120		13

45-Me2-1A-Tet-NO3 4,5-dimethyl-1-amino-tetrazolium nitrate Shreeve #46 Object of Bob's Lust?	C3H8N5-NO3 =C3H8N6O3		129.52	30.9	1.5	-59	unk					
5-Aminotetrazolium nitrate	CH4N6O3		-29.3076	-7.0	1.74	-	unk					13
Greg's un-namable 5-R-Tetrazolium Nitrate, aka 1-H-5 hydrazinium-1,2,4 triazolium nitrate	C3H7N7O4		-334.944	-80.0	1.7	-	unk					
G-5AT (J Shreeve #3)	C2H8N8	144	205.4	49.1	1.5	126	unk					13

MAG-5AT (D Doll / J Shreeve #4)	C2H9N9	159	302.3	72.2	1.5	96	unk					13
GG-5AT (GuanylGuanidinium; Shreeve#5)	C2H8N5 CH2N5 =C3H10N10		306.9	73.3	1.41	141	unk					13
4A-1Me-124Tri-5AT 4-amino-1-methyl-1,2,4-triazolium (5AT) Shreeve #7	C3H7N4 CH2N5 =C4H9N9		546	130.4	1.46	-24	unk					13
4A-1Et-124Tri-5AT 4-amino-1-ethyl-1,2,4-triazolium (5AT) Shreeve #8	C4H9N4 CH2N5 =C5H11N9		523.4	125.0	1.39	-38	unk					13
1-5DA-4Me-1234Tet-5AT-1Et-124Tri-5AT 1,5-diamino-4-methyl-1,2,3,4-tetrazolium (5AT) Shreeve #9	C2H7N6 CH2N5 =C3H9N11		655.1	156.5	1.57	171	unk					13
5AT-5NT 5AT-5-nitro-tetrazolate, Shreeve A	CH3N5 CH2N5O2 =C2H5N10O2		571.4	136.5	1.75	159	unk					

[2-hydroxyethyl-4-amino-124Triazolium][3,5-DiNitro-124-Triazolate], AMT-DNT	[C3H8N4][C2N5O4] =C5H8N9O4	258	318.1968	76.0	1.6	84	234					
Other Heterocycles												
2,4,6-triamino-1-H-pyrimidinium nitrate (TriPyrN)	C4H4N2 C4H8N5-NO3 C4H8N6O3	174	83.736	20.0	1.54	255	300	unk	175	240		13
1-Methyl-Imidazolium Nitrate, [1-MeIm]NO3	[C4H7N2]NO3 = C4H7N3O3	145	-184.7	-44.1	1.25	70	unk					
1-Et-3-Me-Imidazolium Nitrate	[C6H11N2]NO3 = C6H11N3O3					38	unk					
1,2-diamino-imidazolium nitrate	C3H7N5O3		0	0.0	1.63	-	unk					
1,3-Diamino-1H-imidazol-3-ium nitrate	C3H7N5O3		0	0.0	1.63	-	unk					13
[1-amino-3-Methyl-123Triazolium][3,5-DiNitro-124-Triazolate] HEAT-DNT	[C4H9N4O][C2N5O4] =C6H9N9O5	287	0	0.0	1.61	107	200		70			
							unk					

Other Systems							unk					
[4-amino-1,2,4-Triazolium]3* La(NO3)6			-1425.9	-340.6	1.87	81	211					
[1-amino-124-Triazolium][3-nitro-124Tri-5-one]			63.9	15.3	1.67	71	188					
Others - AMRDEC Kickoff Suggestions												
1, 2-dihydroxy-3-aminopropane nitrate	C3H7N5O3		154	-180.0	1.43							13
3-methylammonium-1, 2-propanediol nitrate	C4H12N2O5		168	-185.0	1.24							13
3-Dimethylammonium-1, 2-propanediol nitrate	C5H14N2O5		182	-190.0	1.15							13
3-Diethylammonium-1, 2-propanediol nitrate	C7H18N2O5		210	-200.0	1.12							13
N-methyl-D-glucammonim nitrate	C7H17N2O8		257	-350.0	1.52							13
3-Morpholinium-1, 2-propanediol nitrate	C7H17N3O6		239	-270.0	1.36							13

1-Amino-4-methylpiperazinium nitrate	C5H13N4O3		153	-50.0	1.31							13
1-methyl-piperazinium nitrate	C5H14N3O3		164	-75.0	1.25							13
												13
1,2,4-Triazole-1-carboximidamidimium Nitrate	C2H6N6O3		174	-65.0	1.56							13
1-(2-hydroxyethyl)-4-amino-1,2,4-triazolium nitrate	C3H6N6O3		191	-75.0	1.65							13
1-(2-hydroxyethyl)-4-amino-3, 5-hydroxymethyl 1,2,4-triazolium nitrate	C4H9N5O4		251	-185.0	1.47							13
4-amino-3, 5-hydroxymethyl 1,2,4-triazolium nitrate	C6H13N5O6		207	-110.0	1.57							13
1,4-di-H-3, 5-hydroxymethyl 1,2,4,triazolium nitrate	C4H9N5O5		192	-140.0	1.69							13
												13
1-amino-3-(2-hydroxyethyl) 1,2,3-triazolium nitrate	C4H9N5O4		191	-30.0	1.53							13

Appendix B- Thermochemical Calculations

Table 1: Input deck for the thermochemical program

Water wt%	HAN wt%	Ionic Liquid wt%
10.00	72.00	18.00
10.00	63.00	27.00
10.00	54.00	36.00
10.00	45.00	45.00
15.00	85.00	0.00
15.00	80.75	4.25
15.00	76.50	8.50
15.00	72.25	12.75
15.00	68.00	17.00
15.00	59.50	25.50
15.00	51.00	34.00
15.00	42.50	42.50
20.00	80.00	0.00
20.00	76.00	4.00
20.00	72.00	8.00
20.00	68.00	12.00
20.00	64.00	16.00
20.00	56.00	24.00
20.00	48.00	32.00
20.00	40.00	40.00
25.00	75.00	0.00
25.00	71.25	3.75
25.00	67.50	7.50
25.00	63.75	11.25
25.00	60.00	15.00
25.00	52.50	22.50
25.00	45.00	30.00

25.00	37.50	37.50
30.00	66.50	3.50
30.00	63.00	7.00
30.00	59.50	10.50
30.00	56.00	14.00
30.00	49.00	21.00
30.00	42.00	28.00
30.00	35.00	35.00
40.00	57.00	3.00
40.00	54.00	6.00
40.00	51.00	9.00
40.00	48.00	12.00
40.00	42.00	18.00
40.00	36.00	24.00
40.00	30.00	30.00

Table 2: Alternative M124 Formulations

Water [%]	**HAN [%]**	**M124 [%]**	**Isp** $\left[\frac{lb_f\ s}{lb_m}\right]$
15.00	48.04	36.96	203.21
18.00	48.24	33.76	202.68
21.00	48.44	30.56	202.15
24.00	48.64	27.36	201.63

M123TN1

Water	HAN	Ionic liquid	Ratio HAN/IO	Isp	Pc, K	mol C	mol H	mol N	mol O	Hf [kcal]	Water	HAN
10.00	90.00	0.00	1.00	133.2	880.9	0	0	0	0	0	10	90
10.00	85.50	4.50	0.95	169.4	1196.9	0.092466	0.184932	0.123288	0.092466	-0.15411	10	85.5
10.00	81.00	9.00	0.90	198.5	1490	0.184932	0.369863	0.246575	0.184932	-0.30822	10	81
10.00	76.50	13.50	0.85	235.5	2021.8	0.277397	0.554795	0.369863	0.277397	-0.46233	10	76.5
10.00	72.00	18.00	0.80	264.8	2456.7	0.369863	0.739726	0.493151	0.369863	-0.61644	10	72
10.00	63.00	27.00	0.70	270.3	2541.6	0.554795	1.109589	0.739726	0.554795	-0.92466	10	63
10.00	54.00	36.00	0.60	262.8	2359	0.739726	1.479452	0.986301	0.739726	-1.23288	10	54
10.00	45.00	45.00	0.50	118.1	755	0.924658	1.849315	1.232877	0.924658	-1.5411	10	45
15.00	80.75	4.25	0.95	208.4	1599.6	0.087329	0.174658	0.116438	0.087329	-0.14555	15	80.75
15.00	76.50	8.50	0.90	225.8	1847.1	0.174658	0.349315	0.232877	0.174658	-0.2911	15	76.5
15.00	72.25	12.75	0.85	255.4	2289.6	0.261986	0.523973	0.349315	0.261986	-0.43664	15	72.25
15.00	68.00	17.00	0.80	260.8	2357.2	0.349315	0.69863	0.465753	0.349315	-0.58219	15	68
15.00	59.50	25.50	0.70	253	2169.1	0.523973	1.047945	0.69863	0.523973	-0.87329	15	59.5
15.00	51.00	34.00	0.60	126.2	629.6	0.69863	1.39726	0.931507	0.69863	-1.16438	15	51
15.00	42.50	42.50	0.50	140.9	919.3	0.873288	1.746575	1.164384	0.873288	-1.45548	15	42.5
20.00	76.00	4.00	0.95	215.6	1672.8	0.082192	0.164384	0.109589	0.082192	-0.13699	20	76
20.00	72.00	8.00	0.90	245.4	2108	0.164384	0.328767	0.219178	0.164384	-0.27397	20	72
20.00	68.00	12.00	0.85	250.6	2161.5	0.246575	0.493151	0.328767	0.246575	-0.41096	20	68
20.00	64.00	16.00	0.80	242.9	1981.1	0.328767	0.657534	0.438356	0.328767	-0.54795	20	64
20.00	56.00	24.00	0.70	113.8	504.6	0.493151	0.986301	0.657534	0.493151	-0.82192	20	56
20.00	48.00	32.00	0.60	124.3	781.7	0.657534	1.315068	0.876712	0.657534	-1.09589	20	48
20.00	40.00	40.00	0.50	156.7	1036.8	0.821918	1.643836	1.09589	0.821918	-1.36986	20	40
25.00	71.25	3.75	0.95	234.6	1918.2	0.077055	0.15411	0.10274	0.077055	-0.12842	25	71.25
25.00	67.50	7.50	0.90	239.7	1964.1	0.15411	0.308219	0.205479	0.15411	-0.25685	25	67.5
25.00	63.75	11.25	0.85	232.4	1796.8	0.231164	0.462329	0.308219	0.231164	-0.38527	25	63.75
25.00	60.00	15.00	0.80	100.3	380	0.308219	0.616438	0.410959	0.308219	-0.5137	25	60
25.00	52.50	22.50	0.70	129.9	644	0.462329	0.924658	0.616438	0.462329	-0.77055	25	52.5
25.00	45.00	30.00	0.60	139.9	887.7	0.616438	1.232877	0.821918	0.616438	-1.0274	25	45
25.00	37.50	37.50	0.50	167.5	1114.4	0.770548	1.541096	1.027397	0.770548	-1.28425	25	37.5
30.00	66.50	3.50	0.95	228.1	1768.9	0.071918	0.143836	0.09589	0.071918	-0.11986	30	66.5
30.00	63.00	7.00	0.90	221.5	1616	0.143836	0.287671	0.191781	0.143836	-0.23973	30	63

Atomic Weights

C	H	N	O	
12	1	14	16	-5

	C	H	N	O	MW
Water	0	2	0	1	18
HAN	0	4	2	4	96
IL	3	6	4	3	146

↓	C1	C2	C3	C4	C5	C6	C7	C8	C9	C10	C11	C12	C13	C14	C15	C16	C17	C18
	Water	mol water	HAN	mol han	Ionic liquid	Mol Han/Mol IO	Ratio HAN/IO	O/C Ratio	Isp	Pc, K	Ivol	mol C	mol H	mol N	mol O	Hf [kcal]	ISP_fit	FITS
1	10	0.55556	85.50	0.890625	4.50	28.8958	0.95	45.5	169.4	1196.9	9.7981	0.09247	0.18493	0.12329	0.09247	-0.1541	171.029	1270.88
2	10	0.55556	81.00	0.843750	9.00	13.6875	0.90	22.3	198.5	1490.0	11.3860	0.18493	0.36986	0.24658	0.18493	-0.3082	203.059	1627.93
3	10	0.55556	72.00	0.750000	18.00	6.0833	0.80	10.6	235.5	2021.8	13.2846	0.36986	0.73973	0.49315	0.36986	-0.6164	230.213	1934.52
4	10	0.55556	63.00	0.656250	27.00	3.5486	0.70	6.7	264.8	2456.7	14.6964	0.55479	1.10959	0.73973	0.55479	-0.9247	249.167	2150.54
5	10	0.55556	54.00	0.562500	36.00	2.2813	0.60	4.8	270.3	2541.6	14.7611	0.73973	1.47945	0.98630	0.73973	-1.2329	266.070	2343.93
6	10	0.55556	45.00	0.468750	45.00	1.5208	0.50	3.6	262.8	2359.0	14.1255	0.92466	1.84932	1.23288	0.92466	-1.5411	282.153	2528.26
7	15	0.83333	80.75	0.841146	4.25	28.8958	0.95	49.1	155.8	1057.4	8.7201	0.08733	0.17466	0.11644	0.08733	-0.1455	158.930	1099.70
8	15	0.83333	76.50	0.796875	8.50	13.6875	0.90	24.0	186.0	1337.2	10.3323	0.17466	0.34932	0.23288	0.17466	-0.2911	191.398	1461.51
9	15	0.83333	72.25	0.752604	12.75	8.6181	0.85	15.7	208.4	1599.6	11.4870	0.26199	0.52397	0.34932	0.26199	-0.4366	206.897	1635.87
10	15	0.83333	68.00	0.708333	17.00	6.0833	0.80	11.5	225.8	1847.1	12.3535	0.34932	0.69863	0.46575	0.34932	-0.5822	218.153	1763.36
11	15	0.83333	59.50	0.619792	25.50	3.5486	0.70	7.3	255.4	2289.6	13.7635	0.52397	1.04795	0.69863	0.52397	-0.8733	236.423	1971.48
12	15	0.83333	51.00	0.531250	34.00	2.2813	0.60	5.2	260.8	2357.2	13.8485	0.69863	1.39726	0.93151	0.69863	-1.1644	252.572	2156.18
13	15	0.83333	42.50	0.442708	42.50	1.5208	0.50	4.0	253.0	2169.1	13.2395	0.87329	1.74658	1.16438	0.87329	-1.4555	267.872	2331.49
14	20	1.11111	76.00	0.791667	4.00	28.8958	0.95	53.0	140.9	919.3	7.6396	0.08219	0.16438	0.10959	0.08219	-0.1370	146.617	926.15
15	20	1.11111	72.00	0.750000	8.00	13.6875	0.90	26.0	172.0	1186.3	9.2605	0.16438	0.32877	0.21918	0.16438	-0.2740	179.631	1293.90
16	20	1.11111	68.00	0.708333	12.00	8.6181	0.85	17.0	198.0	1436.4	10.5871	0.24658	0.49315	0.32877	0.24658	-0.4110	195.036	1467.08
17	20	1.11111	64.00	0.666667	16.00	6.0833	0.80	12.5	215.6	1672.8	11.4484	0.32877	0.65753	0.43836	0.32877	-0.5479	206.039	1591.61
18	20	1.11111	56.00	0.583333	24.00	3.5486	0.70	8.0	245.4	2108.0	12.8541	0.49315	0.98630	0.65753	0.49315	-0.8219	223.644	1792.03
19	20	1.11111	48.00	0.500000	32.00	2.2813	0.60	5.7	250.6	2161.5	12.9485	0.65753	1.31507	0.87671	0.65753	-1.0959	239.048	1968.12
20	20	1.11111	40.00	0.416667	40.00	1.5208	0.50	4.4	242.9	1981.1	12.3855	0.82192	1.64384	1.09589	0.82192	-1.3699	253.571	2134.49
21	25	1.38889	71.25	0.742188	3.75	28.8958	0.95	57.6	124.3	781.7	6.5357	0.07705	0.15411	0.10274	0.07705	-0.1284	134.050	749.74
22	25	1.38889	67.50	0.703125	7.50	13.6875	0.90	28.3	156.7	1036.8	8.1860	0.15411	0.30822	0.20548	0.15411	-0.2568	167.736	1124.87
23	25	1.38889	63.75	0.664063	11.25	8.6181	0.85	18.5	183.5	1274.9	9.5255	0.23116	0.46233	0.30822	0.23116	-0.3853	183.090	1297.34
24	25	1.38889	60.00	0.625000	15.00	6.0833	0.80	13.6	204.6	1499.8	10.5553	0.30822	0.61644	0.41096	0.30822	-0.5137	193.862	1419.15
25	25	1.38889	52.50	0.546875	22.50	3.5486	0.70	8.7	234.6	1918.2	11.9529	0.46233	0.92466	0.61644	0.46233	-0.7705	210.822	1612.10
26	25	1.38889	45.00	0.468750	30.00	2.2813	0.60	6.3	239.7	1964.1	12.0617	0.61644	1.23288	0.82192	0.61644	-1.0274	225.491	1779.72
27	25	1.38889	37.50	0.390625	37.50	1.5208	0.50	4.8	232.4	1796.8	11.5526	0.77055	1.54110	1.02740	0.77055	-1.2842	239.243	1937.21
28	30	1.66667	66.50	0.692708	3.50	28.8958	0.95	62.7	129.9	644.0	6.6288	0.07192	0.14384	0.09589	0.07192	-0.1199	121.172	569.88
29	30	1.66667	63.00	0.656250	7.00	13.6875	0.90	30.8	139.9	887.7	7.0971	0.14384	0.28767	0.19178	0.14384	-0.2397	155.686	954.10
30	30	1.66667	59.50	0.619792	10.50	8.6181	0.85	20.2	167.5	1114.4	8.4487	0.21575	0.43151	0.28767	0.21575	-0.3596	171.041	1126.45
31	30	1.66667	56.00	0.583333	14.00	6.0833	0.80	14.9	191.2	1328.1	9.5906	0.28767	0.57534	0.38356	0.28767	-0.4795	181.607	1245.82
32	30	1.66667	49.00	0.510417	21.00	3.5486	0.70	9.6	223.1	1725.8	11.0635	0.43151	0.86301	0.57534	0.43151	-0.7192	197.949	1431.59
33	30	1.66667	42.00	0.437500	28.00	2.2813	0.60	6.9	228.1	1768.9	11.1860	0.57534	1.15068	0.76712	0.57534	-0.9589	211.896	1590.88
34	30	1.66667	35.00	0.364583	35.00	1.5208	0.50	5.3	221.5	1616.0	10.7428	0.71918	1.43836	0.95890	0.71918	-1.1986	224.885	1739.57
35	10	0.55556	85.50	0.890625	4.50	34.6354	0.95	34.2	165.9	1164.8	9.6239	0.10286	0.18000	0.10286	0.10286	-2.3143	169.198	1246.80

Appendix C- University of Delaware Report (See Attachment in SEMS)

Environmentally Sustainable Liquid Gas Generator Formulations, WP-2400

Final Report

Prepared for Aerojet Rocketdyne by:

Craig Warren Davis Ph. D. and Dominic M. Di Toro, Ph. D.

Department of Civil & Environmental Engineering

University of Delaware

Newark, DE 19716

cwdavis@udel.edu **dditoro@udel.edu**

6/15/2016

TABLE OF CONTENTS

LIST OF TABLES 3
LIST OF FIGURES 4
EXECUTIVE SUMMARY 7
PROJECT GOALS 8

1 BACKGROUND 10

1.1 Ionic Liquids 10
1.2 Quantitative Structure Activity Relationships (QSARs) 11
1.3 Poly-parameter Linear Free Energy Relationships (pp-LFERs) 14

2 ESTIMATING PHYSICAL CHEMICAL PARAMETERS OF ENERGETIC IONIC LIQUID (EIL) ION-PAIRS 17

2.1 Experimental Data – Imidazolium & pyridinium-based ILs 17
2.2 Energetic Ionic Liquids (EILs) 17
2.3 Physical Chemical Parameters 18

3 RESULTS – PREDICTING OCTANOL/WATER PARTITIONING OF TIGHT ION PAIRS 19

3.1 Metrics for Comparing Model Performance – RMS Error & the Spearman Correlation Coefficient 19
3.2 Comparison of Predictive Models 21

3.2.1 Model 1 – EPI Suite: Bare Cation 21
3.2.2 Model 2 – EPI Suite: Neutralized Cation 23
3.2.3 Model 3 – EPI Suite: Tight Ion Pair 24
3.2.4 Model 4 – Abraham pp-LFER: Anion Correction 28
3.2.5 Model 5 – COSMO SAC 30
3.2.6 Summary of Model Performance 32

4 PREDICTIONS OF PHYSICAL CHEMICAL PARAMETERS FOR EIL TIGHT ION PAIRS 34

4.1 Calibrated Anion Fragments for Energetic Ionic Liquids 34
4.2 Computed Thermodynamic Properties of Nitrate-containing EILs 36

4.2.1 Octanol-Water Partitioning - log$\boldsymbol{Kow}$ 36
4.2.2 Air-Water Partitioning (Henry's Law Constant) - log$\boldsymbol{Kaw}$ 38
4.2.3 Aqueous Solubility – logS 39
4.2.4 Organic Carbon-Water Partitioning - log$\boldsymbol{Koc}$ 40

4.2.5 Indirect Vapor Pressure (log$\boldsymbol{Kaw}$, $\mathbf{log}\boldsymbol{S}$) - $\boldsymbol{Pvap}$ 41

4.3 Summary 43

5 FUTURE WORK.....44

5.1 Disassociation of the Tight Ion Pair 44

5.2 Acid-Base Behavior of Energetic Ionic Liquid (EIL) Cations 45

A SUPPLEMENTAL INFORMATION 0

A.1 Imidazolium and pyridinium-based IL training set 0

LIST OF TABLES

Table 1. Summary of Experimental Ionic Liquid (IL) Data. 17

Table 2. List of Energetic Ionic Liquids and Reference Compounds to be Studied..... 17

Table 3. List of Physical Chemical Parameters to be Estimated for the Energetic Ionic Liquid (EIL) Compounds. 18

Table 4. Summary of methods for predicting the octanol-water partition coefficients for IL tight ion pairs..... 19

Table 5. Summary of model performance for predicting the octanol-water partition coefficients of 66 imidazolium and pyridinium-based IL tight ion pairs. 32

LIST OF FIGURES

Figure 1. An Imidazolium-based IL (1-butyl-3-methyl-imidazolium hexafluorophosphate) (left) and Triazolium-based EIL (1-amino-3-methyl-1,2,3-triazolium nitrate, AMTri) (right). 10

Figure 2. EPI Suite predicted vs. experimental octanol-water partition coefficient for a training set of 2447 neutral organic compounds. $R^2 = 0.982$, SD = 0.217. Solid line represents 1:1 agreement. 12

Figure 3. EPI Suite predicted vs. experimental octanol-water partition coefficient for a validation set of 10,946 neutral organic compounds. $R^2 = 0.943$, SD = 0.479. Solid line represents 1:1 agreement. 13

Figure 4. Comparison of the cation-only EPI Suite predicted vs. experimental octanol-water partition coefficients for the tight ion pair. Solid line represents 1:1 agreement, dashed lines represent ± 1 order of magnitude error in the predicted values. The RMS error for the model was 1.294 with a Spearman correlation coefficient, $Sp^2 = 0.259$ for 61 IL tight ion pairs. 22

Figure 5. Comparison of the neutralized cation-only EPI Suite predicted vs. experimental octanol-water partition coefficients for the tight ion pair. Solid line represents 1:1 agreement, dashed lines represent ± 1 order of magnitude error in the predicted values. The RMS error for the raw computated partition coefficients was 4.526, while the RMSE for the linear fit to the experimental data was 1.012. The Spearman correlation coefficient was identical for both, $Sp^2 = 0.281$ for 61 IL tight ion pairs. 23

Figure 6. Comparison of the covalent cation-anion "supermolecular" EPI Suite predicted vs. experimental octanol-water partition coefficients for the tight ion pair. Solid line represents 1:1 agreement, dashed lines represent ± 1 order of magnitude error in the predicted values. The RMS error for the computated partition coefficients was 1.200 (0.747 when XXX is excluded). The Spearman correlation coefficient was $Sp^2 = 0.640$ for 22 IL tight ion pairs. 25

Figure 7. Comparison of the full EPI Suite predicted vs. experimental octanol-water partition coefficients for the tight ion pair. Solid line represents 1:1 agreement, dashed lines represent ± 1 order of magnitude error in the predicted values. The RMS error for the model was 0.8396 with a Spearman correlation coefficient, Sp^2 = 0.836 for 60 IL tight ion pairs. Grey symbols are direct EPI Suite predicted values for the cation-anion covalently bonded complex, blue symbols utilize fitted fragment values for the missing anions listen within the figure. 27

Figure 8. Comparison of the full Abraham pp-LFER predicted vs. experimental octanol-water partition coefficients for the tight ion pair. Solid line represents 1:1 agreement, dashed lines represent ± 1 order of magnitude error in the predicted values. The RMS error for the model was 0.387 with a Spearman correlation coefficient, Sp^2 = 0.894 for 62 IL tight ion pairs. 29

Figure 8. Comparison of COSMO-SAC predicted vs. experimental octanol-water partition coefficients for the tight ion pair. Solid line represents 1:1 agreement; dashed lines represent ± 1 order of magnitude error in the predicted values. The RMS error for the model was 0.8123 with a Spearman correlation coefficient, Sp^2 = 0.755 for 66 IL tight ion pairs. 31

Figure 9. Abraham pp-LFER predicted octanol-water partition coefficients for the nitrate-containing energetic ionic liquid (EIL) tight ion pairs (Eq. (4-3)) ordered by increasing octanol-water partition coefficients. Blue points represent the experimental compounds; red points represent the reference compounds. 36

Figure 10. Abraham pp-LFER predicted air-water (Henry's constant) partitioning for the nitrate-containing energetic ionic liquid (EIL) neutralized cation species ordered by increasing octanol-water partition coefficients. Blue points represent the experimental compounds; red points represent the reference compounds.....38

Figure 11. Abraham pp-LFER predicted aqueous solubility (log(Csat)) [mmol EIL / L water] for the nitrate-containing energetic ionic liquid (EIL) neutralized cation species ordered by increasing octanol-water partition coefficients. Blue points represent the experimental compounds; red points represent the reference compounds. 39

Figure 12. Abraham pp-LFER predicted organic carbon - water partition coefficients for the nitrate-containing energetic ionic liquid (EIL) neutralized cation species ordered by increasing octanol-water partition coefficients. Blue points represent the experimental compounds; red points represent the reference compounds. 40

Figure 13. Calculated (Equation (4-5)) liquid vapor pressure [mol - EIL / mol - air] for the nitrate-containing energetic ionic liquid (EIL) neutralized cations ordered by increasing octanol-water partition coefficients. Blue points represent the experimental compounds; red points represent the reference compounds. 42

EXECUTIVE SUMMARY

The purpose of this report is to summarize the work completed as part of the SERPD project WP-2400 Environmentally Sustainable Liquid Gas Generator Formulations. In this work, Abraham poly-parameter linear free energy (pp-LFER) models were used to predict thermodynamic properties related to the fate and transport of a selection of energetic ionic liquids (EILs). These predictions were based on existing Abraham solute descriptors (E, S, A, B, V) for the neutralized form of the EIL cations with applied empirical corrections for both the cation charge effect as well as the effect of the counter anion (NO_3^-). These corrections were based on a training set of octanol-water partition coefficients for structurally similar ionic liquid (IL) compounds. However, empirical corrections could not be made for the remaining thermodynamic properties, since similar training sets were not available. Consequently, relative predictions for the remaining thermodynamic properties were obtained, with absolute prediction values requiring further calibration with additional training sets.

While absolute predictions of the remaining thermodynamic properties can not be made without additional calibration, the pp-LFER models have been demonstrated to correctly rank the training set ILs as well as the energetic compounds of interest. These estimates of the thermodynamic parameters for the candidate EIL compounds can be used to down select ideal compounds for further testing as well as formulation development as outlined in the scope of work for the project.

PROJECT GOALS

As part of a SERDP-funded "Environmentally Sustainable Liquid Gas Generator Formulations, WP-2400" effort, Aerojet Rocketdyne seeks to balance development of high performance gas generator compositions with environmental sustainability and human safety. This balancing calls for Environmental Safety and Occupational Health (ESOH) predictive modeling of 15-20 candidate compounds anticipated to be taken largely from the energetic ionic liquid (EIL) family of chemical compounds. Aerojet Rocketdyne is contracting with Prof. Dominic Di Toro and the University of Delaware to perform the following ESOH-related tasks.

1. Perform Environmental Safety and Occupational Health (ESOH) analysis of 15-20 candidate compounds. These compounds will consist primarily of energetic ionic liquid (EIL) salt systems. The list of candidate compounds is identified in Table 2 (Section 2.2) below.
    a. Conduct a literature review of physical and toxicological considerations for the candidate gas generator components identified in Table 2 (Section 2.2). Compounds with structure suggesting specific toxicity should be identified for further modeling / testing at advanced stages in formulation development.
    b. Use available quantitative structure-activity relationship (QSAR) and poly-parameter linear free energy (pp-LFER) models to determine chemical / physical properties relating to toxicity, fate, and transport of candidate EILs identified in Table 2 (Section 2.2).
        i. Modeling work will make use of existing models rather than develop new ones, and use known molecular and electronic structural

properties. Depending on the current state-of-the art for modeling routines, the computational work may rely on extrapolation from neutral molecules to the charged species (i.e. ignoring charge effects of anions and cations.)

2. The following properties will be generated in order to estimate the extent of toxicity, fate and transport of subject materials in accordance with ASTM E 2552-08, "Standard Guide for Assessing the Environmental and Human Health Impacts of New Energetic Compounds.":
    a. ***Water solubility***
    b. ***Henry's law constant***
    c. ***Liquid-phase vapor pressure***
    d. ***Affinity to organic carbon (log(Koc))***
    e. ***Lipid solubility (log(Kow))***
3. Refine upon parameters 2(a-e) generated by the preliminary QSAR models using other available approaches (e.g. poly-parameter linear free energy relationships) to determine chemical / physical properties relating to toxicity, fate, and transport of materials identified in Table 2.
4. Assess the data generated in 2(a-e) for pertinent toxicological endpoints characterizing inhalation, oral, and topical fate and transport of materials identified in table 2 using existing Abraham pp-LFER models developed for neutral species.

    a. Assess limits of the toxicity, fate and transport predictions generated above and identify routes to improve the predictive models.

Chapter 1

BACKGROUND

1.1 Ionic Liquids

Ionic liquids (ILs) are salts which are liquid at or near ambient temperatures and pressures. ILs have a unique set of physical chemical properties, most notably their extremely low vapor pressures, high thermal and chemical stability, high ionic conductivity, and broad liquid temperature ranges[1-5]. Because there are near infinite combinations of cationic and anionic components, these properties can be fine-tuned for various applications (e.g., solvents, liquid-liquid-extraction, electrolytes)[2]. Consequently, being able to accurately and easily predict physical chemical behavior for IL compounds based on their chemical structures is extremely important in determining their fate, risk, and transport in the natural environment.

Due to their high thermal and chemical stability as well as their extremely low vapor pressures, ILs have been explored as alternatives to traditional organic propulsion fuels (e.g. hydrazine). Specifically, a subset of ionic liquids with high molecular nitrogen-to-carbon ratios (N:C > 3:1). These ILs, generally congeners of 5-membered aromatic azole rings, are referred to as energetic ionic liquids (EILs).

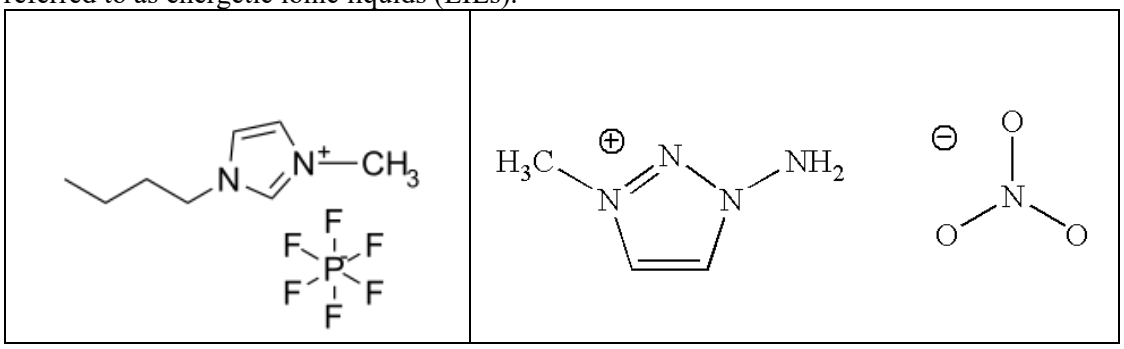

Figure 1. An Imidazolium-based IL (1-butyl-3-methyl-imidazolium hexafluorophosphate) **(left)** and Triazolium-based EIL (1-amino-3-methyl-1,2,3-triazolium nitrate, AMTri) **(right)**.

217 Experimental solvent-water partitioning data exists for some of these ionic liquids,
218 however, reliable physical chemical data is often incomplete or missing entirely for other EIL
219 and IL compounds. This is due likely in part to the complicated natureand many potential
220 combinations of ILs.

221 Because ionic liquids can dissociate to different extents in different solvents,
222 measured partition coefficients for the ion-pair as well as the individual ions are difficult to
223 obtain experimentally. Often, reported experimental partition coefficients, K_{sw}, are
224 distribution coefficients between the two phases, measuring the total distribution of IL
225 between the two phases (i.e. for AMTri, since the anion is inorganic, the two species of
226 interest would be the neutral ion pair and the dissociated organic cation). This is not unlike the
227 measurement of distribution coefficients for organic acids and bases between solvent phases
228 (ignoring the hydrogen ion in the distribution calculation).

229 Often in pure phases or highly concentrated solutions of ILs, dissociation is ignored
230 and the thermodynamic properties are assumed to be those of the neutral tight ion pair.
231 Consequently for calculating physical chemical parameters such as the liquid or solid vapor
232 pressure, the neutral tight ion pair should be the species of concern. However when the
233 concentration of IL is low, especially in the presence of a water phase, dissociation may be
234 complete and the individual ionic species may dominate the system (e.g., air-water partition
235 coefficients (K_{aw}), octanol-water partition coefficients (K_{ow}), or organic carbon – water
236 partition coefficients (K_{OC})). Consequently, accurate methods for obtaining physical chemical
237 parameters are needed for both the ion pair and individual cationic and anionic IL species.

238 **1.2 Quantitative Structure Activity Relationships (QSARs)**

239 QSAR models, which estimate thermodynamic equilibrium properties from structural
240 fragments of the chemical species, have been well-established for neutral organic species. One

241 such method is the EPI Suite set of QSAR models developed by the US EPA. Utilizing a large
242 database of molecular structural fragments, EPI Suite can make accurate predictions of various
243 thermodynamic properties for neutral compounds (e.g. octanol-water, air-water, and organic
244 carbon-water partition coefficients, melting and boiling points, and vapor pressure).

245 The figures below show the predicted vs. observed partition coefficients for training
246 (n=2447) and validation (n=10946) sets of neutral organic chemicals.

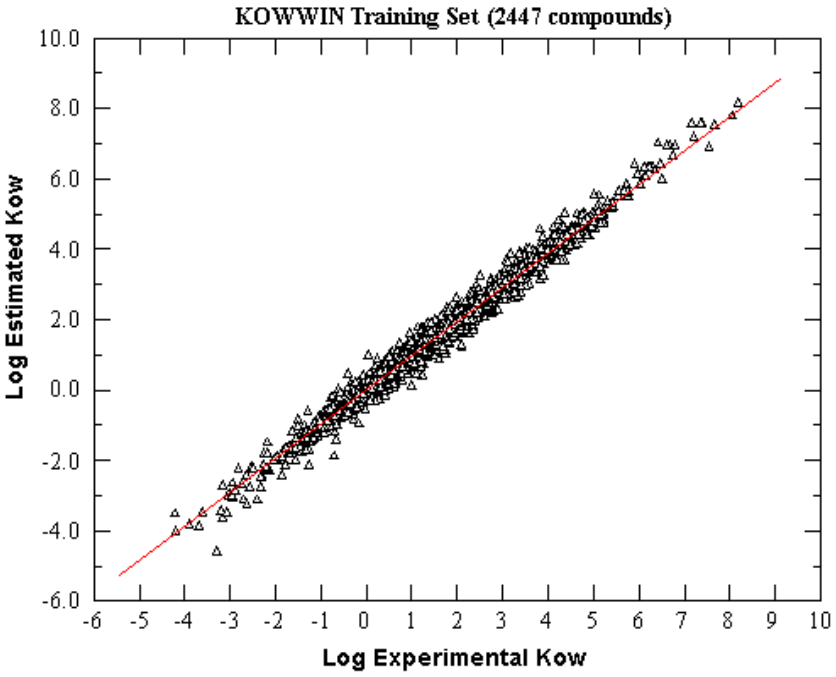

247

248 **Figure 2.** EPI Suite predicted vs. experimental octanol-water partition coefficient for a
249 training set of 2447 neutral organic compounds. $R^2 = 0.982$, SD = 0.217. Solid
250 line represents 1:1 agreement. Reproduced from EPI Suite v4.1 (US EPA 2016).

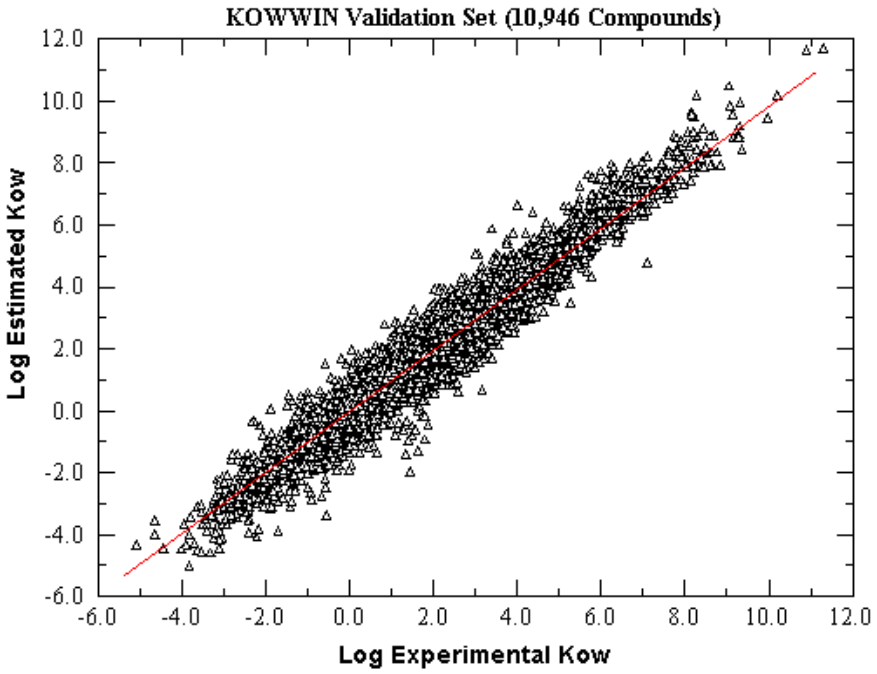

Figure 3. EPI Suite predicted vs. experimental octanol-water partition coefficient for a validation set of 10,946 neutral organic compounds. $R^2 = 0.943$, SD = 0.479. Solid line represents 1:1 agreement. Reproduced from EPI Suite v4.1 (US EPA 2016).

Figures 2 and 3 show that for neutral organic species, the fragment-based QSAR model can accurately predict the octanol-water partition coefficients. For the training set, EPI Suite can predict the $logK_{ow}$ to within a factor of 3 (SD = 0.479).

EPI Suite can also make predictions for singularly charged cations and anions, utilizing alternative fragment values for the atom/fragment containing the charge. However, charged species are not well-represented in the training/calibration data sets of the EPI Suite models. As such, the errors in the predicted values for charged species can be significantly larger than those for neutral species. Similarly, EPI Suite can make predictions for ion pairs. It accomplishes this by forming a discrete covalent bond between the site of positive charge on the cation (e.g. the aromatic nitrogen atom of a pyridinium cation) and the site of negative

charge on the anion (e.g. the singly-bonded oxygen on an acetate anion). As is the case for charged species, the model was not trained on ion-pairs and as such the errors on the estimated parameters for ion-pair species may be significantly higher than those of fully covalently-bonded neutral organic species.

It should be noted however, that these errors are shown to be similar in magnitude to those obtained through straight quantum-chemical computation of the partition coefficients for ionic liquid ion pairs (see Section 3).

1.3 Poly-parameter Linear Free Energy Relationships (pp-LFERs)

Linear free energy relationships (LFERs), like those developed by Abraham et al., are widely used to predict aqueous solubility, solvent-water partitioning, soil-water partitioning, and chemical toxicity to aquatic organisms for neutral organic chemicals[6-14]. These pp-LFER models use a linear combination of physical-chemical properties of the target chemical to predict the total partitioning between various bulk phases (e.g., air-water, octanol-water, fish lipid-water, organic carbon-water). The generalized form of the Abraham pp-LFER can be expressed as follows:

$$\log(K_{i,sw}) = e_{sw}E_i + s_{sw}S_i + a_{sw}A_i + b_{sw}B_i + v_{sw}V_i + c_{sw} \quad (1\text{-}1)$$

where the upper case letters represent the solute (*i*), contributions to the energy of solvation; *E*, molar refractivity, *S*, polarizability, *A*, hydrogen bond donating; and *B*, hydrogen bond accepting capacities, and *V*, the energy required to form a cavity. The lower case letters represent the complementary solvent (*s*) relative to water (w); excess molar refractivity, polarizability, hydrogen bond accepting and donating, and cavitation energy terms, respectively. The c_{sw} term accounts for any non-specific binding interactions not predicted by the Abraham solute parameter product terms ($e_{sw}E_i$, $s_{sw}S_i$, $a_{sw}A_i$, $b_{sw}B_i$, and $v_{sw}V_i$) and varies with the selected units of $K_{i,sw}$.

289 For the prediction of octanol-water partition coefficients of neutral organic
290 solutes, the Abraham pp-LFER method has been demonstrated to be accurate, with an
291 RMS error of 0.56 for set of 992 neutral test compounds. This is comparable to the
292 accuracies obtained using the EPI Suite fragment-based QSAR models. Further, the
293 physical chemical descriptors used in the Abraham pp-LFER model (E, S, A, B, and
294 V) have been calibrated to large sets of experimental data, and have been shown to
295 reproduce experimental values with a high degree of accuracy (RMSE = 0.12, 0.22,
296 0.07, 0.15, 0.01 with N = 5631, 5522, 5719, 5510, 5537, respectively).
297 Experimental solvent-water descriptors (e, s, a, b, v, and c) have been
298 determined for over 400 unique solvent/sorbent-water systems and toxicological
299 endpoints (e.g., air-water, octanol-water, organic carbon – water, liver-water,
300 respiratory irritation, odor threshold, etc…). Unlike the QSAR-based approach, whose
301 fragment-descriptors and regressions are unique for each thermodynamic property, the
302 Abraham solute descriptors (E, S, A, B, V) are universal and can be applied to any
303 solvent-water system whose system parameters (e, s, a, b, v, c) are already known.
304 Additionally, the Abraham pp-LFER model can make estimates of properties
305 for permanently charged cationic species (e.g., quaternary amine). Similar to the EPI
306 Suite QSAR methods, it accomplishes this using a smaller training set of charged
307 partitioning data. Because the fraction of charged species within the training set is
308 small, it is expected that larger errors will result for predictions of ionic solvent-water
309 partitioning and associated toxicological endpoints. However, it has been determined
310 for a set of carboxylate anions in several solvent-water systems (e.g., acetone-,
311 acetonitrile-, dimethylsulfoxide-, and methanol-water) that these increases in RMS
312 error are generally small (RMSE = 0.636, 0.590, 1.11, 0.389 for N = 44, 48, 47, and

313 41, respectively), with dimethylsulfoxide (DMSO) being the only solvent-water
314 system which showed a significant increase in prediction error for the charged species
315 relative to predictions for neutral species in octanol-water (RMSE = 0.56, N = 992). It
316 should be noted that these calculations are for bare cation partitioning, and do not take
317 into account the partitioning of the tight-ion pair. Unlike EPI Suite which can form a
318 discreet covalent bond between the cation and anion, making an estimate of
319 partitioning for the entire tight ion pair, the Abraham pp-LFER method can make
320 predictions for the cation, only, requiring an additional calibration of the effect of the
321 counter-ion on the partitioning behavior. This is discussed in detail in Section 3.2.4 of
322 this report.
323 It should be noted, however, that a similar calibration is required for most
324 anion species in the EPI-Suite model (with the exception of Cl and Br) and a
325 comparison of the accuracies of the two models is presented consequently (Section
326 3.2.5).

Chapter 2

ESTIMATING PHYSICAL CHEMICAL PARAMETERS OF ENERGETIC IONIC LIQUID (EIL) ION-PAIRS

2.1 Experimental Data – Imidazolium & pyridinium-based ILs

While experimental data for energetic ionic liquids is sparse, data for similarly-structured ionic liquids (i.e., imidazolium- and pyridinium-based ionic loquids) are not. Significant experimental data for aqueous solubility, octanol-water partition coefficients, hydrophobicity, activated carbon-water, soil-water partition coefficients, and toxicity exist for these classes of ILs. A summary of significant sources of experimental data is shown in the table below.

Table 1. Summary of Experimental Ionic Liquid (IL) Data.

Parameter	Ionic Liquids[a,b]	N	Notes	Reference
K_{ow}	Im, Py	67		Lee, Lin (2013)
K_{ow}	Im, Py	46		Cho et. al (2011)
S_w	Im, Py	37		Cho et. al (2011)
K_{GAC}, K_{oc}	Im	16, 3		Jungnickel et. al (2011)
EC50	Im, Py	50	AChel, vibrio fischeri, E coli, lemna minor, daphnia magna	Pham, Cho (2009)

[a]Imidazolium-based (Im), [b]Pyridinium-based (Py)

2.2 Energetic Ionic Liquids (EILs)

For this study 10 EILs and 3 neutral reference energetic compounds were selected. The table below summarizes the various EILs and their structural composition.

Table 2. List of Energetic Ionic Liquids and Reference Compounds to be Studied.

No	Energetic Ionic Liquids	Abbreviation
1	Ammonium Nitrate	AN

2	Hydrazinium Nitrate (HN)	HN
3	HydroxyEthylHydrazinium Nitrate	HEHN
4	4-Amino-1,2,4-Triazolium Nitrate	ATriN
5	4-Amino-1-Methyl-1,2,4-Triazolium Nitrate	AMTriN
6	Guanidinium Nitrate	GuN
7	MonoAmino-Guanidinium Nitrate	MAGN
8	1-Hydroxyethan-1,2,4-Triazolium Nitrate	HETN
9	1-amino-1,2,3-triazolium Nitrate	A3TriN
	Reference Compounds	
1	Hydrazine	HZ
2	5-Amino-Tetrazole	5AT
3	3-Nitro-1,2,4-Triaminotriazol-5-One	NTO

2.3 Physical Chemical Parameters

The following thermodynamic properties were generated in order to estimate the extent of toxicity, fate and transport of candidate EIL compounds (Table 2):

Table 3. List of Physical Chemical Parameters to be Estimated for the Energetic Ionic Liquid (EIL) Compounds.

Parameter	Description
MW	Molecular weight
S_w	Water solubility
K_{aw}	Henry's law constant
$p/p_o\|_l$	Vapor pressure (liquid)
K_{OC}	Affinity to organic carbon (sorption)
K_{ow}	Lipid solubility (octanol/water coefficient)

Chapter 3

RESULTS – PREDICTING OCTANOL/WATER PARTITIONING OF TIGHT ION PAIRS

Several methods were explored to determine the most accurate method for ranking the octanol-water partition coefficients for ionic liquids tight ion pairs (as they would exist in pure liquid solution or at very high aqueous concentrations). Three of the methods utilize EPI Suite KOWWIN QSAR predictions based on various molecular structures. These are compared to a fourth method, utilizing the Abraham pp-LFER method, based on the physical-chemical descriptors of the solute and solvent systems. And a fifth method, utilizing direct quantum chemical computation of the octanol-water partition coefficients using COSMO-SAC. A summary of the methods is as follows:

Table 4. Summary of methods for predicting the octanol-water partition coefficients for IL tight ion pairs.

1) EPI Suite prediction of $\log(K_{ow})$ using the IL cation structure only
2) EPI Suite prediction of $\log(K_{ow})$ using the neutral form of the IL cation only (e.g. removing a hydrogen from the charged nitrogen site of an imidazolium or pyridinium based IL cation)
3) EPI Suite prediction of $\log(K_{ow})$ using the full IL ion-pair (with the cation and the anion covalently bonded into a single structure)
4) Abraham pp-LFER prediction of $\log(K_{ow})$ using the full IL ion-pair (with anion correction)
5) COSMO-SAC direct quantum-chemical computation of the full IL ion-pair structure (not covalently bonded)

3.1 Metrics for Comparing Model Performance – RMS Error & the Spearman Correlation Coefficient

In order to compare the accuracy of the various models quantitatively, metrics must be selected that describe both the overall accuracy of the predictive methods and, more importantly for the task of screening potential EILs, the accuracy with which the model ranks

the various thermodynamic properties of the EILs (particularly the vapor pressures and octanol-water partition coefficients).

The first of these metrics, the root mean square (RMS) error is a measure of the average error in a set of data between the observed values and the values predicted by a given model. For this reason, it is a valuable tool for comparing the accuracies of several different predictive models against a single set of observed experimental data. The RMS error for a given set of observed experimental and model predicted values can be expressed as follows:

$$RMSE = \sqrt{\frac{\sum(Y_i - X_i)^2}{N}} \tag{3-1}$$

where X_i and Y_i represent the observed and predicted values for the i-th observation, and N represents the total number of observations. The RMS error for logarithmic variables is approximately equal to the standard deviation, and as such an RMS error of 0.5 log units (± 0.5σ) corresponds to 68% of the predictions being within an order of magnitude of the experimental values.

The second metric, the Spearman Rank Correlation Coefficient (Sp) is a nonparametric measure of the statistical correlation between two variables. It quantifies how well the relationship between two variables can be described using a monotonic function. The observed (X_i) and predicted (Y_i) variables are ranked from low to high, and the ranks are used to compute the Spearman coefficient (Sp), as follows:

$$Sp = \frac{6\sum(y_i - x_i)^2}{n(n^2 - 1)} \tag{3-2}$$

where x_i and y_i represent the ranks of the observed and predicted values for the i-th observation, and n represents the total number of observations. The Spearman coefficients of the various models can then be compared to determine the accuracy with which the models correctly rank the given property.

3.2 Comparison of Predictive Models

The performance of the models listed above (Table 4) were evaluated using a training set of structurally similar ionic liquids to those listed in Table 2. These consist of 66 imidazolium- and pyridinium-based ionic liquid tight ion pairs. While not themselves energetic ILs, these compounds are structural analogues, containing 5-membered nitro-substituted aromatic rings and various structural moieties (e.g. aliphatic chains) similar to the tri and tetrazolium-based EILs in Table 2. A full list of these training compounds can be found in Appendix A1.

3.2.1 Model 1 – EPI Suite: Bare Cation

Model 1 (Table 4) compares the EPI Suite predicted $\log K_{ow}$ values for the charged cation to the experimental $\log K_{ow}$ for the tight ion pair. This model ignores the effect of different anions on the partitioning of the tight ion pair between the two solvent phases. The results of the model are illustrated in figure 4 below:

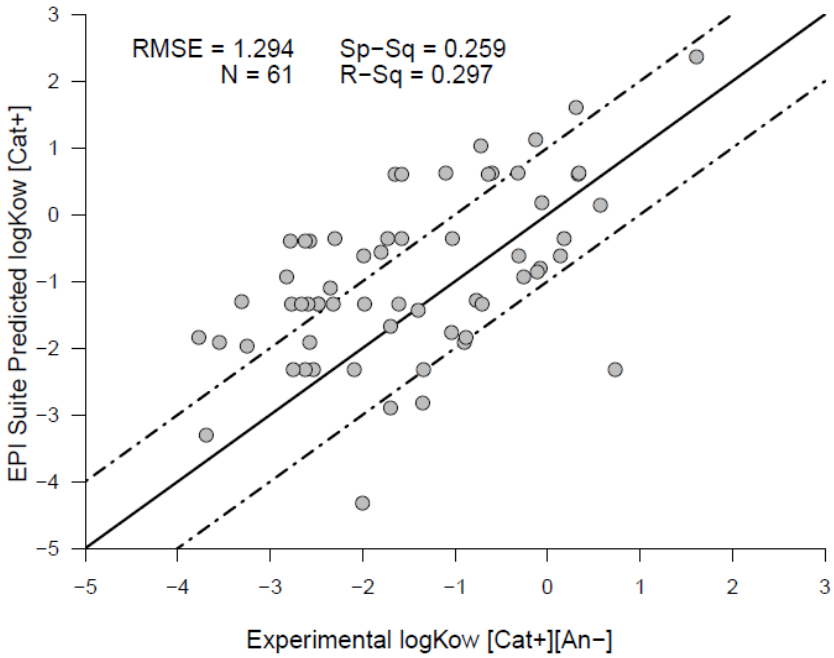

Figure 4. Comparison of the cation-only EPI Suite predicted vs. experimental octanol-water partition coefficients for the tight ion pair. Solid line represents 1:1 agreement, dashed lines represent ± 1 order of magnitude error in the predicted values. The RMS error for the model was 1.294 with a Spearman correlation coefficient, Sp^2 = 0.259 for 61 IL tight ion pairs.

Figure 4 clearly shows that both the error of the EPI Suite cation predicted $\log K_{ow}$ values (RMSE = 1.294) and the ability to rank the $\log K_{ow}$ of the 61 ionic liquids for which EPI Suite made predictions were poor (Sp^2 = 0.259). It is clear in the figure that there are horizontal groupings of individual cations with different anions, strongly suggesting that the effect of the anion on the partitioning of the tight ion pair cannot be ignored.

3.2.2 Model 2 – EPI Suite: Neutralized Cation

Model 2 (Table 4) compares the EPI Suite predicted $\log K_{ow}$ values for the neutralized cation to the experimental $\log K_{ow}$ for the tight ion pair. This model also ignores the effect of different anions on the partitioning of the tight ion pair between the two solvent phases. The results of the model are illustrated in figure 5 below:

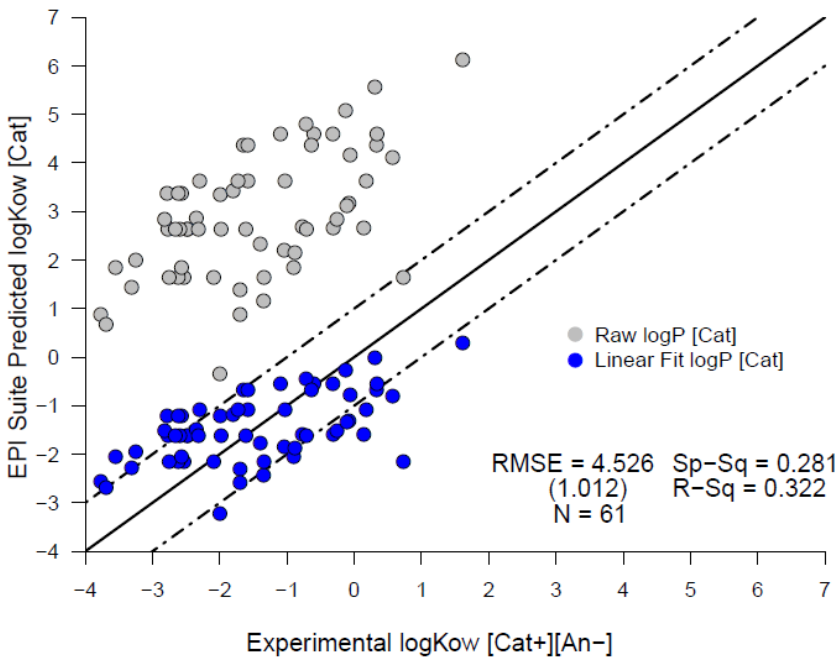

Figure 5. Comparison of the neutralized cation-only EPI Suite predicted vs. experimental octanol-water partition coefficients for the tight ion pair. Solid line represents 1:1 agreement, dashed lines represent ± 1 order of magnitude error in the predicted values. The RMS error for the raw computated partition coefficients was 4.526, while the RMSE for the linear fit to the experimental data was 1.012. The Spearman correlation coefficient was identical for both, $Sp^2 = 0.281$ for 61 IL tight ion pairs.

Figure 5 clearly shows that the raw EPI Suite computed $\log K_{ow}$ values for the neutralized cation do not agree well with the experimental $\log K_{ow}$ values for the tight ion pair (RMSE = 4.526). A linear correction can be applied to the EPI Suite predictions such that:

$$logK_{ow,corr} = m * logK_{ow,raw} + b \quad (3\text{-}3)$$

where $logK_{ow,raw}$ is the raw EPI Suite computed partition coefficient for the neutralized cation, m and b are the fitted slope and intercept, respectively, and $logK_{ow,corr}$ is the corrected EPI Suite predicted value of $\log K_{ow}$ for the tight ion pair.

While a linear correction greatly reduces the RMS error ($RMSE_{corr}$ = 1.012) it has no effect on the ability of the model to predict the correct ordering of the $\log K_{ow}$ for the tight ion pairs (Sp^2 = 0.281).

Both the RMSE and Spearman coefficients are similar for the charged and neutralized cation models (1 & 2). Further, we see a similar horizontal grouping of cations with different anions in both models, suggesting the need for a model which incorporates the anion in predicting the $\log K_{ow}$ for the tight ion pairs.

3.2.3 Model 3 – EPI Suite: Tight Ion Pair

Since models 1 and 2 show a clear anion-specific effect on the $\log K_{ow}$ for the tight ion pairs, a model which explicitly incorporates the anion into the EPI Suite predictions of $\log K_{ow}$ was examined. One difficulty is that EPI Suite cannot represent tight ion pairs as they exist naturally, two individual covalently-bonded ions interacting with each other via electrostatics and hydrogen bonding interactions. However, the tight ion pairs can be approximated as a single "super molecule" with a single covalent bond between the positively charged site on the cation and the negatively charged site on the anion. The result of this method (model 3) is illustrated in the figure below:

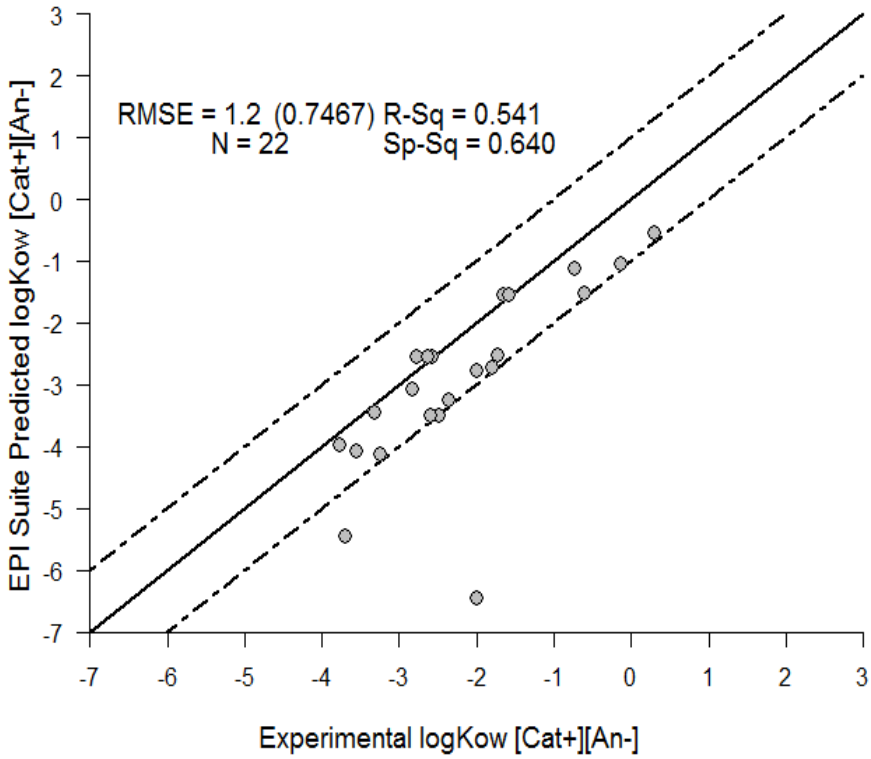

Figure 6. Comparison of the covalent cation-anion "supermolecular" EPI Suite predicted vs. experimental octanol-water partition coefficients for the tight ion pair. Solid line represents 1:1 agreement, dashed lines represent ± 1 order of magnitude error in the predicted values. The RMS error for the computated partition coefficients was 1.20 (0.747 when [C1COOMIM][Cl] is excluded). The Spearman correlation coefficient was $Sp^2 = 0.640$ for 22 IL tight ion pairs.

Since EPI Suite cannot accurately represent some multi-atomic inorganic anion species (e.g., nitrate, tetrafluoroborate, perfluorophosphate, & bis-trifluoromethylsulfonyl-imide), some of the tight ion pairs could not be estimated directly as a single supermolecule (method 3). For these ion pairs (N=39) new fragment values were calibrated using the EPI Suite predicted $\log K_{ow}$ for the cation-chloride supermolecule and the experimental $\log K_{ow}$ for the tight ion pair as follows:

$$E(\delta logK_{ow,an}) = \sum_{i=1}^{n} (logK_{ow,expt} - (logK_{ow,cat-Cl} + \delta logK_{ow,an}))^2 \quad (3\text{-}4)$$

$$logK_{ow,cat-an} = logK_{ow,cat-Cl} + \delta logK_{ow,an} \quad (3\text{-}5)$$

where $\delta logK_{ow,an}$ is the anion-specific fragment contribution to logK_{ow}, $logK_{ow,expt}$ is the experimental octanol-water partition coefficient for the tight ion pair, $logK_{ow,cat-Cl}$ is the EPI Suite predicted octaol-water partition coefficient for the cation-chloride supermolecule, $E(\delta logK_{ow,an})$ is the error function to be minimized using Solver, and $logK_{ow,cat-an}$ is the computed octanol-water partition coefficient for the tight ion pair. When the ion pairs with estimated anion fragment values are added to the EPI Suite direct calculated predictions for the previous 22 tight ion pairs (figure 6) the results are as follows:

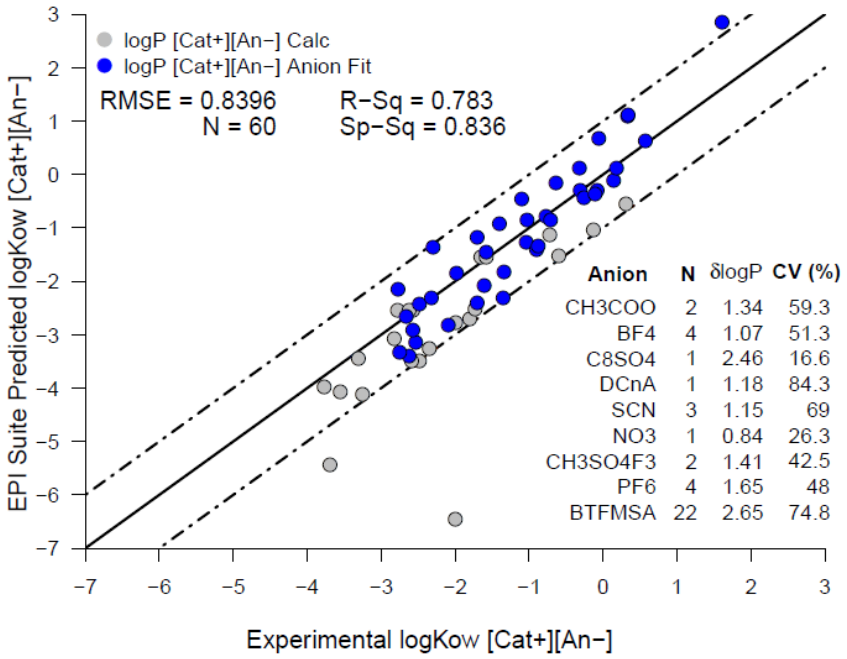

Figure 7. Comparison of the full EPI Suite predicted vs. experimental octanol-water partition coefficients for the tight ion pair. Solid line represents 1:1 agreement, dashed lines represent ± 1 order of magnitude error in the predicted values. The RMS error for the model was 0.8396 with a Spearman correlation coefficient, Sp^2 = 0.836 for 60 IL tight ion pairs. Grey symbols are direct EPI Suite predicted values for the cation-anion covalently bonded complex, blue symbols utilize fitted fragment values for the missing anions listen within the figure.

Figure 7 clearly shows that when the anion fragment contributions to the experimental tight ion pair $\log K_{ow}$ are combined with the EPI Suite estimates for the $\log K_{ow}$ of the bare cations, the resulting predicted $\log K_{ow}$ show strong agreement to the experimental $\log K_{ow}$ of the tight ion pairs. The RMS error (RMSE = 0.840) is significantly smaller than those for models 1 and 2, which do not include the anion contribution to the tight ion pair $\log K_{ow}$. Additionally, the Spearman correlation coefficient (Sp^2 = 0.836) is significantly higher than those of the previous models which only consider the cation species. The resulting predictions

of the cation-anion supermolecule model (method 3) strongly suggest that the anion of the tight ion pair plays a pivotal role in accurately describing the partitioning behavior of the tight ion pair.

3.2.4 Model 4 – Abraham pp-LFER: Anion Correction

Similar to the EPI Suite model (Section 3.2.3), the Abraham pp-LFER model cannot estimate solute descriptors (E, S, A, B, V) directly for non-covalently bonded ion-pairs (e.g., salts, ionic liquids). However, the underlying assumption of the Abraham pp-LFER model is that the contributions of individual solvent-water interactions with the solute molecule are separable and additive. This is not unlike the fragment-based treatment in the EPI Suite model. Consequently, the interaction between the anion and the solvent and water phases can be considered to be a separate term in the Abraham pp-LFER model as follows:

$$\log(K_{i,sw}) = e_{sw}E_i + s_{sw}S_i + a_{sw}A_i + b_{sw}B_i + v_{sw}V_i + c_{sw} + \delta\log(K_{anion,sw}) \quad (3\text{-}6)$$

where the upper and lower case Abraham descriptors are for the cation, directly, and the $\delta\log(K_{anion,sw})$ term accounts for the contribution of the counter-ion to the overall partitioning of the tight ion pair. This approach is very nearly identical to that discussed previously for the EPI Suite model (Section 3.2.3, Eqs. (3-4) and (3-5)).

The results for the Abraham pp-LFER method (with anion corrections) are shown below:

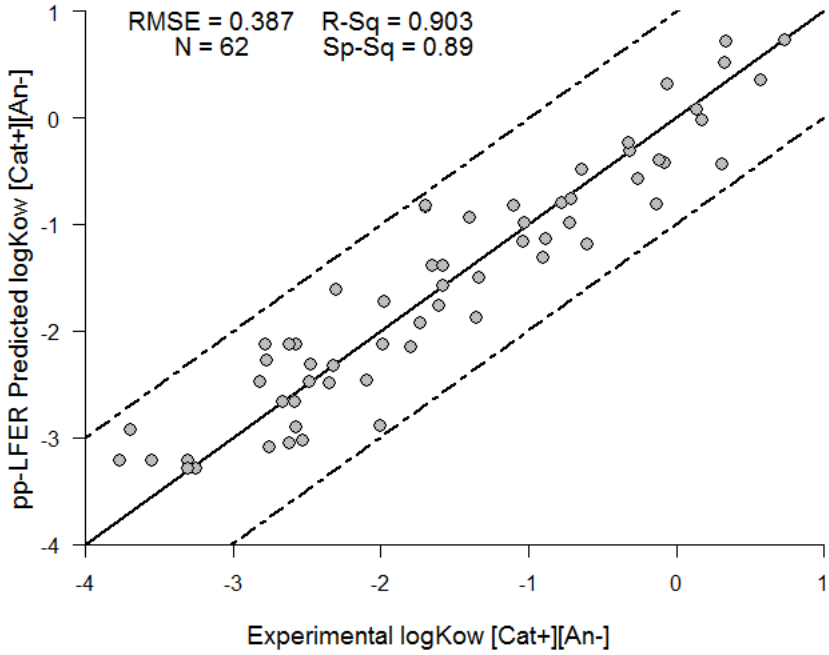

Figure 8. Comparison of the full Abraham pp-LFER predicted vs. experimental octanol-water partition coefficients for the tight ion pair. Solid line represents 1:1 agreement, dashed lines represent ± 1 order of magnitude error in the predicted values. The RMS error for the model was 0.387 with a Spearman correlation coefficient, Sp^2 = 0.89 for 62 IL tight ion pairs.

Figure 8 clearly shows that when the anion fragment contributions to the experimental tight ion pair $\log K_{ow}$ are combined with the Abraham pp-LFER estimates for the $\log K_{ow}$ of the bare cations, the resulting predicted $\log K_{ow}$ show strong agreement to the experimental $\log K_{ow}$ of the tight ion pairs. The RMS error (RMSE = 0.387) is significantly smaller than those for models 1 – 3. Additionally, the Spearman correlation coefficient (Sp^2 = 0.894) is significantly higher than those of the previous models (1, 2) which only consider the cation species as well as slightly higher than the anion-corrected EPI Suite model (3). The resulting predictions of the Abraham pp-LFER model (method 4) further suggests that the anion of the

tight ion pair plays a pivotal role in accurately describing the partitioning behavior of the tight ion pair.

3.2.5 Model 5 – COSMO SAC

Finally, the EPI Suite and Abraham pp-LFER methods for predicting $\log K_{ow}$ for the tight ion pairs were compared to a direct quantum-chemical computation. Using COSMO-SAC and a Pitzer Debye-Huckle correction for high ionic strength, the partitioning of the quantum-mechanically bound tight ion pairs were computed directly. The results are illustrated in the figure below:

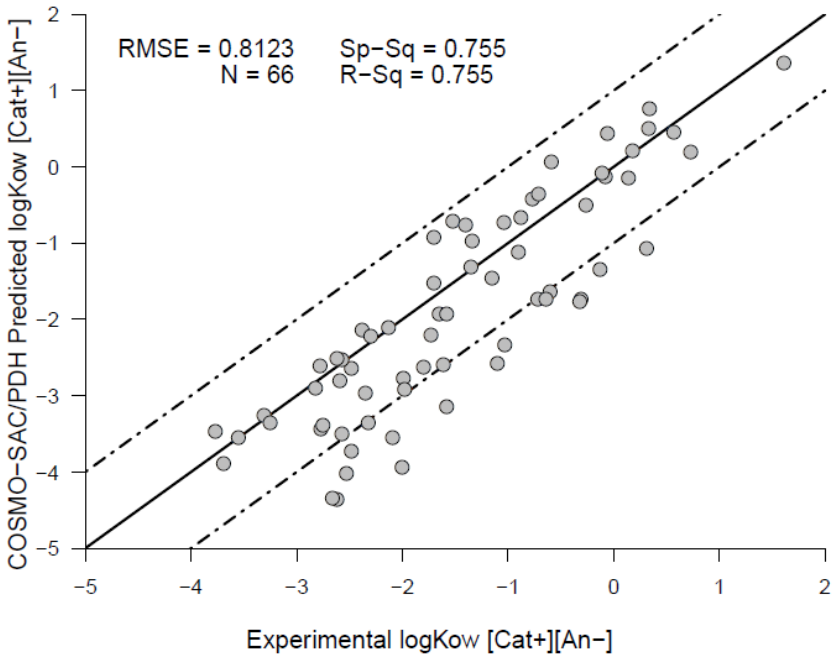

Figure 8. Comparison of COSMO-SAC predicted vs. experimental octanol-water partition coefficients for the tight ion pair. Solid line represents 1:1 agreement; dashed lines represent ± 1 order of magnitude error in the predicted values. The RMS error for the model was 0.8123 with a Spearman correlation coefficient, Sp^2 = 0.755 for 66 IL tight ion pairs.

Figure 8 clearly shows that the COSMO-SAC computed values for the octanol-water partition coefficients of the tight ion pairs show poor agreement with the experimental values for the tight ion pair (RMSE = 0.8123) compared to those predicted by the Abraham pp-LFER model (method 4). While the Spearman correlation coefficient is slightly lower for the direct COSMO-SAC computations (Sp^2 = 0.755) compared to the EPI-Suite and Abraham pp-LFER predictions with calibrated anion fragments (methods 3 and 4), it still demonstrates a clear ability to accurately reproduce the order of the experimental $\log K_{ow}$ for the tight ion pairs. It should be noted, however, that the direct quantum-chemical computation (method 5) does not

require linear corrections or calibration of anion fragments. It is an a priori direct computation of the partition coefficient.

3.2.6 Summary of Model Performance

The relative performance of the methods (Table 4) is summarized in the table below:

Table 5. Summary of model performance for predicting the octanol-water partition coefficients of 66 imidazolium and pyridinium-based IL tight ion pairs.

Method	Description	N	RMSE	Sp	R	Sp-Sq	R-Sq
1	EPI [Cat+]	61	1.294	0.509	0.545	0.259	0.297
2	EPI [Cat]	61	4.526	0.530	0.568	0.281	0.322
3	EPI [Cat+][An-]	60	0.775	0.914	0.885	0.836	0.783
4	Abraham pp-LFER	62	0.387	0.945	0.950	0.894	0.903
5	COSMO + PDH	66	0.813	0.869	0.869	0.755	0.755

It is clear from table 5 that the anion-cation supermolecule predictions from EPI-Suite (method 3) and the Abraham pp-LFER (method 4) as well as the direct COSMO-SAC quantum chemically computed $\log K_{ow}$ demonstrate a strong ability to correctly order the experimental $\log K_{ow}$ values for the imidazolium and pyridinium-based IL tight ion pairs. However, the Abraham pp-LFER method demonstrates a significant improvement in prediction accuracy over the EPI Suite and even the direct quantum chemical prediction methods. The errors for the methods which ignore the contribution of the anion (1, 2) are

548 significantly larger than the other methods (3-5). Further, the low Spearman correlation
549 coefficients for methods 1 & 2 strongly suggest that the anion effect on the partitioning of the
550 IL tight ion pair cannot be ignored.

Chapter 4

PREDICTIONS OF PHYSICAL CHEMICAL PARAMETERS FOR EIL TIGHT ION PAIRS

4.1 Calibrated Anion Fragments for Energetic Ionic Liquids

Because the 5-amino tetrazolate (5AT) and NTO anions were not present within the training set, correction values to the Abraham pp-LFER model (Eq. (3-6)) for these anions could not be determined. Consequently, EILs containing 5AT and NTO as the anion were omitted in the ranking of the predicted thermodynamic properties of the EIL compounds of concern. Additionally, Abraham pp-LFER descriptors are unavailable for one of the EIL compounds, HAN. Consequently, HAN was not analyzed via the Abraham pp-LFER method for the thermodynamic properties in Table3.

Further, since the EIL cations of concern are ionizable (organic acids/bases) and are not permanently charged, Abraham solute descriptors exist only for the neutral species. However, similar to the EPI Suite fragment-based approach, a single $[N^+]$ to $[N]$ correction can be applied to the cations. This fragment correction is expressed as follows:

$$\delta N_{charge} = \delta\log(K_{ow,[N^+]}) - \delta\log(K_{ow,[N]}) \quad (4\text{-}1)$$

where $\delta\log(K_{ow,[N^+]})$ is the 5-valent nitrogen fragment value in the EPI-Suite computed octanol-water partititon coefficient for the cationic species, $\delta\log(K_{ow,[N]})$ is the 4-valent nitrogen fragment value in the EPI-Suite computed octanol-water partititon coefficient for the neutralized cation species, and δN_{charge} is the difference between these two fragment values. These fragment corrections are easily obtained, by computing the difference between the two EPI suite-estimated octanol-water partition coefficients. Consequently, this same value can be applied as a correction to the Abraham pp-LFER estimates for the octanol-water partition coefficients for the EIL cationic species (i) as follows:

$$\log(K_{i,ow})_{cation} = \log(K_{i,ow})_{neut} + \delta N_{charge} \quad (4\text{-}2)$$

where $\log(K_{i,ow})_{neut}$ is the Abraham pp-LFER computed partition coefficient using the neutral species Abraham solute descriptors available from Absolv and $\log(K_{i,ow})_{cation}$ is the corrected partition coefficient for the cationic EIL species, using the correction factor in equation (4-1). The partition coefficient for the tight ion pair can then be computed identically to that for the EPI suite tight ion pair model (Section 3.2.3, Eq. (3-5):

$$logK_{ow,cat-an} = logK_{ow,cation} + \delta logK_{ow,an} \quad (4\text{-}3)$$

Finally, it is not clear whether the observed anion correction values obtained for the octanol-water partitioning data set are universal or specific for that solvent-water system. Consequently, for the remaining thermodynamic properties to be estimated, relative thermodynamic properties are computed, such that the differences between various EIL cations are absolute, however the magnitudes are relative and are dependent on an anion-corrected value for the anion of concern (in this case, nitrate (NO_3^-)) and the thermodynamic property of interest. Resulting computed thermodynamic properties for the nitrate-containing EIL compounds are summarized in the Sections below (4.2 - 4.2.5)

4.2 Computed Thermodynamic Properties of Nitrate-containing EILs

4.2.1 Octanol-Water Partitioning - logK_{ow}

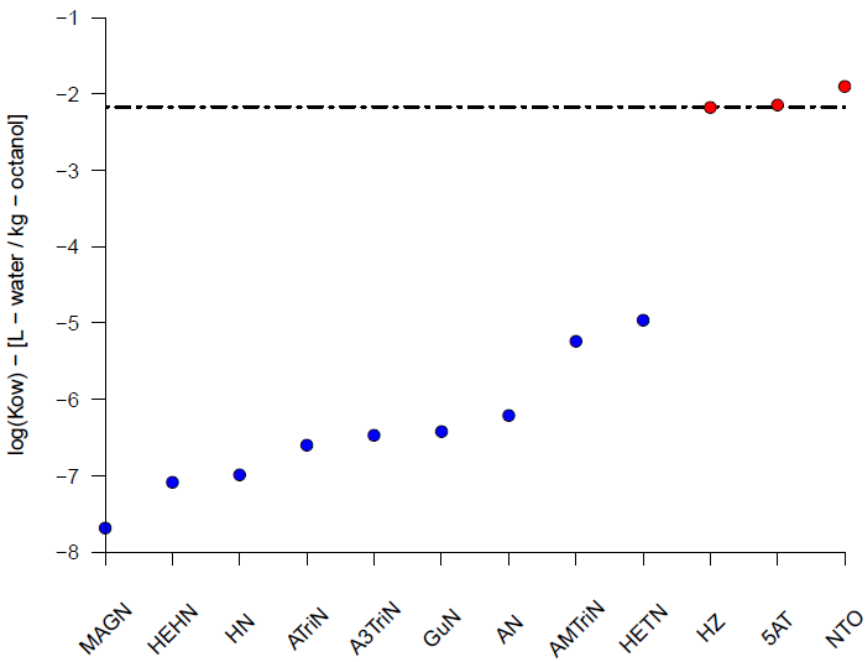

Figure 9. Abraham pp-LFER predicted octanol-water partition coefficients for the nitrate-containing energetic ionic liquid (EIL) tight ion pairs (Eq. (4-3)) ordered by increasing octanol-water partition coefficients. Blue points represent the experimental compounds; red points represent the reference compounds.

It is clear from figure 9 that there is significant variation in the magnitude of the octanol-water partition coefficients for the various EIL compounds. The $logK_{ow}$ values for the EIL compounds range from -7.68 to -4.96, approximately 3 orders of magnitude. Further, it is clear that the $logK_{ow}$ values for the EIL compounds are significantly lower than those of the reference compounds. There is an approximately 3 order of magnitude gap between the most hydrophobic EIL (MAGN) and the most hydrophilic reference compound (NTO). As a rule of

thumb, compounds with log(Kow) < 4.0 will not bioaccumulate significantly in the lipid phases of aquatic organisms. Figure 9 shows that the octanol-water partition coefficients of both the EIL compounds and the reference compounds are significantly smaller than 4.0. Consequently, we would not expect any of them to bioaccumulate in the lipid phases of aquatic organisms.

It should be noted, however, that the calibrated fragment value for the nitrate anion is based on a single observation within the training set and consequently, there is a large degree of uncertainty in the calibrated value. Since the EILs in figure 9 all contain the same anion, error in the calibrated fragment value does not affect the ordering of the EILs relative to one another. Consequently, the remaining thermodynamic properties were computed for the neutralized EIL cation species only, to illustrate the relative orders, not the absolute magnitudes, since the calibrated anion fragment and charge corrections for $logK_{ow}$ should not be applied to the remaining properties without further calibration of IL species to other thermodynamic data.

4.2.2 Air-Water Partitioning (Henry's Law Constant) - $\log K_{aw}$

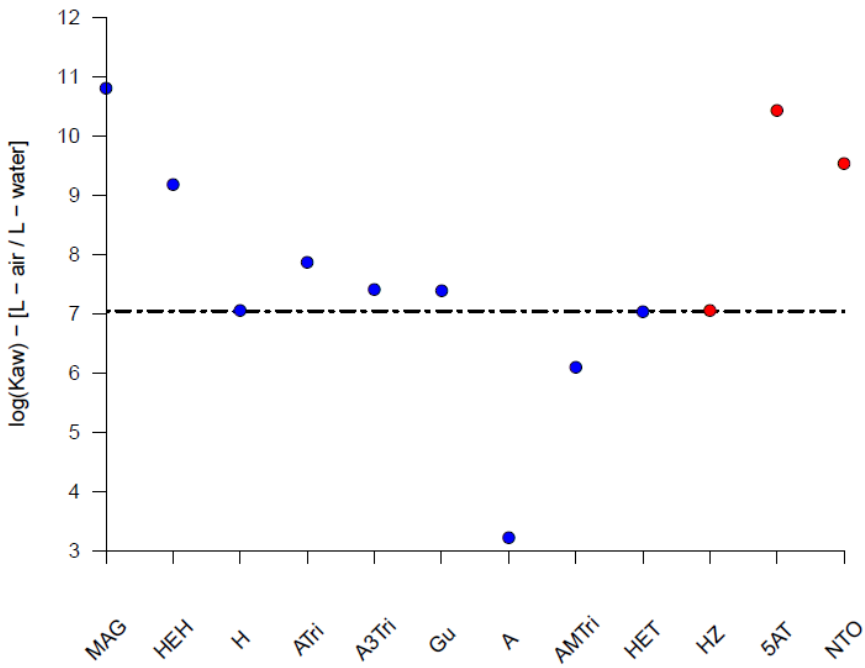

Figure 10. Abraham pp-LFER predicted air-water (Henry's constant) partitioning for the nitrate-containing energetic ionic liquid (EIL) neutralized cation species ordered by increasing octanol-water partition coefficients. Blue points represent the experimental compounds; red points represent the reference compounds.

It is clear from figure 10 that the relative order of the Henry's law constants for the nitrate-containing EILs is nearly perfectly inverse to that of the computed octanol-water partition coefficients, with the notable exception of the A species (which when neutral, is simply aqueous ammonia ($NH_{3,(aq)}$)). This is unsurprising, since ammonia is a small inorganic molecule, for which the Abraham pp-LFER and EPI Suite databases were not calibrated for. Further, the range of the air-water partition coefficients for the EILs is quite large, spanning approximately 5 orders of magnitude (excluding A). Finally, it is worth noting that the predicted Henry's law constant for the most hydrophobic (relative to air) EIL is an order of

magnitude larger than hydrazine, with the other 8 EIL compounds being equivalent or smaller. This strongly suggests that any of the other 8 EIL compounds will be equally or less volatile in dilute (aqueous) solutions than hydrazine, indicating a lower potential toxicological exposure through the air above energetic-laden aqueous phases.

4.2.3 Aqueous Solubility – logS

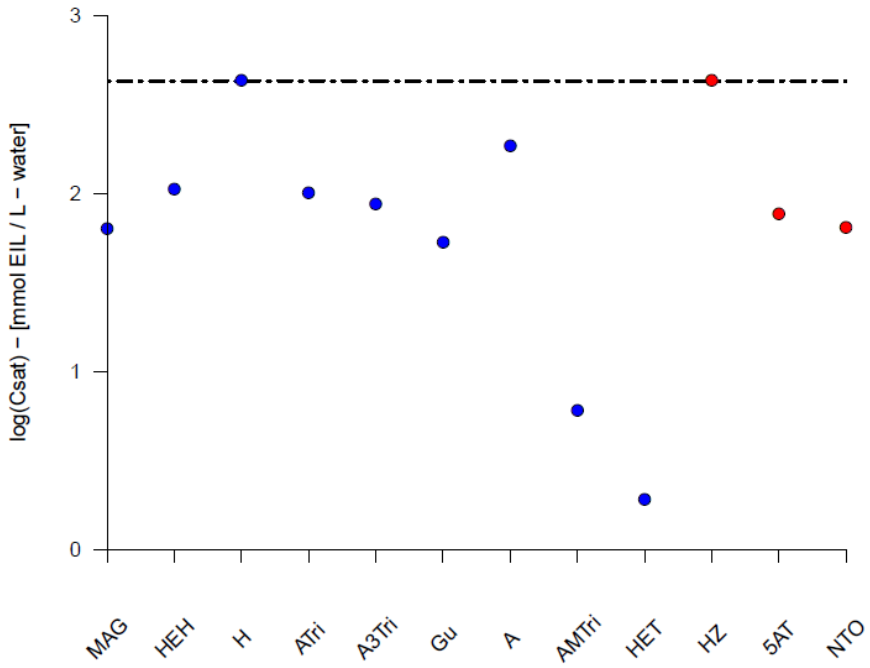

Figure 11. Abraham pp-LFER predicted aqueous solubility (log(Csat)) [mmol EIL / L water] for the nitrate-containing energetic ionic liquid (EIL) neutralized cation species ordered by increasing octanol-water partition coefficients. Blue points represent the experimental compounds; red points represent the reference compounds.

Figure 11 shows that there is little variation in the aqueous solubility of the EIL compounds (approximately 0.5 orders of magnitude) with the exceptions of AMTri and HET. This is not surprising, as they are ionic salts and are expected to dissociate completely in

water. Further, it can be seen that the EIL compounds largely have solubilities similar to those of the neutral reference compounds. Further, the range of solubility is very small, indicating that while the partitioning behavior between solvent phases is highly dependent on the structure of the EIL, the aqueous solubilities are not.

It is important to note that while the small range of solubility observed does not serve to differentiate the EILs, the aqueous solubilities can be used to compute vapor pressures for the EILs (using the Henry's law constants, see Section 4.2.5).

4.2.4 Organic Carbon-Water Partitioning - logK_{oc}

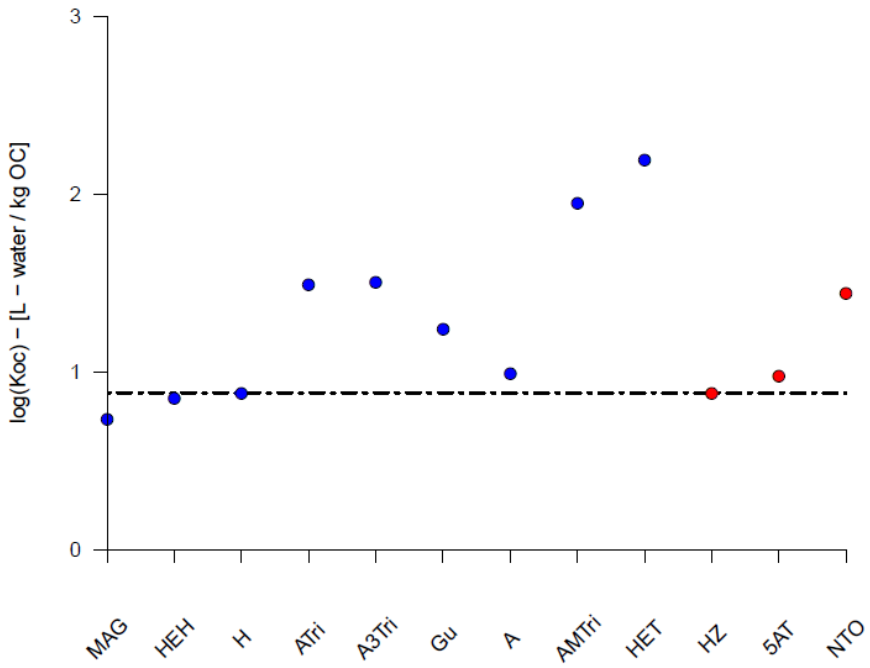

Figure 12. Abraham pp-LFER predicted organic carbon - water partition coefficients for the nitrate-containing energetic ionic liquid (EIL) neutralized cation species ordered by increasing octanol-water partition coefficients. Blue points represent the experimental compounds; red points represent the reference compounds.

Figure 12 shows that there is generally good agreement in the ordering of organic-carbon – water partition coefficients for the larger EIL (and reference) compounds, relative to their partitioning in octanol-water systems. While absolute values for the tight ion pairs can not be determined, since there is no calibrated anion fragment to corrected the cation pp-LFER model with, the relative ordering and the strong relationship to the octanol-water values suggest that these compounds should behave similarly in organic carbon – water systems. Interestingly, the range for the predicted $\log(K_{OC})$ for the EIL compounds is significantly smaller (approximately 1.5 orders of magnitude) than the range in octanol – water (approximately 3 orders of magnitude). This however is consistent with the previous linear energy relationships developed between octanol-water and organic carbon – water systems, used by EPI Suite:

$$\log(K_{OC} = 0.553\log(K_{ow}) + 0.925 + \sum f_i \quad (4\text{-}4)$$

where $\sum f_i$ represents the sum of all fragment-based correction factors for specific fragment / chemical classes. Consequently, a range of 3 orders of magnitude in $\log(K_{ow})$ should correspond with a range in $\log(K_{oc})$ of 1.5 orders of magnitude. Finally, we see that uncorrected, none of the EIL compounds exhibit smaller values of $\log(K_{oc})$ than hydrazine, suggesting comparable mobility in groundwater systems.

4.2.5 Indirect Vapor Pressure ($\log K_{aw}$, $\log S$) - P_{vap}

Vapor pressure (pure liquid solute phase – air equilibrium) of the energetic ionic liquids can be computed from the equilibrium between water – pure phase (aqueous solubility) and water – air (Henery's law) equilibria, as follows:

$$P_{vap,calc} = 22.71 * K_{a,w} * S \quad (4\text{-}5)$$

where $K_{a,w}$ is the air –water partition coefficient in $^{L-\ water}/_{L-air}$, S is the aqueous solubility in $^{mol}/_{L-water}$, and $P_{vap,calc}$ is the resulting vapor pressure, in units of [mol

EIL / mol – air]. Using the Abraham pp-LFER predicted values for $K_{a,w}$ (figure 10) and aqueous solubility, S (figure 11), the vapor pressures can be computed as follows:

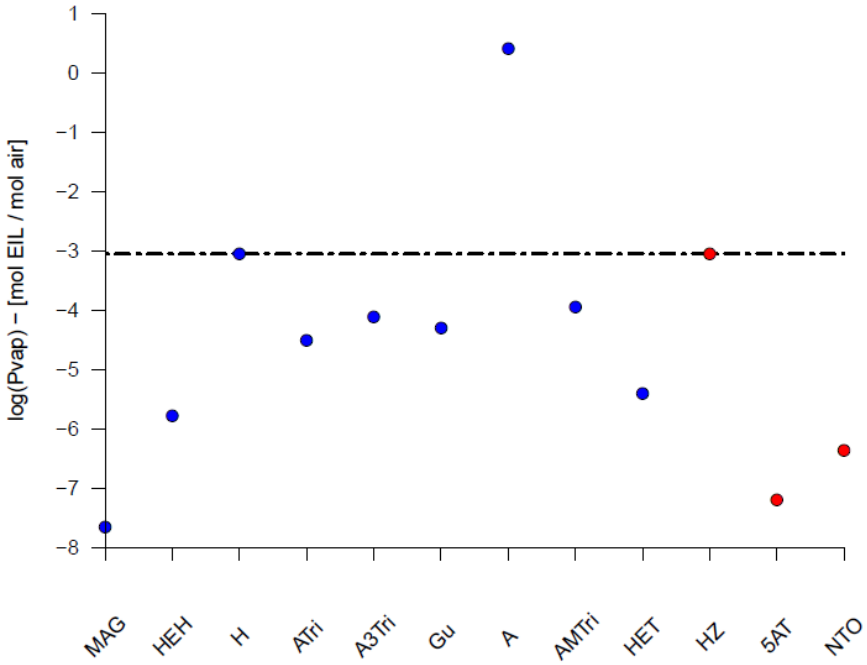

Figure 13. Calculated (Equation (4-5)) liquid vapor pressure [mol - EIL / mol - air] for the nitrate-containing energetic ionic liquid (EIL) neutralized cations ordered by increasing octanol-water partition coefficients. Blue points represent the experimental compounds; red points represent the reference compounds.

This indirect method of computing the vapor pressures for the nitrate-containing EIL cation species shows similar trends for the EIL compounds relative to the octanol-water partition coefficients. The notable exceptions are hydrazine (H) and ammonium (A) neutralized cations. This is unsurprising, since both compounds are small, inorganic molecules for which the previous models (EPI Suite and Abraham pp-LFER models) are not well calibrated. It is clear that the order of the computed vapor pressures for the remaining EIL

compounds is nearly identical to those of the octanol –water partition coefficients, however. Finally, there is significant variation in the vapor pressures for the EILs, spanning approximately 5 orders of magnitude. Since the vapor pressure will directly impact the inhalation and eye irritation exposure to the energetic compound from the pure liquid phase, it is important to note the significantly lower air-liquid partitioning of most of the EILs compared to hydrazine.

4.3 Summary

It is clear from figures 9,10,12, and 13 that the nitrate-containing EILs follow similar trends for the thermodynamic properties discussed above ($logK_{ow}$, $logK_{aw}$, $logK_{oc}$, $and\ logP_{vap,calc}$). This suggests that for the properties of the tight ion pair, selection of an EIL with a low vapor pressure (relative to hydrazine), will not preclude the selection of an EIL compound with low lipophilicity ($logK_{ow}$), low affinity for sorption onto organic carbon / soil ($logK_{oc}$), or low fugacity when dissolved in an aqueous phase ($logK_{aw}$). Further, the low vapor pressures and Henry's law constants computed by EPI suite for the nitrate-containing EILs is consistent with low vapor pressures observed for other IL salts and ionic species in general. Finally, the ability of the Abraham pp-LFER to accurately rank the imidazolium and pyridinium-based ILs in the training set (figure 8) strongly suggests the applicability of the method (method 4) for the structurally similar energetic compounds and their counter-ions (Table 2). However, further work is necessary to more accurately determine the appropriate anion fragment values for 5-aminotetrazolate (5AT) and NTO in octanol –water as well as N anion fragment values for the remaining physical chemical parameters, in order to accurately determine the magnitudes of the EILs, relative to the reference compounds for the remaining thermodynamic properties.

Chapter 5

FUTURE WORK

5.1 Disassociation of the Tight Ion Pair

An additional complication in predicting potential toxicological risk and exposure to EILs and other ionizable species in the environment is determining the method of exposure. Exposure to the direct liquid phase versus exposure to the dilute EIL in the water phase will not only determine the concentration to which the organism is exposed, but the dominant species to which it is exposed (i.e. the neutral tight ion pair or the cationic EIL species). Consequently, it is necessary to determine which major species (i.e. the tight ion pair, or the individual EIL anion and cation species) will be present in the exposure / risk pathways.

For direct exposure to the concentrated ionic liquid, it is expected that disassociation of the EIL tight ion pair will be minimal, as the concentration of EIL is extremely high. Consequently, we would expect that existing models for the neutral species and models developed for the tight ion pair (Eq. (4-3)) would be applicable to these systems with further calibration for necessary counter-ions and the various thermodynamic-equilibrium systems for which calibration data was not available.

For systems in which the exposure route is through an aqueous phase (e.g., soil pore water and vapor over aqueous mixtures of EILs) disassociation of the EIL tight ion pair is expected to be significant. Since the EIL systems are nitrate salts, which have been shown to be highly soluble (Fig. 11), models which utilize the tight ion pair or the neutral EIL species may not be directly applicable. Consequently, further model refinement is required.

We propose the development and calibration of new Abraham pp-LFER solute descriptors for the EIL cation species directly, using methods developed previously for primary - quaternary amine cations in octanol-water and organic carbon – water systems.

These challenges will be addressed in an extension to SERDP WP-2400 as outlined in the WP-2400 extension scope of work (SoW).

5.2 Acid-Base Behavior of Energetic Ionic Liquid (EIL) Cations

Confounding the effects of ion pair disassociation for EIL compounds is that all of the EIL cations studied (Table 2) are organic bases. Consequently, the speciation of the EIL cations is pH dependent. As shown previously, estimates of thermodynamic properties (e.g., octanol-water partition coefficients) can differ by 2-3 orders of magnitude for a cation and its neutral species (Figure 5). Consequently, the speciation and potential toxicological risk of the EIL cations in various environmental systems can vary significantly with soil or aqueous pH.

Since pKa values for the EIL cations (Table 2) are well-characterized within the literature, the main challenge in estimating the speciation and risk for these species is to determine accurately the thermodynamic properties for the ionized EIL species. This challenge will be incorporated into the extension to SERDP WP-2400 as outlined in the WP-2400 extension scope of work (SoW).

Appendix A

SUPPLEMENTAL INFORMATION

A.1 Imidazolium and pyridinium-based IL training set

IL	Name	logKow (Expt)
[C2MIM][Ac]	1-ethyl-3-methylimidazolium Acetate	-2.530
[C4MIM][Ac]	1-butyl-3-methylimidazolium Acetate	-2.770
[C2MIM][BF4]	1-ethyl-3-methylimidazolium Tetrafluoroborate	-2.615
[C4MIM][BF4]	1-butyl-3-methylimidazolium Tetrafluoroborate	-2.477
[C6MIM][BF4]	1-hexyl-3-methylimidazolium Tetrafluoroborate	-1.580
[C8MIM][BF4]	1-octyl-3-methylimidazolium Tetrafluoroborate	-1.097
[C4MIM][Br]	1-butyl-3-methylimidazolium Bromide	-2.480
[C5COOMIM][C8SO4]	3-Methyl-1-(pentoxycarbonylmethyl)imidazolium Octylsulfate	-0.310
[Bz2MIM][Cl]	1-Methyl-3-(2-phenylethyl)-imidazolium Chloride	-1.990
[Bz4C1MIM][Cl]	1-Methyl-3-(4-methylbenzyl)-imidazolium Chloride	-1.800
[BzMIM][Cl]	1-Benzyl-3-methylimidazolium Chloride	-2.350
[C10MIM][Cl]	1-decyl-3-methylimidazolium Chloride	0.311
[C1COOMIM][Cl]	3-Methyl-1-(carboxymethyl)imidazolium Chloride	-2.000
[C1OC2MIM][Cl]	1-(2-Methoxyethyl)-3-methyl-imidazolium Chloride	-3.770

[C2OMIM][Cl]	1-(Ethoxymethyl)-3-methyl-imidazolium Chloride	-3.310
[C2py][Cl]	1-ethylpyridinium Chloride	-3.550
[C32=MIM][Cl]	1-Methyl-3-(2-propenyl)-imidazolium Chloride	-3.250
[C4-2C1py][Cl]	1-Butyl-2-methylpyridinium Chloride	-2.780
[C4C1py][Cl]	1-butyl-4-methylpyridinium Chloride	-2.570
[C4DC1Apy][Cl]		-2.130
[C4DC1py][Cl]		-2.380
[C4MIM][Cl]	1-butyl-3-methylimidazolium Chloride	-2.585
[C4Mpy][Cl]	1-butyl-3-methylpyridinium Chloride	-2.620
[C4py][Cl]	1-butylpyridinium Chloride	-2.820
[C6C1py][Cl]	1-hexyl-4-methylpyridinium Chloride	-1.650
[C6DC1Apy][Cl]		-1.150
[C6MIM][Cl]	1-hexyl-3-methylimidazolium Chloride	-1.730
[C6Mpy][Cl]	1-Hexyl-3-methylpyridinium Chloride	-1.580
[C8MIM][Cl]	1-octyl-3-methylimidazolium Chloride	-0.600
[C8py][Cl]	1-octylpyridinium Chloride	-0.720
[C9MIM][Cl]	1-nonyl-3-methylimidazolium Chloride	-0.130
[POHMIM][Cl]	1-(3-Hydroxypropyl)-3-methylimidazolium Chloride	-3.691
[C4MIM][DCA]	1-butyl-3-methylimidazolium Dicyanamide	-2.320
[C2MIM][F3Ac]	1-ethyl-3-methylimidazolium Thiocyanate	-2.750
[C2py][F3Ac]	1-ethylpyridinium Thiocyanate	-2.570
[C6MIM][F3Ac]	1-hexyl-3-methylimidazolium Thiocyanate	-2.300
[C4MIM][NO3]	1-butyl-3-methylimidazolium Nitrate	-2.660
[C4MIM][OTf]	1-butyl-3-methylimidazolium Trifluoromethylsulfonate	-1.610
[C6Mpy][OTf]	1-Hexyl-3-methylpyridinium Trifluoromethylsulfonate	-0.638
[C2MIM][PF6]	1-ethyl-3-methylimidazolium Hexafluorophosphate	-2.090

[C4MIM][PF6]	1-butyl-3-methylimidazolium Hexafluorophosphate	-1.977
[C6MIM][PF6]	1-hexyl-3-methylimidazolium Hexafluorophosphate	-1.030
[C8MIM][PF6]	1-octyl-3-methylimidazolium Hexafluorophosphate	-0.321
[C1MIM][TF2N]	1-methyl-3-methylimidazolium Bis(trifluoromethylsulfonyl)imide	-1.350
[C2COOpy][TF2N]	1-(2-Ethoxycarbonyl)methylpyridinium Bis(trifluoromethylsulfonyl)imide	-1.700
[C2DMIM][TF2N]	1-ethyl-2,3-dimethylimidazolium Bis(trifluoromethylsulfonyl)imide	-1.040
[C2MIM][TF2N]	1-ethyl-3-methylimidazolium Bis(trifluoromethylsulfonyl)imide	-1.336
[C2OCOOMIM][TF2N]	3-Methyl-1-(2-ethoxy)ethoxycarbonylmethyl)imidazolium Bis(trifluoromethylsulfonyl)imide	-1.520
[C2py][TF2N]	1-ethylpyridinium Bis(trifluoromethylsulfonyl)imide	-0.900
[C3DMIM][TF2N]	1-propyl-2,3-dimethylimidazolium Bis(trifluoromethylsulfonyl)imide	-0.770
[C3MIM][TF2N]	1-propyl-3-methylimidazolium Bis(trifluoromethylsulfonyl)imide	-0.880
[C3OHpy][Tf2N]	1-(3-Hydroxypropyl)pyridinium Bis(trifluoromethylsulfonyl)imide	-1.700
[C3py][TF2N]	1-propylpyridinium Bis(trifluoromethylsulfonyl)imide	-1.400
[C4DMIM][TF2N]	1-butyl-2,3-dimethylimidazolium Bis(trifluoromethylsulfonyl)imide	-0.076
[C4MIM][TF2N]	1-butyl-3-methylimidazolium Bis(trifluoromethylsulfonyl)imide	-0.711
[C4OCOOMIM][TF2N]	3-Methyl-2-(2-butoxy)ethoxycarbonylmethyl)imidazolium Bis(trifluoromethylsulfonyl)imide	-0.585
[C4py][TF2N]	1-butylpyridinium Bis(trifluoromethylsulfonyl)imide	-0.260
[C5COOMIM][TF2N]	3-Methyl-1-(pentoxycarbonylmethyl)imidazolium Bis(trifluoromethylsulfonyl)imide	0.137
[C5MIM][TF2N]	1-pentyl-3-methylimidazolium Bis(trifluoromethylsulfonyl)imide	-0.110
[C6DMIM][TF2N]	1-hexyl-2,3-dimethylimidazolium Bis(trifluoromethylsulfonyl)imide	-0.062
[C6MIM][TF2N]	1-hexyl-3-methylimidazolium Bis(trifluoromethylsulfonyl)imide	0.177
[C6Mpy][TF2N]	1-Hexyl-3-methylpyridinium Bis(trifluoromethylsulfonyl)imide	0.326

[C7MIM][TF2N]	1-heptyl-3-methylimidazolium Bis(trifluoromethylsulfonyl)imide	0.570
[C8iQuin][TF2N]	N-Octylisoquinolinium Bis(trifluoromethylsulfonyl)imide	1.610
[C8MIM][TF2N]	1-octyl-3-methylimidazolium Bis(trifluoromethylsulfonyl)imide	0.340
[C2MIM][TF5P]	1-ethyl-3-methylimidazolium Tris(pentafluoroethyl)trifluorophosphate	0.732

757

References

(1) Pandey, S. Analytical applications of room-temperature ionic liquids: A review of recent efforts. *Analytica Chimica Acta* **2006**, *556*, 38-45.

(2) Marciniak, A. Influence of cation and anion structure of the ionic liquid on extraction processes based on activity coefficients at infinite dilution. A review. *Fluid Phase Equilibria* **2010**, *294*, 213-233.

(3) Armand, M.; Endres, F.; MacFarlane, D. R.; Ohno, H.; Scrosati, B. Ionic-liquid materials for the electrochemical challenges of the future. *Nat Mater* **2009**, *8*, 621-629.

(4) Marsh, K. N.; Boxall, J. A.; Lichtenthaler, R. Room temperature ionic liquids and their mixtures—a review. *Fluid Phase Equilibria* **2004**, *219*, 93-98.

(5) Vidal, L.; Riekkola, M.-L.; Canals, A. Ionic liquid-modified materials for solid-phase extraction and separation: A review. *Analytica Chimica Acta* **2012**, *715*, 19-41.

(6) Schenzel, J.; Goss, K.-U.; Schwarzenbach, R. P.; Bucheli, T. D.; Droge, S. T. J. Experimentally Determined Soil Organic Matter-

Water Sorption Coefficients for Different Classes of Natural Toxins and Comparison with Estimated Numbers. *Environmental Science & Technology* **2012**, *46*, 6118-6126.

(7) Neale, P. A.; Escher, B. I.; Goss, K.-U.; Endo, S. Evaluating dissolved organic carbon-water partitioning using polyparameter linear free energy relationships: Implications for the fate of disinfection by-products. *Water Research* **2012**, *46*, 3637-3645.

(8) Card, M. L.; Chin, Y.-P.; Lee, L. S.; Khan, B. Prediction and Experimental Evaluation of Soil Sorption by Natural Hormones and Hormone Mimics. *Journal of Agricultural and Food Chemistry* **2012**, *60*, 1480-1487.

(9) Hawthorne, S. B.; Grabanski, C. B.; Miller, D. J.; Arp, H. P. H. Improving Predictability of Sediment-Porewater Partitioning Models using Trends Observed with PCB-Contaminated Field Sediments. *Environmental Science & Technology* **2011**, *45*, 7365-7371.

(10) Bronner, G.; Goss, K.-U. Predicting Sorption of Pesticides and Other Multifunctional Organic Chemicals to Soil Organic Carbon.

Environmental Science & Technology **2011**, *45*, 1313-1319.

(11) de Ridder, D. J.; Villacorte, L.; Verliefde, A. R. D.; Verberk, J. Q. J. C.; Heijman, S. G. J.; Amy, G. L.; van Dijk, J. C. Modeling equilibrium adsorption of organic micropollutants onto activated carbon. *Water Research* **2010**, *44*, 3077-3086.

(12) Endo, S.; Grathwohl, P.; Haderlein, S. B.; Schmidt, T. C. LFERs for Soil Organic Carbon-Water Distribution Coefficients (K-OC) at Environmentally Relevant Sorbate Concentrations. *Environmental Science & Technology* **2009**, *43*, 3094-3100.

(13) Sun, H.; Zhou, Z. Impacts of charcoal characteristics on sorption of polycyclic aromatic hydrocarbons. *Chemosphere* **2008**, *71*, 2113-2120.

(14) Goss, K. U.; Schwarzenbach, R. P. Linear free energy relationships used to evaluate equilibrium partitioning of organic compounds. *Environmental Science & Technology* **2001**, *35*, 1-9.

Appendix D- DSC of AMRDEC EILs

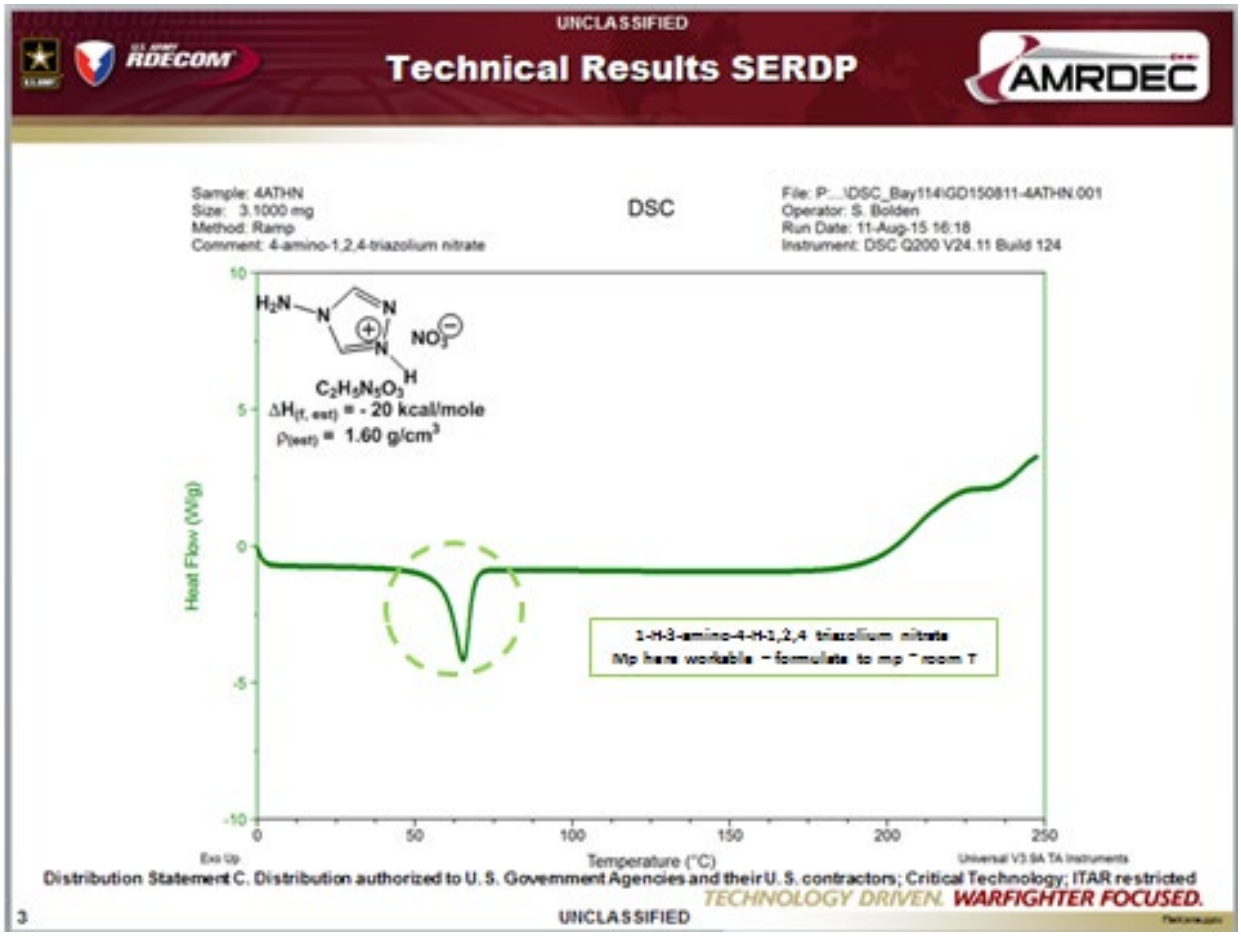

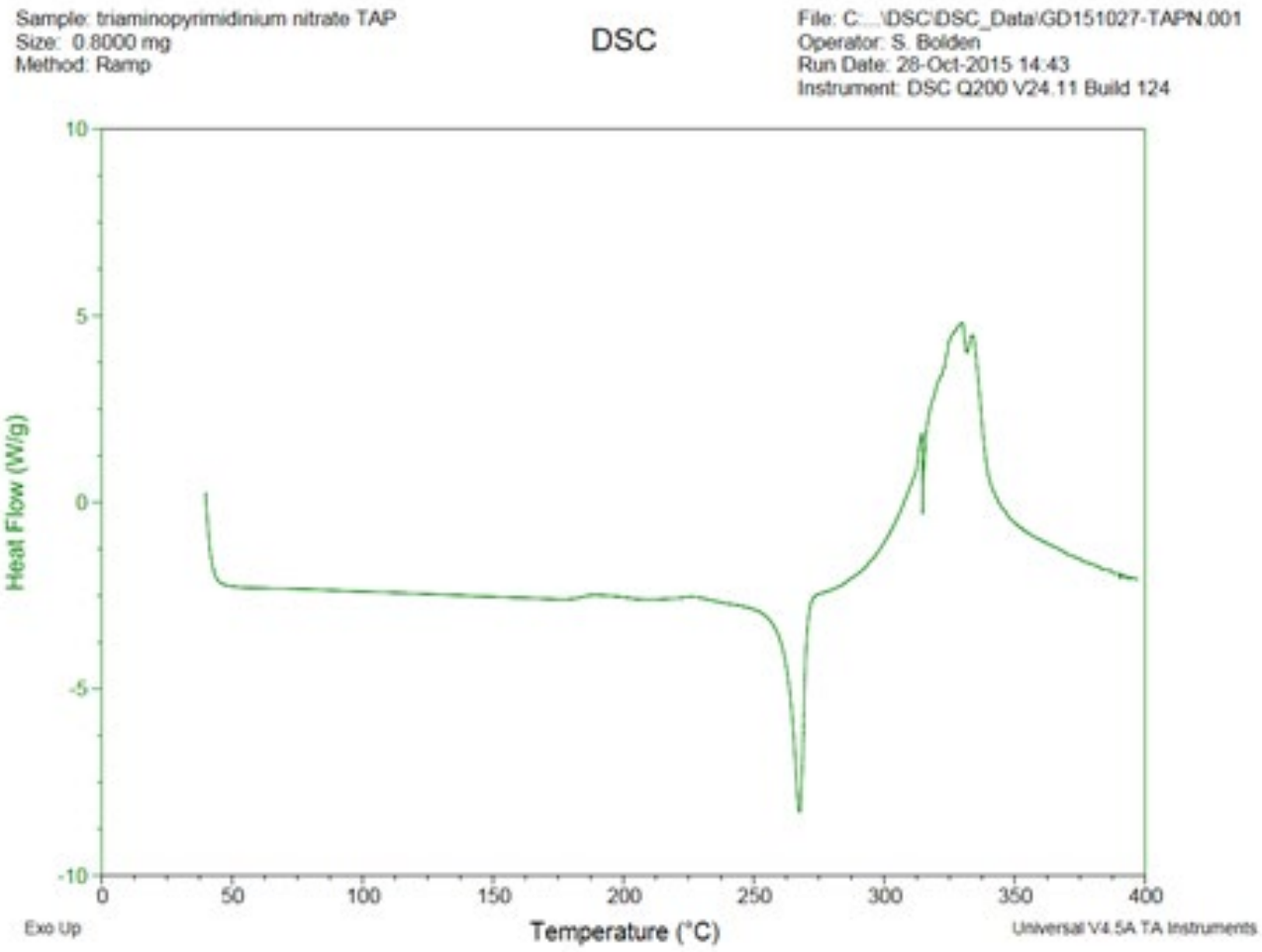
Sample: triaminopyrimidinium nitrate TAP
Size: 0.8000 mg
Method: Ramp
DSC
File: C:...\DSC\DSC_Data\GD151027-TAPN.001
Operator: S. Bolden
Run Date: 28-Oct-2015 14:43
Instrument: DSC Q200 V24.11 Build 124
Heat Flow (W/g)
10
5
0
-5
-10
0
50
100
150
200
250
300
350
400
Exo Up
Temperature (°C)
Universal V4.5A TA Instruments

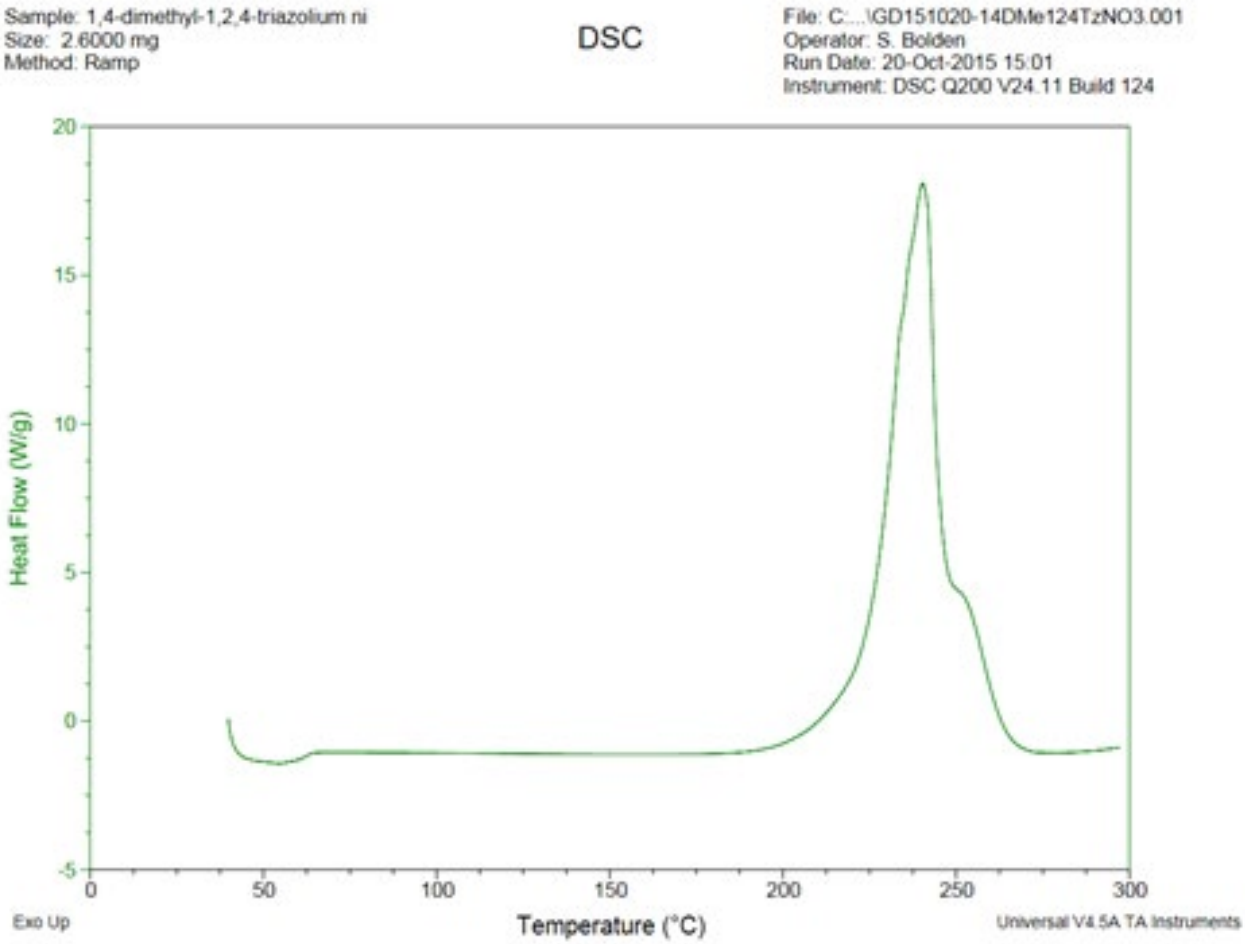
Sample: 1,4-dimethyl-1,2,4-triazolium ni
Size: 2.6000 mg
Method: Ramp
DSC
File: C:...\GD151020-14DMe124TzNO3.001
Operator: S. Bolden
Run Date: 20-Oct-2015 15:01
Instrument: DSC Q200 V24.11 Build 124
Heat Flow (W/g)
20
15
10
5
0
-5
0
50
100
150
200
250
300
Temperature (°C)
Exo Up
Universal V4.5A TA Instruments

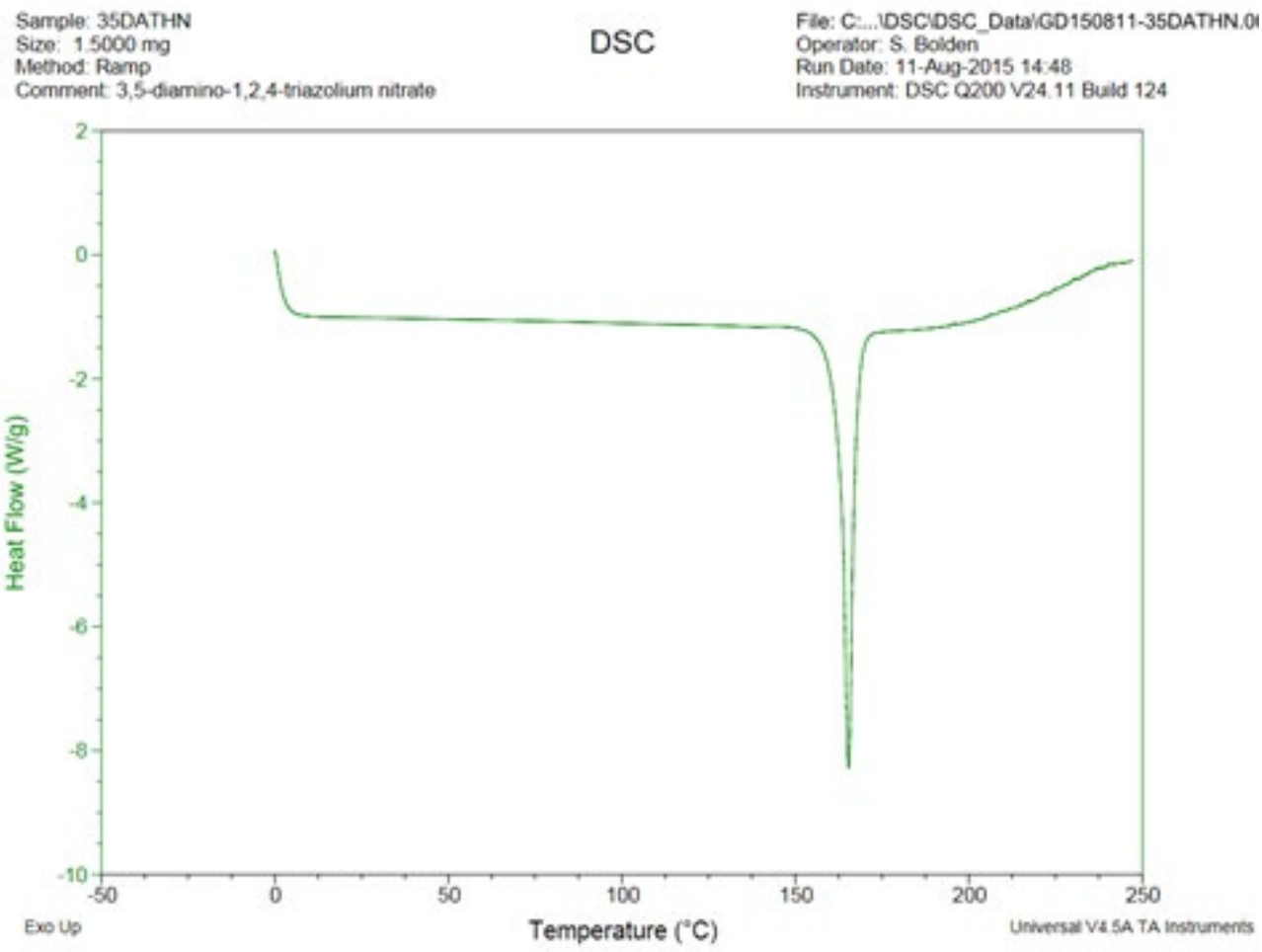
Sample: 35DATHN
Size: 1.5000 mg
Method: Ramp
Comment: 3,5-diamino-1,2,4-triazolium nitrate
DSC
File: C:...\DSC\DSC_Data\GD150811-35DATHN.0
Operator: S. Bolden
Run Date: 11-Aug-2015 14:48
Instrument: DSC Q200 V24.11 Build 124
Heat Flow (W/g)
2
0
-2
-4
-6
-8
-10
-50
0
50
100
150
200
250
Temperature (°C)
Exo Up
Universal V4.5A TA Instruments

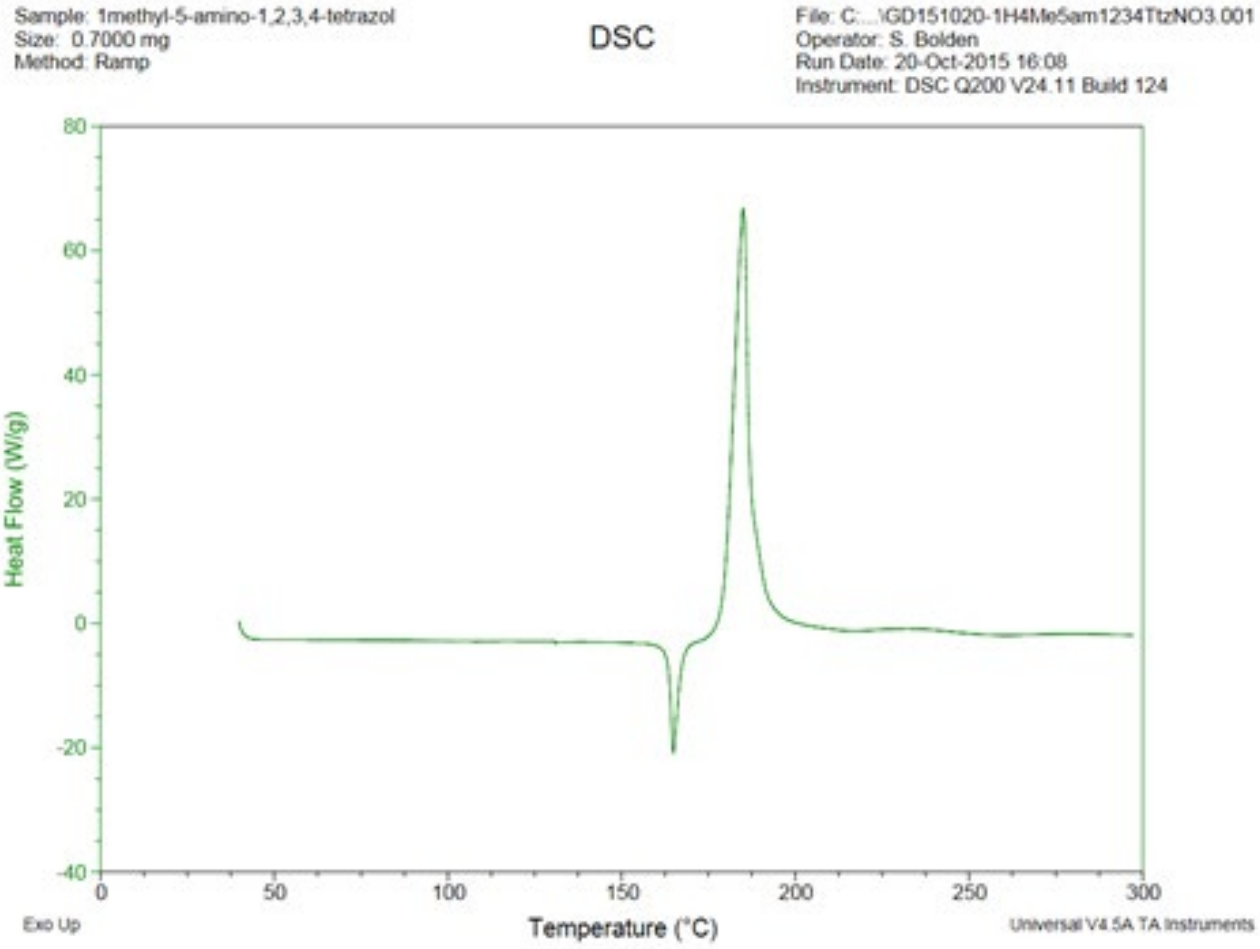
Sample: 1methyl-5-amino-1,2,3,4-tetrazol
Size: 0.7000 mg
Method: Ramp
DSC
File: C:...\GD151020-1H4Me5am1234TtzNO3.001
Operator: S. Bolden
Run Date: 20-Oct-2015 16:08
Instrument: DSC Q200 V24.11 Build 124
Heat Flow (W/g)
80
60
40
20
0
-20
-40
0
50
100
150
200
250
300
Temperature (°C)
Exo Up
Universal V4.5A TA Instruments

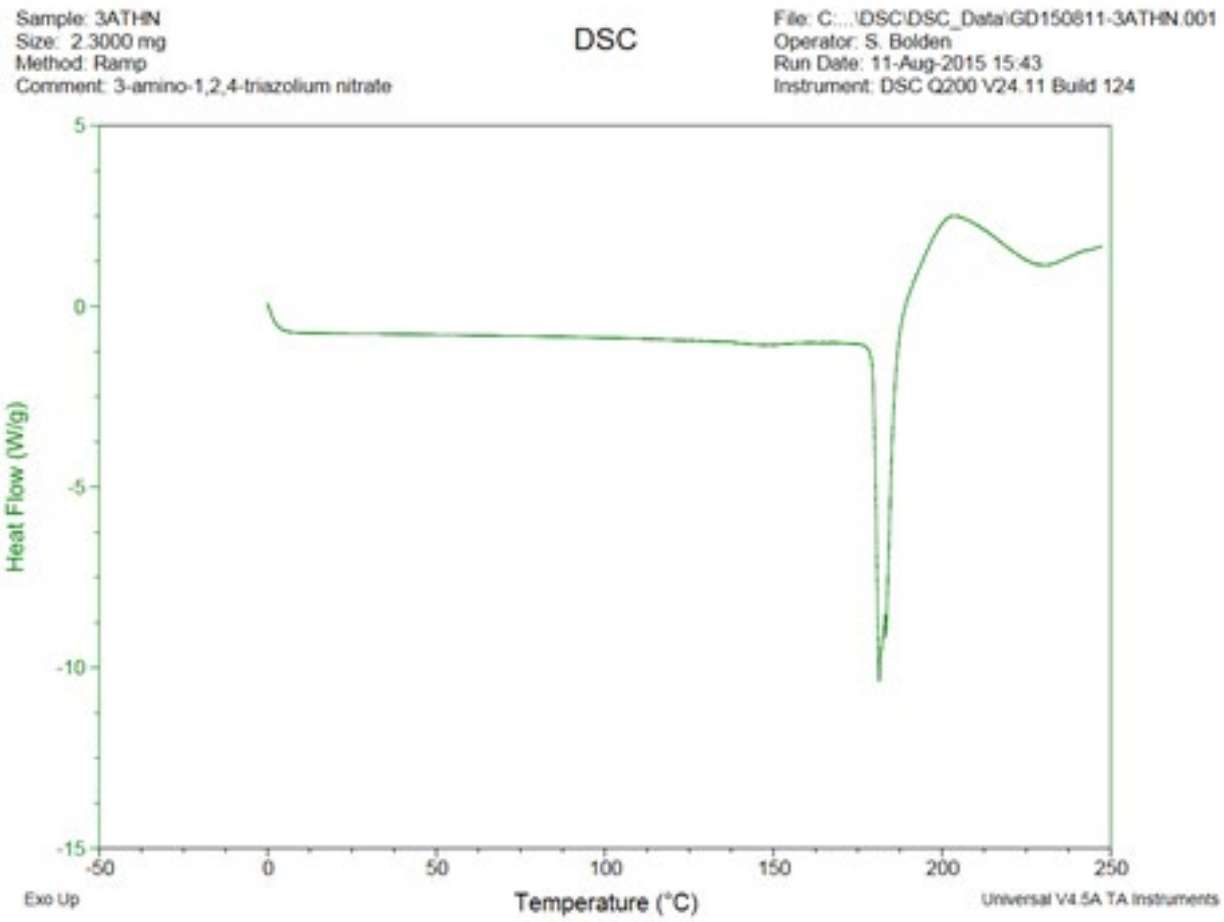
Sample: 3ATHN
Size: 2.3000 mg
Method: Ramp
Comment: 3-amino-1,2,4-triazolium nitrate
DSC
File: C:...\DSC\DSC_Data\GD150811-3ATHN.001
Operator: S. Bolden
Run Date: 11-Aug-2015 15:43
Instrument: DSC Q200 V24.11 Build 124
Heat Flow (W/g)
5
0
-5
-10
-15
-50
0
50
100
150
200
250
Temperature (°C)
Exo Up
Universal V4.5A TA Instruments

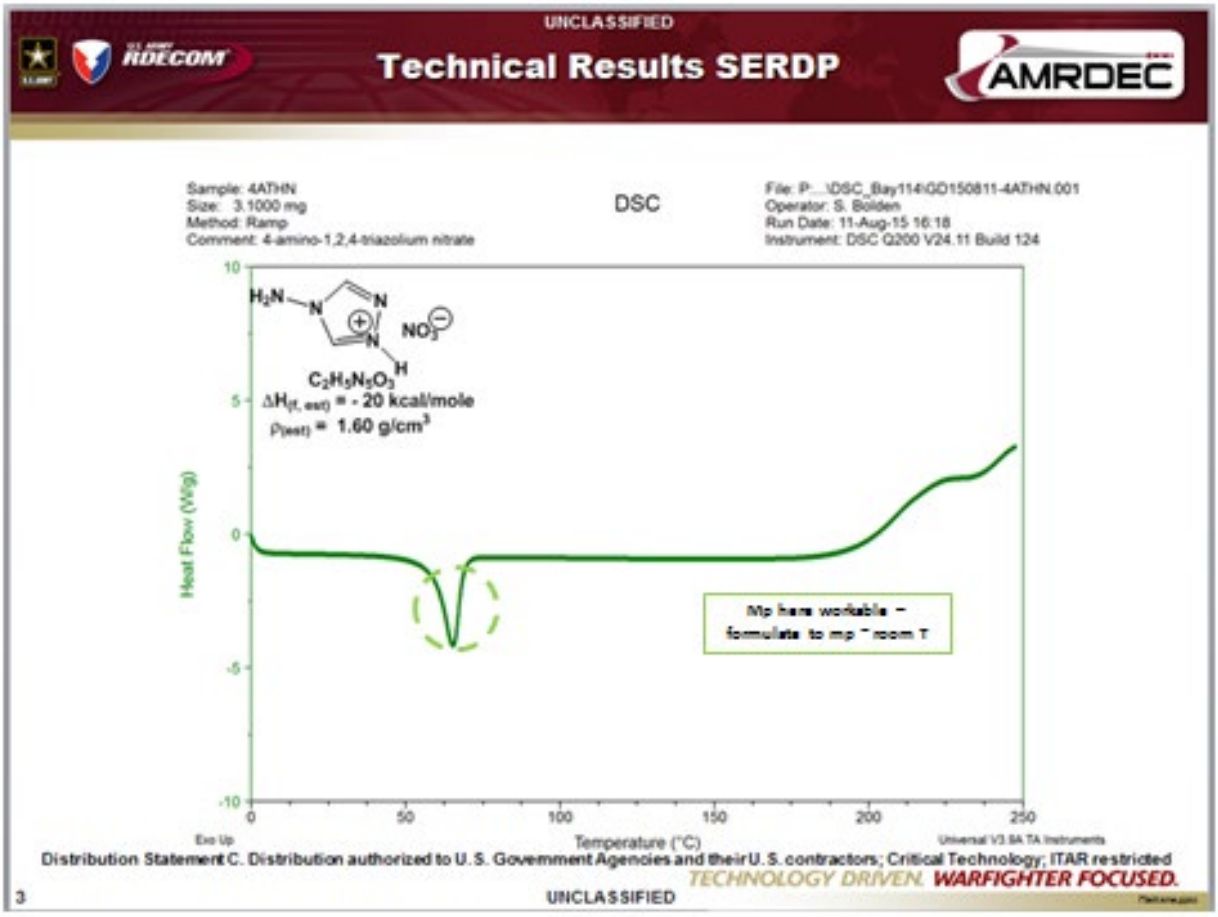
UNCLASSIFIED
Technical Results SERDP
AMRDEC
Sample: 4ATHN
Size: 3.1000 mg
Method: Ramp
Comment: 4-amino-1,2,4-triazolium nitrate
DSC
File: P:...\DSC_Bay114\GD150811-4ATHN.001
Operator: S. Bolden
Run Date: 11-Aug-15 16:18
Instrument: DSC Q200 V24.11 Build 124
$C_2H_5N_5O_3$
$\Delta H_{(f, est)}$ = - 20 kcal/mole
$\rho_{(est)}$ = 1.60 g/cm^3
Mp here workable – formulate to mp ~ room T
Heat Flow (W/g)
Temperature (°C)
Exo Up
Universal V3.8A TA Instruments
Distribution Statement C. Distribution authorized to U.S. Government Agencies and their U.S. contractors; Critical Technology; ITAR restricted
TECHNOLOGY DRIVEN. WARFIGHTER FOCUSED.
3
UNCLASSIFIED

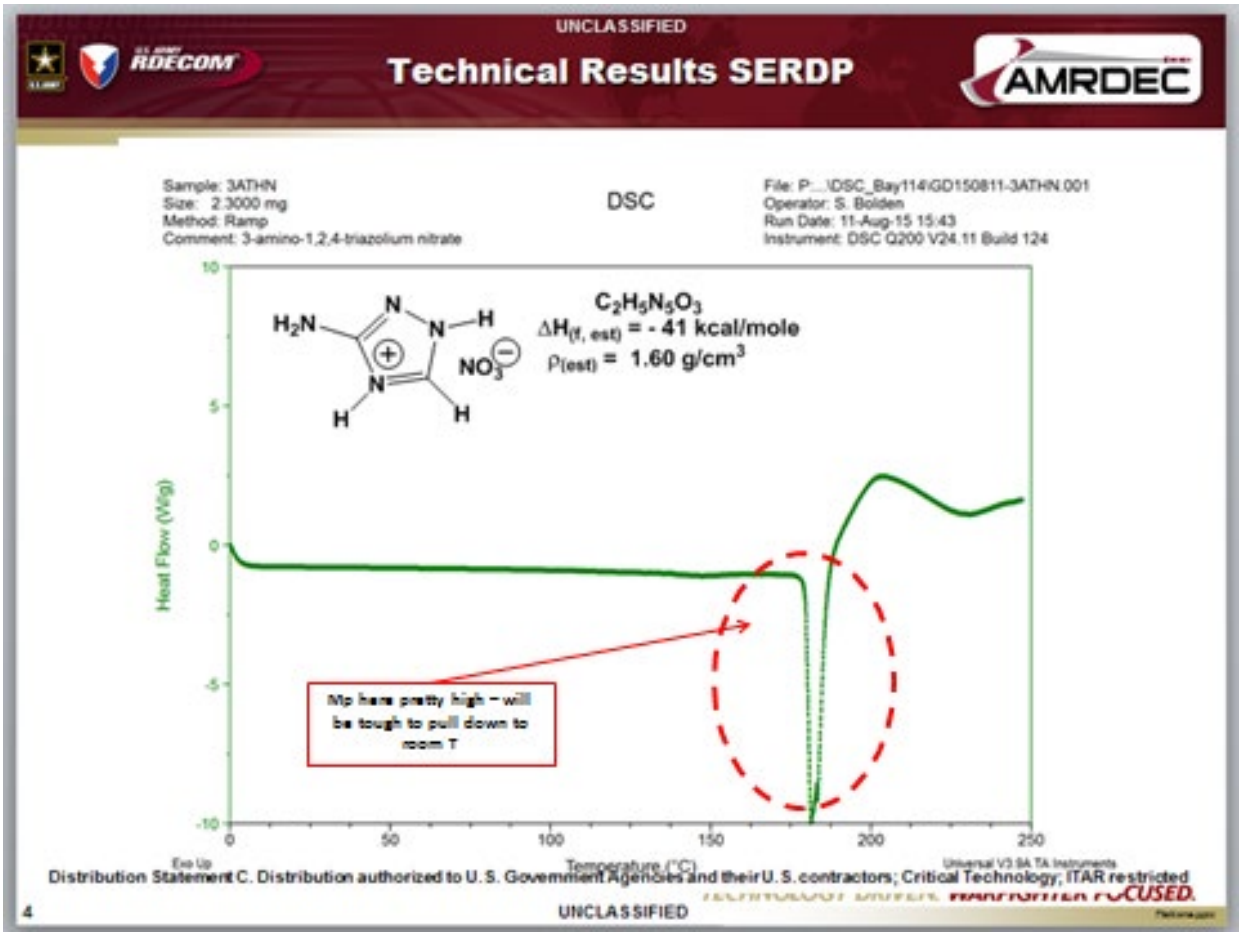
UNCLASSIFIED
RDECOM
Technical Results SERDP
AMRDEC
Sample: 3ATHN
Size: 2.3000 mg
Method: Ramp
Comment: 3-amino-1,2,4-triazolium nitrate
DSC
File: P:...\DSC_Bay114\GD150811-3ATHN.001
Operator: S. Bolden
Run Date: 11-Aug-15 15:43
Instrument: DSC Q200 V24.11 Build 124
$C_2H_5N_5O_3$
$\Delta H_{(f, est)}$ = - 41 kcal/mole
$\rho_{(est)}$ = 1.60 g/cm^3
Mp here pretty high – will be tough to pull down to room T
Heat Flow (W/g)
Temperature (°C)
Exo Up
Universal V3.9A TA Instruments
Distribution Statement C. Distribution authorized to U.S. Government Agencies and their U.S. contractors; Critical Technology; ITAR restricted
4
UNCLASSIFIED

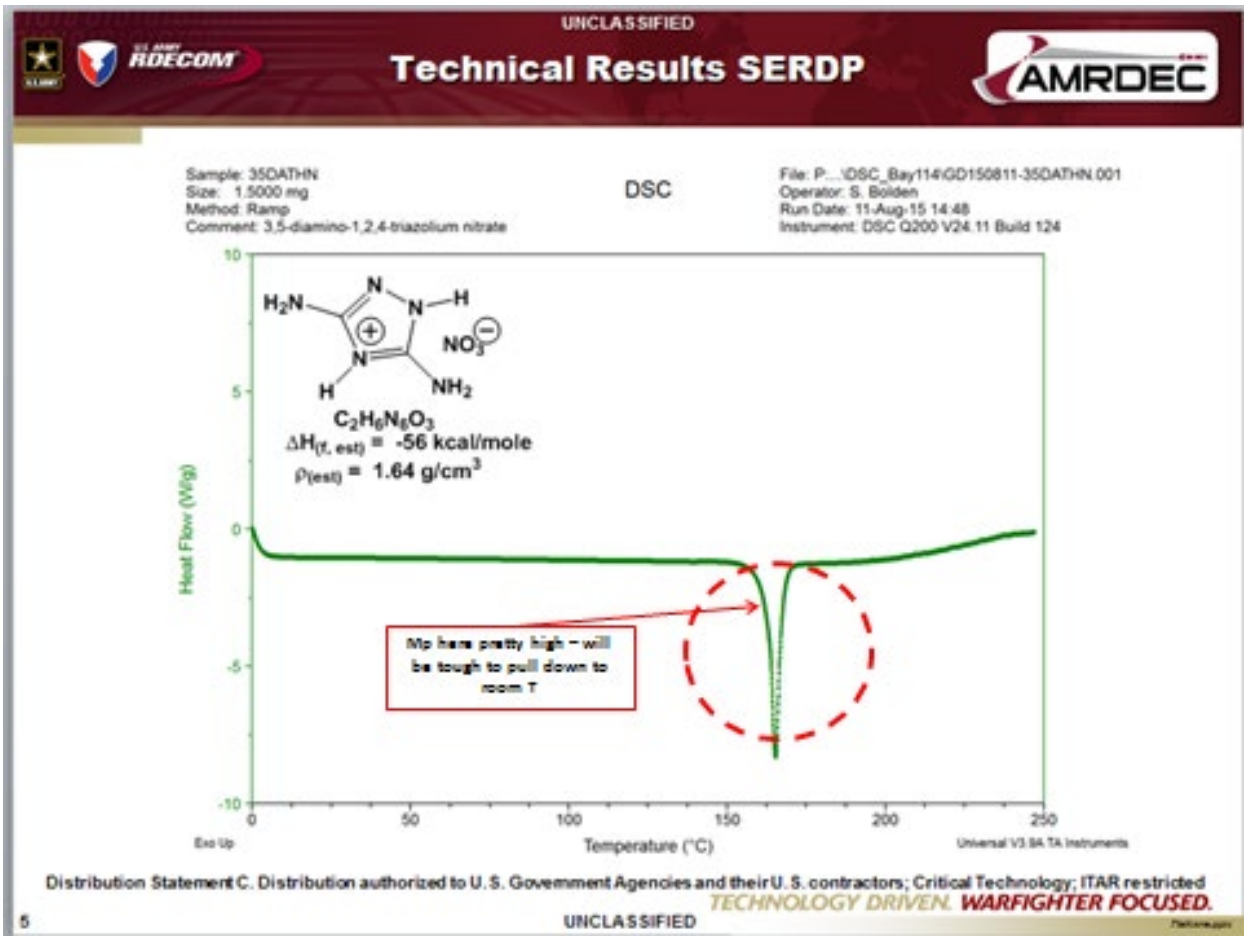
UNCLASSIFIED
RDECOM
Technical Results SERDP
AMRDEC
Sample: 35DATHN
Size: 1.5000 mg
Method: Ramp
Comment: 3,5-diamino-1,2,4-triazolium nitrate
DSC
File: P:...\DSC_Bay114\GD150811-35DATHN.001
Operator: S. Bolden
Run Date: 11-Aug-15 14:48
Instrument: DSC Q200 V24.11 Build 124
$C_2H_6N_6O_3$
$\Delta H_{(f, est)}$ = -56 kcal/mole
$\rho_{(est)}$ = 1.64 g/cm^3
Mp here pretty high – will be tough to pull down to room T
Heat Flow (W/g)
Temperature (°C)
Exo Up
Universal V3.9A TA Instruments
Distribution Statement C. Distribution authorized to U.S. Government Agencies and their U.S. contractors; Critical Technology; ITAR restricted
TECHNOLOGY DRIVEN. WARFIGHTER FOCUSED.
5
UNCLASSIFIED

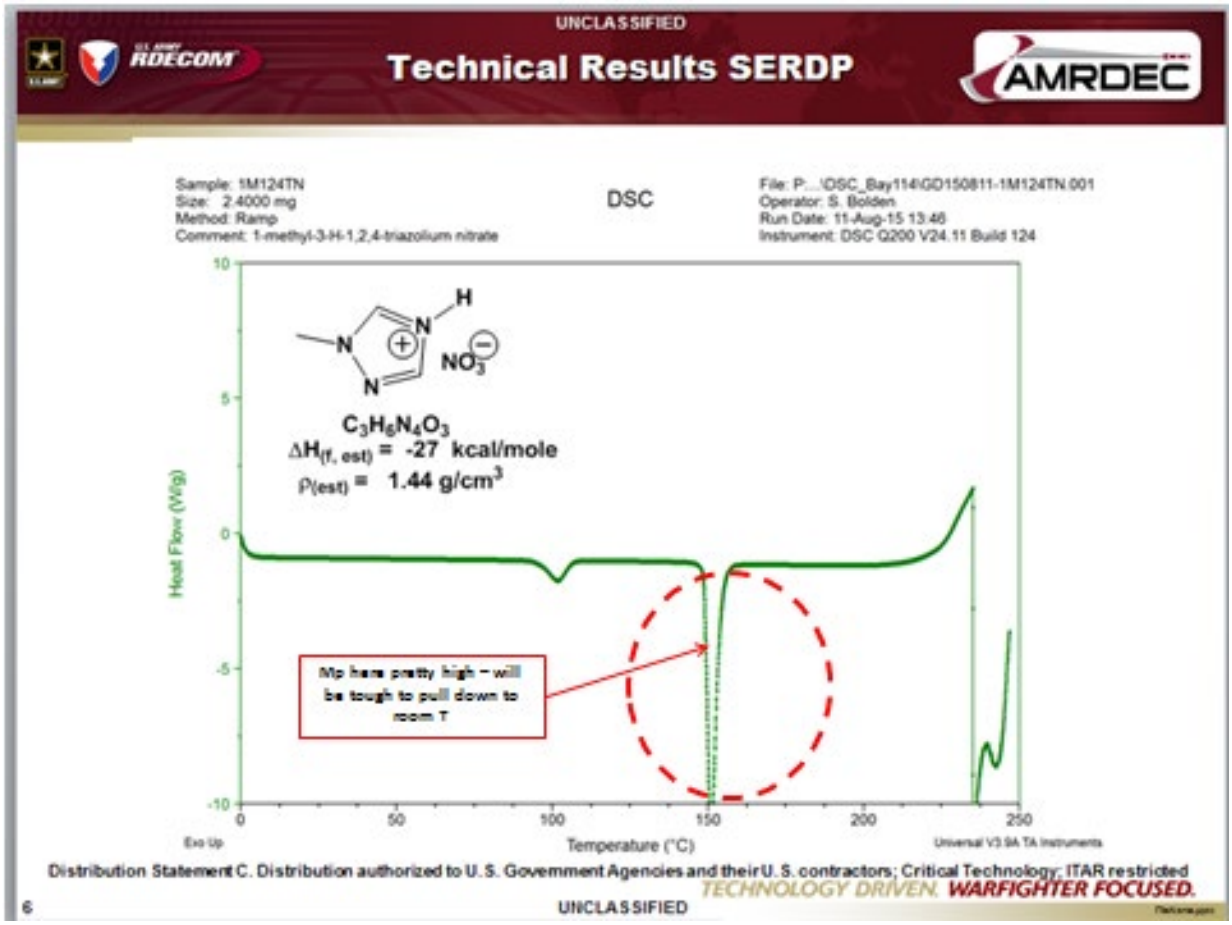
UNCLASSIFIED
RDECOM
Technical Results SERDP
AMRDEC
Sample: 1M124TN
Size: 2.4000 mg
Method: Ramp
Comment: 1-methyl-3-H-1,2,4-triazolium nitrate
DSC
File: P:...\DSC_Bay114\GD150811-1M124TN.001
Operator: S. Bolden
Run Date: 11-Aug-15 13:46
Instrument: DSC Q200 V24.11 Build 124
C3H6N4O3
ΔH(f, est) = -27 kcal/mole
ρ(est) = 1.44 g/cm3
Mp here pretty high – will be tough to pull down to room T
Heat Flow (W/g)
Temperature (°C)
Exo Up
Universal V3.9A TA Instruments
Distribution Statement C. Distribution authorized to U.S. Government Agencies and their U.S. contractors; Critical Technology; ITAR restricted
TECHNOLOGY DRIVEN. WARFIGHTER FOCUSED.
6
UNCLASSIFIED

Appendix E- AFRL JANNAF Paper

LOW TEMPERATURE LIQUID GAS GENERATOR FORMULATIONS

Phu Quach [1], Adam J. Brand [2], and David Scharfe [1]

[1] ERC, Incorporated

Edwards AFB, CA

[2] Air Force Research Laboratory, Propulsion Directorate

Edwards AFB, CA

ABSTRACT

The Air Force Research Laboratory (AFRL), in collaboration with Aerojet Rocketdyne and the Army, has developed a series of low combustion temperature, liquid gas generator/monopropellant formulations under a Strategic Environmental Research and Development Program (SERDP). The program aims to address the increasing concern over the environmental impact of hydrazines for rocket propulsion, but more specifically identifying low toxicity, low flammability liquid Divert Attitude Control Systems (DACS) formulations suitable for shipboard use. The approach of this study was to build upon existing formulations AFRL has developed for spacecraft propulsion and by exploring new ionic liquid formulations with reduced toxicity and low flammability that maintain, or surpass the performance of hydrazine in respect to Density-Specific Impulse (ρ-Isp).

For use in DACS, these formulations maintain theoretical combustion temperatures less than the 1450 K upper-operational limit of Inconel thrusters. This work details three series of ionic liquid formulations: 1) HAN-based AF-M315E-type; 2) triazole salt-based; 3) HAN-free. These formulations explore different energetic salts ranging from triazole-based salts to ammonium nitrate. The theoretical performance of each formulation is presented along with the small scale hazards data. Additionally, data from catalytic reactivity studies and thruster firings of some of these formulations are also reported.

INTRODUCTION

The steady interest in green energy and technology has spurred the development of innovative, environmentally-friendly rocket propellants. The Air Force Research Laboratory (AFRL) has been on the forefront of identifying and characterizing energetic ionic liquids for use in liquid propellants [1]. Ionic liquids are defined as salts with melting points at or below 100 °C. Some benefits conferred by energetic ionic liquids are: low handling hazards (low vapor pressure, largely insensitive to impact, friction, and electrostatic discharge), high density and heats of formation, and thermal stability [2]. Of particular note, the low vapor pressure and vapor toxicity of ionic liquids strongly distinguishes them from the current state-of-the-art hydrazine.

AFRL has been steadily proposing and synthesizing a wide variety of ionic compounds ranging from hydrazinium salts to triazole-based salts. Many nitrogen-rich heterocyclic rings have been synthesized as potential energetic ingredients in monopropellant formulations [3]. This paper focuses on triazolium nitrate salts that have an anticipated high-reactivity to iridium catalysts such as S405. The high nitrogen content, high heat of formation, low melting points, and good thermal stabilities make them particularly attractive for monopropellant formulations. In addition, other hydrazine-salts such as the balanced Hydroxyethyl hydrazinium nitrate (HEHN) have been used in the AFRL formulation AF-M315E.

AF-M315E has been selected for demonstration under the NASA funded Green Propellant Infusion Mission (GPIM) [4, 5]. This green monopropellant offers a 50% increase in ρ-Isp over hydrazine, in addition to reducing the vapor pressure and toxicity over a wide range of temperatures and pressures. The use of the highly toxic and volatile hydrazine necessitates a plethora of time-consuming and expensive mission considerations. Some of the concerns include long-term safe storage, lengthy handling and disposal procedures, and the imperative use of a Self-Contained Atmospheric Protective Ensemble (SCAPE) suit. The higher performance characteristics grant a wider range of volume-limited missions with an increased duration at a lower overall cost. Unfortunately, the high combustion temperature (2165 K) requires the use of exotic and expensive rhenium-based materials for the propulsion system. This study presents some of the joint work completed to address this concern and NAVY shipboard compatibility for liquid propellants.

A collaborative effort with Aerojet Rocketdyne and the Army was formed to develop formulations intended for use in satellite thrusters or as replacements for gas generators in SM-3 Block IIB Solid DACS. The program aims to formulate monopropellants with lower combustion temperatures that would still meet shipboard liquid propellant requirements such as low flammability and low toxicity. Aerojet Rocketdyne is the prime contractor responsible for propellant development, characterization, and thruster testing of new formulations. AMRDEC was contracted to synthesize energetic materials, while AFRL was tasked to provide candidate

formulations and characterize their small scale hazards. Additional funds were provided to AFRL to investigate potential HAN-free formulations that used various energetic salts. Before any blends were made, the salts were assessed for catalytic reactivity on preheated S405.

In an effort to minimize program cost and duration, formulation work centered on identifying new formulations using pre-existing and well characterized materials such as HAN. Some of the technical objectives of the effort are outlined in **Table 1**. In a broad sense, this effort aims to match or surpass the performance of hydrazine while simultaneously reducing the hazards to below that of hydrazine. However, due to the high combustion temperatures typically encountered in many ionic liquid based monopropellants, a principal concern was maintaining compatibility with standard Inconel (nickel alloys) thrusters. Accordingly, much of the formulation effort was directed towards reducing the combustion temperature to around the maximum operating temperature of Inconel and alumina-catalysts at 1450 K. In addition, an upper threshold limit was defined to include formulations with combustion temperatures around 1800 K. Although not ideal, these high performance blends could still be used with higher temperature ceramic catalysts and thruster body materials. These lower combustion temperatures will allow for better thermal management in the propulsion system and possibly an infinite duty cycle.

Table 1. SERDP program objectives

Parameter	**Performance Guideline**
Storage	≤ -20 °C
ρ-Isp	+20% of N2H4
Long-term storage stability	10 year
Low vapor pressure/toxicity	Less than N2H4
Combustion temperature	< 1450 K
Liquid viscosity	< 100 cP @ 20 °C
Decomposition onset	> 150 °C by DSC
Synthesis	≤ 2 steps
Flammability	No flammability with air up to 130 °F
Hazard classification	U.S. DOT 1.3
Ignition delay	≤ 50 ms

Leveraging AFRL's previous work in monopropellants, various candidate formulations were identified and tested in a subscale "microreactor." A preliminary study of ignition delay and combustion properties were compared to firings of the baseline AF-M315E propellant. The results of previous Aerojet Rocketdyne thruster firings of similar formulations are presented as a substitute for any diluted variants. Most of the formulations contain some combination of known energetic salts such as: AN, HAN, and HEHN. Note that although HAN makes an excellent liquid oxidizer, it imparts many undesirable concerns such as: material incompatibility (most metals), sensitivity to impurities leading to poor thermal stability, and poor ignitability. Because of these issues, several HAN-less formulations were also investigated in this study. AFRL's ultimate approach was to provide a candidate formulation from each of the three following classes: 1) HAN-based, 315E type; 2) triazole salt based; and 3) HAN-free. All of these formulations conform to most of the desirable small-scale safety properties listed in **Table 2**.

Table 2. Desirable monopropellant small-scale safety properties

Characteristic	**Objective**
Thermal stability	<2% wt. decomposition for 48 hrs at 75 °C
Unconfined ignition response	No explosive response
Impact sensitivity (Olin Mathiesen drop weight)	>20 kg-cm
Friction sensitivity (Julius Peters sliding friction)	Insensitive at >300N
Detonability (NOL card gap)	Negative at zero-cards (Class 1.3)
Adiabatic compression (U-Tube test)	Insensitive (Pressure ratio >35)
Electrostatic discharge sensitivity	Insensitive to static spark discharge (1J)
Vapor toxicity	Low hazard (No SCBA requirement)

PROPELLANT FORMULATIONS

Two distinct sets of monopropellants were formulated to meet the optimal and threshold combustion temperatures of 1450 K and 1800 K. Some of the blends were diluted variants of previously tested formulations, simply reformulated to meet the program goals; these formulations are identified with the "-D" at the end of the name. The first set of formulations contain a diluted variant of 315E, a HAN-free 315F, and a HN/AN based 1028B. The second set of formulations are high performance, triazole-based blends containing variants of a previously tested 1107P and a novel 824S monopropellant. The constituents of the candidate formulations are presented **Table 3**; note that all of the propellants contain water as the diluent. Most of the ingredients listed are well-known in the industry, with the exception of the triazolium-nitrate salts: HEATN and MATN. HEATN is a thermally stable nitrate salt: 1-hydroxyethyl-4-amino-1,2,4-triazolium nitrate. MATN is a highly energetic nitrate salt: 1-methyl-4-amino-1,2,4-triazolium nitrate. These salts were chosen due to their high heats of formation, low melt points, and potential reactivity to S405 catalyst.

Table 3. Propellant formulations in weight percent.

	315E-D	**315F**	**1028B**	**1107P**	**824S**
AN	--	17.0	7.7	--	--
H2O	32.0	10.0	25.0	28.0	25.0
HEATN	--	--	--	--	24.0
HEHN	34.0	73.0	43.0	5.0	--
HN	--	--	14.3	--	--
MATN	--	--	--	20.0	--
MeOH	--	--	--	--	--
S-HAN5^{++}	34.0	--	10.0	47.0	51.0

$^{++}$Stabilized HAN containing 1 wt% 2-bipyridyl and 5 wt% AN.

Note: 1028B utilizes a eutectic mixture of 65%/35% of HN/AN.

RESULTS AND DISCUSSION

The propellant performance characteristics, hazards, and physical properties are presented in

Table 4. A clear distinction can be made between ionic liquid monopropellants and hydrazine in regards to an immense increase in combustion temperature, yet similar performance. Hydrazine has a high performance relative to its low combustion temperature due to the low molecular weight gases (N2, H2, NH3) it outputs during catalytic decomposition in a thruster. On the contrary and in the case of the carbon-containing ionic liquids, an oxidizer must be used to balance the formulation for complete combustion. Since this produces higher molecular weight gases, the Isp detriment must be offset by a higher combustion temperature. Although the theoretical Isp of 315E-D and 1028B do not surpass hydrazine, the ρ-Isp still outperforms hydrazine by 20 to 30%. The real performance gain for the ionic liquids originates in their superior density (~1.4 vs 1.0 g/mL). More importantly, however, the ionic nature of the formulations impart many favorable traits in regards to propellant hazards such as lower: vapor toxicity, flammability, and handling concerns.

Table 4: Propellant performance characteristics, hazards, and physical properties

	315E-D	**315F**	**1028B**	**1107P**	**824S**
Isp vac. (s, theo.)$^{+}$	221	239	227	244	243
Tc (K, theo.)	1453	1457	1433	1887	1900
Density (g/mL)	1.318	1.393	1.330	1.362	1.402
Impact (kg-cm, 5 neg.)	128	100*	125	129	133
Friction (N, 5 neg.)	>353	88*	>353	>353	>353
ESD (J)	>1	--	>9.4	>9.4	>9.4
TGA (%wt. loss/day, 75 °C)	0.43*	0.20	0.25	0.48*	0.43*
Melt Point (°C)	Glass*	<-35	-7	Glass	Glass
Viscosity (cP, 25 °C)	<25	38	<25	<15	<25
NOL Card Gap (0 cards)	Neg.*	Neg.*	Neg.	Pos.* (12-20)	--

Adiabatic Compression (at 25 °C)	10/10 neg. @200:1	5/5 neg. @135:1	10/10 neg. @200:1	5/5 neg. @200:1	5/5 neg. @200:1

[+]Calculated with Beckman-Acree code at: Pc = 300 psia to vac, ε = 50:1.

*Results from undiluted variants; not expected to deviate significantly for diluted variants.

The formulations were largely insensitive to friction and ESD, with the exception of 315F. The four formulations containing HAN had friction and ESD values at the upper end of the test equipment. This is expected, as the ionic nature of the constituents make them highly electrically conductive. The impact sensitivities of the propellants were in line with typical ionic liquid monopropellants, noting that the maximum value is 200 N. The 315F formulation containing AN had a higher sensitivity to impact and friction. Although this friction sensitivity is higher than other ionic liquid monopropellants, it should still be comparatively safe in day-to-day use. In conjunction with the Zero-Card NOL Card Gap results, all of these formulations would be considered a Class 1.3 explosive.

Another attractive property of the formulations is their thermal stability. All of the blends had less than 1 wt% decomposition per day at 75 °C. Notably, the formulations lacking HAN as the primary oxidizer (315F and 1028B) had a weight loss only half that of the other formulations. This provides further impetus for identifying more formulations that omit HAN as the oxidizer. To gauge the thermal stability of the triazole formulations, a simulated slow cook off in a TGA (3 C/hour ramp to 60 °C, 3 hour soak) was performed on undiluted 315E, 1107P, and 824S. The onset temperatures of the three blends were found to be 137, 113, and 141 °C, respectively. It was evident that MATN was decidedly less thermally stable than HEATN in a similar propellant system. In-house studies have found that this is likely due to the stabilizing effect of the hydroxyethyl group (on HEATN) to HAN.

Per program agreement, AFRL also assessed the adiabatic compression sensitivity of the propellants using a custom U-tube apparatus [6]. The U-tube design allows for evaluating the sensitivity of the propellants at elevated temperatures in a closed system that has compression rates and response times comparable to spacecraft isolation valves. These tests simulate a sudden shock to the propellant from the rapid opening or closure of valves or a direct hit to a propellant storage tank.

Previous studies showed that neat 315E had a threshold-pressure initiation of roughly 300 psi at 25 °C (19/19 neg.), corresponding to a compression ratio of about 20 to 1 [7]. These results also held true at 60 °C and 90 °C under the same conditions. This compression ratio is an order of magnitude more sensitive than those of the formulations currently presented. The initiation level for four of the five propellants was 200 to 1 or 3000 psi in the test setup. This value is the maximum burst pressure available in-house and the highest compression ratio ever seen in similar

monopropellant tests. 315F had a lower, albeit still respectable compression ratio of 135 to 1. The substantial water dilution likely suppressed any high level adiabatic response by reducing overall explosive energy or partially attenuating the shock wave. The new propellants are also expected to retain their low adiabatic compression sensitivity at elevated temperatures (≤ 90 °C) when considering the previous results of thermally damaged 315E [7].

CATALYTIC REACTIVITY TESTS

In order to identify potential propellants that lacked HAN as the primary oxidizer, a series of oxygen balanced salts were synthesized and screened for catalytic reactivity. The candidates investigated and their respective reactivity are listed in **Figure 2**. A few of these materials—such as 5-nitro-3-oxytetrazole—were first synthesized by SRI international and explored for use as potential melt cast explosives; however, they have never been evaluated in monopropellant formulations. These nitrogen-rich materials have high heats of formation and densities of upwards of 40 kcal/mol and 1.70 g/mL. In addition, the adjacent nitrogen atoms are theorized to improve catalytic reactivity on standard hydrazine catalysts. Preliminary Isp calculations showed that some of the salts could be formulated with an appropriate oxidizer and diluent to meet the program goals. The exhaust products were primarily N_2, CO_2, and H_2O with no solid particulate and trivial amounts of methane.

The catalytic reactivity of the salts were gauged qualitatively using a drop test on hot S405 (0.1g at ~220 °C), which was ranked numerically from 1 to 5. If the salt was a solid, it was first dissolved in a small amount of compatible solvent such as water or acetonitrile. The progressive scale is defined as such: 1) slow bubbling; 2) bubbling and light fuming, no flame; 3) fuming off with delayed ignition and flame; 4) rapid fuming and quick ignition with flame; 5) very rapid, violent ignition. As a reference point, undiluted 315E is assigned a rank of 4. Note that the undiluted variants of the formulations presented were subjected to this qualitative test, and were rated on par with 315E with a rank of 4. However, as discussed later, the ignition delay of any diluted variants should be expected to progressively degrade as the dilution is increased.

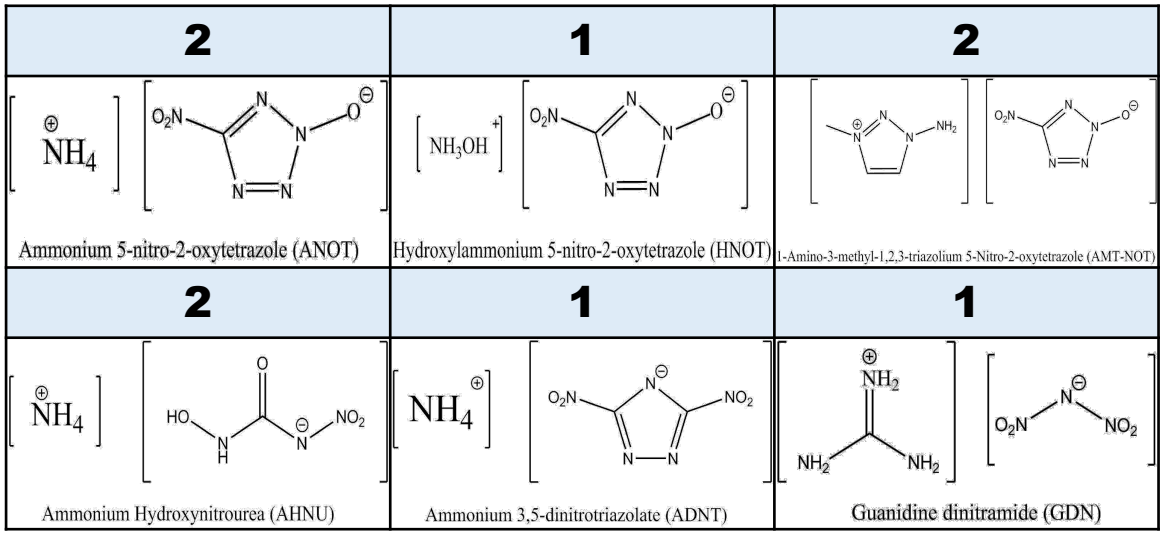

Figure 2. Nitrogen-rich salts investigated and their respective catalytic reactivity (S405 at 220 °C).

The salts investigated did not have much reactivity to the S405 catalyst at the set preheat temperature. The dissolved salts simply bubbled and fizzed upon contact with the catalyst; subsequent drops did not illicit any appreciable reaction with the exception of ADNT. There was a delayed response for ADNT, with a quick, bright flash occurring after approximately 3 minutes. However, this exceedingly delayed reaction does not warrant further investigation of this particular salt. Although these proposed salts did not appear to be catalytically reactive at this temperature, the cations could possibly be exchanged with more reactive ones such as hydrazinium. There are a myriad energetic salts that could be synthesized and tested in future studies with different catalysts or preheat temperatures.

AFRL MICROREACTOR HARDWARE

A “microreactor” was designed at AFRL to serve as an inexpensive modular testbed for studying the combustion properties of monopropellants. The microreactor and feed system shown

in **Figure 3** is made of slightly modified, off-the-shelf parts—allowing for rapid screening of new monopropellant blends. The microreactor has been fired with pulse lengths ranging from 0.5 seconds up to 10 seconds. The bedplate is a 1/2" diameter Ultramet SiC foam bedplate coated with $LaAlO_3$, allowing for a 10 minute reactor lifetime. All firings discussed in this study were conducted with a feed pressure target of 400 psi and a catalyst bed preheat target of 400 °C. The granular catalyst used was Sienna SSC-0103 at 18-25 mesh. This system has been demonstrated in previous studies and in the testing of a Busek Microthruster [8, 9].

The hardware is fired inside of a large vacuum chamber, reaching a base pressure of 20 mTorr. A pair of diagnostics have been implemented to measure the feed rate of the propellant: 1) graduated sight glass video/ measurements of propellant and 2) GN2 volumetric flow rate. The mass flow rate of the propellant is monitored using a graduated sight glass filled with propellant and a gas volumetric flow meter measuring the displacement of GN2 as it backfills the propellant outflow .Video recordings of the propellant in the sight glass, combined with a calibration of distance and the known internal cross-sectional area of the sight glass tubing, allow for rough estimates of the propellant flow. This unique system for measuring mass flow rate was implemented due to the incompatibility between HAN and most transition metals commonly found in Coriolis meters. Additionally, the "spin up time" in these types of meters can result in a significant delay in volume measurements. These transients are not of concern in long, steady burns, but cause inaccurate measurements for short or rough test pulses.

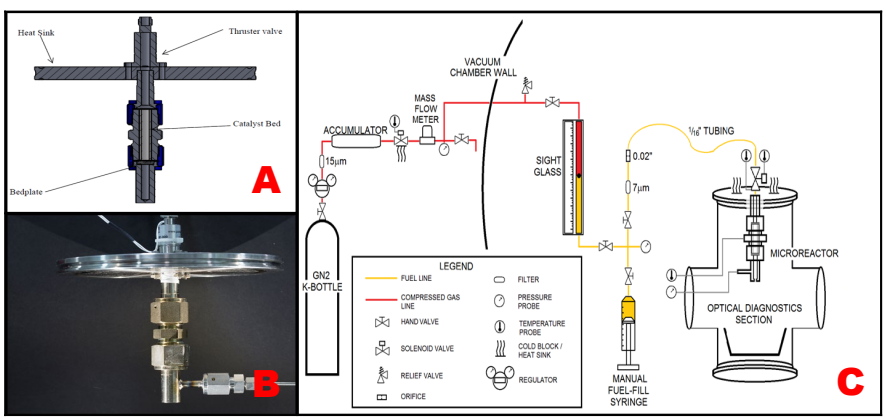

Figure 3. A) CAD model of microreactor, B) image of fully assembled microreactor, and C) feed system schematic.

AFRL MICROREACTOR FORMULATIONS

AFRL developed 315F as a HAN-free monopropellant with a low combustion temperature. The benefits of omitting the acidic HAN are numerous, i.e. the AN substitute not attacking metallic hardware. Furthermore, HAN becomes less thermally stable and has a lower onset temperature as

it absorbs metal ions; this reaction is autocatalytic as it produces higher levels of nitric acid. On the other hand, a realistic concern about using such a fuel rich formulation in a small satellite thruster: the production of solid particulates or soot. Theoretical thermoequilibrium calculations, however, showed that methane was a primary exhaust product rather than soot. This speculation was verified in observations made during the test firings shown below. Another justifiable concern is the high viscosity of the formulation, originating from the considerable amount of HEHN present. This has an appreciable effect on the final propulsion system design and can be addressed via reformulation if the propellant proves viable.

The 824 series was formulated to investigate the use of energetic nitrogen-rich heterocycles in a monopropellant. It has a high energy density and is more thermally stable than other formulations containing similar triazole salts (MATN). A diluted form of this propellant, 824S, was proposed specifically to meet the combustion temperature objective of this program. Both 315F and 824S demonstrated high reactivity with preheated S405 and SSC-0103 in the qualitative drop test. However, neither of these propellants has ever been fired in a catalytic reactor or thruster until this current study. The results of AFRL's microreactor experiments on 315E baseline, 315F, and 824S are presented below. Note that these firings are primarily qualitative experiments to demonstrate and compare the catalytic reactivity of the propellants to the 315E baseline. The results are not a definitive measure of propellant performance in an actual thruster. Any poor ignition delays observed are likely a function of the hardware or other associated factors.

MICROREACTOR FIRINGS OF 315F

A series of 0.5 to 4 second firings were performed on both neat 315E and 824S at a nominal feed pressure of 400 psi and 400 °C preheat. A representative 4 second steady-state pressure trace of both propellants is shown in **Figure 4**. The severe pressure roughness and prolonged ignition delays indicate suboptimal hardware and firing conditions. Nonetheless, a few important combustion characteristics of 315F can still be gleaned from the results.

Neat 315E appeared to have an ignition delay on the order of 1 second, while 315F took closer to 1.25 seconds. This is likely due to the higher catalytic reactivity of HAN in 315E than the AN in 315F. 315F had a slightly smoother steady state pressure, oscillating around 175 psi. This is noticeably lower than the roughly 200 to 225 psi achieved with neat 315E under the same conditions. This is expected, as the performance of 315F is significantly lower than that of neat 315E. The results are promising as the propellant was able to sustain combustion for an extended period of time with little pressure degradation. Additionally, there was no evidence of soot found in the catalyst bed nor the disassembled nozzle post-firing. The clear exhaust observed during the firing is encouraging in regards to the production of solid particulates caused by the fuel-rich formulation. In short, these results confirm the catalytic reactivity of 315F and its potential as a low temperature 315E replacement.

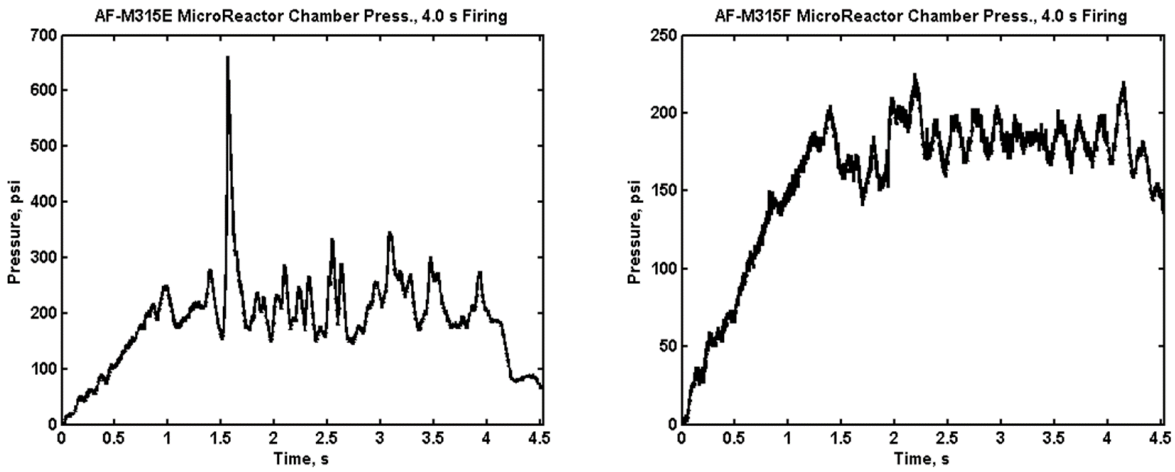

Figure 4. Representative 4 second firing of 315E (left) and 315F (right) under identical conditions.

MICROREACTOR FIRINGS OF 824S

The diluted variant 824S underwent a series of 0.5 to 2 second firings with a representative 2 second test shown in **Figure 5**. A 4 second firing was not completed due to the chamber pressure reaching the maximum threshold operating pressure of the system. 824S had a much smaller pressure roughness than neat 315E—such that the oscillations were almost imperceptible. 824S had a steadily increasing pressure from 300 to 350 psi, while neat 315E reached about 200 to 250 psi. The progressive trace of 824S suggests that the bed was not preheated to an optimal level before combustion or there was a delayed combustion of excess propellant. Notably, the mass flow meter was pegged at its maximum for the duration of the 824S test. There was also evidence of propellant splatter on the walls and on the optical view port of the test chamber. Water condensation was ruled out as the system was still under high vacuum shortly after the test sequence. These results indicate that either the 400 psi feed pressure was too high or that the feed system orifice was too large for the less viscous 824S. Despite this, the outcome is still promising as the propellant was able to sustain extended combustion with a lower pressure roughness. Although the firings demonstrate the catalytic reactivity and smoother combustion of 824S, much more work must be completed on optimizing the parameters for more accurate results.

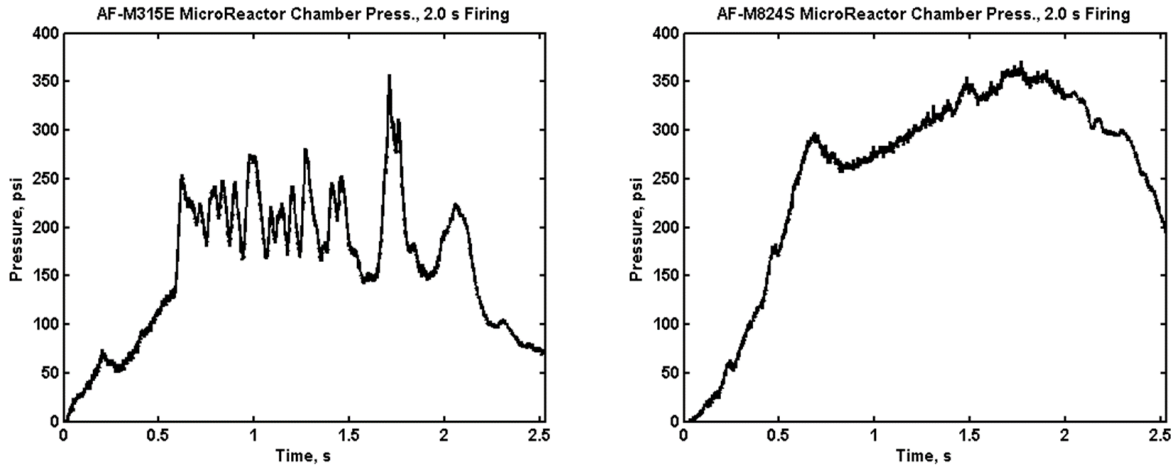

Figure 5. Representative 2 second firing of 315E (left) and 824S (right) under identical conditions.

AEROJET ROCKETDYNE THRUSTER FIRINGS

The development of a diluted variant of 315E was focused on finding the minimum dilution required to achieve a lower combustion temperature of 1450 K. The 1107 and 1028 series were both developed to reduce the minimum catalyst preheat temperature and combustion temperature of IL formulations. Leveraging previous work completed by Aerojet Rocketdyne, these propellants were reformulated to attain a combustion temperature of 1450 to 1900 K. This section presents the characterization and firings previously completed by Aerojet Rocketdyne to achieve these goals. Although the diluted formulations presented were not actually fired, Aerojet Rocketdyne's results suggest that the propellants are catalytically reactive and diluted variants can be successfully employed with some optimization.

Aerojet Rocketdyne investigated the progressive dilution of 315E using an existing 0.2 lbf test thruster. 315E was diluted with water—starting at 20%—and fired until catalyst bed washout was imminent or the thruster performance was deemed unacceptable. For the second series of testing, the 1028A and 1107A blends were fired at preheat temperatures of 600 to 900 °F (315 to 482 °C).

AEROJET ROCKETDYNE FIRINGS OF 315E AND 315E-D

The most notable result from this study was the transient startup periods of the diluted propellants were not significantly different from that of the neat propellant. The ignition

delay and thrust roughness of the diluted propellants were on par with the neat propellant. Furthermore, nearly all of the diluted variants reached thermal equilibrium within 15 seconds, albeit they took higher feed pressures to maintain the target 300 psia chamber pressure. As expected, the higher feed pressures and water content had an adverse effect on the ultimate Isp and C* of the propellants. There were detrimental effects on the catalyst, as the bed temperature takes longer to reach equilibrium and eventually washes out at higher dilutions**.** A study on the preheat temperature of diluted 315E found that the minimum value was comparable to that of neat propellant. There was a noticeable improvement in the responsiveness of the propellant as the preheat was increased to upwards of 900 °F (482 °C). In short, the results confirm that a water-diluted 315E variant can be successfully fired at various preheat temperatures. The dilution also does not appear to drastically affect the ignitability of the propellant; the excess water simply reduces the combustion temperature and performance of the propellant. These results are promising in regards to test firing other diluted formulations for low temperature applications where performance is not the primary objective.

AEROJET ROCKETDYNE FIRINGS OF 1028A

Aerojet Rocketdyne also fired a higher performance variant of 1028B, known as 1028A. This formulation has an Isp of 246 and a theoretical combustion temperature of 1829 K. The effect of preheat temperature on the propellant is shown in **Figure 6.** The minimum preheat temperature required for reliable ignition was around 700 °F (371 °C); lower temperatures did not produce a sufficient chamber pressure rise. The ignition delay of the propellant was notably slower than neat 315E, not reaching steady state until after 0.75 seconds and with a slight increase in pressure roughness. Nonetheless, the ignition delay was only marginally slower than some of the diluted 315E blends, and with a more linear pressure rise transient. Although not shown, the performance of the propellant took a severe hit as the feed pressure had to be increased to 820 psig to attain a chamber pressure of 300 psia. As a reference point, neat 315E only required about 600 psig feed pressure. The peak gas exhaust temperature of 1028A was around 1450 °F (788 °C), whereas the peak temperature of neat 315E was around 1400 °F (786 °C).

These results indicate that the 1028 series is capable of being reliably fired in a test thruster using standard catalysts. Although admittedly, it does not provide any significant benefit in regards to the original goal of a lower preheat temperature. In consideration of the encouraging results of the diluted 315E test series and the firings of 1028A, the diluted variant 1028B is anticipated to perform in a similar manner. As expected, the performance (Isp) of the propellant will be diminished, but the combustion and catalytic reactivity should not be dramatically affected.

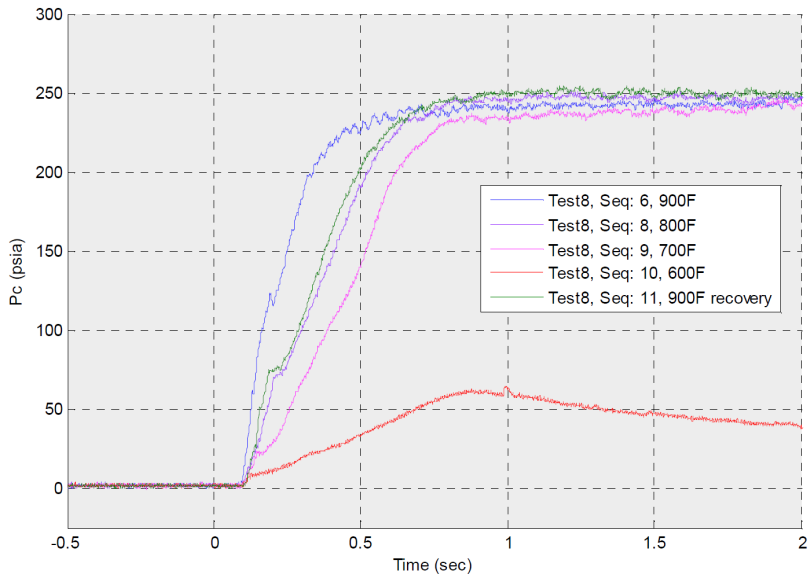

Figure 6. Test firings of 1028A at 600 to 900 °F (315 to 482 °C) catalyst preheat temperatures.

AEROJET ROCKETDYNE FIRINGS OF 1107A

A high performance, triazole-based 1107 series was also fired to test its performance in an actual thruster. 1107P is simply a lower combustion temperature variant in the 1107 series presented below. The propellant underwent the same series of tests that 1028A was subjected to; however, the thruster was not repacked and used the same LCH-240 catalyst from previous testing. **Figure 7** reveals the effect of preheat temperature on chamber pressure for 1107A. As with previous results, the pressure rise rate decreased in tandem with the preheat temperature. The pressure trace at the various preheat temperatures had a more striking difference in shape when compared to other propellants.

The substantial reduction in pressure rise rate and pressure spikes around 1 second (for 600 and 700 °F) suggest that the propellant may have pooled in the catalyst bed before ignition. Additionally, smoke was observed emanating from the nozzle during the firings at the lower preheat temperatures. The propellant likely experienced partial combustion and possible cook-off in a propellant pool close to the injector. 1107A appeared to be more sensitive to preheat temperatures than 315E or 1028A, yet still had an acceptable pressure roughness and ignition delay

comparable to neat 315E. The 1107A propellant also achieved a similar chamber pressure to 315E at roughly the same feed pressure.

The results of these firings demonstrate that the triazole-based 1107A is capable of being fired for extended periods in a test thruster with existing catalysts. Although the propellant proved more sensitive to preheat temperatures than 315E or 1028A, it is still had a higher performance than both under similar conditions. Again, in consideration of the results of the 315E dilution study, a diluted variant, 1107P, is expected to ignite and combust reliably for a lower temperature application.

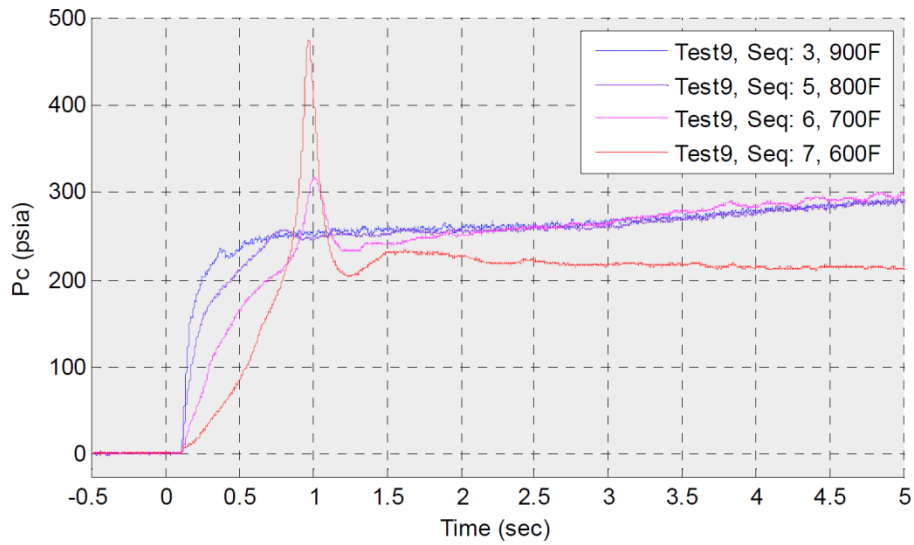

Figure 7. Test firings of 1107A at 600 to 900 °F (315 to 482 °C) catalyst preheat temperatures.

CONCLUSIONS AND FUTURE WORK

This study summarizes the physical properties, hazards, and test firings of five candidate ionic liquid monopropellants with combustion temperatures between 1450 and 1800 K. These formulations were based on well-known and proven ingredients that have some degree of reactivity to standard iridium catalysts such as S405. In accordance with the broader SERDP goals, these formulations have ideal hazards characteristics that mitigate many of the issues associated with handling hydrazine. Various energetic salts were also tested for catalytic reactivity using a qualitative drop test. Although none of the proposed salts had an appreciable reactivity to preheated S405, an exchange for more reactive cations/anions should improve the results.

The 824S and 315F formulations were tested for the very first time in a modular AFRL catalytic microreactor. Although the pressure traces obtained had significant roughness and substantial ignition delays, the results provide fundamental insight into the propellants' combustion characteristics and catalytic reactivity. In addition, Aerojet Rocketdyne demonstrated

diluted variants of 315E in their 0.2 lbf research thruster—finding only moderate disadvantages that could be addressed with system optimization. Despite not attaining the original goal of a lower preheat temperature, 1107A and 1028A were also successfully fired in the same testbed. Note that the diluted variants presented, 1107P and 1028B, were never tested in the microreactor nor a subscale thruster. However, in light of the favorable dilution study performed by Aerojet Rocketdyne, these diluted variants are expected to perform in a similar manner to diluted 315E. In place of actual firing data, a bridge can be drawn between the diluted 315E results and other diluted variants.

As mentioned before, the microreactor system must undergo optimization studies for each of the new propellants to be tested. There are many improvements to be made in terms of injector design, feed pressure, flow rate, or catalyst bed packing before an accurate assessment can be performed. Currently, it cannot provide a definitive combustion performance metric in terms of C* efficiency due to the limitations of the mass flow rate measurement.

A down select for the three most promising candidates yielded: 315E-D, 315F, and 824S. Future work will focus on additional characterization (adiabatic compression, shock sensitivity, etc.) and providing these candidates to Aerojet Rocketdyne for test firing in a more realistic thruster. 315E-D was chosen as a simple, diluted variant of the comprehensively characterized and tested AF-M315E. 315F was selected as a HAN-free variant of the 315 series, mitigating many of the drawbacks of using HAN in a monopropellant system. Although the preliminary results are promising, the high viscosity and possible soot formation must be addressed before moving forward. Finally, 824S was picked as a formulation that omitted any substituted hydrazine ingredient, and instead, employed a triazolium-nitrate salt as the fuel. In order to fill in any gap in knowledge of the propellant hazards, a sample of HEATN will be sent to the Army for toxicology screening. It would be encouraging to know whether or not the triazolium salts confer any improved toxicological properties over substituted hydrazine derivatives. It is also perceivable for any non-critical propellant flaw to be mitigated through slight reformulation.

The two other formulations (1028B and 1107P) were not down selected due to intrinsic flaws that are not likely alleviated by reformulation. 1028B has a higher melting point than desired for space applications and HN/AN could perceivably fall out of solution if the water is lost by any means. The presence of a Class 1.1 solid HN presents a handling hazard that many labs cannot contend with. Furthermore, the stability of the eutectic between HN and AN in an ionic solution has yet to be exhaustively studied. The 1107P formulation suffers from the relatively weak thermal stability of MATN when compared to other ILs. The synthesis of MATN also uses fairly expensive precursors, which would severely limit scale-up production for further thruster testing.

ACKNOWLEDGEMENTS

The authors would like to thank Dr. Marcus Young, Gerald Gabrang, and Paul Adkison at AFRL for their seminal work on the microreactor system. Much gratitude is extended to Drs. EJ Wucherer, Gary Holland, and Bob Masse at Aerojet Rocketdyne for funding the work and test firing the formulations.

REFERENCES

[1] G. Drake, et al., "Energetic, low-melting salts of simple heterocycles," *Propellants, Explosives, Pyrotechnics,* vol. 28, no. 4, pp. 174-180, 2003.

[2] P. Nancarrow and H. Mohammed, "Ionic Liquids in Space Technology–Current and Future Trends," *ChemBioEng Reviews,* 2017.

[3] Q. Zhang and J. N. M. Shreeve, "Energetic ionic liquids as explosives and propellant fuels: a new journey of ionic liquid chemistry," *Chemical reviews,* vol. 114, no. 20, pp. 10527-10574, 2014.

[4] C. H. McLean, et al., "Green propellant infusion mission program overview, status, and flight operations," in *51st AIAA/SAE/ASEE Joint Propulsion Conference*, Orlando, 2015.

[5] R. A. Spores, et al., "GPIM AF-M315E propulsion system," in *51st AIAA/SAE/ASEE Joint Propulsion Conference*, Orlando, 2015.

[6] I. M. Ismail and T. W. Hawkins, "Adiabatic Compression Sensitivity of Liquid Fuels and Monopropellants," *DTIC,* 1999.

[7] P. Quach, G. Warmoth and A. Brand, "Adiabatic Compression Sensitivity of AF-M315E," in *51st AIAA/SAE/ASEE Joint Propulsion Conference*, Orlando, 2015.

[8] D. B. Scharfe, G. Gabrang, P. Adkison, et al., "Microreactor testing with AF-M315E," in *JANNAF Propulsion Meeting*, Phoenix, 2016.

[9] P. Adkison, G. Gabrang, et al., "Drop In Testing of AFM315E and AFM315Q with Busek 0.5N Thruster," in *JANNAF Propulsion Meeting*, Phoenix, 2016.

[10] F. Kamal, B. Yann, B. Rachid and K. Charles, "Application of ionic liquids to space propulsion," *Applications of Ionic Liquids in Science and Technology,* 2011.

[11] T. W. Hawkins, A. J. Brand, M. B. McKay and M. Tinnirello, "Reduced toxicity, high performance monopropellant at the US Air Force Research Laboratory (No. AFRL-RZ-ED-TP-2010-219," *DTIC,* 2010.

[12] A. J. Brand and G. W. Drake, "Energetic hydrazinium salts". U. S. Patent 6,218,577, 17 April 2001.

Appendix F- Army Public Health Center Report (See Attachment in SEMS)

USAPHC

U.S. ARMY PUBLIC HEALTH COMMAND

5158 Blackhawk Road, Aberdeen Proving Ground, Maryland 21010-5403

Toxicology Report No. S.0026122-15 (Draft Version 3.0)
U.S. Department of Defense
Strategic Environmental Research and Development Program (SERDP)
March 2018

Toxicology Assessment for Environmentally Sustainable Liquid Gas Generator Formulations (SERDP Project WP-2400)

Prepared by

William S. Eck, Ph.D.

Distribution C: Authorized to U.S. Government Agencies and their contractors only; proprietary information, critical technology : December 2017. Requests for this document must be referred to Program Manager, Weapons Systems and Platforms, Strategic Environmental Research and Development Program (SERDP), 4800 Mark Center, Suite 17D08, Alexandria, VA 22350.
.

ARIMS Designation: 500c

CHPPM/PHC FORM 433-E (MCHB-CS-IP), SEP 10

DESTRUCTION NOTICE - Destroy by any method that will prevent disclosure of contents or reconstruction

ACKNOWLEDGEMENTS

The authors would like to acknowledge the support and encouragement provided to this effort by Dr. Robin Nissan, Program Manager, Weapons Systems and Platform, SERDP.

Table of Contents

Page

1 Summary 1

1.1 Overview 1
1.2 Purpose 1
1.3 Conclusions 1
1.4 Recommendations 1

2 References 1

3 Authority 2

4 Background 2

5 Statement of the Problem 2

6 Methods 3

7 Results 5

7.1 Physical and Chemical Properties 5
7.2 Summaries 5
7.3 Hydroxylammonium nitrate [HAN]
7.4 Hydroxyethylhydrazinium nitrate [HEHN]
7.5 Ammonium nitrate[AN]
7.6 2,2-Bipyridyl [BP]
7.7 1-Methyl-4-amino-1,2,4-triazolium nitrate [AMTN]
7.8 Hydrazine

8 Discussion 11

8.1 Compound Summaries 11
8.2 Regulations and Standards 12
8.3 Summary and Conclusions 12

9 Recommendations 13

10 Point of Contact 13

Appendices

A References A-1

Figures

1.
2.
3.
4.
5.

Tables

1. Formulation Components 4
2. Categorization Criteria used in the Development of Environmental Safety and Occupational Health Severity 5
3. Physical and Chemical Properties 14
4. Toxicity Data 15
5. Toxicity Assessment 16
6. Ecotoxicity Assessment 16

Toxicology Report No. S.0026122-15 (Draft Ver 3)
Environmentaly Sustainable Liquid Gas Generator Formulations
March 2018

1 Summary

1.1 Overview

Research, development, testing, training, and use of substances potentially less hazardous to human health and the environment is vital to the readiness of the US military. Safeguarding the health of Service Members, civilians, and the environment requires an assessment of alternatives before they are fielded. Continuous assessments begun early in the Research, Development, Testing and Evaluation (RDT&E) process can save significant time and effort during RDT&E, as well as over the life cycle of the items developed. Residues of pyrotechnics, propellants, explosives and incendiaries that cost the Department of Defense billions of dollars and were part of mission essential activities have been found in soil, air, surface and ground water samples, creating environmental problems and interfering with training activities.

1.2 Purpose

Several U.S. missile and satellite systems or their components use hydrazine as a fuel. Hydrazine is a colorless oily liquid that fumes in air, has a penetrating odor resembling ammonia, and is explosive in the presence of air. It is also unstable in the presence of metal ions, ultraviolet light, and is highly toxic and corrosive to skin which it readily penetrates. Hydrazine is mutagenic and is a suspected human carcinogen. Replacing this dangerous and difficult to handle material would improve prospects for human health and the environment, as well as reducing life cycle costs.

1.3 Conclusions

1.4 Recommendations

2 References

See Appendix A for list of references

3 Authority

Funding for this work was provided under Military Interdepartmental Purchase Request No. W74RDV41496835, dated 29 May 2014 and W74RDV70976015, dated 7 April 2017. This Toxicology Assessment addresses, in part, the environment, safety and occupational health (ESOH) requirements outlined in Department of Defense Instruction (DoDI) 4715.4. The Sponsor is the U.S. Department of Defense Strategic Environmental Research and Development Program (SERDP), Weapons Systems and Platforms program. The Principle Investigator (PI) is Dr. Nora Dimas, Aerojet Rocketdyne, Gainesville, VA.

4 Background

There is currently strong international demand for a high performance, environmentally benign replacement for hydrazine in propulsion applications, especially related to spacecraft maneuver. Hydrazine fuel, typically used in such applications, comes with multiple safety concerns and added costs that could be eliminated from the life cycle costs for satellites and similar systems. DOD Missile Defense applications also have a strong interest in replacing the current toxic fuels that are used in programs like SM-3 (Standard Missile-3) and THAAD (Theater High Altitude Area Defense/Terminal High Altitude Area Defense) systems, both of which are part of the U.S. national missile defense system. This program seeks to develop a new, environmentally benign missile propellant formulation.

Current regulations require assessment of human health and environmental effects arising from exposure to substances in soil, surface water, and ground water. Applied after an item has been fielded, these assessments can reveal the existence of adverse environmental and human health effects that must be addressed, often at substantial cost. It is more efficient to begin the assessment of exposure, effects, and environmental transport of military-related compounds/ substances early in the research, development, test and evaluation (RDT&E) process in order to avoid unnecessary costs, conserve physical resources, and sustain the health of our forces and others potentially exposed.

In an effort to support this preventive approach, the U.S. Army Public Health Center (APHC) has been tasked with creating a phased process to identify ESOH effects impacting readiness, training, and development costs. This is an on-going effort, and this report represents the status of information available for this work unit as of the date of publication.

5 Statement of Problem

Spacecraft and missile warhead guidance systems currently use the hypergolic fuel hydrazine for maneuvering. Hydrazine is extremely hazardous to handle, requiring personnel to be in full protective suits including self-contained breathing apparatus. Also, hydrazine fuels have a measureable shelf life, requiring that they be periodically replaced, causing additional concerns associated with disposal and potential environmental release. Users of space and missile systems are interested in developing an alternative to hydrazine that imposes fewer human and environmental health hazards, and is easier to handle during fueling and refueling operations.

6 Methods

In order to determine the human health and environmental impact of compounds employed in these formulations, it is necessary to correctly identify each compound and to determine its physical, chemical, and toxicological properties. The primary means of identification employed for each compound in this program is its Chemical Abstracts Service Registry Number (CAS RN) (see Table 1). While all compounds do not necessarily have a single CAS RN, the CAS RN is an unambiguous way of accessing information for chemical substances. The CAS RN is readily used as a keyword for searching online databases and is often cross-referenced with both systematic and trivial (i.e., “common” or non-systematic) names for chemical substances. In some cases, synonyms and trade names are also used to identify structures.

The properties necessary to assess fate and transport in the environment (FTE) include—

- Molecular weight (MW).
- Boiling point (bp).

- Octanol-water partition coefficient (log K_{OW}).
- Organic carbon partition coefficient (log K_{OC}).
- Water solubility
- Henry's law constant (K_H).
- Vapor pressure (vp).

Basic physical and chemical properties are usually determined by consulting tertiary sources when such information is available.

Toxicological information needed to estimate potential human health risks includes reported toxicity effects of oral, inhalation, dermal, and ocular exposures; potential for developmental or reproductive toxicity, mutagenesis and carcinogenesis; and mode(s) and mechanisms of toxicity. Toxicological information is derived directly from primary sources whenever possible.

Sources used in this search included publications from the U.S. Department of Health and Human Services Agency for Toxic Substances and Disease Registry (ATSDR), *The Merck Index* (O'Neil, 2006, Budavari 1996), Chemical Propulsion Information Agency's (CPIA) *Hazards of Chemical Rockets and Propellants* (CPIA 1985), and the EPA's *Drinking Water Health Advisory: Munitions* (USEPA 1992). The USEPA ECOTOXicology Database System (ECOTOX) and the National Institute of Environmental Health Sciences (NIEHS) National Toxicology Program (NTP) databases were used. Primary sources are identified and retrieved using PubMed®, the Ovid® Technologies Journals, and the EBSCOhost® Research Database. (DTIC® is a registered trademark of the Defense Technical Information Center, TOXNET®, ChemIDPlusLite®, ChemIDPlus®, HSDB®, DIRLINE®, TOXLINE®, PubMed® are registered trademarks U.S. National Library of Medicine; OVID®, is a registered trademark of Ovid Technologies, Inc.; and EBSCOhost® is a registered trademark of EBSCO Publishing.)

Additional sources may include the Defense Technical Information Center (DTIC®), Food and Agriculture Organization of the United Nations (FAO), the World Health Organization (WHO), the International Agency for Research on Cancer (IARC), the International Chemical Safety Cards (ICSC) developed by the National Institute for Occupational Safety and Health (NIOSH), and the U.S. National Library of Medicine's Toxicology Data Network (TOXNET®) that provides access to information from the National Institutes of Health (NIH) and the U.S. Environmental Protection Agency (USEPA). The TOXNET is a suite of individual databases including ChemIDPlusLite® (CIDPL) and ChemIDPlus® Advanced (i.e., chemical and registration numbers, and chemical identification and structure, searches respectively), Hazardous Substances Data Bank (HSDB®), Chemical Carcinogenesis Research Information System (CCRIS), Developmental and Reproductive Toxicology (DART/ETIC), Directory of Information Resources Online (DIRLINE®), Genetic Toxicology (GENE-TOX), Haz-Map (database linking chemicals, jobs and diseases), Household Products Databank (HPD) (potential health effects of chemicals in common household products), Integrated Risk Information System (IRIS), International Toxicity Estimates for Risk (ITER), Toxicology Information Online (TOXLINE®), Toxic Release Inventory (TRI), and Lactation Database (LactMed) (database of drugs and other chemicals to which breastfeeding mothers may be exposed). Commercial suppliers may provide results of in-house research that do not appear in the open literature.

Persistence, bioaccumulation, human health toxicity, and ecotoxicity were assigned to general categories of risk (i.e., low, moderate, or high) using criteria modified from Howe et al. (2006). Table 2 describes the criteria used in the categorization, though the relative proportions of each substance were also factored into the final assessment. In addition, classification in the Globally

Harmonized System (GHS; OSHA 2012) is also included for many of these compounds (See Appendix B).

If no experimental data can be located in the literature, toxicity values for the various parameters aree predicted using Quantitative Structure Activity Relationship (QSAR) software where possible. Modeling packages include US EPA's EPI Suite™ 4.0 (USEPA, 2008a), ECOSAR™ (USEPA, 2007) and TOPKAT (BIOVIA Inc.). (EPI Suite™ and ECOSAR™ are trademarks of the USEPA.)

Table 1. Formulation Components

Chemical Substance	Percent composition*	CAS Number
M315E Mod Han-Based (AFRL 315E Diluted)		
HEHN	34	
S-HAN5**	34	
HEHN (No HAN) (AFRL 315F)		
HEHN	73	
AN	17	
1- Hydroxylethyl-4-amino-1,2,4-triazolium nitrate (No Substituted Hydrazine) (AFRL 824S)		
HEATN	24	
S-HAN5**	51	
1-Methyl-4-amino-1,2,4-triazolium nitrate [AMTN] (AFRL 1107P)		
AMTN	20	
HEHN	5	
S-HAN5**	47	
Carbohydrazide [CBZ]		
Carbohydrazide		497-18-7

*Percent compositions brought to 100% by addition of water.
**Stabilized HAN containing 1 wt% 2-bipyridyl and 5 wt% AN

Table 2. Categorization Criteria used in the Development of Environmental Safety and Occupational Health Severity (modified from Howe et al. 2006)

	Low	Moderate	High
PERSISTENCE	Readily biodegrades (<28 days)	Degradation ½ life: water <40 days , soil <120 days	Degradation ½ life: water >40 days soil > 120 days
TRANSPORT	Water sol. < 10 mg/L log K_{OC} > 2.0	Water sol. 10-1000 mg/L log K_{OC} 2.0-1.0	Water sol. > 1000 mg/L log Koc <1.0
BIOACCUMULATION	log K_{OW} <3.0	log K_{OW} 3.0-4.5	log K_{OW} >4.5
TOXICITY	No evidence of carcinogenicity/ mutagenicity; Subchronic LOAEL > 200 mg/kg-d	Mixed evidence for carcinogenicity/mutagenicity (B2, 2); Subchronic LOAEL 5-200 mg/kg-d	Positive corroborative evidence for carcinogenicity /mutagenicity; LOAEL < 5 mg/kg-d
ECOTOXICITY	Acute LC_{50}/LD_{50} >1 mg/L or 1500 mg/kg; Subchronic EC_{50} >100 µg/L or LOAEL >100 mg/kg-d	Acute LC_{50}/LD_{50} 1-0.1 mg/L or 1500-150 mg/kg; Subchronic EC_{50} 100-10 µg/L or LOAEL – 10-100 mg/kg-d	Acute LC_{50}/LD_{50}<100 µg/L or <150 mg/kg; Subchronic LOAEL <10 mg/kg-d

Notes:
mg/L - milligrams per liter
LOAEL - lowest-observed adverse effect level
LC_{50} – concentration expected to result in 50 percent lethality to a population of test animals.
mg/kg-d - milligrams per kilogram per day
µg/L - micrograms per liter

7 Results

7.1 Physical and Chemical Properties

Physical and chemical properties are summarized in Table 3. When data were not found, "nd" (no data) is inserted. In some cases the property named is not applicable ("n/a") to the substance being described. For example, if the compound is a nonvolatile solid or an inorganic salt, vapor pressure, K_{OW}, K_{OC}, and the Henry's Law constant (K_H) are typically negligible.

7.2 Summaries

The summaries of the mammalian toxicity data are collected in Table 4. Assessments of human health and environmental toxicity for each of the formula components are presented in Tables 5 and 6, respectively. Each characterization is generally based on the criteria set forth in Table 2. The final risk characterization also incorporates assessment of the uncertainty associated with available data, the amount of each compound present in the formulation, and the nature of potential exposure associated with use of the end item.

7.3 Hydroxyl ammonium nitrate [HAN]

7.3.1 General Information

Hydroxylammonium nitrate is the nitrate salt of hydroxylamine.

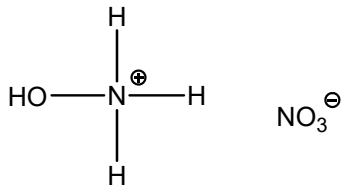

Fig. 1. HAN

7.3.2 Toxicology Data

HA, and presumably HAN, rapidly induces methemoglobin formation as well as depletion of glutathione levels. It is believed HA causes damage to blood via two separate mechanisms—production of free radicals and inihibition of the enzymes glutathione S-transferase (GST) and NADPH methemoglobin reductase (NADPH-HbR). Blood cell cytotoxicity is also observable in formation of Heinz bodies and increased lipid peroxidation. Riboflavin availability is also decreased. HA is a potent inhibitor of platelet aggregation. In rats, brain levels of GABA (γ-aminobutyric acid) are observed, followed by paralysis and cessation of breathing (Evelo et al. 1998). Data gaps for HA cannot be filled by TOPKAT modeling because the molecule contains no carbon atoms.

7.3.2.1 Oral

The oral lethal dose in humans is estimated to be between 50 and 500 mg/kg. In animals, a fatal overdose causes seizures, paralysis of the respiratory muscles and death. Sublethal signs and symptoms of exposure include headache, vertigo, restlessness, tinnitus, dyspnea, nausea, vomiting, proteinuria, hematuria, anemia, leukocytosis, platelet aggregation, jaundice, and splenomegaly. Ingestion of hydroxylamine also causes methemoglobinemia and depletion of glutathione, indicating production of reactive oxygen species (HSDB 2003).

7.3.2.2 Inhalation

The neutral compound hydroxylamine is highly irritating to mucous membranes. Due to its salt nature, and presumed lack of volatility, HAN is likely to only be present in particulate form for inhalation, but will have the same effects as hydroxylamine (HA). Ingestion of HA leads to rapid, significant methemoglobinemia and depletion of glutathione. HA has also caused dose-related hypotension in test animals (HSDB 2003).

7.3.2.3 Dermal

HA and its salts are corrosive to skin. Repeated exposure may enhance allergic reaction, particularly of hands and forearms beginning 1-2 weeks to 2-5 years after initial exposure. Cases of eczema may be observed after prolonged contact (HSDB 2003).

7.3.2.4 Ocular

HA and its salts are highly irritating to eyes and mucous membranes. Nystagmus has been observed in test animals; a yellow-brown deposit on the conjunctiva and cornea are possible (HSDB 2003).

7.3.2.5 Development and Reproduction

Malformations have been observed in rabbits following exposure to HA (HSDB 2003).

DeSesso et al. (2000) observed cellular debris, an indicator of cell death, in limb buds of gestation day 12 rabbit embryos 4 hours after injection of hydroxylamine hydrochloride and various other related compounds via either intracoelomic (2.66 µmol/embryo) or subcutaneous injection (8.55 mmol/kg). Early cell death was not observed. The authors concluded the data were consistent with a free radical mechanism involving a terminal hydroxylamine group.

7.3.2.6 Neurotoxicity

Hydroxylamine elevates brain γ-aminobutyric acid (GABA) levels in rats; systemic poisoning is characterized by cyanosis, convulsions, and coma (HSDB 2003).

7.3.2.7 Genotoxicity

HA has been observed to cause point mutations in DNA replication (Chatake et al. 1999). HA is negative in *in vitro* leukocyte and lymphocyte tests (HSDB 2003).

7.3.2.8 Carcinogenicity

Hydroxylamine is not listed as a human carcinogen (HSDB 2003). Although HA is a potent mutagen *in vitro*, it has not been shown to possess carcinogenic capabilities, and has shown carcinostatic activity against certain tumors in animals (Gross 1985).

7.3.2.9 Ecotoxicology

7.3.2.9.1 Fate and Transport

If released to air, HAN will exist solely in particulate form due to its salt nature. Airborne HAN will be degraded in the atmosphere by reaction with photochemically-produced hydroxyl radical. The half-life for this reaction is estimated to be 18 hours (HSDB 2003).

If released to water, HAN is likely to be highly mobile, and may pose a hazard to ground, surface, and drinking water (HSDB 20003).

If released to soil, HAN is expected to have high mobility, based upon an estimated K_{OC} of 14. The pK_a of HA is 5.94, indicating HA and HAN will exist as both ionic and protonated species in the environment, and exhibit the same fate and transport characteristics. Volatilization from moist soil surfaces is not expected to be an important fate process for HAN, based upon an estimated Henry's Law Constant of 6.9×10^{-9} atm-m^3/mol for HA; the protonated form will not volatilize (HSDB 2003).

An estimated bioconcentration factor (BCF) of 3 suggests the potential for bioconcentration in aquatic organism is low (HSDB 2003).

7.3.2.9.2 Ecotoxicity

HA-HCl treatment of wheat seed induced chromosome aberrations in mitotic and meiotic cells of resulting plants. Frequency of chromosomal aberration was 2-3 fold high than for seed soaked in distilled water (HSDB 2003).

EPA's ECOSAR program models HA as a neutral organic, and estimates a 96-hour EC_{50} in green algae of 1970 mg/L, a 48-hour LC_{50} in *Daphnia* of 9073 mg/L, and a 96-hour LC_{50} in fish of 21,530 mg/L. Since these values are based upon general narcosis, experimental values would likely be lower.

7.3.2.8.3 Degradation/Treatment

Abiotic photodegradation of HA by photochemically produced peroxy radicals is an important environmental fate in surface waters, with a half-life of about 2 hours (HSDB 2003).

EPA's EPI Suites program predicts HA, and therefore HAN, will be poorly removed (<2 percent) by standard

7.4 Hydroxyethylhydrazinium nitrate [HEHN]

7.4.1 General Information

HEHN is a component of a proposed monopropellant, AF-M315E. The new formulation is designed to have less vapor toxicity than hydrazine, but greatly improved volumetric and specific impulse.

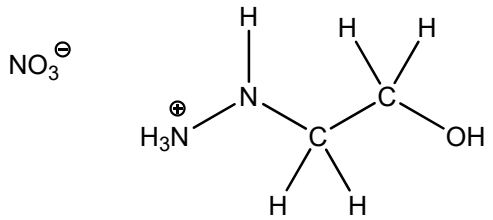

Fig. 2. HEHN

7.4.2 Toxicology Data

7.4.2.1 Oral

The Air Force Research Lab determined the oral LD_{50} in rats to be 367 mg/kg (CPIAC 2009). The TOPKAT model prediction for the neutral compound is very similar, at 283.1 mg/kg. The chronic LOAEL is predicted by TOPKAT to be 19.4 mg/kg-day.

7.4.2.2 Inhalation

No experimental data were found. TOPKAT modeling predicts the median inhalation toxicity (LC_{50}) in rats to be 0.549 g/m^3-hour.

7.4.2.3 Dermal

HEHN was found to be a slight dermal irritant (CPIAC 2009). TOPKAT modeling predicts HEHN will not be a skin sensitizer.

7.4.2.4 Ocular

No experimental data were found. TOPKAT modeling predicts HEHN is probably an ocular irritant.

7.4.2.5 Development and Reproduction

No experimental data were found. TOPKAT modeling predicts HEHN will be a developmental or reproductive toxicant at high confidence.

7.4.2.6 Genotoxicity

HEHN is reported to be positive in the Ames mutagenicity assay, but the available information does not indicate whether this was with or without microsomal activation (AFRL 2002).

7.4.2.7 Carcinogenicity

No experimental data were found. TOPKAT modeling of HEHN suggests only a moderate likelihood of carcinogenicity. The reference compound, hydrazine, is categorized as a possible human carcinogen, which correlates well with the modeling prediction.

7.4.2.8 Ecotoxicology

7.4.2.8.1 Fate and Transport

HEHN has a high aqueous solubility and low log K_{OC}, making transport in ground water a significant hazard. Partition to the atmosphere from water or wet surfaces is highly unlikely, as is vaporization from dry surfaces, due to the salt-nature of HEHN. EPA's EPI Suite predicts a log BCF of 0.50, indicating no tendency to bioaccumulate.

7.4.2.8.2 Ecotoxicity

No experimental data were found. For the neutral compound, TOPKAT predicts an EC_{50} in *Daphnia* of 93.3 mg/L at moderate confidence, and an LD_{50} in fish of 15.0 mg/L at low confidence.

EPA's ECOSAR program models HEHN as a hydrazine, and predicts a 96-hour EC_{50} in green algae of 3.52 mg/L, a 48-hour LC_{50} in *Daphnia* of 231.8 mg/L, and a 96-hour LC_{50} in fish of 19.46 mg/L.

7.4.2.8.3 Degradation/Treatment

No experimental data were found. For the neutral compound, TOPKAT predicts an EC_{50} in *Daphnia* of 93.3 mg/L at moderate confidence, and an LD_{50} in fish of 15.0 mg/L at low confidence.

EPA's ECOSAR program models HEHN as a hydrazine, and predicts a 96-hour EC_{50} in green algae of 3.52 mg/L, a 48-hour LC_{50} in *Daphnia* of 231.8 mg/L, and a 96-hour LC_{50} in fish of 19.46 mg/L.

7.5 Ammonium nitrate [AN]

7.5.1 General Information

Ammonium nitrate is a common, simple inorganic compound formed from the condensation of hydrochloric acid and ammonia. Physically, it is forms white, orthorhombic crystals. The dry solid is hygroscopic. It's most common use is as a fertilizer, but when mixed with an organic fuel can be used to make field-expedient explosives of significant power; a truck containing an ammonium nitrate-fuel oil (ANFO) mixture was used to devastate the Murrah Federal Office building in Oklahoma City, OK, in April, 1995. Ammonium nitrate is also used in medical icepack replacements, as the heat of solution is strongly endothermic, producing a cold pack "on demand" (HSDB 2007). As with other nitrate salts, consumption may produce methemoglobinemia due to oxidation of the Fe^{2+} ion.

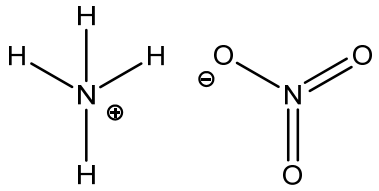

Fig. 3. AN

7.4.2 Toxicology Data

Workers producing AN have professional contact with the substance in both the aerosol and gaseous (ammonia) forms. Illnesses of the respiratory apparatus and musculoskeletal system predominate in the morbidity structure. Clinical examination of workers in the production of AN shows frequent cases of chronic bronchitis and radiculonephoprathy. Function studies show damage to the airways, myocardiodystrophy, and changes in EEG T-waves (Tsimakuridze et al. 2005).

7.4.2.1 Oral

According to the European Commission EUCLID dataset, the oral LD_{50} in rats is reported to be 2217 mg/kg or 2800 mg/kg (HSDB 2014).

A single oral dose of 2 g/kg to sheep caused death 12 hours to 17 days after administration (HSDB 2014).

7.4.2.2 Inhalation

According to the European Commission EUCLID dataset, the LC_{50} for a 4-hour inhalation in rats is >88.8 mg/L (HSDB 2014).

Inhalation is irritating to mucous membranes of the respiratory tract, causes severe lung congestion, coughing, difficulty breathing, and acid urine. Inhalation of large amounts of AN also causes system acidosis and abnormal hemoglobin (HSDB 2014).

Twenty normal and 19 asthmatic human subjects were exposed for 2 hours to an ammonium nitrate aerosol at concentrations of 200 $\mu g/m^3$ with intermittent exercise and heat stress. Neither

the normal nor asthmatic subjects showed significant differences in their lung function tests or symptom scores, and no other significant symptoms occurred (Kleinman et al. 1980).

Sprague-Dawley rats were exposed to 1 mg/m^3 ammonium nitrate 6 hours/day, 5 days/week for 4 weeks. The exposure had no effect on body weights, lung volume, vital capacity, or histologic structure of ciliated epithelial cells of the respiratory tract (HSDB 2014).

7.4.2.3 Dermal

A clinical case of contact dermatitis was reported by Pasricha and Gupta (1983) to a farmer after sowing sorghum and wheat using urea and calcium-ammonium nitrate (CAN) fertilizers. Patch tests revealed that the CAN fertilizer was the source of the sensitivity.

AN was found to be moderately irritating in rabbits by the Draize test. The mean erythema and edema scores were calculated to be 0.1 and 0, respectively following a simple 4-hour application. O erythema was observed in any animals 48 or 72 hours following decontamination. Repeated (x5) applications of 500 mg of test sample to each rabbit caused only very slight edema in two of the rabbits and slight erythema in the third (HSDB 2014).

7.4.2.4 Ocular

Ammonium nitrate is an eye irritant (HSDB 2014).

7.4.2.5 Development and Reproduction

A mixture designed to mimic agricultural run-off consists of five pesticides and ammonium nitrate fertilizer. The chemicals and their relative concentrations were determined on the basis of survey data from California (pesticides) and Iowa (fertilizer). The mixture was administered in drinking water to Sprague-Dawley rats on gestation days (GD) 6 to 20 at 3 dose levels: 1X, 10X and 100X median concentration in the environment. Dams were monitored daily for signs of toxicity, and fetuses were removed on GD 20 for evaluation. Maternal body weights, food and water consumption, and clinical signs were all similar to control values. No adverse effects were observed for measures of embryo/fetal toxicity, including resorptions per litter, live litter size, and fetal body weight. The mixture did not cause an increased incidence of malformations or variations (Heindell et al. 1992)

In an experiment parallel to the one in the preceding paragraph, but conducted in mice, George et al. (1993) dosed Swiss mice at 1X, 10X and 100X median concentration in the environment for a period of 18 weeks. F0 mice were fertile throughout the exposure, and the mixture did not affect reproductive competence, F0 body weight, food or water consumption, organ weights, or sperm parameters at necropsy. No treatment-related clinical signs were noted. F1 pre-weaning growth and maturation were unaffected, and no treatment-related clinical signs or adverse effects on F1 reproductive competence, food and water consumption, male or female body weight, or selected male and female organ weights, sperm parameters, vaginal cytology, or histology of selected organs.

7.4.2.6 Mutagenesis

Ammonium nitrate at 5 mg/plate was negative in *S. typhimurium* strains TA1535, TA1537, TA1538, TA98, and TA100 with or without metabolic activation (HSDB 2014).

7.4.2.7 Carcinogenesis

Nitrates can be transformed to nitrites by certain microorganisms in the soil, and by

microorganisms found in the mouth and stomach, followed by nitrosation of secondary amines and amides in the diet. The resulting nitrosamines are mutagenic, but humans are naturally exposed to the precursors as a part of a normal diet. The average Western diet contains 1-2 mmol nitrate/person/day (Hotchkiss et al. 1992).

According to the USEPA, available information on the carcinogenic potential of nitrates is equivocal. The results of some carcinogenicity studies suggest that nitrates may cause tumors in laboratory animals, while others do not (USEPA 1991a). The possible carcinogenicity of nitrate depends on the conversion of nitrate to nitrite and the reaction of nitrite with secondary amines, amides, and carbamates to form N-nitroso compounds that are carcinogenic (Bouchard et al. 1992).

7.4.2.8 Ecotoxicology

7.4.2.8.1 Fate and Transport

Ammonium nitrate is readily soluble in water and will be solubilized when water is present. However, both the cation and anion are essential nutrients for plants, and therefore will be readily removed from soil when plants are present. Small discharges to surface water are also expected to be taken up by plants, but larger discharges can result in toxicity to aquatic species or to ecological upset due to rapid plant (algae) growth and subsequent death. Nitrates can also be metabolized by bacteria, especially in anaerobic environments (HSDB 2014).

7.4.2.8.2 Ecotoxicity

Influence of ammonium nitrate on embryonic and larval stages of anuran amphibians (i.e. frogs, toads and tree frogs) has been studied. Significant differences were observed in sensitivity to ammonium nitrate as a function of developmental stage in Iberian painted frog (*Discoglossus galgano*), Western spadefoot toad (*Pelobates cultripes*), and Natterjack toads (*Bufo calamita*). In *D. galganoi* and *P. cultripes* younger individuals displayed greater acute effects than older individuals. All (100 percent) of the *P. cultripes* hatchlings died after 4-days exposure to a nominal concentration of 225.8 mg nitrogen (as ammonium nitrate)/L, where fewer than 40 percent of individuals from older larval stages died when exposed to this concentration. *B. calamita* showed a higher sensitivity in later larval stages after 12 days of exposure (Ortiz et al. 2004).

The minimum lethal toxicity of ammonium nitrate for *Rana temporaria chensinensis* tadpoles was 0.91 g/L, and the maximum tolerance concentration was 0.83 g/L. In field experiments, ammonium nitrate concentrations of 0.25 g/L had no adverse effects on the tadpoles, as reflected by their growth rates (Oldham et al. 1997; HSDB 2014).

In the Pacific tree frog (*Pseudacris regilla [Baird and Girard]),* the 4-day LC_{50} was 135.4 mg/L, and decreased to 55.2 mg/L for a 10-day exposure. The comparable values in the common laboratory African clawed toad (*Xenopus laevis [Daudin]*) were 100.7 mg/L for a 4-day exposure and 52.9 mg/L for a 10-day exposure. The LOAEL for ammonium nitrate was calculated at 24.6 mg/L in *P. regilla*, and 99.5 mg/L for *X. laevis* (Schuytema and Nebeker 1999).

In the common toad (*Bufo bufo*), ammonium nitrate LC_{50}'s of 2199 mg/L and 2112 mg/L for 96-hour and 168-hour exposures, respectively, were determined. The exposure of tadpoles to nominal concentrations of 100 mg/L ammonium nitrate (measured as nitrate) for 24-, 48-, or 72-hours caused a significant decrease in tadpole activity, but no clear reduction in food consumption or delay of development (Xu and Oldham 1997).

Puglis and Boone (2007) exposed *Rana catesbiana* egg masses to 0, 5, or 10 mg nitrate/L for seven days. Ammonium nitrate was found to have no effect on hatching and survival of tadpoles

at these concentrations.

Ruminants may develop methemoglobinemia by consumption of quantities of nitrate. This is due to the reducing environment of the rumen, resulting in rapid conversion of nitrates to the more toxic nitrites. Clinical signs may be non-specific, but in cattle often involve decreased weight gain and food efficiency, decreased milk production, poor reproductive capacity, and impaired health of epithelial tissues as expressed by digestive tract and respiratory disorders (HSDB 2014).

An EC_{50} for a 24-hour exposure to *Daphnia* was reported to be 555 mg/L (HSDB 2014).

LC_{50} for ammonium nitrate in Rainbow trout (*Oncorhynchus mykiss*) for a 96-hour exposure is 6000 mg/L, and 74 mg/L in Common carp (*Cyrinus carpio*) for a 48-hour exposure (HSDB 2014).

Effect of ammonium nitrate contaminated soil on snapping turtle (*Chelydra serpentina*) eggs survivorship was evaluated by deSolla and Martin (2007). Eggs were incubated in garden soil that had received ammonium nitrate at rates up to 2000 kg/ha in 2005. In the field, the ammonium nitrate was observed to have no impact on hatching success or development of the young turtles, despite overt toxicity to endogenous plants. In the lab, hatching success was reduced, body mass of young was less, and there was reduced post-hatch survival compared to controls. The difference in outcome between the lab and field exposures is probably attributable to reduction in fertilizer concentration via soil leaching and atmospheric loss (of ammonia).

Abdel-Hamid et al. (1997) found that ammonium nitrate negatively impacted egg-laying by the snail *Biomphalaria alexandrina* more than phosphorous- or sulfur-containing fertilizers.

Larvae of the newt *Triturus vulgaris (L.)* were exposed to ammonium nitrate at 0, 100, 200, or 500 mg/L in artificial pond water. Larvae exposed at 200 or 500 mg/L for periods of 24, 48, or 72 hours were significantly smaller than controls at metamorphosis, however survival was high (HSDB 2007).

Marco et al. (2004) collected wild, gravid females of Carbonell wall lizards (*Podarcis carbonelli*) and Spanish wall lizards (*Podarcis hispanica*) from areas in which they were abundant. Eggs were obtained within 15 days of the females being captured. Eggs were exposed to one of 4 distinct environments: 1) plants (to absorb some of the ammonium nitrate fertilizer) and fertilizer, 2) plants and control, 3) no plants and fertilizer, and 4) no plants and control. Ammonium nitrate was initially applied at a rate equal to 100 mg/L of soil; eggs were exposed to treatment for an average of 50 days. Mortality was only observed for eggs exposed to fertilizer in the absence of plants (treatment 3), where 27% of the eggs died. Hatchlings from eggs incubated with fertilizer were significantly smaller in length and mass; effects that were not mitigated by the presence of plants. A test of hatchling running speed indicated no differences among any of the treatment groups over a distance of 100 cm.

7.4.2.8.3 Degradation/Treatment

Ammonium nitrate is readily taken up by both terrestrial and aquatic plants as an essential nutrient. It will also be consumed by bacteria (HSDB 2014).

7.5 2,2-Bipyridyl [BP]

7.5.1 General Information

BP is a white, crystalline solid at room termperature. It is used as a chemical intermediate for the production of the herbicide diquat, as n indicator for photometric determination of Ag, Cd, Cu, Fe,

and Mo, and as an iron chelating agent. Synonyms for this compound include α,α'-bipyridyl, α,α'-bipyridine, bipyridine, 2,2'-bipridin, α,α'-dipyridine, and 2-(2-pyridyl)pyridine.

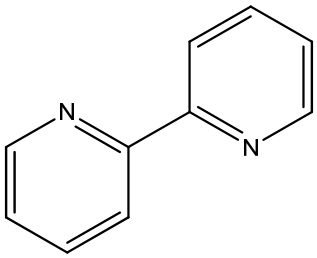

Fig. 4. BP

7.5.2 Toxicology Data

7.5.2.1 Oral

The oral LD_{50} in rats is reported to be 100 mg/kg (HSDB 2002). TOPKAT modeling predicts chronic LOAEL of 60.9 mg/kg-day at high confidence.

BP administered to rats either orally or intraperitoneally in doses of 50, 100, or 250 mg/kg caused tremors and slight ptosis which completely disappeared in 24 hours (Taylor et al. 1969). Under similar circumstances, BP was noted to decrease the level of norepinephrine and inhibited dopamine β-hyrdroxylase activity in the brain in a dose-dependent manner. However, dopamine and hydroxytryptamine levels were not affected, and observed tremors, hypothermia and hypotension from administration of BP did not appear to be related to depletion of norepinephrine (HSDB 2002).

7.5.2.2 Inhalation

TOPKAT modeling predicts an inhalation LC_{50} in rats of 9.1 g/m^3-hour at high confidence.

Pyridine and its derivatives cause local irritation on contact with the skin, mucous membranes, and cornea (HSDB 2002).

7.5.2.3 Dermal

The dermal LD_{50} for BP is reported to be 938 mg/kg in the rat (Sigma-Aldrich 2015).

Pyridine and its derivatives cause local irritation on contact with the skin, mucous membranes, and cornea (HSDB 2002). TOPKAT modeling predicts BP is unlikely to be a dermal sensitizer.

7.5.2.4 Ocular

Pyridine and its derivatives cause local irritation on contact with the skin, mucous membranes, and cornea (HSDB 2002).

A SDS for the compound indicates BP produces mild irritation (Sigma-Aldrich 2015).

7.5.2.5 Development and Reproduction

Data in the TOPKAT database indicates BP is a recognized developmental toxicant.

Rats treated with 0.5 percent solutions of BP (1-2 mL/kg-day) had alterations of testicular parenchyma involving both cells of the seminal epithelium and to a less extent those of the interstitial tissue. Effects were more marked in the peripheral tubules (Palmieri et al. 1978).

7.5.2.6 Mutagenesis

BP is reported to be mutagenic in the Ames test (HSDB 2002).

7.5.2.7 Carcinogenesis

No experimental data were found. TOPKAT modeling predicts BP is not likely to be carcinogenic.

7.5.2.8 Ecotoxicology

7.5.2.8.1 Fate and Transport

With an estimated water solubility of nearly 6000 mg/L and log K_{OC} of 2.11, BP is expected to have a moderate ability to migrate in groundwater, possibly posing a hazard to surface and drinking water. BP is expected to not readily evaporate from water or wet surfaces based upon its Henry's Law Constant, and will exist in the atmosphere as a vapor-particulate mix. BP will be removed from the atmosphere by both wet and dry deposition. Vapor-phase BP will be degraded in the atmosphere by reaction with photochemically-produced hydroxyl radicals, with an estimated half-life of 12.5 days. BP is not predicted to bioaccumulate.

7.5.2.8.2 Ecotoxicity

BP was a strong inhibitor of axenically grown *Entamoeba histolytica*, a causative agent of amebiasis (HSDB 2002).

TOPKAT modeling predicts an EC_{50} in *Daphnia* of 5.5 mg/L at high confidence, and an LC_{50} in fathead minnow of 1.7 mg/L at moderate confidence.

EPA's ECOSAR program predicts a 96-hour EC_{50} in green algae of 145.8 mg/L, a 48-hour LC_{50} in *Daphnia* of 247.98 mg/L, and a 96-hour LC_{50} in fish of 462.4 mg/L.

7.5.2.8.3 Degradation/Treatment

EPA's EPI Suite 4.11 models predict BP will be biodegraded poorly, with environmental persistence of weeks to months. Removal by wastewater treatment plants is also expected to be poor (< 2 percent), primarily due to sludge adsorption.

7.6 1-Methyl-4-amino-1,2,4-triazolium nitrate [AMTN]

7.6.1 General Information

AMTN is under evaluation as a component for a monopropellant formulation to replace hydrazine.

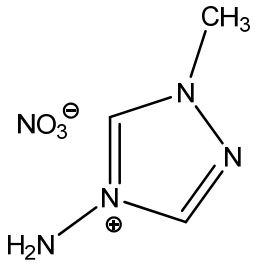

Fig. 4. AMTN

7.6.2 Toxicology Data

No experimental data were found. All information below is based upon QSAR analysis using TOPKAT (Biovia 2015), EPI Suite 4.11 (EPA 2015a) and ECOSAR (EPA 2015b).

7.6.2.1 Oral

TOPKAT modeling predicts an oral LD_{50} in rats of > 10,000 mg/kg at high confidence; the chronic LOAEL is predicted to be 30.0 mg/kg-day at low confidence. Based upon the acute toxicity prediction, AMTN is essentially non-toxic.

7.6.2.2 Inhalation

TOPKAT modeling predicts an inhalation LC_{50} in rats of >10 g/m^3-hour at high confidence, making AMTN non-toxic via inhalation.

7.6.2.3 Dermal

TOPKAT modeling predicts AMTN is unlikely to be either a dermal irritant or sensitizer at moderate confidence.

7.6.2.4 Ocular

TOPKAT modeling predicts AMTN is possibly an ocular irritant at moderate confidence.

7.6.2.5 Development and Reproduction

TOPKAT modeling predicts AMTN will not be a developmental or reproductive toxicant at moderate confidence.

7.6.2.6 Genotoxicity

TOPKAT modeling predicts AMTN will not be mutagenic in the Ames mutagenicity test at high confidence.

7.6.2.7 Carcinogenicity

TOPKAT modeling of AMTN for carcinogenicity is indeterminate.

7.6.2.8 Ecotoxicology

7.6.2.8.1 Fate and Transport

Based upon a high predicted solubility and a predicted log Koc of -1.14, AMTN is expected to be readily transported in groundwater and will probably pose a hazard to surface and drinking water. Based upon a predicted Henry's Law constant of 4.43 x 10^{-14} atm-m^3/mol, AMTN is not expected to partition to the atmosphere from water or wet surfaces. AMTN will exist in the atmosphere only in particulate form. The salt nature of the compound also makes it unlikely to vaporize from dry surfaces. Bioaccumulation in aquatic species is expected to be negligible based upon a predicted log Kow of -3.86.

7.6.2.8.2 Ecotoxicity

No experimental data were found. TOPKAT modeling predicts an EC_{50} in *Daphnia* of 3800 mg/L at low confidence. A prediction could not be made for fathead minnow due to lack of a suitable model.

EPA's ECOSAR program models AMTN as a non-fused triazole, and predicts a 96-hour EC50 in green algae of 5585 mg/L, a 48-hour LC_{50} in *Daphnia* of 1325 mg/L, and an LC_{50} in fish of 1.8 x 10^6 mg/L, which may be greater than the compound's solubility (i.e, no effects at saturation).

7.6.2.8.3 Degradation/Treatment

AMTN is expected to be moderately persistent in the environment with persistence of days to weeks.

The half-time for AMTN degradation by hydroxyl radicals in the atmosphere is predicted to be 12.5 hours.

AMTN is predicted to be poorly removed (< 2 percent) by physical processes at wastewater treatment plants.

7.7 Carbohydrazide [CBZ]

7.7.1 General Information

Carbohydrazide (CBZ) is a white crystalline solid (Sigma-Aldrich 2014). Synonyms include 1,3-diaminourea, carbonic dihydrazide, carbonohydrazide, and 4-amino-semicarbazide, as well as several others. Industrial uses include in corrosion inhibitors, anti-scaling agents, fuels, additives, and lubricants (PubChem 2018) and in water desalinization plants in place of hydrazine (Rahman et al. undated).

7.7.2 Toxicity data

CBZ decomposes to produce hydrazine (Rahman et al. undated).

7.7.2.1 Oral

The oral LD_{50} in female rats is reported to be 311 mg/kg; this corresponds to classification in the GHS of Category 4 (Sigma-Aldrich 2014). TOPKAT modeling predicts a chronic LOAEL of 274.1 mg/kg-day.

7.2.2 Inhalation

CBZ is reported to cause respiratory tract irritation (PubChem 2018). TOPKAT modeling predicts an inhalation LC_{50} in rats of 1.2 g/m^3-hour.

7.7.3 Dermal

CBZ is both a skin irritant and sensitizer (PubChem 2018).

7.7.4 Ocular

CBZ is a serious eye irritant (PubChem 2018).

7.7.5 Development and reproduction

No experimental data were found. TOPKAT modeling predicts carbohydrazide will be a developmental or reproductive toxicant at high confidence.

7.7.6 Neurotoxicity

Methyldithiocarbazinate, a sulfur analog of carbohydrazide has been noted to cause convulsions in laboratory animals. Activity of the enzyme glutamide decarboxylase in whole brain homogenates from mice sacrificed at the onset of seizures, was significantly reduced. Pretreatment of the animals with pyridoxal phosphate conferred protection against seizures and death (Meldrum et al. 1975).

7.7.7 Genotoxicity

No experimental data were found. TOPKAT modeling predicts CBZ will be mutagenic in the Ames assay.

7.7.8 Carcinogenicity

No experimental data were found. TOPKAT modeling is indeterminate.

7.7.9 Ecotoxicology

7.7.9.1 Fate and transport

As CBZ is freely soluble in water, it will be highly mobile in groundwater, and will likely pose a hazard to surface and drinking water. CBZ will not partition to the atmosphere from water or wet surfaces. CBZ will exist in the atmosphere only in particulate form. CBZ is not expected to bioaccumulate in aquatic organisms.

7.7.9.2 Ecotoxicity

A manufacturer's SDS classifies CBZ in GHS Category 2 for both acute and chronic aquatic toxicity (Sigma-Aldrich 2014).

The 72-hour EC_{50} for green algae is reported to be 9.5 mg/L, the 48-hour LC_{50} for *Daphnia* is 96 mg/L, and the 96-hour LC_{50} in Bluegill (*Lepomis macrochirus*) is 190.0 mg/L (Sigma-Aldrich 2014).

7.7.9.3 Degradation/Treatment

EPA's EPI Suite predicts CBZ will not readily degrade in the environment, with persistence in the environment of days to weeks.

EPA's EPI Suite also predicts CBZ will be poorly removed by wastewater treatment plants (< 2 percent), primarily by sludge adsorption.

7.8 Hydrazine [N_2H_4]

7.8.1 General Information

Hydrazine is a colorless oily liquid that fumes in air with an ammonia-like odor. It is used as a propellant in liquid-fuel missiles. It has a penetrating odor resembling ammonia, and burns with a violet flame. Hydrazine will explode during distillation if air is present, and is also affected by UV light and metal ion catalysts. It can be stored for years if sealed in glass and protected from light (O'Neil, 2006). There is a relatively large amount of data available on hydrazine, particularly in laboratory animals. The examples cited below represent only a portion of the available information, but should be considered representative.

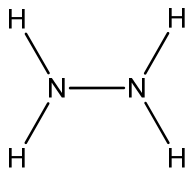

Fig. 5. Hydrazine

7.8.2 Toxicology Data

Toxic effects of hydrazine include conjunctivitis, pulmonary edema, hemolytic anemia, ataxia, convulsions, and kidney and liver toxicity (HSDB 2005).

7.8.2.1 Oral

Oral toxicity values for hydrazine are reported to be 59 mg/kg in the mouse and 60 mg/kg in the rat (CIDPL 2009). In cases of acute human poisoning, vomiting, severe irritation of the respiratory tract with development of pulmonary edema, central nervous system depression, and hepatic and renal damage (HSDB 2005).

Golden hamsters administered daily doses of 0.74 or 0.68 mg hydrazine over a 15-20 week period developed liver lesions, reticuloendothelial cell proliferation, cirrhosis, bile-duct proliferation, and degenerative fibrous cells in hyalinized tissues (Sheftel 2000).

Administration of hydrazine to mice, rats, and hamsters was found to result in rapid methylation of liver DNA guanine for which endogenous formaldehyde appeared to be the source of the methyl moiety. Hamsters were given hydrazine sulfate at 170, 340, and 510 mg/L in drinking water for 2 years, during which levels of methylation of DNA guanine in liver, kidney and lung was observed. Hepatocellular carcinomas were observed in hamsters treated with the highest doses of hydrazine sulfate after 78 weeks of exposure; the incidence of liver cancer was dose-related over the course of the experiment (Bosan et al. 1987).

7.8.2.2 Inhalation

The LC_{50} for inhalation of hydrazine in rats is reported to be 570 ppm (CIDPL 2009).

Groups of dogs, monkeys, rats and mice were exposed either 24 hours/day, 7 days/week to 6.2 or 1 ppm, or 6 hours/day, 5 days/week to 1 or 5 ppm hydrazine for 6 months. Mortality was seen in mice and dogs, but not in monkeys or rats. Dogs showed hematologic deficits and increased numbers of reticulocytes. Liver changes that consisted of moderate to severe fatty infiltration were marked in mice and dogs, were slight to moderate in monkeys, and were absent in rats (HSDB 2005).

Ninety-seven percent pure hydrazine vapor was administered to mice, rats, Syrian golden hamsters and beagles by MacEwen et al. (1981). Exposure concentrations were up to 1.0 ppm for C57BL/6 mice and dogs, and 5.0 ppm for F344 rats and hamsters. Animals were exposed for 6 hours/day, 5 days/week, for 1 year, followed by a variable observation period (12-38 months). Significant increases over controls were reported for lung adenomas in mice at the highest dose; nasal cavity adenoma and adenocarcinoma in rats; and nasal cavity polyps in hamsters. No significant increases in tumor induction were noted at the lower doses, nor were treatment-related neoplasms reported in dogs (the observation period for dogs was considered inadequate for development of neoplasms in dogs).

Occupational exposure to hydrazine has been reported to produce systemic problems to include lung and liver damage, conjunctivitis, tremors, lethargy, long-term neurobehavioral impairment, and ultimately death (HSDB 2005).

7.8.2.3 Dermal

Hydrazine is corrosive to skin, producing caustic-like, severe, penetrating burns. It will also dissolve hair. Hydrazine exposure is also suspected in a human case of epithelioid sarcoma in an individual occupationally exposed to hydrazine fuel. Hydrazine exposure has been shown to produce dermatitis and skin sensitization (HSDB 2005).

A dermal LD_{50} is reported to be 91 mg/kg in rabbits, and 190 mg/kg in guinea pigs (HSDB 2005).

7.8.2.4 Ocular

Exposure to the eyes can produce temporary blindness. Liquid splashes to the eyes can produce corneal injuries and burns (HSDB 2005).

7.8.2.5 Development and Reproduction

Groups of rats exposed orally during gestation to 8 mg hydrazine hydrochloride/kg body weight resulted in maternal body weight loss and mortality, along with fetal toxicity that included reduced fetal weight and viability. Although some fetuses were pale and edematous, no major congenital malformations occurred (ACGIH 2001).

A developmental toxicity study carried out in rats receiving oral doses of 0, 2.5, 5, or 10 mg hydrazine/kg from days 6-15 of gestation resulted in both maternal and fetal toxicity at the 5 and 10 mg/kg dose rates, with 2.5 mg/kg being an apparent NOEL. Developmental delays, but no terata, were seen in the fetuses (ACGIH 2001).

Eggs of the South African clawed toad (*Xenopus laevis*) in the cleavage state were exposed to hydrazine until hatching. Survival and development into normal larvae occurred at exposures below 10 mg/L. At 10 mg/L, 35 percent of the embryos were malformed at hatching; the effect was dose-related. Additional studies revealed that teratogenic effects appeared until neurulation. When *Xenopus* larvae were exposed to 1.0 mg hydrazine/L water for 120 hours, all died 24-48

hours after exposure. No significant effects on survival and development were observed after exposure to 0.1 mg/L, the next lowest concentration tested (HSDB 2005).

7.8.2.6 Genotoxicity

Mutagenicity of hydrazine has been demonstrated in both *in vitro* and *in vivo* assays, tested as hydrazine sulfate, hydrazine hydrate, or hydrazine hydrochloride. Reverse mutations were induced in the Ames assay using *Salmonella typhimurium* (Kimball 1977; Anderson and Styles 1978; McMahon et al. 1979; Tosk et al. 1979; Parodi et al. 1981, and Rogan et al. 1982) and in tryptophan auxotrophs of *E. coli* (McMahon et al. 1979, Von Wright and Tikkanen 1980), and in host-mediated assay with mice given a single dose of hydrazine sulfate by gavage (Simmon et al. 1979, IRIS 2009).

7.8.2.7 Carcinogenicity

Hydrazine is categorized as a probable human carcinogen (Group 2B), based upon inadequate evidence in humans, but sufficient evidence in experimental animals (HSDB 2005).

Toth (1972) administered 0.001 percent hydrazine in drinking water to 50 Swiss mice/sex for their lifetimes. Lung adenomas and adenocarcinomas were induced in 24/50 of the males and 27/50 females (48-54 percent) (IRIS 2009)

7.8.2.8 Ecotoxicology

7.8.2.8.1 Fate and Transport

Because of its miscibility with water and low predicted log K_{OC}, hydrazine is expected to be easily transported in the environment. Evaporation from wet surfaces is not expected, but is possible from dry surfaces. Hydrazine has a pKa of 7.96, indicating presence of the protonated form is likely, which will also inhibit evaporation (HSDB 2005).

If released to the atmosphere, hydrazine is expected to exist solely as a vapor. Atmospheric degradation by photochemically-induced hydroxyl radicals is expected, with a half-life estimated at 6 hours (HSDB 2005).

Because of a low K_{OW}-value, the potential for bioconcentration of hydrazine appears low. As a cation, hydrazine can participate in cation-exchange reactions (HSDB 2005).

7.8.2.8.2 Ecotoxicity

Hydrazine poses a particular risk to aquatic organisms or and terrestrial organisms that consume hydrazine-contaminated water. A fairly large amount of ecotoxicity information exists for hydrazine. EC_{50} values reported for green algae range from 0.5 µg/L to an upper value of about 37 µg/L depending upon species and exposure time (ECOTOX 2009).

The 48-hour EC_{50} in green algae (*Selenastrum capricornutum*) was 0.02 µL/L (0.02 µg/L). The 48-hour LC_{50} for *Daphnia pulex* is 0.19 mg/L.

The lowest 96-hour LC_{50} reported for finfish (Bluegill, *Lepomis macroshirus*) 1.08 mg/L in a static system. A 96-hour continuous flow exposure of bluegills (*Lepomis macrochirus*) resulted in a no lethal effects concentration of 0.43 mg/L (HSDB 2005).

A 96-hour LC_{50} reported for aquatic sowbugs (*Asellus spp.*) is 1.3 mg/L (HSDB 2005).

Laboratory exposures of fathead minnows (*Pimephales promales*) have resulted in LC_{50} values from 8.98 mg/L for an 18-hour exposure, to a minimum of 2.25 mg/L for a 4-day exposure (Velte 1984, Brooke 1987). LC_{50} values for other higher finfish range from 0.28 mg/L for 2-day exposures of Bluegills (*Lepomis macrochirus*) to 1.0 mg/L for 4-day exposure of channel catfish (*Ictalurus punctatus*) and 1.17 mg/L for 1-day exposures of Zebra danios (*Danio rerio*) to 3.40 mg/L for 4-day exposures of threespine sticklebacks (Gasterosteus aculeatus)(Brooke 1987, Harrah 1978, Hunt et al. 1981).

Toxicities of hydrazine and phenylhydrazine to embryos and larvae of Zebrafish (*Brachyodanio rerio*) were studied under standardized conditions. Exposure to the chemical started at the blastula stage and the effect on hatching and survival were monitored for 15 days. The results showed that toxicities of phenylhydrazine to both embryos and larvae were more than for hydrazine. The LOEL for hatching with hydrazine was 0.049 mg/L, and the LOEC for survival of larvae was 0.00035 mg/L for hydrazine. The NOAEL for hatching was 0.0245 mg/L for hydrazine and the NOAEL for survival of larvae was 0.00175 mg/L for hydrazine (HSDB 2005).

Minimum LC_{50}'s for amphibians (salamanders and African clawed toads) are about 2120 µg/L for a 4-day exposure in salamanders (Slonim 1986) and 10-25 mg/L in the African clawed toad (*Xenopus laevis*)(Greenhouse 1976).

Hydrazine at levels between 50-1000 ppm in soil have been found to induce chromosome breakage in broadbean plants (*Vicia faba*) after only 2 days of exposure (Gupta and Grover 1970). Sixteen-day-old seedlings of cotton (*Gossypium hirsutum*) in a hydroponic culture were exposed to hydrazine in growth medium for 9 days at concentrations between 0 and 1000 mg/L and a temperature of 22-29ºC. Plants died within 48 hours of exposure to 300 mg/L and within 30 hours at the higher concentrations. Injury was first noted as foliar dehydration, without chlorosis or necrosis, after 9 days of exposure to 50 mg/L or within 24 hours of exposure to 300 mg/L or more (WHO 1987).

7.8.2.8.3 Degradation/Treatment

Hydrazine appears to degrade more rapidly in soil than in water, with oxidation and biodegradation as the main removal processes. In water, the half-life for hydrazine degradation is predicted to be 8.3 days. Vapor phase hydrazine will react with both photochemically-produced hydroxyl radicals and ozone. The half-life for reaction with hydroxyl radicals is predicted to be about 6 hours, while the half-life for degradation by ozone in the natural troposphere about 2 hours (HSDB 2005).

8 Discussion

8.1 Compound Summaries

8.1.1 Hydroxylammonium nitrate [HAN]

Precise values for acute toxicity are not available, but HAN should be treated as a toxic substance, although it does not appear to be carcinogenic. Precautions must be taken in occupational health environments to prevent inhalation, dermal and ocular exposure. There is information from animals that HA, and by extrapolation HAN, may have developmental or reproductive impacts potentially leading to malformations but not death.

A similar lack of precision is found for ecotoxicity information. The matter is somewhat complicated by the fact that HA/HAN can exist in various chemical forms, depending upon the pH and ionic environment.

8.1.2 Hydroxyethylhydrazine nitrate [HEHN]

The acute oral toxicity of HEHN compares favorably with that of hydrazine (367 mg/kg vs. 60 mg/kg in rats). Inhalation toxicity is also moderate. Ecotoxicity also appears to be relatively low, although ground water transport is highly likely. Occupational health hazard is moderate, except for the likelihood that HEHN will be a developmental or reproductive toxicant.

8.1.3 Ammonium nitrate [AN]

Assessing the impact of ammonium requires determining the impact of three separate components—the nitrate anion, change in pH from dissociation of the ammonium cation, and decomposition of the ammonium ion to release ammonia. Ammonium nitrate is relatively non-toxic as long as significant quantities are not involved. Because of its ionic nature, ammonium nitrate is readily transported in the environment, but is rapidly taken up by plants since both of the ions represent essential nutrients for plants. Over time, there is a potential for acidification of water by the ammonium cation.

8.1.4 2,2'-Bipyridyl [BP]

2,2'-Bypyridyl is acutely toxic via oral ingestion, and is predicted to be a developmental or reproductive toxicant. Inhalation toxicity is low. BP is mutagenic in the Ames test, but is not predicted to be carcinogenic. Occupational hazards are moderate to skin and eyes.

Environmental hazards are moderate to low, with toxicity toward benchmark species low, but some hazard of groundwater transport and relatively high environmental persistence.

8.1.5 1-Methyl-4-amino-1,2,4-triazolium nitrate [AMTN]

AMTN is predicted to demonstrate low toxicity via oral, inhalation, and dermal routes of exposure. It is a possible ocular irritant, but this is a prediction at moderate confidence. AMTN is not predicted to be mutagenic, and although the carcinogenicity prediction from TOPKAT is indeterminate, a negative result in the Ames test indicates carcinogenicity is unlikely.

8.1.6 Carbohydrazide

CBZ is a moderately toxic solid with high aqueous solubility, but negligible vapor pressure. Inhalation toxicity is low, but the compound is an ocular irritant and dermal irritant and sensitizer. CBZ is expected to be positive in the Ames mutagenicity assay.

CBZ will have an environmental persistence of days to weeks, and is not readily biodegradable. Toxicity toward aquatic organisms is low.

8.1.7 Hydrazine

Hydrazine is extremely toxic to humans by all routes of exposure, and is a probable human carcinogen. In an occupational environment, complete physical protection, to include self-contained breathing apparatus, is required.

Ecotoxicity is also very high for hydrazine, although degradation in the environment appears to be relatively rapid. Release to the air, water, or soil should be proscribed.

8.2 Regulations and Standards

8.2.1 Hydroxylammonium nitrate

8.2.2 Hydroxyethylhydrazine nitrate [HEHN]

No regulations or standards pertaining to HEHN were found.

8.2.3 Ammonium nitrate

Ammonium nitrate is readily taken up by both terrestrial and aquatic plants as an essential nutrient. It will also be consumed by bacteria (HSDB 2014).

8.2.4 2,2-Bipryidyl [BP]

BP is listed as a Community Right to Know compound in New Jersey and Pennsylvania (Sigma-Aldrich 2015).

8.2.5 AMTN

No regulations relating to AMTN were found

8.2.6 Carbohydrazine

Carbonohydrazide is listed under the Right-to-Know regulations of Pennsylvania and New Jersey (Sigma-Aldrich 2014).

8.2.7 Hydrazine

Hydrazine is regulated under the Clean Air Act as a Hazardous Air Pollutant (HAP). OSHA has established an 8-hour TWA limit of 1 ppm (1.3 mg/m^3), and the ACGIH has established an 8-hour TWA TLV of 0.01 ppm. The IDLH level is 50 ppm. Hydrazine is also regarded as carcinogenic (HSDB, 2005).

Releases of greater than 1 lb (0.454 kg) of hydrazine are reportable under CERCLA/SARA (Comprehensive Environmental Response, Compensation and Liability Act [Superfund]/Superfund Amendments and Reauthorization Act).

8.3 Summary

8.3.1 M315E HAN-based

8.3.2 M315F HAN-free

8.3.3 HEATN-based (AFRL 824S)

8.3.4 AMTN-based (AFRL 1107P)

8.3.5 Carbohydrazide

9 Recommendations

10 Point of Contact

The Point of Contact for this report is Dr. William S. Eck, telephone 410-436-3980, DSN: 584-3980; e-mail: usaphctoxinfo@amedd.army.mil.

Table 3. Physical Properties.

	Molar Mass (g/mol)	**Melting Point (ºC)**	**Boiling Point (ºC)**	**Aqueous solubility (mg/L) @ 25ºC**	**log K_{OW}**	**log K_{OC}**	**Henry's Law Constant (atm-m^3/mol) @ 25ºC**	**Vapor Pressure mmHg @ 25°C**
HAN	96.06[1]	ND	Decomposes near boiling point[3]	ND	ND	ND	ND	10.5[3?] @ 0°C
HEHN	139.04[1]	-70[4]	219[4]	1E+06[4] (miscible)	-1.98[5]	-0.06[5]	1.54E-12[5]	0.023[5]
AN	80.06[1]	169.6[2]	210[2] (dec)	192,000[2]	n/a	n/a	n/a	n/a
BP	156.19[1]	72[6]	273.5[6]	5.93E+03[4]	1.50[6]	2.11[4]	7.09E-10[4]	1.35E-05[4]
Hydroxyethyl triazolium								
AMTN	162.13	Nd	Nd	1E+06	-3.86[b]	-1.14[b]	4.43E-14[b]	0.198[b]
Carbohydrazide								
Hydrazine	32.05[7]	70.71[8]	113.5[7]	Miscible[7]	-2.07[8]	2[8]	6.1E-07[8]	14.4[8]

Notes: (dec) = Decomposes
1=Calculated from molecular formula and standard atomic weights.
2=Dean 1992.
3=HAN decomposes near the boiling point of the aqueous solution (Sassie and Klein 1979).
4=EPI Suite 4.11 database value
5=EPI Suite 4.11 estimate for neutral compound
6=Lide 2000.
7=O'Neil 2006
8=HSDB 2005

Table 4. Toxicity data.

Compound	Acute Oral LD_{50} (mg/kg)	Chronic Oral LOAEL (mg/kg-d)	Inhalation LC_{50} (g/m^3-h)	Dermal	Ocular	Mutagenicity	Carcinogenicity
HAN	325[2]	ND	ND	Moderate irritant[1]	Probable irritant[3]	Negative[2]	Negative[3]
HEHN	367[4]	19.4[3]	0.549[3]	Slight irritant[4]	Probable irritant[3]	Positive[4]	Possible[3]
AN	2217[1]	ND	>88.8[1] (rat)	Irritant[1]	Irritant[1]	Negative[1]	Negative[1]
BP	100[5]	60.9[3]	9.1[3]	Irritant[5]; unlikely sensitizer[3]	Irritant[3]	Positive[5]	Unlikely[3]
AMTN	>10,000a	30.0a	>10.0a	Unlikely irritant or sensitizera	Possible irritanta	Negativea	Indeterminatea
Hydroxyethyl triazolium							
Carbohydrazide							
Hydrazine	59[6] (mouse) 60[6] (rat)	ND	570 ppm/4 hr[6]	Highly corrosive; LD_{50}=91 mg/kg (rabbit)[6]	Corrosive; can produce temporary blindness[6]	Positive[6]	Positive in animals;likely in humans[6]

Notes:
1=HSDB 2014
2=AFRL Operational Toxicology Branch.
3=TOPKAT model estimate
4=CPIAC 2009
5=HSDB 2002.
6=HSDB 2005

Table 5. Toxicity Assessment

Compound	Oral	Inhalation	Dermal	Ocular	Mutagenicity	Carcinogenicity	Comments
HAN	Mod	Unk	Mod	Mod		Low	
HEHN	Mod	Mod	Mod	Mod		Mod	
AN	Low	Low	Low	Low		Low	Methemoglobinemia most readily expressed clinical sign.
BP	High	Low	Mod	Mod		Low	pKa = 4.33[1]; Positive developmental toxicant
Hydroxyethyl triazolium							
AMTN	Low	Low	Low	Low	Low	Not predicted to be a developmental or reproductive toxicant	Low
Carbohydrazide							
Hydrazine	High	High	High	High	High	Carcinogenic to animals	

1=HSDB 2002

Table 6. Ecotoxicity assessment

Compound	Aquatic	Terrestrial Invertebrates	Terrestrial Plants	Mammals	Birds	Comments
HAN	Low	Low	Mod	Mod	Unk	
HEHN	Low	Unk	Unk	Mod	Unk	
AN	Low	Low	Low	Low	Low	Amphibians most sensitive
BP	Low	Unk	Unk	High	Unk	Some data on aquatic and terrestrial plants but data are uninterpretable.
Hydroxyethyl triazolium						
AMTN						
Carbohydrazide						
Hydrazine	High	High	Mod	High	Unk	

Prepared By:

_____ _____
William S. Eck, Ph.D. ..... Date
Biologist, HERP

Approved by:

_____ _____
Michael J.Quinn, Ph.D. ..... Date
Program Manager, Health Effects Research

_____ _____
Mark S. Johnson, Ph.D., D.A.B.T. ..... Date
Portfolio Director, Toxicology

Appendix A

References

Abdel-Hamid, A.Z., Farrag, E., Rizk, M., Omar, M.T. and Mantawy, M.M. 1997. Effect of nitrogen, sulpher & phosphorous containing fertilizers and organophosphorous insecticide on reproduction of *Biomphalaria alexandrina* snails. *Egypt. J. Pharm. Sci.* 38(1-3): 147-158. [Abstract only]

ACGIH. 2001. Documentation of Threshold Limit Values for Chemical Substances and Physical Agents and Biological Exposure Indices for 2001. American Conference of Governmental Industrial Hygienists, Cincinnati, OH.

AFRL. 2002*. In vitro* rat hepatocyte toxicity and bacteria genotoxicity evaluation of high energy chemicals for replacement of hydrazine. U.S. Air Force Research Laboratory Report No. AFRL-HE-WP-TR-2003-0077. Wright-Patterson AFB, Dayton, OH. DTIC Report: ADA424199.

AFRL. 1998. High Performance Reduced Toxicity Monopropellant Development. U.S. Air Force Research Laboratory Report No. AFRL-PR-ED-TP-1998-070. Edwards Air Force Base, CA. DTIC Report:

Anderson, D. and Styles, J.A. 1978. An evaluation of four short-term tests for detecting organic chemical carcinogens. Appendix 2. The bacterial mutation test. *Br. J. Cancer* 37: 924-930.

BIOVIA. 2015. TOPKAT, Toxicity Prediction Komputer Assisted Technology, Dassault Systems, BIOVIA Corp., 5005 Wateridge Vista, San Diego, CA.

Bosan, W.S., Shank, R.C., MacEwen, J.D., Gaworski, C.L. and Newberne, P.M. 1987. Methylation of DNA guanine during the course of induction of liver cancer in hamsters by hydrazine or dimethylnitrosamine. *Carcinogenesis*. 8(3): 439-444.

Brooke, L. 1987. Report of the flow-through and static acute test comparisons with fathead minnows and acute tests with an Amphipod and Cladoceran. Center for Lake Superior Environmental Studies. University of Wisconsin-Superior, Superior, WI. 24pp. In: ECOTOX, 2009.

Chatake, T., Ono, A., Ueno, Y., Matsuda, A. and Takenaka, A. 1999. Crystallographic studies on damaged DNAs. I. An N(6)-methoxyadenine residue forms a Watson-Crick pair with a cytosine residue in a B-DNA duplex. *J. Mol. Biol.* 294:1215-1222.

CIDPL. 2009a. *Ammonium nitrate.* ChemIDPlusLite. TOXNET database, National Library of Medicine, National Institutes of Health. URL: https://toxnet.nlm.nih.gov/.

CIDPL. 2009b. *Hydrazine*. ChemIDPlusLite, TOXNET, National Library of Medicine, National Institutes of Health. URL: http://toxnet.nlm.nih.gov/.

CPIAC. 2009. *AF-M315E Summary of Properties*. Chemical Propulsion Information Agency, Monopropellant Unit 37. Johns Hopkins University.

Dean, J.A. 1992. *Lange's Handbook of Chemistry, 14th Ed.* New York: McGraw-Hill, p.3-17.

DeSesso, J.M., Jacobson, C.f., Scialli, A.R. and Goeringer, G.C. 2000. Hydroxylamine moiety of developmental toxicants is associated with early cell death: a structure-activity analysis. *Teratology* 62:346-355.

deSolla, S.R. and Martin, P.A. 2007. Toxicity of nitrogenous fertilizers to eggs of snapping turtles (*Chelydra serpentina*) in field and laboratory exposures. *Environ. Toxicol. Chem.* 26(9): 1890-1895.

ECOTOX. 2009. U.S. Environmental Protection Agency Ecotoxicity Database, URL: http://cfpub.epa.gov/ecotox/.

Evelo, C.T., Spooren, A.A., Bisschops, R.A., Baars, L.G. and Neis, J.M. 1998. Two mechanisms for toxic effects of hydroxylamines in human erythrocytes: involvement of free radicals and risk of potentiation. *Blood Cells Mol. Dis.* 24:280-295.

George, J.D., Fail, P.A., Grizzle, T.B., Yang, R.S. and Heindel, J.J. 1993. Reproductive toxicity evaluation of a pesticide/fertilizer mixture administered in the drinking water to mice. *Toxicologist* 13(1): 77.

Greenhouse, G. 1976. Evaluation of the teratogenic effects of hydrazine, methylhydrazine, and dimethylhydrazine on embryos of *Xenopus laevis*, the South African Clawed Toad. *Teratology* 13: 167-178. In: ECOTOX, 2009.

Gross, P. 1985. Biologic activity of hydroxylamine: a review. *Crit. Rev. Toxicol.*14:87-99.

Gupta, A.K. and Grover, N.S. 1970. Hydrazine induced breaks in chromosomes of *Vicia faba. Mutat. Res*. 10: 514-520. In: ECOTOX, 2009.

Harrah, C.B. 1978. Biological effects of aqueous hydrazine solutions. In: CEEDO-TR-78-14, Proc. Conf. Environ. Chem. Hydrazine Fuels, Sept. 13, 1977, Tyndall AFB, FL: 167-176. In: ECOTOX, 2009.

Heindel, J.J., Price, C.J., George, J.D., Marr, M.C., Myers, C.B., Schwetz, B.A. and Yang, R.S. 1992. Developmental toxicity evaluation in rats of a pesticide/fertilizer mixture selected to mimic environmental exposure. *Teratology* 45(5): 500.

HSDB. 2014. *Ammonium nitrate*. Hazardous Substances Databank. TOXNET database, National Library of Medicine, National Institutes of Health. URL: https://toxnet.nlm.nih.gov/. Accessed 7 May 2015.

HSDB. 2005. *Hydrazine.* Hazardous Substance Data Bank, TOXNET, National Library of Medicine, National Institutes of Health. URL: http://toxnet.nlm.nih.gov/. Accessed 11 May 2015.

HSDB. 2003. *Hydroxylamine*. Hazardous Substances Data Bank, National Library of Medicine, National Institutes of Health. URL: http://toxnet.nlm.nih.gov/. Accessed 25 Sep 2014.

HSDB. 2002. *2,2'-Bipyridine.*Hazardous Substances Data Bank, TOXNET, National Library of Medicine, National Institutes of Health. URL: http://toxnet.nlm.nih.gov/. Accessed 8 May 2015.

Hunt, T.P., Fisher, J.W., Livingston, J.M. and Putnam, M.E. 1981. Temperature effects on hydrazine toxicity to bluegills. *Bull. Environ. Contam. Toxicol.* 27(5): 588-595. In: ECOTOX, 2009.

IRIS. 2009. *Hydrazine*. Integrated Research Information System, U.S. Environmental Protection Agency, URL: http://www.epa.gov/iris/.

Kimball, R.F. 1977. The mutagenicity of hydrazine and some of its derivatives. *Mutat. Res.* 39(2): 11-126.

Kleinman, M.T., Linn, W.S., Bailey, R.M., Jones, M.P. and Hackney, J.D. 1980. Effect of ammonium nitrate aerosol on human respiratory function and symptoms. *Environ. Res*. 21:317-326.

MacEwen, J.D., Vernot, E.H., Haun, C.C., Kinkead, E.R., and Hall III, A., 1981. Chronic inhalation toxicity of hydrazine: Oncogenic effects. Air Force Aerospace Medical Research Laboratory, Wright-Patterson Air Force Base, Ohio. NTIS.

Marco, A., Hidalgo-Vila, J. and Diaz-Paniagua, C. 2004. Toxic effects of ammonium nitrate on flexible-shelled lizard eggs. *Bull. Environ. Contam. Toxicol.* 73: 125-131.

McMahon, R.E., Cline, J.C. and Thompson, C.Z. 1979. Assay of 855 test chemicals in ten tester strains using a new modification of the Ames test for bacterial mutagens. *Cancer Res.* 39(3): 682-693.

Oldham, R.S., Latham, D.M., Hilton-Brown, D., Towns, M., Cooke, A.S. and Burn, A. 1997. The effect of ammonium nitrate fertiliser on frog (*Rana temporaria*) survival. *Agricultural Ecosystems & Environment* 61(1): 69-74.

O'Neil, M.J. 2006. *The Merck Index, 13th Ed*. Whitehouse Station: Merck, Sharpe and Dohme.

Ortiz, M.E., Marco, A. Saiz, N. and Lizana, M. Impact of ammonium nitrate on growth and survival of six European amphibians. *Arch. Environ. Contam. Toxicol*. 47:234-239.

Palmieri, B., Asole, A., Panu, R. and Branca, A. 1978. [Testicular lestions in rat treated with an iron-chelating agent (alph,alpha-dipyridyl)]. *Boll. Soc. Ital. Biol.Sper.*54:229-232. [Article in Italian, PMID: 6872429]

Parodi, S., DeFlora, S., Cavanna, M., et al. 1981. DNA-damaging activity in vitro and bacterial mutagenicity of 16 hydrazine derivatives as related quantitatively to their carcinogenicity. *Cancer Res.* 41(4): 1469-1482.

Pasricha, J.S. and Gupta, R. 1983. Contact dermatitis due to calcium ammonium nitrate. *Contact Dermatitis* 9(2): 149.

PubChem. 2014. *Hydrazine, nitrate*. PubChem Open Chemistry Database, National Center for Biotechnology Information, National Library of Medicine. URL: http://pubchem.ncbi.nlm.nih.gov/compound/166817. Accessed 4 May 2015.

Puglis, H.J. and Boone, M.D. 2007. Effects of a fertilizer, an insecticide, and a pathogenic fungus on hatching and survival of bullfrog (*Rana catesbiana*) tadpoles. *Environ. Toxicol. Chem.* 26(10): 2198-2201.

Rogan, E.G., Walker, B.A., Gingell, R., Nagel, D.L. and Toth, B. 1982. Microbial mutagenicity of selected hydrazines. *Mutat. Res.* 102(4): 413-424.

Sasse, R.A. and Klein, N. 1979. Thermal initiation of hydroxylammonium-based gun propellants, Proceedings of the 15th JANNAF Combustion Meeting, Vol. 1, p. 313, CPIA Pub 297.

Schuytema, G.S. and Nebeker, A.V. 1999. Comparative toxicity of ammonium and nitrate compounds to Pacific treefrog and African clawed toad tadpoles. *Environ. Toxicol. Chem.* 18(10): 2251-2257.

SciLab. 2013. *Hydroxylamine*. Safety Data Sheet, Science Lab Corp., Houston, TX. URL: http://www.sciencelab.com/msds.php?msdsId=9924321. Accessed 26 Sep 2014.

Sheftel, V.O. 2000. Indirect Food Additives and Polymers. Migration and Toxicology, Boca Raton, FL: Lewis Publishers, p. 208. In: HSDB, 2009.

Sigma-Aldrich. 2015. *2,2'-Bipyridyl*. Material Safety Data Sheet, Ver. 5.5, dated 3/31/2015. Sigma-Aldrich

Chemical Co., St. Louis, MO. URL: http://www.sigmaaldrich.com/MSDS/MSDS/DisplayMSDSPage.do?country=US&language=en&productNumber=D216305&brand=SIAL&PageToGoToURL=http%3A%2F%2Fwww.sigmaaldrich.com%2Fcatalog%2Fsearch%3Fterm%3D366-18-7%26interface%3DCAS%2520No.%26N%3D0%26mode%3Dmatch%2520partialmax%26lang%3Den%26region%3DUS%26focus%3Dproduct. Accessed 8 May 2015.

Simmon, V.F., Rosenkranz, H.S., Zeiger, E. and Poirer, L.A. 1979. Mutagenic activity of chemical carcinogens and related compounds in the intraperitoneal host-mediated assay. *J. Natl. Cancer Inst.* 62(4): 911-918.

Slonim, A.R. 1986. Acute toxicity of some hydrazine compounds to salamander larvae, *Ambystoma spp*. *Bull. Environ. Contam. Toxicol*. 37(5): 739-746. In: ECOTOX, 2009.

Taylor, R.J., Jr., Stubbs, C.S., Jr. and Ellenbogen, L. 1969. Tyrosine hydroxylase inhibition in vitro and in vivo by chelating agents. *Biochem. Pharmacol*. 18:587-594.

Tosk, J., Schemeltz, I. and Hoffman, D. 1979. Hydrazines as mutagens in a histidine-requiring auxotroph of *Salmonella typhimurium*. *Mutat. Res*. 66(3): 247-252.

Tsimakuridze, M., Saakadze, V. and Tsereteli, M. 2005. [The characteristic state of health of ammonia nitrate producing workers]. *Georgian Med. News*. (122):80-83. [Article in Russian, PMID: 15988092].

US EPA. 2015a. EPI Suite 4.11, Estimation Programs Interface Suite™ for Microsoft® Windows, Version 4.11, U.S. Environmental Protection Agency, Washington, DC.

US EPA. 2015b. ECOSAR, Ecological Structure Activity Relationships, Version 1.11, U.S. Environmental Protection Agency, Washington, DC.

Velte, J.S. 1984. Acute toxicity of hydrazine hydrate to the fathead minnow (*Pimephales promelas*) and Daphnid (*Daphnia pulex*). *Bull. Environ. Contam. Toxicol.* 33(5): 598-604. In: ECOTOX, 2009.

Von Wright, A. and Tikkanen, L. 1980. Hydrazine and methylhydrazine as recA+-independent mutagens in *Escherichia coli. Mutat. Res.* 71(2): 269-271.

Watt, P.J. and Oldham, R.S. 1995. The effect of ammonium nitrate on the feeding and development of larvae of the smooth newt, *Triturus vulgaris (L.)*, and on the behavior of its food source, *Daphnia*. *Freshwater Biology* 33(2): 319-324.

WHO. 1987. Environmental Health Criteria 68: Hydrazine. World Health Organization, Geneva, Switzerland. URL: http://www.inchem.org/documents/ehc/ehc/ehc68.htm#PartNumber:%206

Xu, Q. and Oldham, R.S. 1997. Lethal and sublethal effects of nitrogen fertilizer ammonium nitrate on common toad (Bufo bufo) tadpoles. *Arch. Environ. Contam. Toxicol*. 32;298-303.

Appendix G- Thermal Stability Testing of Carbohydrazide Candidate

Thermal Stability Testing

Initial ~0.5 cc test samples (qty 2) of the carbohydrazide-nitrate based propellant were maintained in sealed vials at 75 ºC for 48 hrs. While no color change or significant mass loss was observed either in the test sample of hydrazine and AF-M315E control samples, comparison of titrations taken pre- versus post-thermal exposure, presented in Figure 3.6-2, indicate appreciable degradation of the carbohydrazide occurred.

1. Initial pH of the experimental propellant samples remained unchanged at around pH 3
2. Equivalents of base needed to complete titration were similar (4.83/4.97 and 5.21/4.99) for both samples held at 75 ºC for 48-hrs.
3. A control sample of the experimental propellant maintained at ambient temperature exhibited a single titration end point at approximately pH 7.5.
4. Both experimental propellant samples held at 75 ºC for 48-hrs showed a first endpoint at pH 6.4 and a second at pH 9.5-9.6.
5. Differential scanning calorimetry traces performed on samples held at 75 ºC for 48-hrs (with the parameters as employed in testing described in Section **Error! Reference source not found.**) showed no appreciable changes from propellant maintained at ambient temperature apart from a possibly significant increase in the magnitude of the endotherm observed around 160 ºC.
6. Titrated solutions of the thermally-exposed samples appeared yellow in color after titration, whereas those maintained at ambient temperature remained clear.
7. Pre- versus post-thermal exposure titration results for the hydrazine and AF-315E control samples were identical.

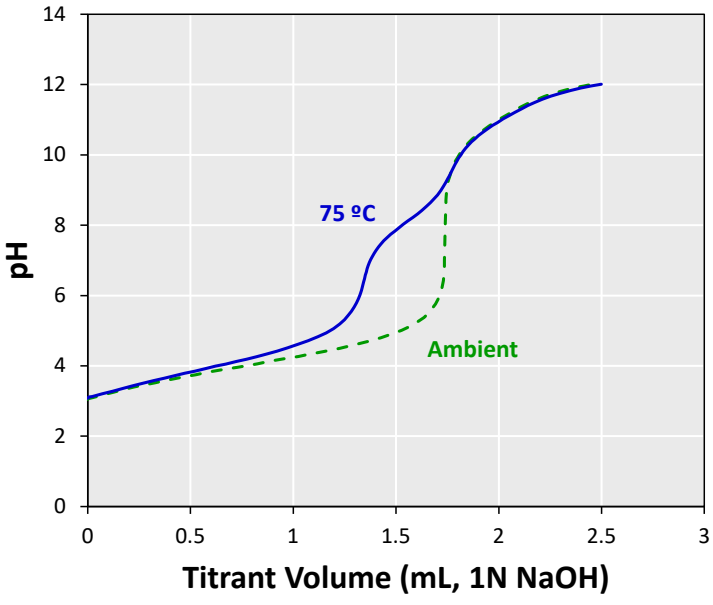

Figure 3.6-2 Comparison of titration curves for carbohydrazide nitrate-based propellant samples stored at ambient temperature versus 75 ºC for 48 hrs.

Subsequently, solutions of the experimental propellant's constituent fractions (EAN and carbohydrazide nitrate/water) were individually subjected to identical thermal exposure testing to assess the nature of the observed degradation process. Whereas post-exposure titrations of EAN showed no change, the carbohydrazide/water sample demonstrated increased degradation (33% of total base needed to react with the degradation product species versus 25% for the experimental propellant samples), suggesting the presence of EAN may provide a degree of stabilization.